DESIGN OF A THERMAL OPERATIONAL AMPLIFIER: THERMICS APPLIED TO HEAT SIGNAL CONTROL

by

ROGER LEE MCCARTHY

A.B., University of Michigan
(1972)

B.S.E. (M.E.) University of Michigan
(1972)

S.M., Massachusetts Institute of Technology
(1973)

Mech. E., Massachusetts Institute of Technology
(1975)

SUBMITTED IN PARTIAL FULFILLMENT
OF THE REQUIREMENTS FOR THE
DEGREE OF

DOCTOR OF PHILOSOPHY

at the

MASSACHUSETTS INSTITUTE OF TECHNOLOGY

March 1, 1977

Signature of Author.....
Department of Mechanical Engineering, March 1, 1977

Certified by.....
Thesis Supervisor

Accepted by.....
Chairman, Department Committee on Graduate Students

DESIGN OF A THERMAL OPERATIONAL AMPLIFIER:

THERMICS APPLIED TO HEAT SIGNAL CONTROL.

by

ROGER LEE MCCARTHY

Submitted to the Department of Mechanical Engineering
on March 1, 1977 in partial fulfillment of the requirements for
the Degree of Doctor of Philosophy.

ABSTRACT

A thermal differential operational amplifier was developed through an experimentally verified analysis of design parameters. In general, an operational amplifier (or Op-Amp) is a device which amplifies a signal by a constant factor, called the amplifier's gain. A thermal differential Op-Amp takes a small temperature difference between its negative and positive inputs and produces a much larger output temperature difference. Conceived as the building block for linear thermal logic, or thermics, the amplifier is an active control element operating totally in the thermal-energy domain, using temperatures for input and output, and heat for power. A detailed seventh-order analytical model of the amplifier used physical dimensions and material properties to predict step-input response (open and closed loop). Predictions agreed with open-and-closed loop dynamic-response tests performed on experimental prototypes. The selection of physical dimensions to produce desired dynamic behavior was accomplished with an optimal-design technique.

The amplifier was constructed from two effort (temperature) controlled resistors (ECR) which were series connected in a push-pull configuration. The trade of gain for range is identified and expressions for each constructed in terms of thermal-resistor parameters. The prototype utilized planar-film ECR's, in which the level of a conducting fluid in an air gap varies thermal resistance. The fluid level is modulated by the temperature difference between negative and positive sensors, which creates an output temperature proportional to the input temperature difference.

When tested open loop, the ratio of amplifier output to input had a constant value of twenty over the amplifier's output operating range, typically $\pm$ 30°F from a reference. Configured closed loop as an effort follower the 90% rise time was less than three minutes. Closed loop operation proved that an amplifier building block for analog thermic circuits was feasible.

Thesis Supervisor: B. Shawn Buckley
Title: Associate Professor of Mechanical Engineering

ACKNOWLEDGMENTS

First, and foremost, the author must express his sincere gratitude to his friend and advisor, Professor B. Shawn Buckley. Space does not permit narration of all the advice, encouragement, insight, and help extended to the author; suffice it to say this is not a customary acknowledgment, but a statement of truly heartfelt appreciation.

Secondly, the author must acknowledge the significant contribution made to this effort, and to his life, by his friend David W. Mercaldi, who had the patience and the misfortune to listen to many of the author's bad ideas, and all of his rude remarks, so that you, the reader, were spared.

The other members of the committee; Prof. Peter Griffith, Prof. Henry M. Paynter, and Prof. David G. Wilson, were universally positive in their attitude, encouraging, and extremely helpful to the author, for which he is deeply grateful.

Cliflex Bellows Corp. of Boston practically donated 8 bellows to the author that made a working prototype possible.

Leslie Regan's undying patience and late hours typing this manuscript deserves special mention.

Finally, to all who made the atmosphere at Tech what it was; Neville, Lampe, Jeff, Tom, Bob, Anna, Woodie, Dave, Rich, Joe, Omezie, Sandy, Fred, Jim, Mark, Jerry, John, and even Steve, I wish to say thank you, in my weaker moments I'll miss you all.

This work was made possible through the generous support of the National Science Foundation, the Dupont Science and Engineering Grant, and the Energy Research and Development Agency.

Dedication:

To my parents,

William H. and
Eloise E. McCarthy

TABLE OF CONTENTS

Page

Page

LIST OF TABLES

LIST OF FIGURES

CHAPTER 1: INTRODUCTION

Section 1-1: Brief chapter summary.

Section 2 defines an amplifier as an effort multiplying device. The different energy domains are summarized, as are the variables associated with each, called "effort" or "flow". The thermal discipline is examined, and temperature is called effort, and heat flux is flow. A thermal amplifier thus amplifies temperatures.

Section 3 describes the history of passive thermal control. Starting with the alchemist's incubator the field has evolved to the temperature modulated heat pipes used in the space program.

Section 4 is an overview of the thesis, with brief indications of the contents of each chapter and the appendices.

Section 1-2: Description and justification

A thermal operational amplifier is a temperature or heat flux amplifier. Since it cannot violate the second law, it requires a separate power input to perform its function, and thus is a three port device as shown in figure 1-2.1.

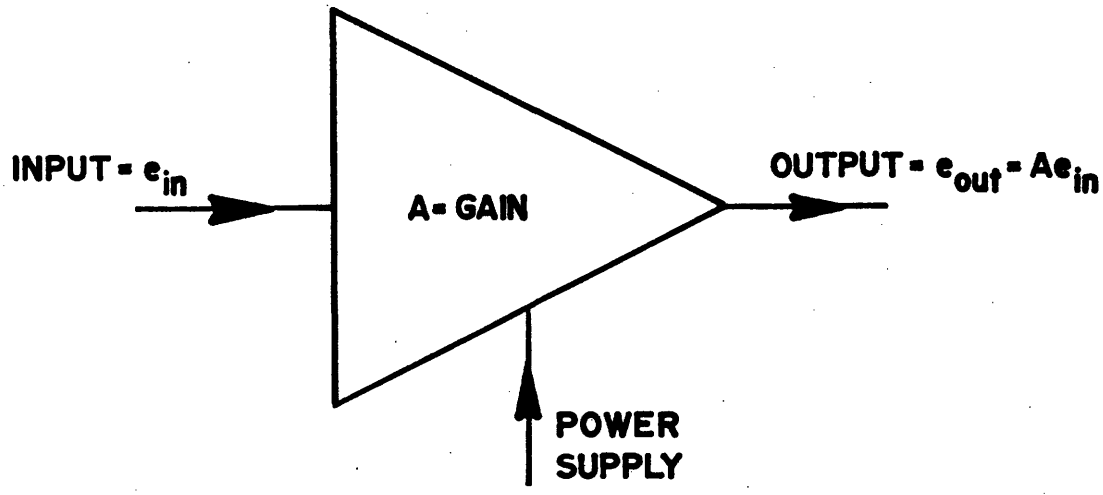

Figure 1-2.1: Operational amplifier as a three port device.

There is an input port, where the variable to be amplified (heat flux or temperature) is sensed. The amplified input appears at the output port, (multiplied by some large factor, called the "gain" of the amplifier). Power to perform this amplification function is drawn from the power port. The electronic symbol for an amplifier is shown in figure 1-2.2, note only the input and output ports are

shown, not the power port.

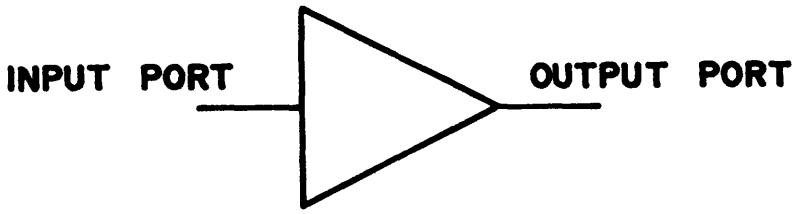

Figure 1-2.2: Electronic amplifier symbol.

The purpose of this device is to be the building block for a logic that controls heat flow or temperature, while using only heat as its power source. A device that can amplify temperature by large factors can be configured in "operational" circuits: circuits which perform mathematical operations on temperatures, such as addition, subtraction, multiplication, integration and differentiation. For this reason the device is called an operational amplifier, which is often shortened to just "op amp". The result is a logic that "thinks" with heat. Temperature control constitutes a large fraction of all control, and is the application to which this device is well suited.

By examining the nature of power, and its control, the reason for developing such a device can be understood. Power can be transferred in many forms. Electric current flow, fluid flow, shaft rotation and heat flow are examples of power being transferred in the electrical, hydraulic, mechanical, and thermal energy domains,

respectively. Power, which has the units of energy per unit time, is energy transfer. The form of energy can vary but in any domain its transfer can be expressed as the product of an effort variable, such as voltage in the electric domain, and a flow variable, such as current. Control of power can be accomplished by manipulation of either variable. Various energy domains, and their associated effort and flow variables are summarized in table 1-2.1. (Ref. 25)

In the thermal discipline two sets of effort and flow variables are currently in use. Temperature is universally the effort variable, while "entropy flow" or heat flux is the flow variable. Throughout this paper heat flux will be the flow variable. The product of temperature and heat flux is not power, heat flux itself has the units of power, but the modeling advantages compensate for this inconvenience. Operational amplifiers can be configured to amplify either the effort or flow variable, but most often used to amplify effort. Thus a thermal operational amplifier would amplify temperatures by some large factor.

Historically, when a power transfer domain has come into wide spread use, a control system has emerged that used this power transfer medium as its thinking medium. For example, the use of electricity spawned electric and electronic controls. These used the medium they controlled as their power source. Later, hydraulic power use led to hydraulic controls, and pneumatic power to pneumatic and fluidic controls. The reason for this tendency is simple. It

TABLE 1-2.1: Summary of energy domain variables.

Primary variables	Hydraulics	Electronics	Pneumatics	Fluidics	Thermics
flow	liquid volume flow	current	air volume flow	fluid volume flow	heat flow
effort	pressure	voltage	pressure	pressure	temperature

is usually more efficient to use a controller that "thinks" in the same medium as its power. Otherwise it is necessary to transduce between the power medium being controlled and that of the controller. This is slow and usually expensive, and when possible, avoided. To eliminate the need for transduction a thermal amplifier has been developed.

Heat exists as an exception to the other power transfer mediums cited above. Heat is a widespread power transfer medium whose control has traditionally been performed by some other means, usually the electrical or mechanical. A thermal amplifier would permit thermal control to be done in the thermal domain. A thermal control system is inherently slower than an electronic one. However, most thermal processes are very slow, and do not require high speed decisions. Thus, the thermal amplifier is ideally suited to the medium it controls.

The thermal operational amplifier is the basic building block for an analog or linear control system, to control heat flux or temperature. It makes possible sophisticated controllers utilizing modern control theory, while eliminating the need for an additional energy medium for control power. The convenience of single medium power and the efficiency gained from avoiding transduction constitute the two justifications for this work.

Section 1-3: Brief history of active thermal control.

Perhaps the earliest use of active thermal control, with temperature feedback was an alchemist's incubator shown in figure 1-3.1 used in the seventeenth century. (Ref. 19)

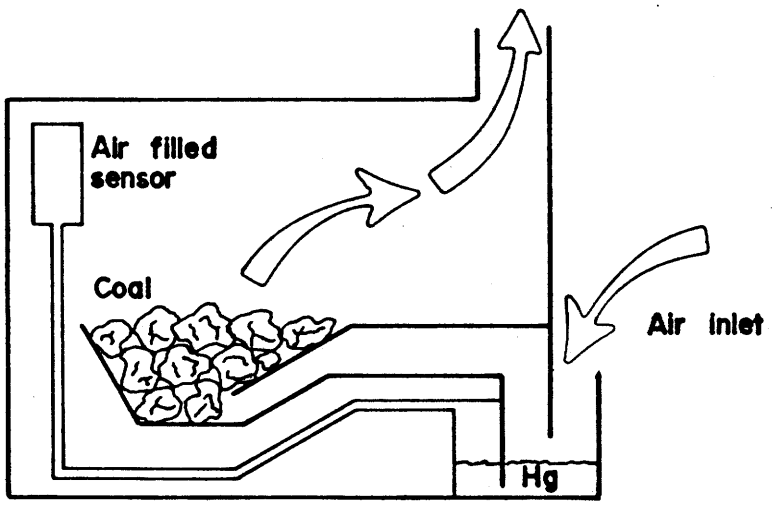

Figure 1-3.1: Alchemist's incubator, invented by Drebbel, circa 1600.

Invented by Cornelis Drebbel (1572-1633), the device was a self contained system that regulated a furnace temperature. An air filled sensor volume controls the flue opening of the furnace fire via a mercury column. As the heated air expands the mercury blocks the flue opening, starving the fire for air. The furnace temperature is controlled using only the furnace heat for an energy source. The control is active because it has a modulator, and draws power to perform its function. A passive element, such as a resistor or capacitor, is a two

port element that uses no power to perform its function.

The heat pipe is probably the most highly developed thermally modulated conductor. The National Aeronautic and Space Administration (NASA) has funded substantial research on these devices and their control. The primary application of heat pipes has been to spacecraft component cooling. Consequently the thermal logic applications were not examined. But several self modulating thermal resistances have been developed and should be noted. A self modulating resistance changes resistance in response to a temperature it senses on a third port.

The thrust of most previous thermal control has been toward temperature regulators. Usually a self modulating resistor is configured to keep a component or package at a constant operating temperature in the face of a variable heat load.

Hughes Aircraft has developed a passive "switching" heat pipe. (Ref. 26) This device employed active sensors that would switch a passive heat pipe between different temperature sinks in response to a small temperature change. A change in sink temperature modulated the heat flux. The sensor provided feedback and the device performed as an infrared detector temperature regulator.

While not strictly active thermal devices, since they work in two energy domains, electrical feedback controlled variable conductance heat pipes have been developed in Germany and the United States (Ref. 11,5,12). The conductance of a heat pipe is varied by

the amount of noncondensing or inert gas present in the pipe. A noncondensing gas "blankets" the heat pipe's condensing section, and interferes with the heat transfer accomplished by the condensing gas. The resistance of the heat pipe is thus a function of the concentration of inert gas, and can be varied over a significant range. The electrical feedback control of the inert gas concentration gave the device a variable set-point feature.

Active variable conductance heat pipes have also been developed (Ref. 4) The noncondensing gas concentration is controlled by the temperature of a sensor volume. They have been used in several applications to control temperature (Ref. 20). A schematic of such a heat pipe is shown in fig. 1-3.2.

The temperature modulated heat pipe is the previous work most closely allied to the topic of this thesis. For the amplifier developed, planar temperature modulated resistors were chosen rather than heat pipes. They can be made in more advantageous geometries, and their properties are easier to tailor. No previous records of heat pipe use for amplifier construction have been found.

Temperature modulated fluid film conduction resistors have had previous application. A resistor utilizing a fluid film to vary conductance was disclosed in patent no. 3,391,728. This device is shown in figure 1-3.3.

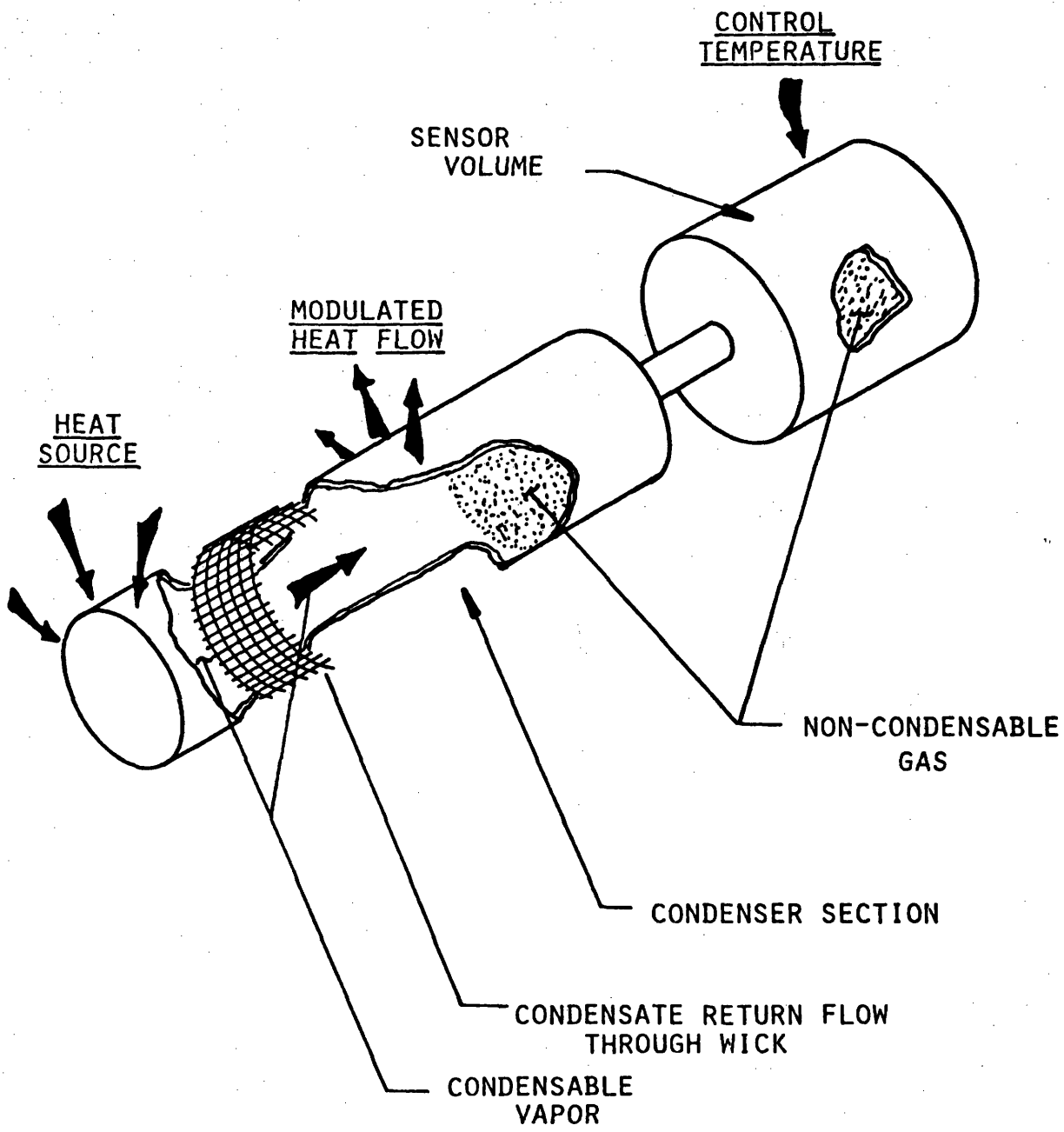

Figure 1-3.2: Variable conductance heat pipe.

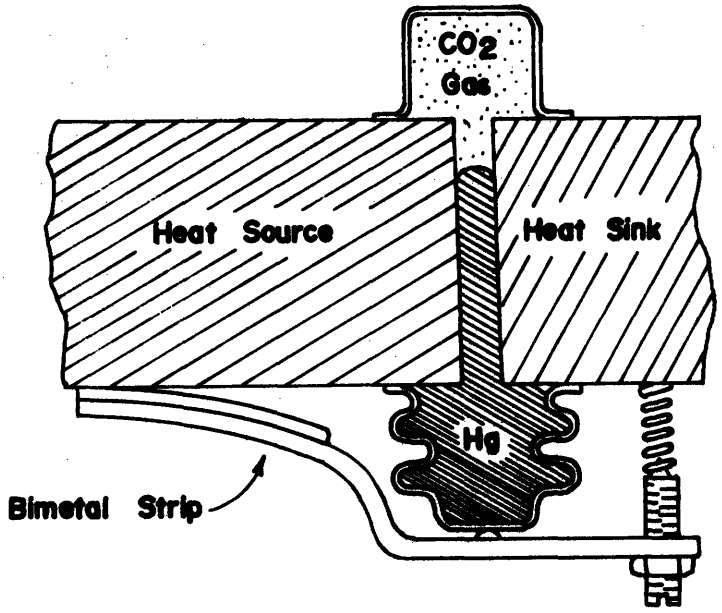

Figure 1-3.3: Modulated fluid film resistor.

A thin mercury film was manipulated to vary thermal conductance. This film resistor was used as a self modulating resistance to maintain a heat source at a constant temperature.

As of this writing the author has no record of another effort to build a thermal operational amplifier. A Northeastern Academic Science Information Center (NASIC) computer data search and a patent search were conducted. The thrust of past research mostly by NASA, was aimed at heat flux modulation rather than thermal signal control. Temperature control with variable conductances has a long history, but such devices were dedicated to a specific

temperature or geometry.

All previous temperature modulated thermal resistors have been single input, usually tied to a source to function as a regulator. In a differential amplifier the third modualting port would be decoupled from the source temperature, and used as a separate input. The next section will outline the resistors and amplifier developed in this thesis.

CHAPTER 2: THEORY OF AMPLIFIER OPERATION

Section 2-1: Brief chapter summary.

This chapter defines an amplifier and describes its functions and applications. The amplifier is treated as a completely general device, without reference to any energy domain.

Section two describes general amplifier theory. The "ideal" differential amplifier is defined, and its symbol introduced.

Section three introduces the parameters used to evaluate nonideal amplifier performance: gain, input impedance, output impedance, frequency response, and common mode rejection ratio. A simple constituitive model of the amplifier, which can account for nonidealities, is explained.

Section four describes the operational applications of the amplifier. Circuits to multiply, sum, integrate and differentiate are illustrated. The equations that govern these circuits are derived assuming the amplifier ideal, and then the effects of nonidealities are indicated, notably finite gain and saturation.

Section 2-2: Definition and description of ideal operational amplifier

An operational amplifier is a device that senses an input signal and produces an output that is a large multiple of the input. The input is usually a physical effort variable, viz. voltage, pressure, or temperature, but by a circuit change they can be the complimentary flow variables: current, volume flow, or heat flux.

An ideal amplifier senses the level of an input, draws no flow (and consequently no power) from the effort being sensed, and outputs an effort level infinitely greater. In other words $e_{out}=Ae_{in}$, where A=infinity and e represents the value of the effort. The output should remain at this value regardless of how much power is drawn from the ideal amplifier. The perfect amplifier will have infinite power available. The amplification factor A, called the "gain", should be infinite, or if finite it should remain constant, and not depend on the absolute value of the input effort variable, e_{in}. Moreover, the amplification factor should be completely insensitive to the rate at which e_{in} changes. The amplifier should respond in zero time, so that the instantaneous value of e_{out} is equal to Ae_{in}.

For the case of the differential amplifier, shown in figure 2-2.1, the input effort level that becomes amplified is the differenence between the inputs on the two terminals, or

$$e_{out} = A(e_1 - e_2) \qquad (2\text{-}2.1)$$

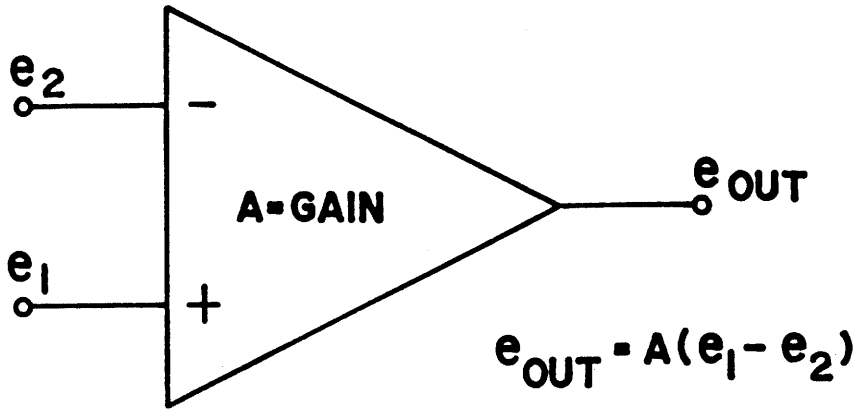

Figure 2-2.1: Symbol of a differential amplifier.

By convention port 1 is called the noninverting input and port 2 the inverting input. The differential amplifier has the most applications. The sign of a variable can be changed while being amplified, a considerable advantage in computation. Thus the symbol of figure 2-2.1 is most commonly used to denote the operational amplifier. The ideal differential amplifier responds only to the difference (with attention to sign) between the two input levels, and ignores their absolute values.

Effort variables, or simply efforts, are usually measured relative to reference or "ground". This ground is the zero effort point, all efforts below this value are negative and all above are positive. A good analogy is atmospheric pressure, used as a reference in fluidics. Values below 14.7 psia are often termed negative, even though these pressures are positive in an absolute sense.

The terms "at zero effort" and "at ground" can be used interchangeably. There is no absolute value for ground, it depends on the circuit and energy domain under study.

Section 2-3: Amplifier nonidealities

There are no ideal amplifiers. They all have finite, and not infinite gains, i.e. the amplification factor A is less than infinity. Actual amplifiers tend to require flow when sensing an input, and thus disturb the source they sense in some small way. The measure of this tendency to draw flow is called input impedance. The input impedance is the ratio of the net effort applied on the amplifier inputs to the flow drawn by the amplifier. This ratio can be expressed;

$$\frac{e_{in}}{f_{in}} = Z_{in} \qquad (2\text{-}3.1)$$

where Z_{in} is called the input impedance. From this expression, for any given effort, e_{in}, the flow can be calculated. Since an amplifier should not disturb the effort it is sensing by drawing flow, it is designed to have the highest practical input impedance.

Actual amplifiers do not have access to infinite power. They will not maintain the output effort level if significant flow is drawn by the load. The measure of this tendency to reduce an effort output level in the face of a large flow is called the output impedance, Z_{out}. The output impedance is defined as:

$$Z_{out} = \frac{e_{out}}{f_{out}} - Z_{load} \qquad (2\text{-}3.2)$$

where Z_{load} is the impedance of the amplifier load. The output impedance of the amplifier becomes important when the load impedance be-

comes small, since the flow drawn from the amplifier becomes high. Beyond a certain limit all amplifiers will suffer an output effort drop because of their inability to supply all the flow a higher effort output level would require.

Real amplifiers do not respond in zero time. It takes a finite interval to sense that the input effort value has changed, and adjust the output accordingly. If the input effort changes slower than the response time of the amplifier, the amplifier output will track the input. However, as the input rate of change approaches the amplifier response time, two things happen. First, the magnitude of the amplifier output begins to attenuate. The amplifier doesn't have enough time to bring the output to full value before the input changes. Second, the amplifier begins to "lag". For a sinusoidal input, the shape of the output will be the shape of the input, but attenuated, and slightly behind in time. This phenomen is called phase lag and is directly related to the speed of response of the amplifier. It is measured in degrees because a sine wave is used to excite the amplifier and the phase lag is the number of degrees the output sine wave lags behind the input sine wave. Both attentuation and phase lag are indicated in figure 2-3.1. The attenuation is measured in decibles, where decibles (db) = $20 \log \frac{\text{output effort}}{\text{input effort}}$. Because high gain amplifiers multiply signals by many orders of magnitude, historically it has been more convenient to use a logarithmic scale.

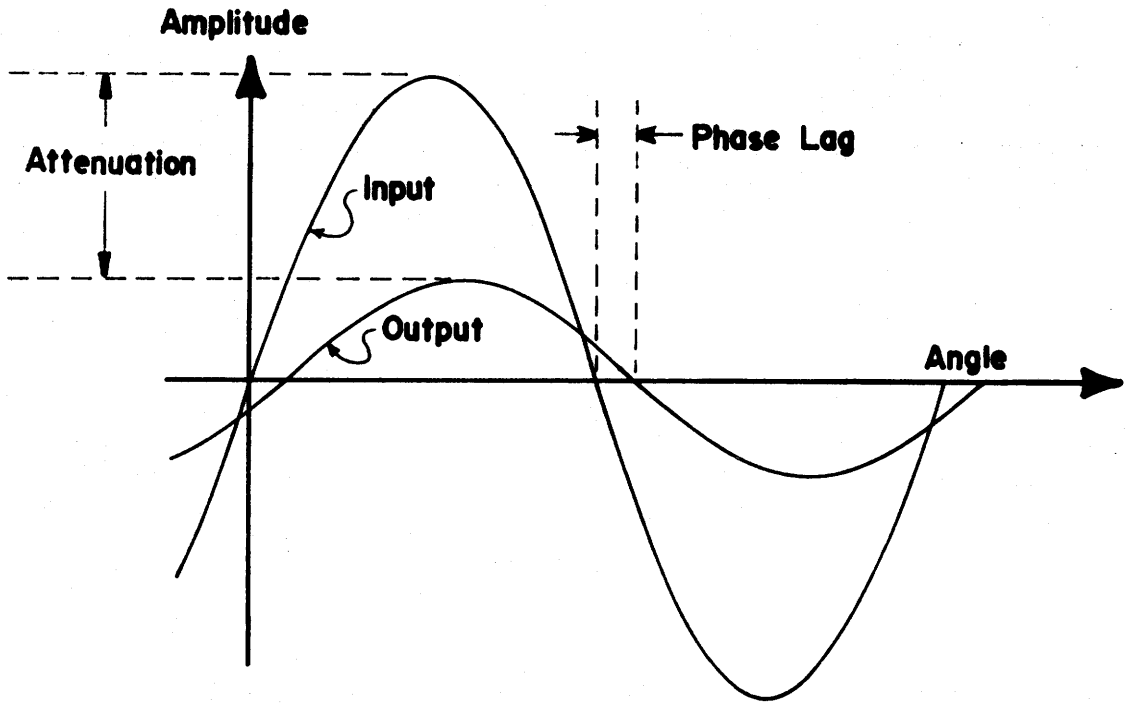

Figure 2-3.1: Definition of attenuation and phase lag.

Attenuation and phase lag are functions of the input sine wave frequency. As the frequency becomes higher the amplifier has less time to respond. At higher frequencies the attention and phase lag increase. This information is summarized in a Bode plot, where attenuation and phase lag (also called phase angle) are plotted as a function of input sine wave frequency. An example is shown in figure 2-3.2.

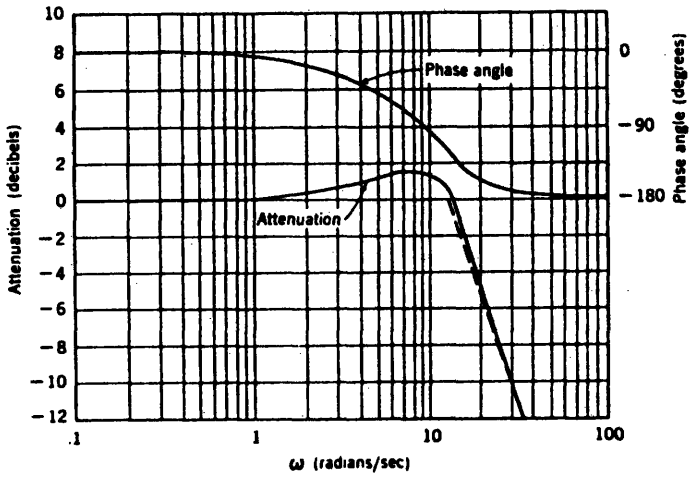

Figure 2-3.2: Bode plot of attenuation and phase lag.

Finally, actual differential amplifiers cannot totally ignore the absolute value of the input signals. Differential amplifiers, designed only to amplify the difference between the inputs, invariably amplify some small portion of the absolute value. For example, in the case of an electronic amplifier, the result of putting 1000.1 volts on the 1 (or positive terminal) of figure 2-2.1 and 1000 volts on the 2 (or negative terminal) will <u>not</u> be the same as putting .1 on the positive and 0 on the negative. The measure of this nonideality is the common-mode rejection ratio (CMRR) expressed in decibles. It is the ratio of the differential signal gain to the common mode signal gain (Ref. 8), or $\text{CMRR} = \frac{A}{A_{\text{common mode}}}$.

This parameter would be infinite for the perfect amplifier, since for identical inputs there should be no output, and $A_{\text{common mode}} = 0$.

Five factors have been described for analyzing amplifier performance. Amplification (or gain), input impedance, output impedance, frequency response, and common mode rejection. This list is not exhaustive. Parameters, such as offset and drift can be just as important in certain applications. Offset is an undesired bias of the output, positive or negative. Drift is a change in the output with time while the input has remained constant.

The five parameters do, however, represent what are perhaps most important performance aspects of an amplifier.

A simple model of an operational amplifier exists (Ref. 23) that describes its function and accounts for its deviation from the ideal. Figure 2-3.3 is a bond graph of a differential operational amplifier. (See appendix 1 for explanation of bond graphs and their use). Each bond represents a power flow, and has an effort and flow variable associated with it. From this bond graph the following constituitive matrix equation can be derived for an actual amplifier:

$$\begin{bmatrix} e_{out} \\ f_{in} \end{bmatrix} = \begin{bmatrix} A_{(\omega)} & -Z_{out} \\ 1/Z_{in} & 0 \end{bmatrix} \begin{bmatrix} e_{in} \\ f_{out} \end{bmatrix} \qquad (2\text{-}3.3)$$

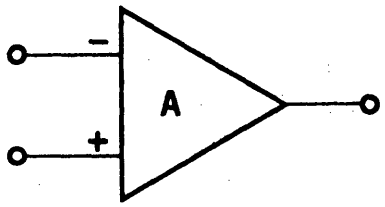

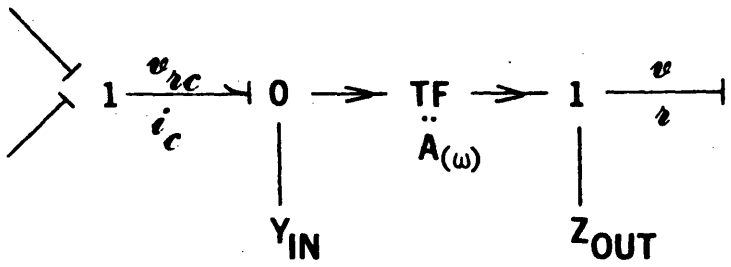

$$\begin{bmatrix} v \\ i_c \end{bmatrix} = \begin{bmatrix} A_{(\omega)} & -Z_{OUT} \\ Y_{IN} & 0 \end{bmatrix} \begin{bmatrix} v_{rc} \\ i \end{bmatrix}$$

where $Y_{in} = \frac{1}{Z_{in}}$

Figure 2-3.3: Bond graph characterization of the operational amplifier.

In this expression $A_{(\omega)}$ is the gain, which is a function of the input effort's frequency, ω. The amplification or gain decreases as ω approaches the natural frequency of the amplifier. Z_{out} & Z_{in} are the output and input impedances respectively. Thus this model takes into account the nonideality of normal amplifiers and allows computation

of output for a given input. For the ideal case Z_{out} is zero, and Z_{in} is infinite, and the matrix expression becomes $e_{out} = A\, e_{in}$. This model is used to explain the applications of the amplifier.

Section 2-4: Use of the amplifier in operational circuits.

The term operational amplifier comes from the amplifier's use in computational circuits, which perform mathematical operations. Figure 2-4.1 shows an amplifier in a circuit that will perform multiplication of an input effort by a predetermined ratio.

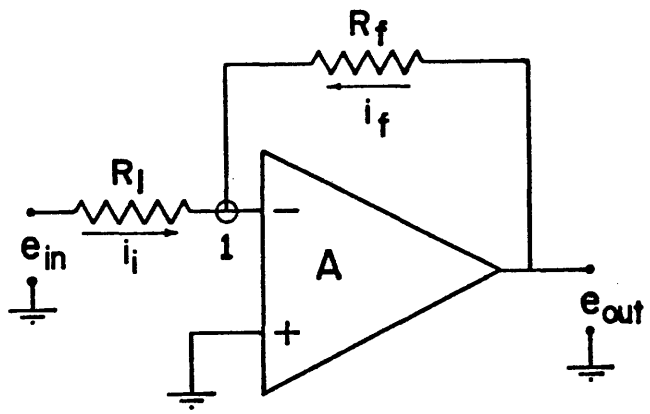

$$e_{out} = \frac{-R_f}{R_i} e_{in}$$

Figure 2-4.1: Fixed ratio multiplier

By examining the circuit the operation can be understood. First, assume the amplifier is ideal. The problems posed by nonideality will be examined later. Note the amplifier is differential, with the positive input tied to ground. By applying Kirchoff's law to junction 1 the relationship between the input and output efforts can be determined. Since the input impedance is infinite, no flow

goes into the amplifier, and

$$i_i + i_f = 0, \tag{2-4.1}$$

therefore,

$$i_i = -i_f. \tag{2-4.2}$$

The value of i_i or i_f would thus determine the efforts everywhere in the circuit. We lack, however, the effort at junction 1. By assuming the amplifier ideal the following argument can be made. If junction 1 were to have an effort value other than 0, the infinite amplification would cause e_{out} to be infinitely large, and of the opposite sign. This would quickly cause flow through the feedback loop, forcing junction 1 to return to a 0 or ground effort level. Junction 1 is thus maintained at "virtual ground". While not actually grounded, the feedback loop to the inverting input causes any deviation above or below ground to be corrected.

Now the values of i_i & i_f can be calculated.

$$i_i = \frac{e_{in} - e_1}{R_i} = \frac{e_1 - e_{out}}{R_f} \quad \text{but } e_1 = 0 \tag{2-4.3}$$

$$\therefore \quad i_i = \frac{e_{in}}{R_i} = -\frac{e_{out}}{R_f} \tag{2-4.4}$$

$$\text{or} \qquad e_{out} = -\frac{R_f}{R_i} e_{in} \tag{2-4.5}$$

The output of this circuit is the input effort multiplied by the ratio of the feedback and input resistors, and inverted in sign. Thus, with an ideal amplifier, an effort can be multiplied or amplified, as desired.

If the assumption of ideality is not valid, and junction 1 is not maintained at virtual ground by an infinite gain, the formulae governing operation are somewhat different. Now assume $e_1 \neq 0$ and $e_{out} = -Ae_1$. Therefore,

$$\text{since } -i_f = i_i = \frac{e_{in} - e_1}{R_i} = \frac{e_1 - e_{out}}{R_f} \qquad (2\text{-}4.6)$$

$$\text{now,} \quad \frac{e_{in} + \frac{e_{out}}{A}}{R_i} = -\frac{[\frac{e_{out}}{A} + e_{out}]}{R_f} \qquad (2\text{-}4.7)$$

$$\text{then,} \quad -\left[\frac{1}{\frac{1}{A} + \frac{R_f}{R_i A} + 1}\right]\frac{R_f}{R_i} e_{in} = e_{out} \qquad (2\text{-}4.8)$$

$$\text{which reduces to } e_{out} = -\left[\frac{A}{\frac{R_i}{R_f}[1+A]+1}\right]e_{in} \qquad (2\text{-}4.9)$$

This function is plotted against gain for a range of resistance ratios in figure 2-4.2. Compared with the curve for an infinite gain, shown as a dotted line, a gain as small as 1000 causes less than 10% deviation from ideal performance.

Other nonidealities produce the following effects. Signal attenuation at high frequency causes the multiplication factor, A, to be instantaneously less. The effects of finite input impedance or non-

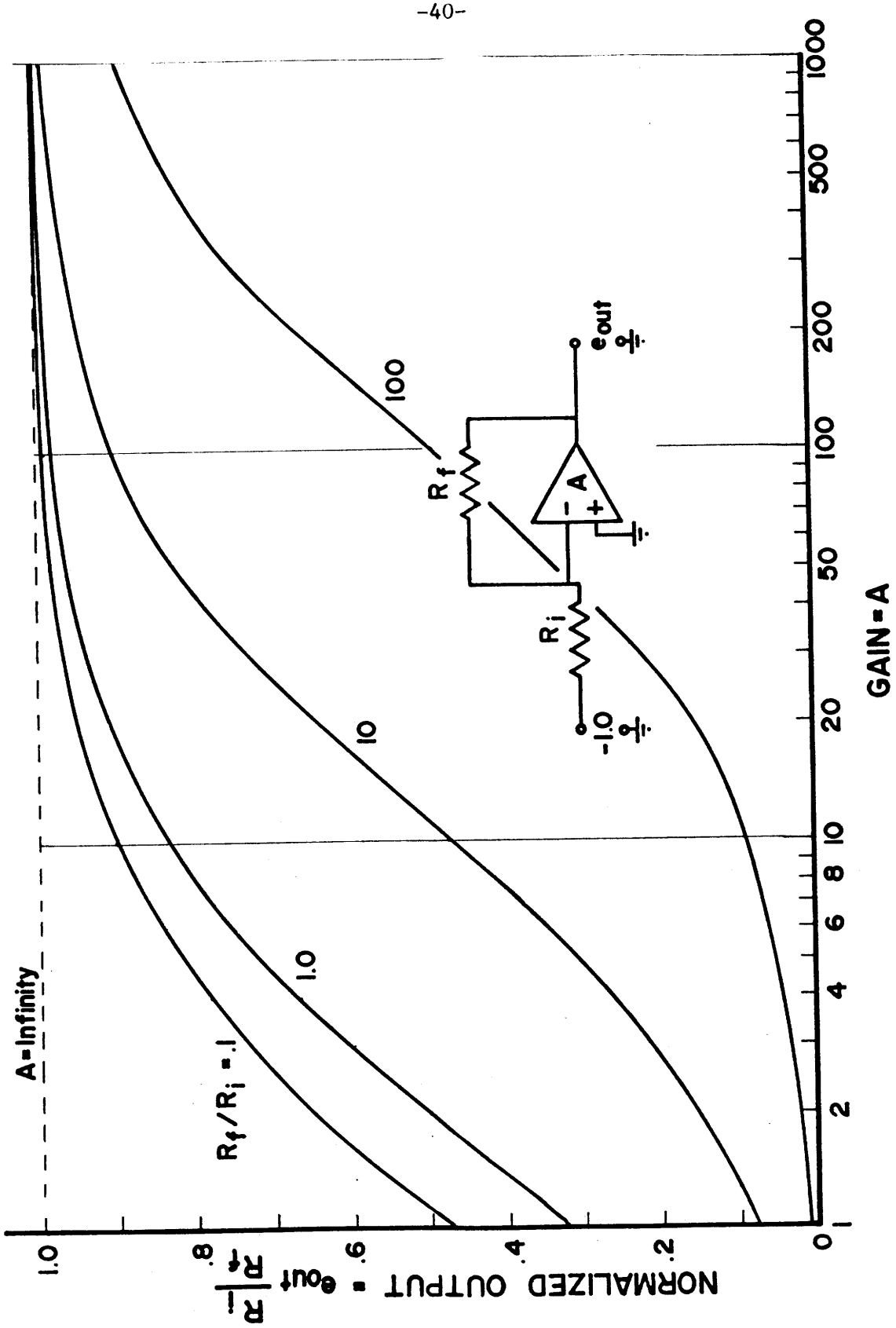

Figure 2-4.2: Normalized output as a function of gain for unity input.

zero output impedance depend on the impedances of the source and load respectively. If the input impedance is much larger than the source impedance, the deviation from ideal will be very small. The same is true if the output impedance is much less than the load impedance the amplifier is trying to drive.

The use of an operational amplifier for multiplication has been examined. It should be noted that the same circuit could be used for division, since the ratio of R_f to R_i was <u>not</u> assured greater than unity. It remains to be demonstrated how the amplifier is used for addition and subtraction, and the time based operations of integration and differentiation.

Addition or subtraction of effort values is performed by the circuit of figure 2-4.3. A circuit that adds or subtracts is a "summer". The equations that describe the summer's operation are derived as for the multiplier. The amplifier is assumed ideal, and junction 1 is assumed at virtual ground. After applying Kirchoff's law to junction one the following expression results for output versus input:

$$e_{out} = - \left[\frac{R_f}{R_1} e_1 + \frac{R_f}{R_2} e_2 + \ldots + \frac{R_f}{R_N} e_N\right] \qquad (2\text{-}4.10)$$

Summation and multiplication can thus be performed simultaneously. If only summation was desired, then all resistor values could be made unity. Subtraction is performed by inverting the sign of the signal

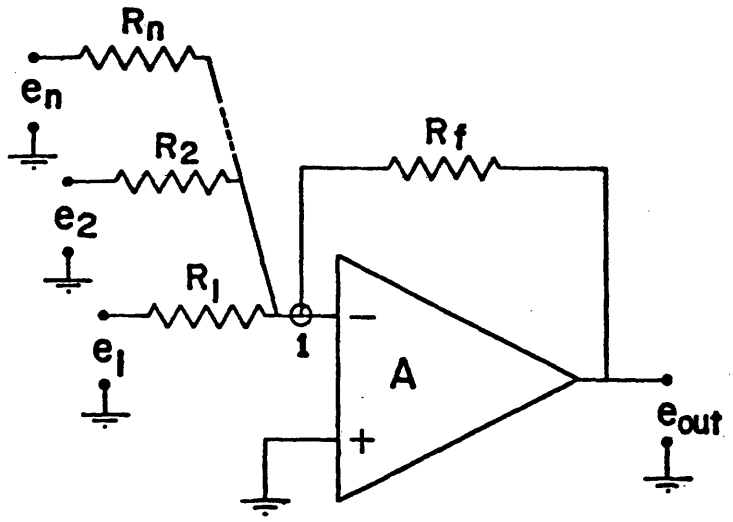

$$e_{out} = -\left(\frac{R_f}{R_1}e_1 + \frac{R_f}{R_2}e_2 + \ldots\ldots + \frac{R_f}{R_n}e_n\right)$$

Figure 2-4.3: Summer circuit.

to be subtracted, and then summing; another amplifier is usually required for this inversion.

Integration of an effort level is accomplished with the circuit of figure 2-4.4. Note the feedback loop now has a capacitor. Again assume the amplifier is ideal, and junction 1 is at virtual ground. Using Kirchoff's law or junction 1 results in the expression:

$$\frac{e_{in} - e_1}{R_i} = - C_f \frac{d}{dt}(e_{out} - e_1) \qquad (2\text{-}4.11)$$

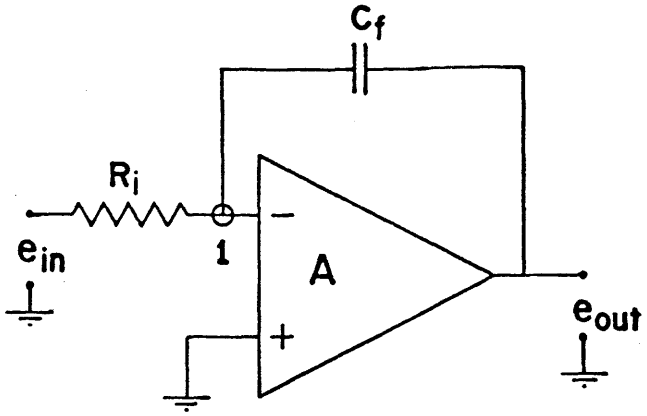

$$e_{out} = \frac{-1}{R_i C_f} \int e_{in}\, dt$$

Figure 2-4.4: Integrator circuit.

The virtual ground assumption implies $e_1 = 0$, so

$$\frac{e_{in}}{R_i C_f} = \frac{de_{out}}{dt} \tag{2-4.12}$$

We need an expression for the circuit output, not its time derivative or rate of change. Integrating both sides gives;

$$\frac{1}{R_i C_f} \int - e_{in} dt = e_{out} + \text{constant} \tag{2-4.13}$$

which rearranged becomes,

$$e_{out} = - \frac{1}{R_i C_f} \int e_{in} dt + e_o \tag{2-4.14}$$

Thus the output effort is the time integrated sum of the input, plus some constant e_o, which is the initial condition. This initial condition is the initial charge on the capacitor. R_iC_f has the units of time and is called the time constant of the circuit. Unfortunately an amplifier will not continue to integrate forever, a phenomena called saturation eventually occurs. A plot of input versus output for a typical electronic integration circuit can be seen in figure 2-4.5.

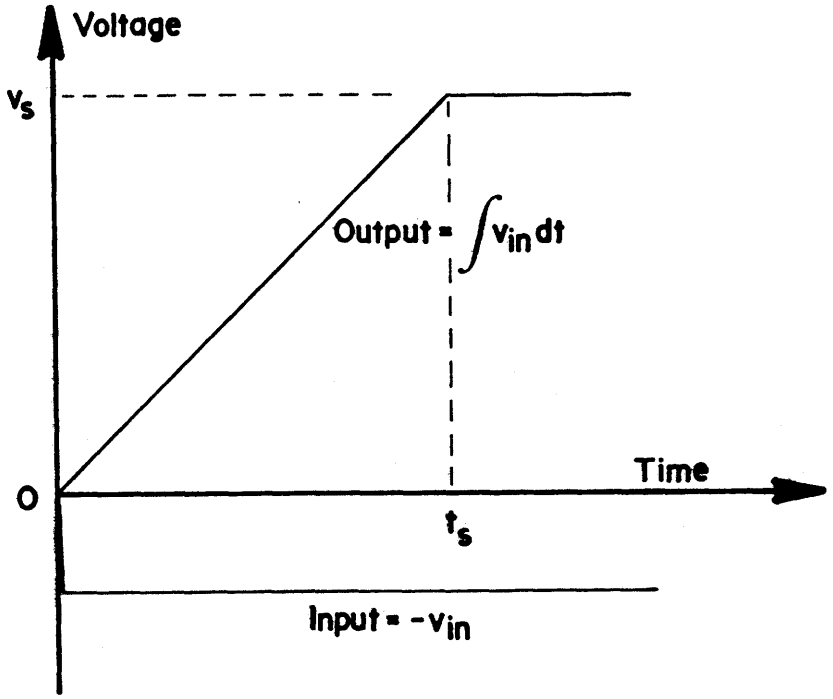

Figure 2-4.5: Illustration of amplifier saturation effect.

Output voltage remains constant beyond t_s, after the output reaches the supply voltage, v_s. This occurs because the amplifier draws its power from a voltage source that has less than infinite effort. It cannot output an effort higher in value than its source.

Thus the amplifier saturates at some effort lower than the supply level. If the input signal changes sign periodically, with a period shorter than the saturation time, the saturation phenomena is not observed.

Differentiation requires a circuit similar to 2-4.4, but with the capacitor and resistor interchanged. The output effort then becomes the derivative input, and is proportional to its rate of change and not its absolute value. Such a circuit has less utility than the others discussed because any "noise" or random disturbance on the input signal, particularly common in electronics, is sensed as signal rate-of-change and differentiated. Thus, the output of a differentiator is usually very noisy.

The preceeding discussion of addition, subtraction, multiplication, division, integration, and differentiation is by no means complete. Other sources (Ref. 2) provide a much more detailed description of the amplifier, and a more detailed account of the effects of nonideality of the amplifier on circuit performance. Applications such as filters, analog simulators, etc. have not been discussed, but are important uses of the operational amplifier. This section is intended only as a general introduction, but specific applications of the thermal amplifier will be described in chapter 6.

To this point the amplifier has been treated as a completely general device. Inputs and outputs were any effort variable of any power domain. The next chapter will discuss the thermal operational

amplifier. The effort variable will be temperature, and the flow variable heat flux, q, which has units of power. The uses of a device with differential inputs that can multiply efforts has been outlined. How such a device works in the thermal domain will be illustrated.

CHAPTER 3: THE THERMAL OPERATIONAL AMPLIFIER

Section 3-1: Brief chapter summary.

This chapter describes the thermal operational amplifier. Section two explains how two temperature modulated thermal resistors can be configured to produce an amplifier.

Section three makes some simple assumptions about the nature of the temperature modulated resistances, and characterizes them with the simple, linear, constituitive relation:

$$R = \left[\frac{r_L + r_v}{2} \right] k\Delta T_{in}$$

Utilizing this relation a simple expression for the amplifier gain, A, is derived:

$$A = \frac{k\ \Delta T_s}{r_v + r_L} .$$

Section four examines the parameters that appear in the gain expression, and explains the significance of each. A two resistor amplifier inherently suffers reduced gain for increased range and vice versa. The nature of this relationship is explained.

Section five is a general introduction to thermal resistors. The topic is narrowed to planar thermal resistors, and three types; film, convection, and pneumatic, are discussed. The film resistors are used in the amplifier, and their particular characteristics are outlined.

Section six details the topology of the two film ECR amplifier. The compensation for inherent film ECR non-linearity is detailed.

Section 3.2: Description of the thermal operational amplifier.

The amplifier has been defined as an effort amplifying device, drawing power from a third port to perform its function. For a thermal amplifier the effort variable is temperature. Therefore a thermal amplifier senses a small temperature input, i.e., a small temperature difference above or below ground, and produces a large temperature difference at the output.

The amplifier designed and investigated in this thesis employs two variable thermal resistors in a "push-pull" configuration. A schematic diagram of the internal amplifier circuit is shown in figure 3-2.1. The resistors are placed in series, and the junction between them is the output.

The inputs change the thermal resistance of R_V and R_L inversely. A small positive (i.e. above ground or zero) temperature input on the positive terminal will cause R_V to decrease its thermal resistance and become more conductive. At the same time R_L will increase its thermal resistance and become more of an insulator. The net effect is to create, for the junction, good thermal communication with the high temperature source, hereinafter just called the source, and poor thermal communication with the low temperature source, called the sink. The temperature of the junction will rise closer to that of the source and away from that of the sink. Resistor R_V tends to "pull" the junction temperature up while resistor R_L tends to "push", hence the term "push-pull". The reverse happens if a small positive

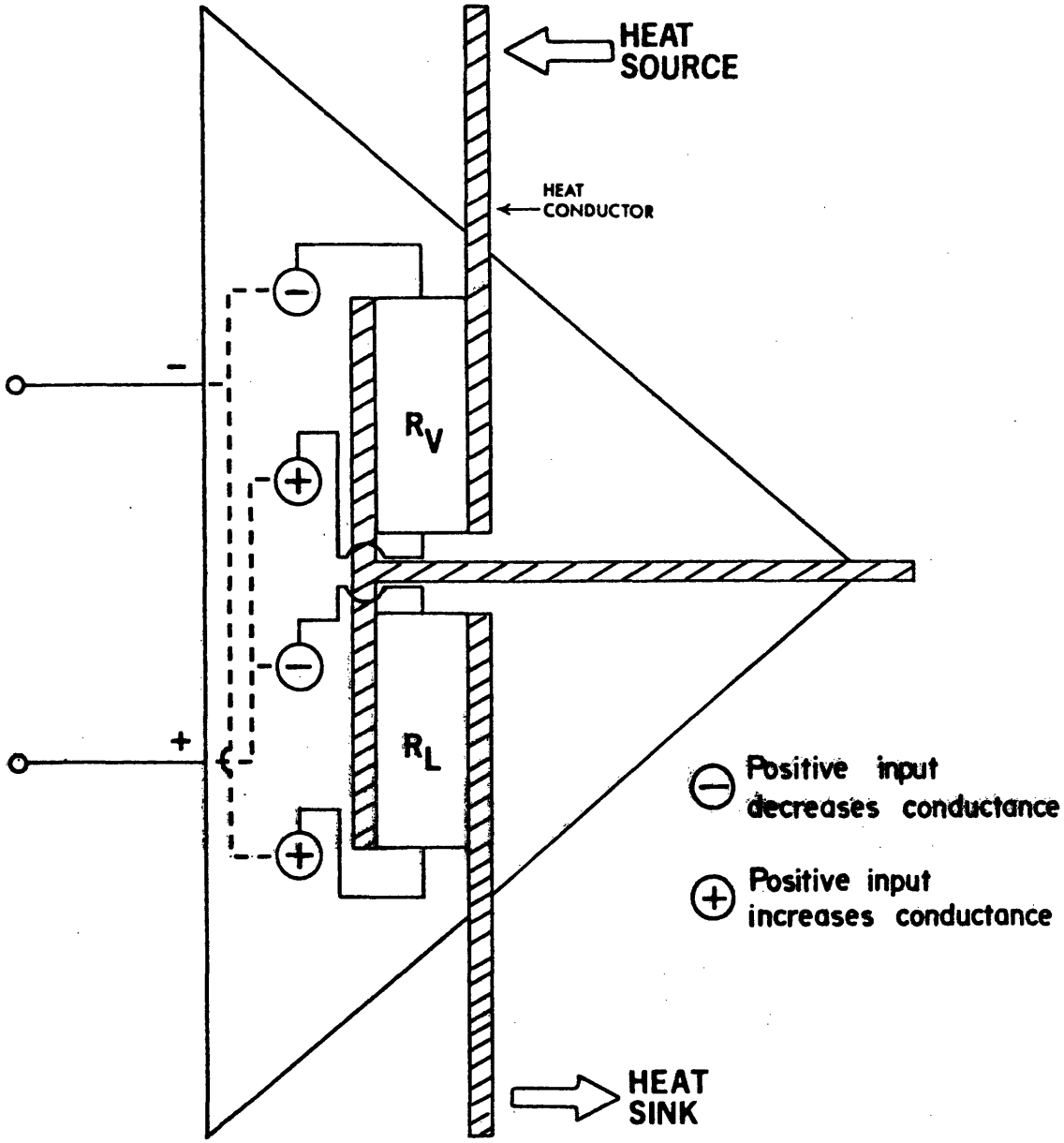

Figure 3-2.1: Diagram of amplifier thermal circuit.

temperature is sensed on the inverting input. Resistor R_L will become conductive, R_v insulating, and the temperature of the junction will move closer to that of the sink. By symmetry, a negative (i.e. less than ground) temperature input at the noninverting terminal will have the same effect as a positive input on the inverting terminal.

With no feedback loop the ratio of the temperature change at the junction to the temperature input is the open loop gain, A. With no input R_v & R_L will assume equal values, and the junction will be at ground, that temperature mid-way between source & sink temperatures. With identical inputs on the inverting and noninverting terminals, the junction should again be at ground, since only differences are amplified.

This particular design was chosen for several reasons. First, the thermal resistance is the simplest thermal element that lends itself to thermal modulation. Control of the amplifier must remain completely in the thermal domain, temperature and heat flux must power all resistance changes. Second, temperature modulated thermal resistances can be conveniently constructed. The thermal conductively of various materials varies over approximately 6 orders of magnitude. Thus the same geometry can enjoy radically different conductivities by exchanging materials. And third, thermal resistance, or conductivity is a well tabled thermal property that is

relatively insensitive to absolute temperature. For the amplifier properties to be predictable, internal component values must remain constant over the temperature range of operation, or at least change in some predictable manner. Thermal conductivities for most materials are readily obtainable, and often the temperature dependence of this value has been tabled.

The above advantages combined to produce the amplifier with the circuit of figure 3-2.1. Note the similiarities of this circuit to the final stage of the μ741 electronic operational amplifier, shown in figure 3-2.2, (Ref. 8). This amplifier is the most commonly used electronic model. Instead of variable resistors the electronic amplifier uses transistors, labeled Q_1 and Q_2, but the method of operation is very similar. The output voltage depends on which transistor is most conductive. Transistors have the advantage of passing very little power when turned "off", behavior a thermal variable resistor cannot completely parallel. The difference, though, is not in structure, but in degree.

The theory behind the thermal amplifier could be made perfectly general by calling the temperature modulated resistors Effort Controlled Resistors (or ECR's). Effort, in this case temperature, controls their resistance value. Any power domain that has a resistor that can be modulated by an effort can also have an amplifier. This amplifier would work in the qualitative manner described.

The next section is a more quantitative, linearized development, which makes some assumptions about the nature of the ECR.

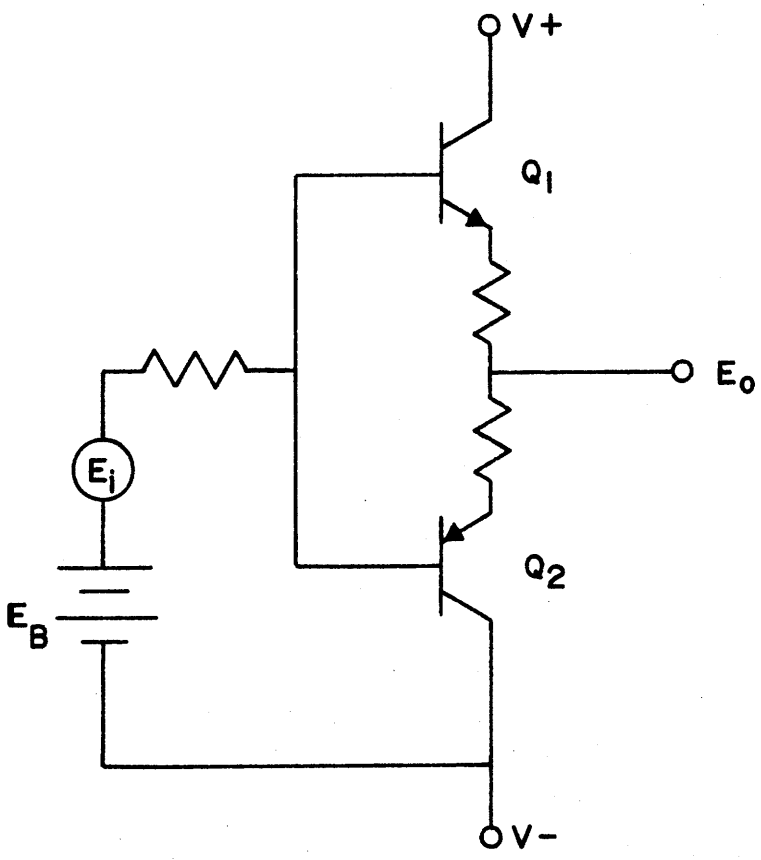

Figure 3-2.2: Circuit of μ741 electronic operational amplifier final stage.

Section 3-3: Linearized amplifier description.

This section will present a linearized analysis of an amplifier with two variable thermal resistors. The term linearized means the resistors will be assumed to change their resistance linearly with input temperature. This is not a necessary condition for amplifier resistors. It represents a simplification of more complex or non-linear resistance versus input temperature behavior. A linear approximation is usually valid for a small range of operation. The behavior of a non-linear resistor can be characterized as a curve on a resistance versus input temperature plot. If the curve is of low order (i.e. has few deflection points) a small length of the curve can be approximated to first order by a line. The line represents a linear approximation of the actual behavior.

The goal of the linear amplifier model is to understand how fixed resistor parameters influence amplifier performance. There are many different types of thermal resistances, with vastly different characteristics. A rational choice of resistors requires understanding how their particular properties affect the amplifier. A quantitative expression for gain will be derived, in terms of fixed system parameters, assuming simple linear resistance changes.

In figure 3-3.1 the amplifier circuit is shown with more detail. Electronic symbols have been used for the thermal elements because of their familiarity. For simplicity, ground temperature is chosen half-way between source and sink temperatures, this is a very

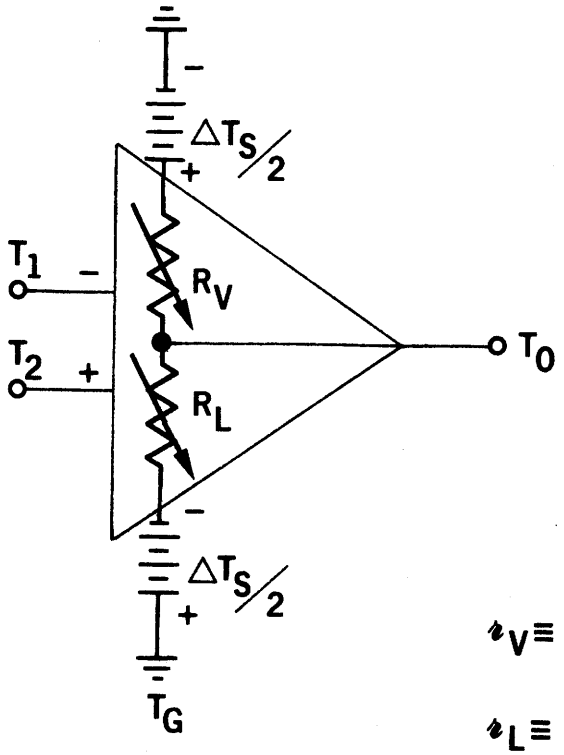

$$[T_2 - T_1] = e_{rc} = \Delta T_{IN}$$

$$T_O - T_G = \Delta T_{OUT}$$

$$R_V = \frac{r_V + r_L}{2} - K\Delta T_{IN}$$

$$R_L = \frac{r_V + r_L}{2} + K\Delta T_{IN}$$

$r_V \equiv$ MAXIMUM RESISTANCE VALUE

$r_L \equiv$ MINIMUM RESISTANCE VALUE

$$Q = \frac{\Delta T_S}{R_V + R_L} = \frac{\Delta T_{OUT} + \Delta T_S/2}{R_L}$$

$$\Delta T_{OUT} = \frac{R_L \Delta T_S}{R_V + R_L} - \frac{\Delta T_S}{2}$$

$$\Delta T_{OUT} = \underbrace{\left[\frac{K\Delta T_S}{r_V + r_L}\right]}_{\text{GAIN}} \Delta T_{IN}$$

Figure 3-3.1: Amplifier gain derivation.

configuration in electronics. The source and sink are shown as batteries, with the source $\Delta T_s/2$ above ground in temperature, and the sink $\Delta T_s/2$ below ground. All temperatures are referenced to ground, and appear as ΔT, meaning the distance from ground temperature. The total temperature drop from source to sink is ΔT_s.

The two effort controlled resistors, R_v and R_L, are analogous to a voltage divider, but instead divide temperature. The amplifier output, T_o, is the temperature of junction 0, between the two resistors. The output temperature can be determined if the resistance values of R_v and R_L are known, as follows:

$$\Delta T_{out} = \Delta T_s \left[\frac{R_L}{R_L + R_v} - \frac{1}{2} \right] \qquad (3\text{-}3.1)$$

The value of R_v or R_L will always be a positive, finite, non-zero number. From this expression it is clear the output can never be higher than the source temperature, nor lower than the sink. The ratio of the resistances divides the temperature between source and sink and produces the output.

If they are geometrically identical the variable thermal resistors, R_v and R_L, will have identical maximum and minimum resistance values, designated r_v and r_L respectively. The value of r_L, the minimum resistance of the variable resistors, can never be zero. There is a limit to how conductive any thermal conductor can be made, so r_L will always have some finite, non-zero value. Conversely,

materials have finite thermal resistivity. There are no perfect insulators, and r_v, the maximum thermal resistance, will never reach infinity, but instead will have a finite value.

To quantify amplifier gain a specific expression for the linear thermal resistance changes must be assured. R_v and R_L were characterized by the following inverse relations:

$$R_v = \frac{r_v + r_L}{2} - k\,\Delta T_{in} \qquad (3\text{-}3.2)$$

where, $\Delta T_{in} = [T_1 - T_2]$

$$R_L = \frac{r_v + r_L}{2} + k\,\Delta T_{in} \qquad (3\text{-}3.3)$$

Both have a fixed resistance that changes with a constant increment with input temperature.

The linearized constituitive relations of R_v and R_L entail that, with no inputs, each variable resistor will assume a value mid-way between minimum and maximum resistance value. This is <u>not</u> a necessary condition for a resistor used in an amplifier. By assuming a zero-input, mid-point resistance value the derivation of a gain expression is simplified. In the actual experimental amplifier the resistors used did not conform to this assumption. The two resistors do, however, have to assume equal values, for no input, if ground is mid-way between source and sink temperature. Otherwise a zero input would result in a non-zero output. The amplifier characteristics, e.g. gain, should remain constant irrespective of whether out-

put is above or below ground. This output symmetry around the ground point is assured if the resistor range is symmetric about the zero-output resistance value. The zero output resistance value is:

$$r_o = r_L + \frac{r_v - r_L}{2} = R_v = R_L \qquad (3\text{-}3.4)$$

and is the value assumed by R_v and R_L for zero input. The $(r_v - r_L/2)$ term is half the resistance value between the minimum and maximum, which is then added to the minimum to get the mid-point value.

In the qualitative description of amplifier operation R_v and R_L were described as varying inversely for the same input. However, identical inputs of different sign should produce identical outputs of different sign. The amplifier of figure 3-3.1 will perform in this manner as if R_v and R_L change their resistance the same amount for each unit of temperature input, above or below ground. The gain will remain constant over the full range of operation if each unit of temperature input produces the same unit resistance change over the full range of resistor operation. This is not a necessary but a sufficient condition for a constant gain. Both resistors can be nonlinear and the gain remain constant over the full range of operation, if they compensate for one another. An amplifier of this type will be discussed in section 5. The assumption of unit resistance change simplifies a gain expression derivation.

Constant gain is most important for <u>open loop</u> amplifier performance. Closing the loop (i.e. feeding the output back to one of the in-

puts) diminishes the impact of a gain change significantly. In figure 2-4.2 the amplifier output was expressed as a function of gain, for the closed loop multiplier circuit shown, and as a function of the multiplier factor.

The constant k is the resistance change per unit of temperature input. The sign difference between the two resistor constituitive expressions causes the opposing resistance changes in R_v and R_L for a given input. Assuming the amplifier has no load the heat flow through the two resistors must equal the flow through one, since they are in series, or:

$$\frac{\Delta T_s}{R_v + R_L} = \frac{\Delta T_{out} + \Delta T_s/2}{R_L} \qquad (3\text{-}3.5)$$

The gain will multiply the input temperature and yield the output in terms of the input. Thus an expression for ΔT_{out} is desired. Rearranging yields:

$$\Delta T_{out} = \left[\frac{R_L \Delta T_s}{R_v + R_L} - \frac{\Delta T_s}{2} \right] \qquad (3\text{-}3.6)$$

Now substituting the previous expressions for R_v and R_L:

$$\Delta T_{out} = \underbrace{\left[\frac{k \Delta T_s}{r_v + r_L} \right]}_{\text{Gain}} \Delta T_{in} = A \Delta T_{in} \qquad (3\text{-}3.7)$$

which is the desired relation. The gain is expressed in time invariant circuit parameters, which are also independent of the input or

output values. In the next section the individual parameters composing the gain expression will be examined in detail.

Section 3-4: Gain parameters.

The gain of a two, effort-controlled variable-resistor thermal amplifier was derived to be $\frac{k\Delta T_s}{r_v + r_L}$ with the assumptions of the preceeding section. The ideal amplifier has an infinite or very large gain. The gain expression will be examined to understand how each term relates to the circuit of the amplifier, and how they might be used to maximize the gain.

The constant k is straightforward. A larger k means more resistance change for a given temperature input, and thus a greater junction '0' (fig. 3-3.1) temperature change, which is the output. Since the gain is the ratio of output to input, it is consistent to find k in the numerator; a larger k means a higher gain.

The total temperature difference between source and sink, ΔT_s, belongs in the numerator. The variable resistors act like a temperature divider, the output is the ratio of resistances multiplied by the temperature difference, specifically,

$$\Delta T_{out} = \Delta T_s \left[\frac{R_L}{R_L + R_v} - \frac{1}{2} \right] \qquad (3\text{-}4.1)$$

A larger ΔT_s results in a larger output and higher gain.

The most subtle terms in the gain expression are r_v and r_L. The sum of the minimum and maximum resistor values appear in the denominator for non-obvious reasons. The total resistance of R_v and R_L is always a constant, and equal to the sum of r_v and r_L, or:

$$R_{total} = R_v + R_L = r_v + r_L \qquad (3\text{-}4.2)$$

If the total temperature difference, ΔT_s, remains fixed, any increase in r_v or r_L will diminish the heat flux through R_v and R_L. The temperature difference across a thermal resistance is directly proportional to the heat flux through it. The highest gain amplifier will produce the most junction temperature change for a fixed resistor value change (k, the resistance change per unit of temperature input, has remained fixed). The amount of junction temperature change for a given resistance change is directly proportional to the heat flux. Thus diminishing the heat flux decreases the junction temperature change and diminishes the gain. Consequently both r_v and r_L appear in the denominator.

This, perhaps unforseen, result puts the amplifier designer in a decision position. The denominator of the gain expression contains both the minimum and maximum thermal resistance of the variable resistors. The amplifier power output will be greatest when r_L has the smallest value, since r_L is the smallest resistance possible between the output (or load) and the power source. Reducing r_L also increases gain. Both these factors guarantee r_L will be made as small as practically possible. Once r_L has been established by technological considerations, r_v, the maximum resistance value, has to be chosen. The r_v value <u>can</u> usually be chosen since it is far easier

to increase thermal resistance than decrease it. For maximum gain r_v should be made as small as possible. Decreasing r_v has the unfortunate consequence of decreasing amplifier range. To understand qualitatively how r_v affects range consider the case where r_v is made almost as small as r_L. This would be the maximum gain situation, but the output would hardly change regardless of input, since maximum and minimum resistance of the variable resistors are almost equal. In other words, they have become essentially fixed resistors, and the term range is meaningless. On the other hand, if r_v is made very large, the amplified output can move over a range slightly less than ΔT_s. But the gain is substantially reduced because each degree of input temperature affects the ratio of R_v to R_L much less, which means less temperature change at the output. The choice of r_v is thus the pivotal decision.

A function relating gain and range to r_v and r_L is necessary. The maximum output occurs in response to an input that totally saturates the amplifier, and drives the two variable resistors to their minimum and maximum values. Analytically this means

$$k\ \Delta T_{in(sat)} = \frac{r_v - r_L}{2}\ , \qquad (3\text{-}4.3)$$

or $k\ \Delta T_{in}$ assumes a value that makes $R_v = r_L$ and $R_L = r_v$. Putting this value of $k\Delta T_{in}$ into the gain expression (eq. 3-3.7) gives:

$$\Delta T_{out} = \left[\frac{r_v - r_L}{2(r_v + r_L)}\right] \Delta T_s \qquad (3\text{-}4.4)$$

The maximum output of the amplifier is less than or equal to $\pm \frac{1}{2} \Delta T_s$. The output can never exceed the effort value of the source. The ratio of actual output to theoretically possible output can now be expressed.

$$\frac{\Delta T_{out}}{\frac{1}{2} \Delta T_s} = \frac{r_v - r_L}{r_v + r_L} \tag{3-4.5}$$

It is most convenient to have the ratio of actual to possible output expressed in terms of the ratio of r_v to r_L. or:

$$\frac{T_{out}}{\frac{1}{2} \Delta T_s} = \frac{\frac{r_v}{r_L} - 1}{\frac{r_v}{r_L} + 1} = \text{Fraction Possible Range} \tag{3-4.6}$$

This function is plotted in figure 3-4.1 as the curve labelled range, as a function of the ratio r_v/r_L.

The second curve shown in figure 3-4.1 is the gain function. This is the fraction of the theoretical maximum gain plotted as a function of r_v/r_L. The expression for gain is:

$$\text{Gain} = \frac{k \ \Delta T_s}{r_v + r_L} \tag{3-4.7}$$

as shown previously. The maximum gain amplifier, in theory has $r_v = r_L$. The ratio of actual to maximum gain is expressed by the relation:

$$\text{Fraction possible gain} = \frac{\frac{k \ \Delta T}{r_v + r_L}}{\frac{k \ \Delta T}{2r_L}} = \frac{2r_L}{r_v + r_L} \tag{3-4.8}$$

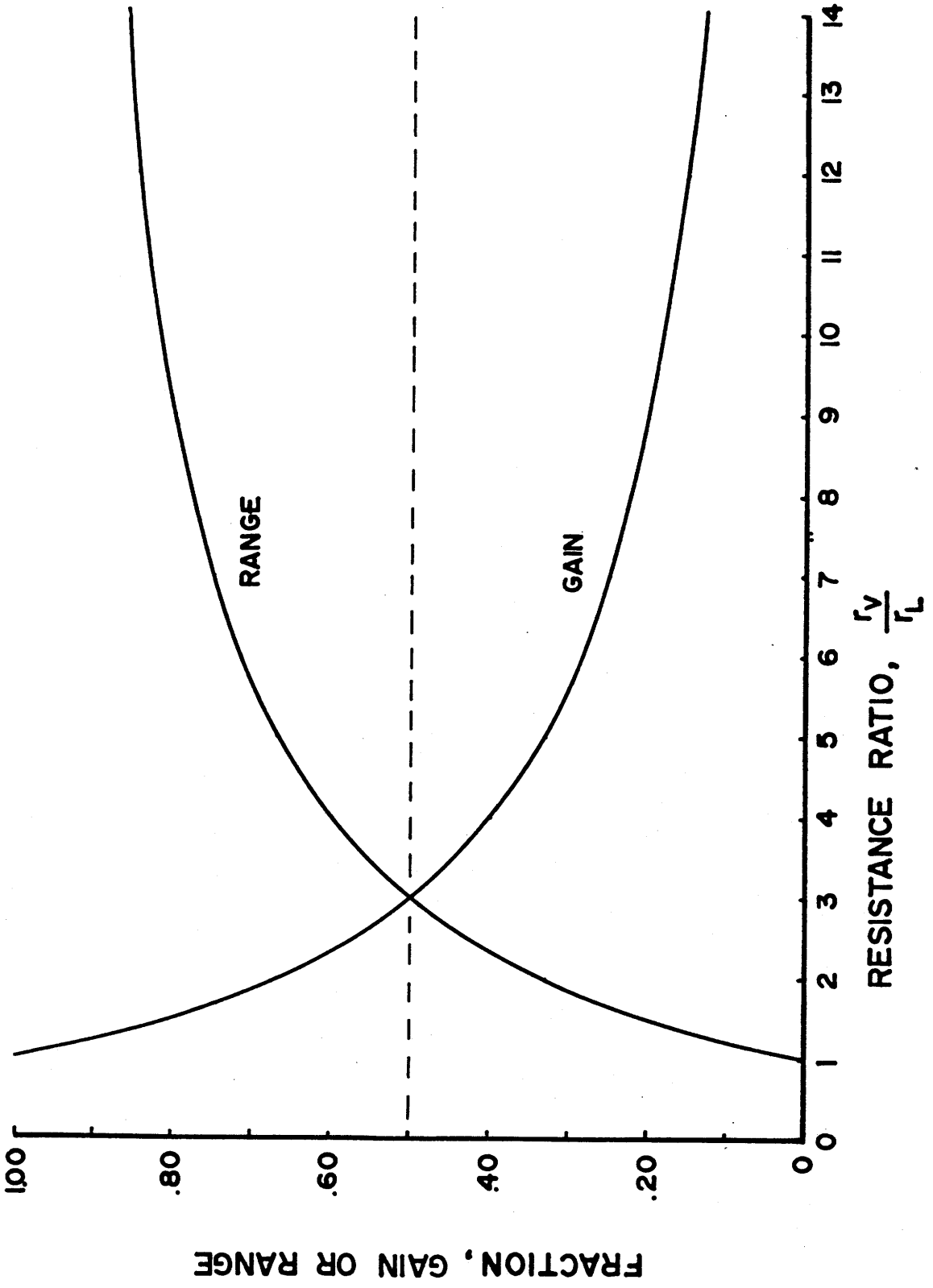

Figure 3-4.1: Fraction of gain and range as a function of resistance ratio.

Rewriting this function with r_v/r_L as the independent variable, yields:

$$\text{Fraction possible gain} = \frac{2}{\frac{r_v}{r_L} + 1} \qquad (3\text{-}4.9)$$

This relation is plotted in figure 3-4.1 and labeled gain.

Two curves of Fig. 3-4.1 illustrate completely the tradeoff of gain for range. As the output range increases the gain decreases and conversely more gain means less range. The curves are exactly symmetric inverses, a line through the .5 point on the ordinate acts as the axis of symmetry. The two functions are highly non-linear, and half the possible range and gain can be achieved with r_v equal to 3 r_L. Depending on the application gain or range will be the most important feature. Once technological constraints have fixed r_L, the amplifiers ultimate range and gain are fixed with the selection of r_v.

All this is <u>a priori</u> to any statement about actual physical construction of the resistors. A few basic assumptions about circuit and resistor behavior have been made, and conclusions about ultimate amplifier performance have been drawn.

The foregoing analysis has reduced the problem of designing a temperature amplifier to designing a temperature modulated thermal resistor. Temperature modulated thermal resistors exist, making an

operational amplifier possible. An effort controlled resistor that can be characterized by the linearized relation:

$$R = \frac{r_v + r_L}{2} - k\Delta T_{in} \qquad (3\text{-}4.10)$$

and can be made into an amplifier. This very general relation is applicable to many complicated, nonlinear resistors over a small range of operation and allows an expression for the amplifier gain to be derived. The gain expression has illustrated the impact of various resistor parameters on ultimate amplifier performance. Effort controlled resistors must now be examined for compatibility with the assumptions made.

Section 3-5: Temperature modulated resistors.

Part 3-5A: General description of thermal resistors.

The problem of building the thermal amplifier was reduced, in the previous section, the problem of building a linear temperature modulated resistor (ECR). There are innumerable temperature modulated resistors, and to consider all would be impossible. Thermal resistances can be classed in several broad categories, which will be examined.

The theory developed thus far is completely general and any resistor with an appropriate constituitive relationship would suffice. A general, but not exhaustive, classification of thermal resistances will include the following nonexclusive categories. First, mechanical resistors, which includes all devices where a temperature causes a mechanical element movement that alters thermal conductivity. An example might employ a bi-metallic strip. These devices generally control heat flow by conduction or contact resistance. Second, there are fluid resistors, the category in which heat exchangers fall. This includes any device that uses a liquid for heat transport purposes, usually controlling heat flux by conduction or convection. Third, there are heat pipes, those devices using an evaporating and condensing gas for their heat transport; actually a special case of fluid resistor. Finally there are radiation resistors, using materials that become more or less opaque, controlling the flow of infrared radiation, and therefore heat.

Planar fluid conduction resistors were chosen for their numerous advantages. The thermal conductivity of fluids covers several orders of magnitude, so resistor properties could be tailored over as wide a range. Moving fluids don't wear like mechanical parts. Because fluids assume the shape of their container they impose few geometry constraints on the amplifier design. Finally, conduction heat transfer is well understood for simple geometries, and amplifier performance can be predicted.

The geometry of fluid conduction resistors is an infinitely wide category; planar resistors were chosen from a practical viewpoint to facilitate construction. Limiting the choice to conduction fluid resistors of a planar construction is not restrictive. For comparison, three of the many possible planar, fluid, conduction or convection temperature modulated resistors will be briefly illustrated.

Part 3-5B: Planar thermal resistors.

Three types of planar, fluid-based, thermal resistors are shown in figures 3-5.1, 3-5.2, and 3-5.3. Each device is associated with sensors: the resistor varies its thermal resistance in response to the temperatures of the sensors. In each case, the sensor contains a volume of fluid which responds to a temperature change by expanding. This expansion is then "piped" to the resistor where it changes the thermal resistance. Hence, the thermal resistance is controlled by the effort variable (temperature) of the sensor: an effort controlled resistor or ECR. Note that expansion due to temperature change in the sensor can be either thermal expansion or the vaporization of the fluid contained.

Each type of ECR changes its thermal resistance in a different manner. In the film ECR, figure 3-5.1 the positive sensor's expansion drives a liquid film between two conducting plates; since liquids conduct heat better than gases, the thermal resistance of the modulator is reduced as liquid rises between the plates. Using air and water, a ten-to-one change in thermal resistance is typical. In the pneumatic ECR, figure 3-5.2, thin diaphragms are deformed by the expansion of one sensor's fluid, changing the gap between the diaphragms and outer plates. Except for very large gaps the thermal resistance is related to the gap thickness, and heat is transferred by conduction.

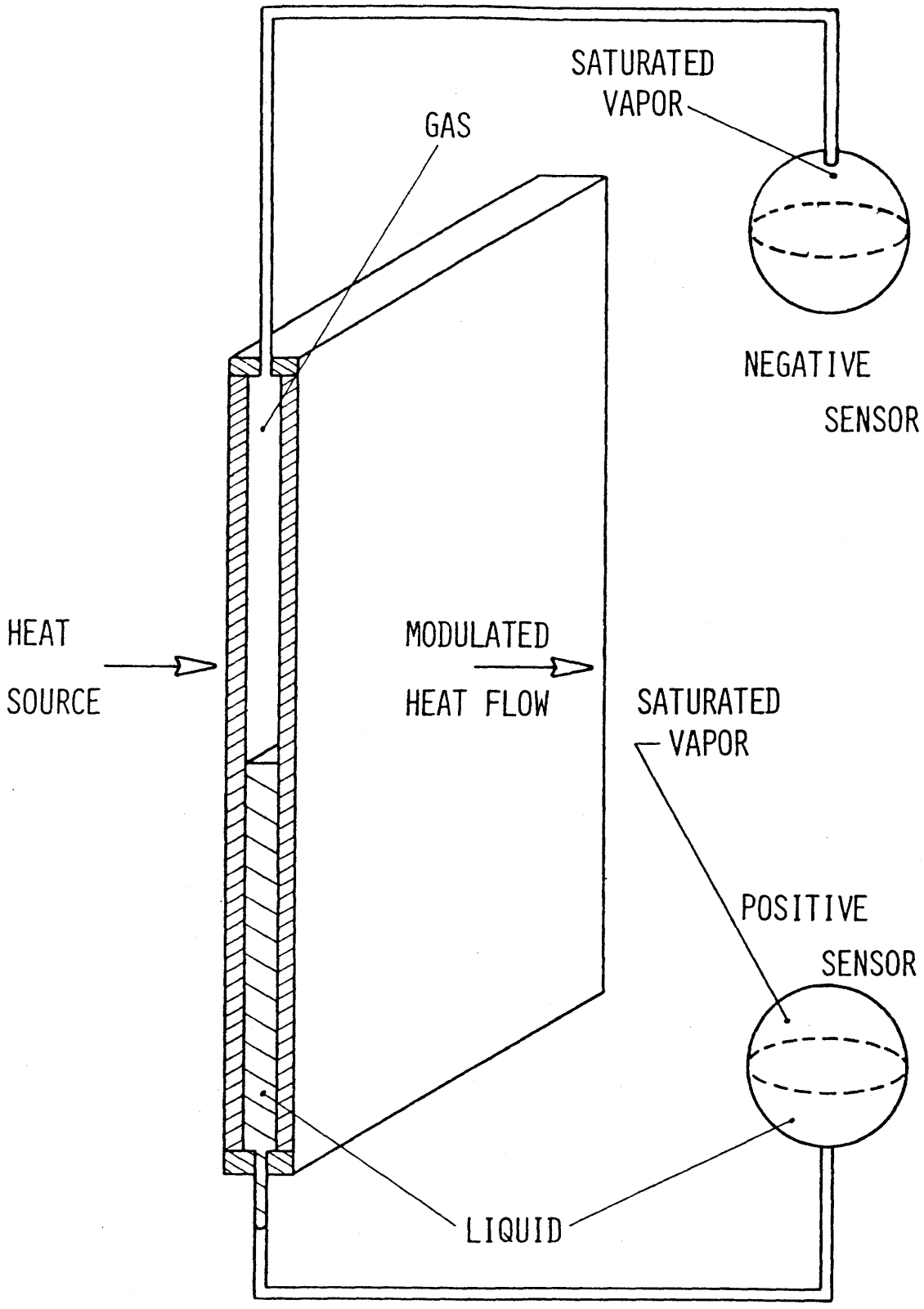

Figure 3-5.1: Film ECR.

Note that the pneumatic amplifier has moving parts (of the flexing variety), and might also be classified in the mechanical category. The convection ECR, figure 3-4.3 using the modulated thermosyphon of Buckley, (Ref. 7) is more complicated because its thermal resistance is only indirectly modified by expansion of sensor fluid. It consists of two enclosed layers of liquid separated by a thick slab of insulation. The vertical-oriented layers are connected top and bottom by ducting to form an enclosed circulation loop. When one layer is heated, buoyancy forces cause the other layer to be heated by natural convection. If both layers are thin, their heat transfer is by conduction, but their bulk motion results from convection. Expansion of the negative sensor fluid is made to block this circulation loop, expansion of the positive sensor fluid opens the loop. One method is a "bubble trap": negative sensor fluid expansion injects a small air bubble in the trap preventing fluid circulation, while expansion in the positive sensor reduces the bubble's size.

In all these ECR's, a temperature increase at the positive sensor reduces thermal resistance through the modulator while an increase in temperature at the negative sensor has the opposite effect. Thus they operate differentially: the temperature difference between the positive and negative sensors changes the device's resistance. Other variations, such as single-input ECR's can be made, but do not easily combine into a thermal operational amplifier.

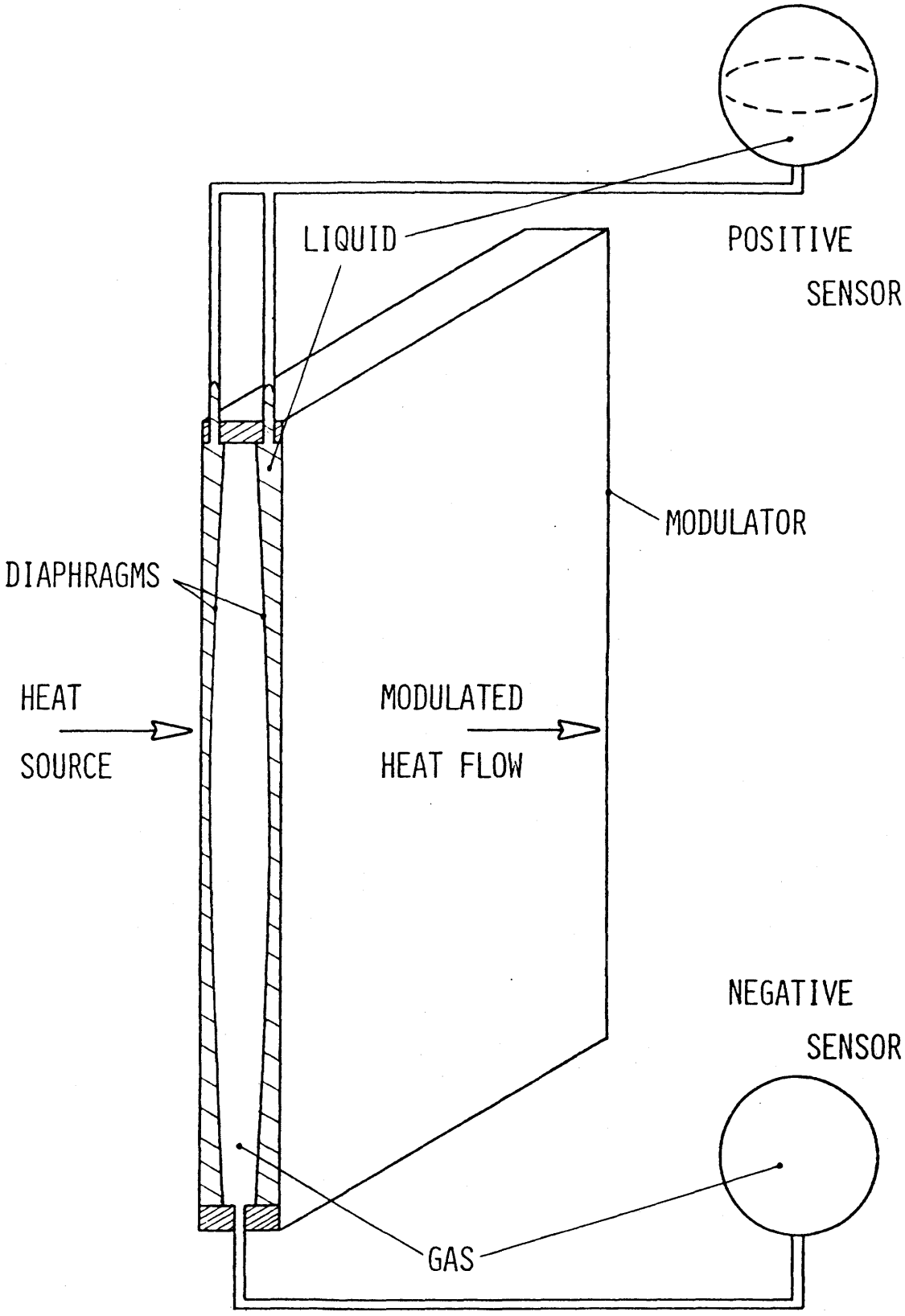

Figure 3-5.2: Pneumatic ECR.

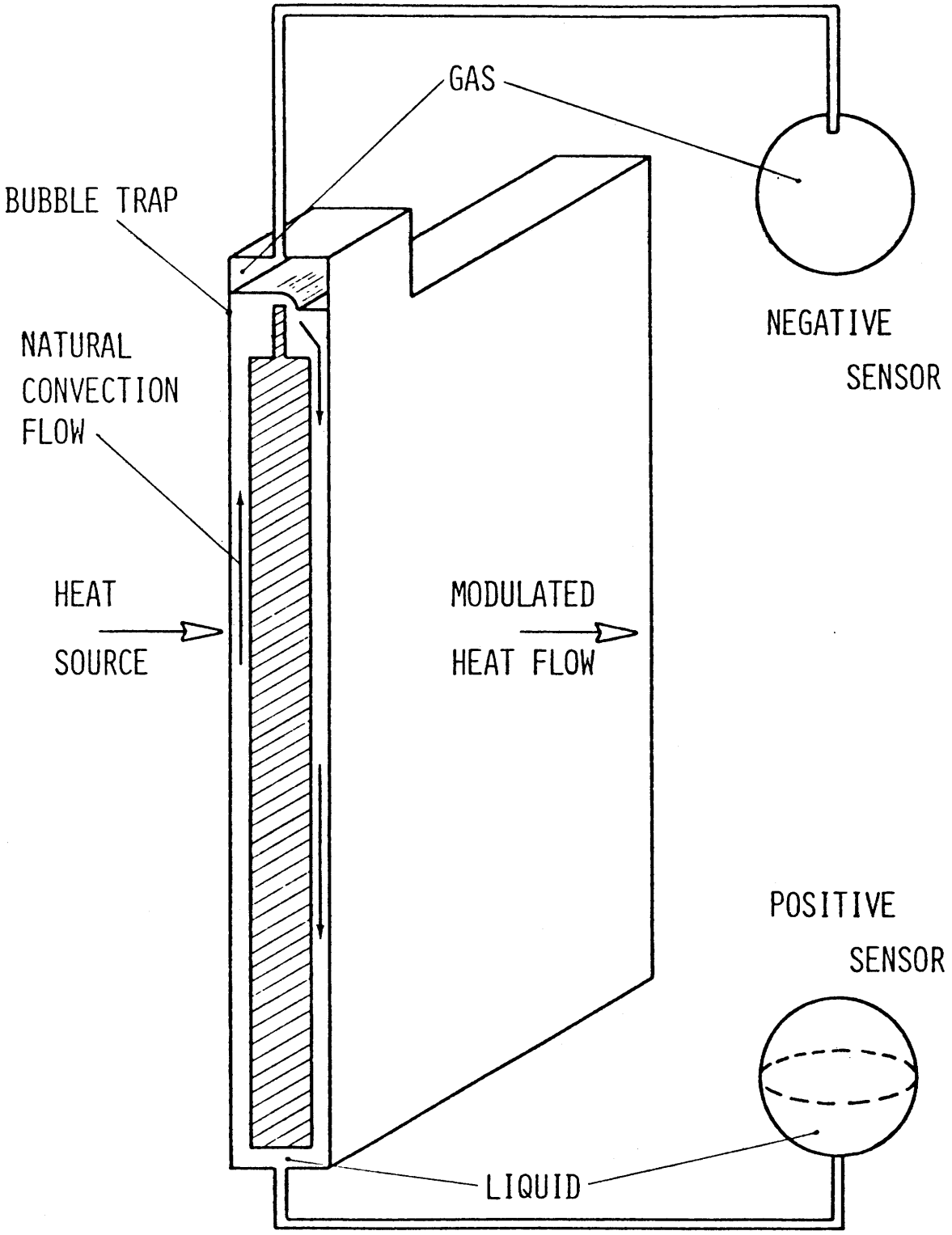

Figure 3-5.3: Convection ECR.

Part 3-5C: The film resistor.

All the ECR's described before are non-linear in resistance change with input temperature, contrary to the assumption of the gain derivation. This does not preclude their use in an amplifier. The non-linearity of the planar film resistor is of a special character. With the identical circuit used for the gain derivation two special non-linear film resistors can be combined to produce a linear amplifier. In addition, the film resistor offers the most flexibility in tailoring the minimum and maximum resistance, r_L and r_v respectively, to particular values. To illustrate how these advantages are inherent to the film ECR, its mechanics will be examined.

A temperature change of the sensor is designed to give a proportional change to the height of the liquid "film" inside the film resistor. The sensor is filled with a liquid which vaporizes, causing a pressure increase in response to temperature increase. The vapor is always saturated because it is in contact with its liquid. The pressure and temperature inside the sensor are no longer independent: they are related by the saturated vapor curve of the phase diagram for the fluid. Most saturated vapor curves are well behaved continuous functions of temperature in non-critical regions. As illustrated by a curve for saturated Freon-113 in figure 3-5.4. Thus, for small temperature ranges, a linear approximation of the temperature-pressure relationship will be adequate.

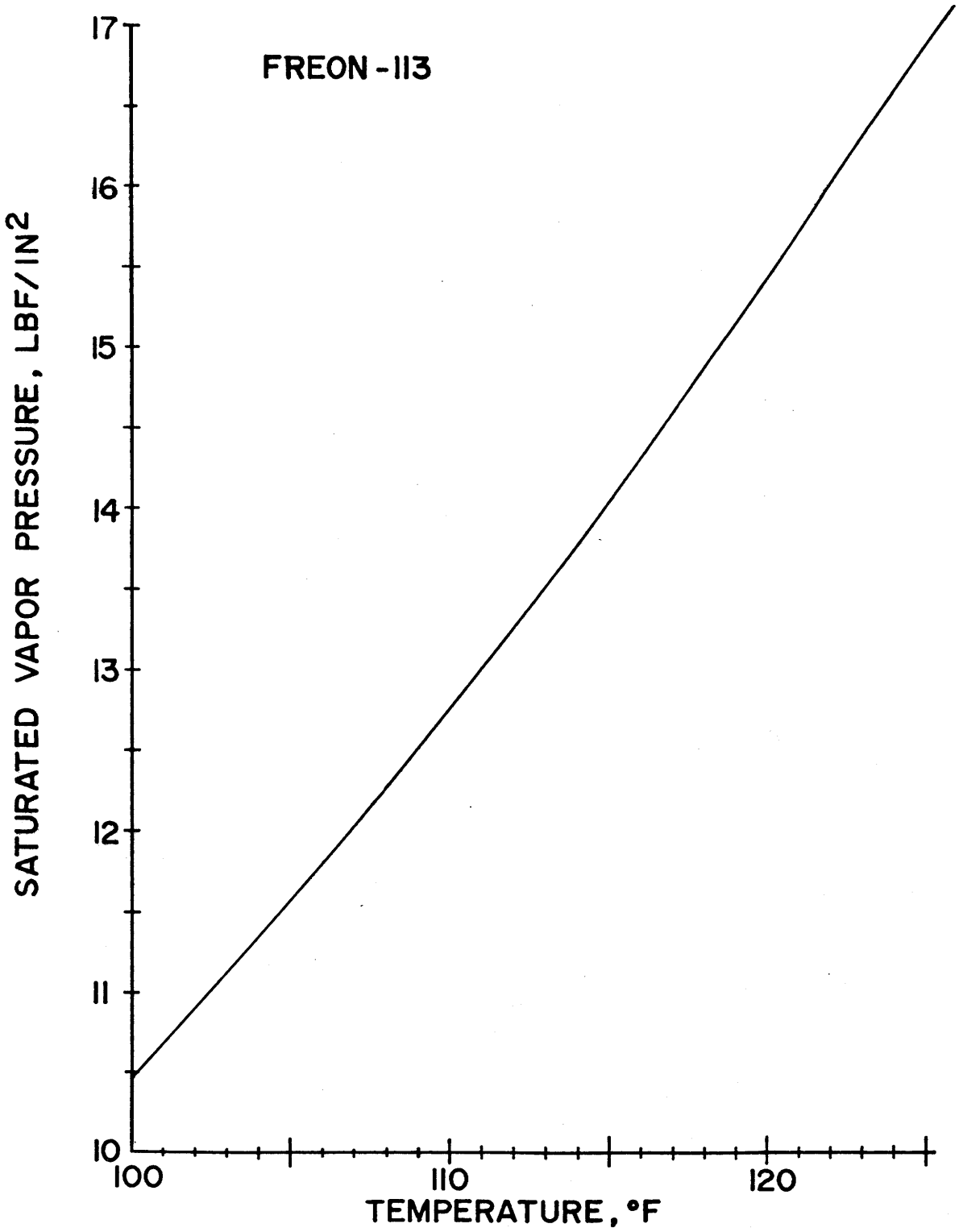

Figure 3-5.4: Saturated vapor-pressure curve for Freon-113.

Part 3-5D: Geometry of the film resistor.

The geometry of a film ECR determines most of its performance characteristics. Figure 3-5.1 was a schematic representation of a film resistor, not an illustration of final configuration. The resistor geometry must cause the resistor performance to conform to previous assumptions.

If the amplifier output is going to change symmetrically about some ground value the film resistors must change their resistance about some equilibrium value which corresponds to the ground value of the output. With no inputs the resistors must assume this equilibrium value, which should be mid-way between the maximum and minimum resistance.

To satisfy the preceeding constraint the resistor geometry of figure 3-5.5 was chosen for the amplifier. The sensors are not shown, but the effect of a positive pressure input is indicated. The thermal resistor is the film section. Conducting fluid for the resistor is stored in the reservoir, and the insulating fluid is assumed a gas. The reservoir and film section form the two legs of a U-shaped manometer, which is filled half full of conducting fluid. With no pressure inputs the fluid level in the film section and reservoir are equal. This satisfies the requirements that the resistor assume and equilibrium value between r_v and r_L, since the fluid exactly half fills the thermal resistor.

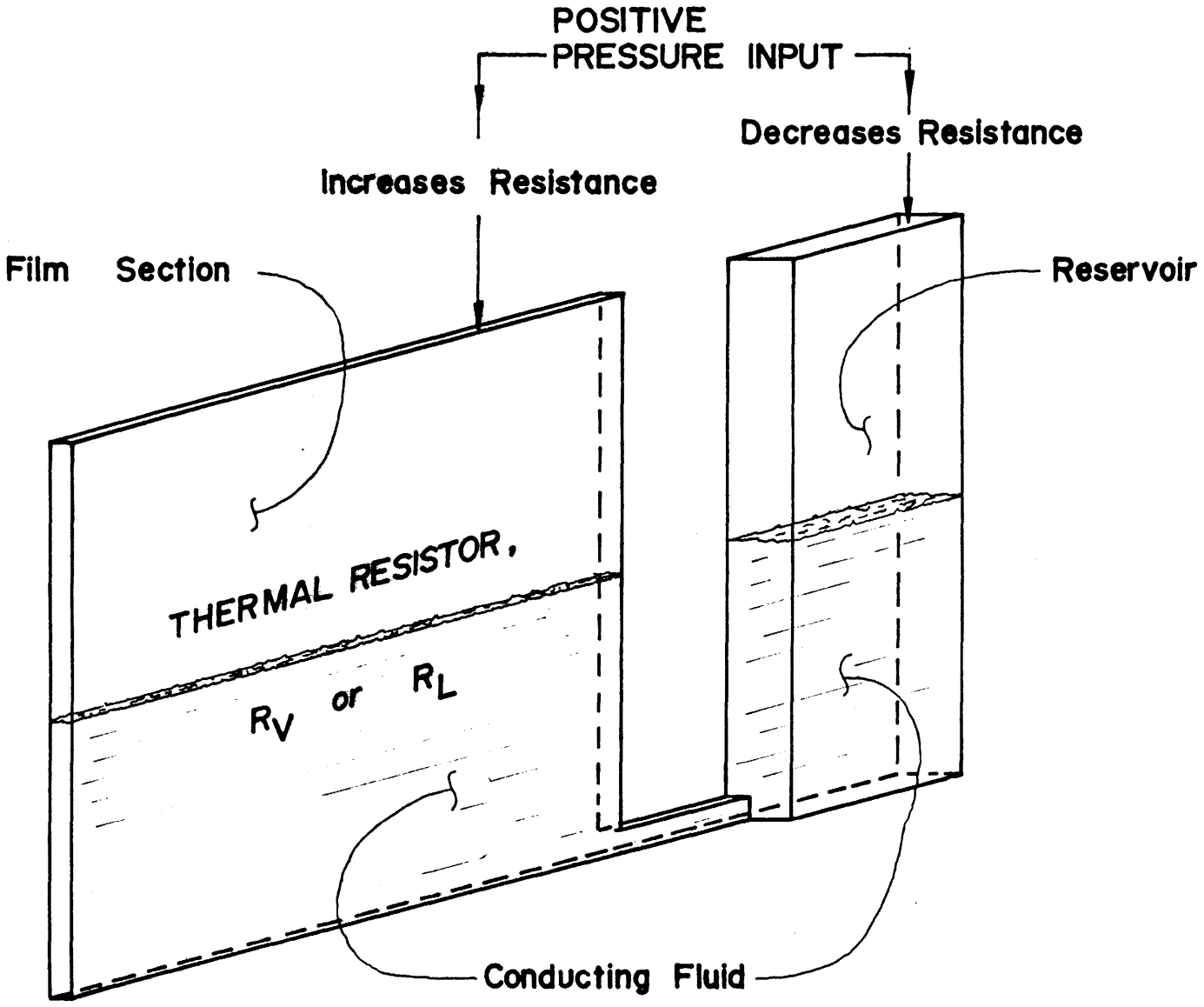
POSITIVE
PRESSURE INPUT
Decreases Resistance
Increases Resistance
Film Section
Reservoir
THERMAL RESISTOR,
R_V or R_L
Conducting Fluid

A pressure input to the reservoir or film section changes the conductivity of the film section. The pressure will cause the fluid level in both film section and reservoir, to change inversely (i.e. one will go down and the other up) until the level difference creates a hydraulic head equal to the pressure difference across the manometer. This effect is illustrated in figure 3-5.6, where the reservoir is shown with the same cross-sectional area as the film section, so the fluid levels deflect symmetrically about the center line. The hydraulic head is equal to the pressure difference, or:

$$P = \rho g \, 2\Delta h \qquad (3\text{-}5.1)$$

The pressure difference across the manometer is generated by the sensors. If the sensors are at the same temperature, the pressures are equal. Insulating gas fills the space above the conducting fluid in the film section and reservoir. A fluid that vaporizes is used in the sensors to generate a pressure in response to a temperature. The vaporizing and insulating fluids can be selected independently if they are physically separated. This is accomplished in the sensor by a completely flexible, impermeable, diaphragm. The pressure generated by the vaporizing fluid on one side of the diaphragm is conveyed through the diaphragm undiminished. The insulating fluid then has the same pressure as the vaporizing fluid, this pressure is conveyed by the insulating fluid to the manometer. The sensor diaphragm also prevents vapor pumping of the sensor fluid to the film section. The temperature of the film section of reservoir could

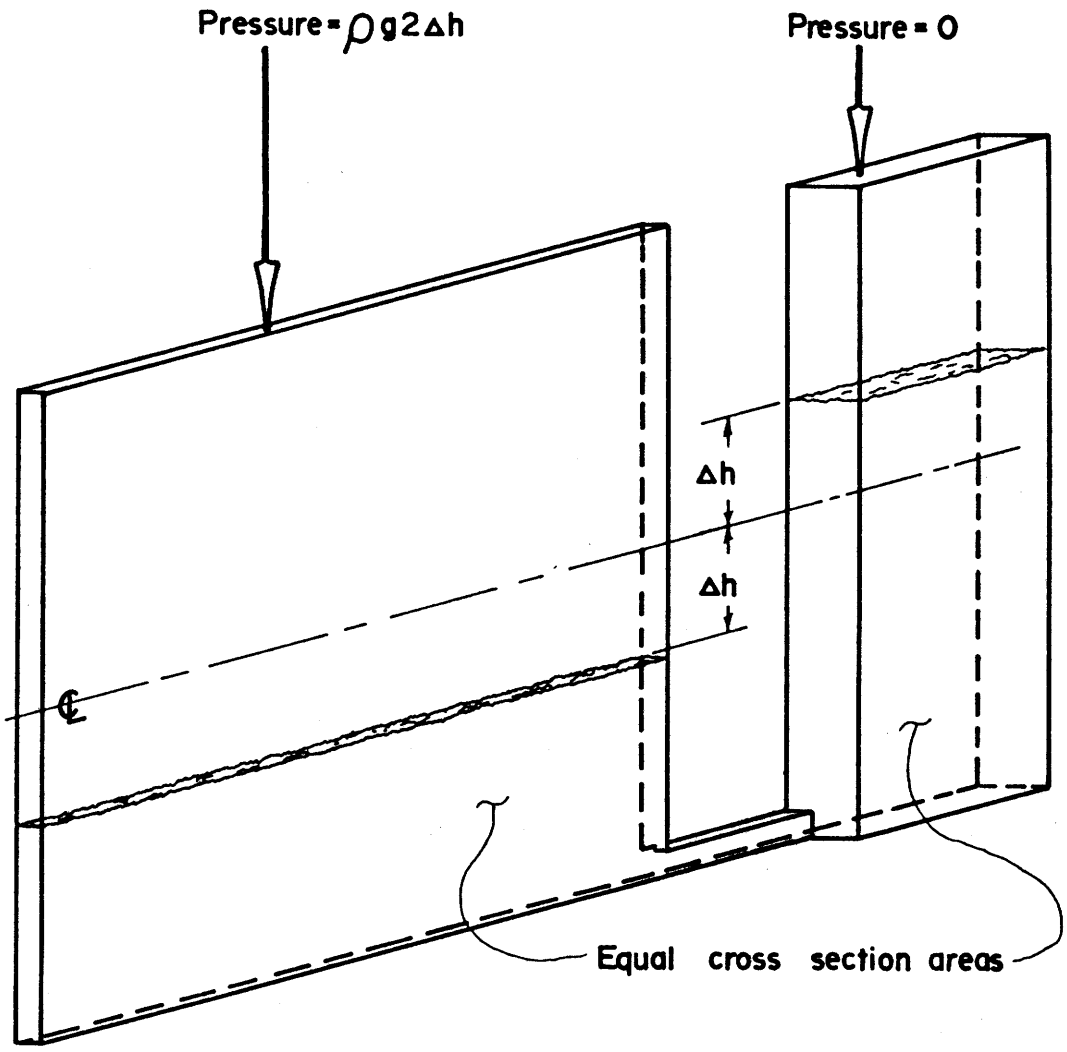

Figure 3-5.6: Conducting fluid deflection in response to pressure difference across manometer.

be lower than the condensation temperature of the vaporizing fluid at the system pressure. If the sensor fluid vapor is allowed to mix with the insulating fluid, or is used as the insulating gas, it could condense in the resistor. This phenomena is called vapor pumping. Condensation in the resistor would make the resistor performance immediately indeterminate. The condensate would form an alternate heat path in the film section, or it could unbalance the manometer if it formed in the reservoir or film section.

The film ECR responds to a pressure difference caused by a temperature difference between sensors. A large temperature difference could saturate the resistor by driving all the fluid out of the film section or reservoir. For small temperature differences the conducting fluid will balance the sensor pressure difference. This difference will cause a conducting fluid height above or below equilibrium. This change in fluid height will change the resistance of the film section.

The film section thermal resistance will be a single-valued function of the conducting fluid height, which will be a single-valued function of the pressure difference between sensors, which will be a single-valued function of the temperature difference. Therefore, the resistance of the film ECR will be a single-valued function of the input temperature difference. The saturated vapor pressure curve of the sensor fluid is an approximately linear function of temperature. The conducting fluid level difference in the manometer is a linear function of the pressure difference across the two legs. The conduct-

ing fluid height will thus be a linear function of the input temperature differences, over a small temperature range.

The density of the conducting fluid is an important resistor parameter. It determines the amount of thermal resistance change per unit of pressure difference. The effect of density can be minimized, or eliminated completely, by tilting the amplifier. The tilt will reduce the net hydraulic head generated by the manometer, but at shallow angles surface tension can become dominant, producing undesirable characteristics. The remainder of this thesis will assume the amplifier vertical, and therefore at lowest gain.

Part 3-5E: Analysis of the Film ECR.

The film section of an ECR can be thermally modeled as shown in figure 3-5.7.

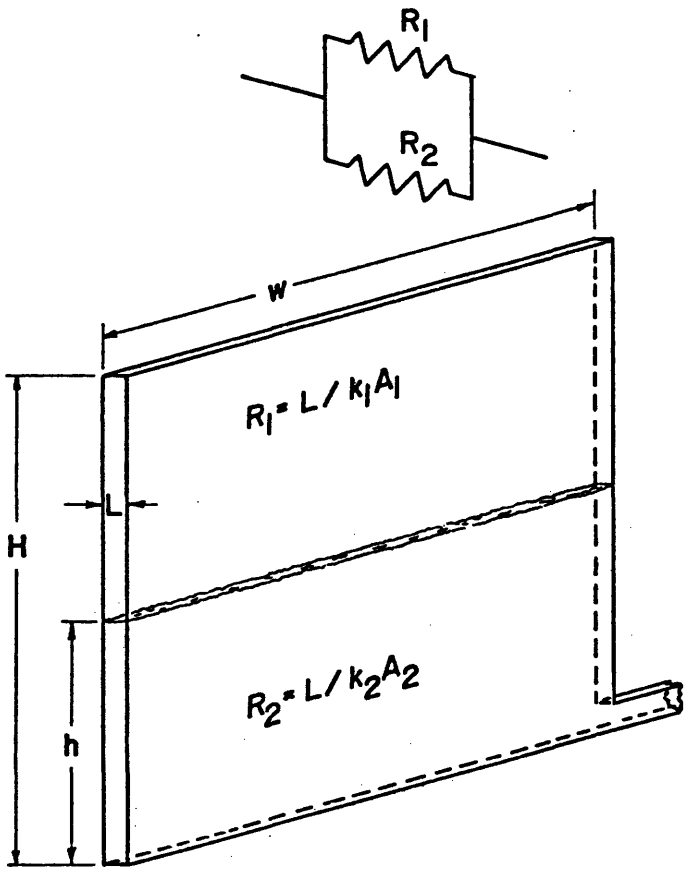

Figure 3-5.7: Parallel thermal resistors in the film ECR.

Assuming temperatures on both sides of the film section are uniform the section acts like two thermal resistances in parallel. The upper resistance, R_1, will be the nonconducting fluid, the lower resistance,

R_2, the conducting fluid. The net thermal resistance of the whole section will be the parallel product of R_1 and R_2, or $R_{net} = \frac{R_1 R_2}{R_1 + R_2}$. If all heat transfer in the section is by conduction the values of R_1 and R_2 can be expressed as follows:

$$R_1 = \frac{L}{K_1 A_1} \qquad (3\text{-}5.2)$$

$$R_2 = \frac{L}{K_2 A_2} \qquad (3\text{-}5.3)$$

L = film thickness

K_1 = conductivity of non-conducting fluid

K_2 = conductivity of conducting fluid

Parameters A_1 and A_2 are the film section areas in contact with the nonconducting and conducting fluid, respectively. The total of A_1 and A_2 will be the total area of the section. Since the conductivities of the fluids are fixed, as is the film thickness, R_1 and R_2 are made to vary by the areas A_1 and A_2. The contact areas are determined by the height of conducting fluid. If this height is designated h, the width of the section w, and the total section height H, then the formulas for R_1 and R_2 can be rewritten:

$$R_1 = \frac{L/w}{K_1[H - h]} \qquad (3\text{-}5.4)$$

$$R_2 = \frac{L/w}{K_2[h]} \qquad (3\text{-}5.5)$$

These two resistances change nonlinearly with input temperature. Conducting fluid height, h, changes linearly with input temperature, but h appears in the denominator of the resistance expressions, so the resistances are not linearly related to h.

The parallel combination of R_1 and R_2 is also a non-linear function of conducting fluid height. Substituting the expressions for R_1 and R_2 into the parallel resistance formula produces;

$$R_{net} = \frac{R_1 R_2}{R_1 + R_2} = \frac{L/w}{(K_2 - K_1)h + K_1 h} \qquad (3\text{-}5.6)$$

which still has the h term in the denominator. The non-linear character of the net resistance requires special attention when two resistors are combined to form an amplifier. The nonlinearity must cancel so the output temperature is a linear function of input temperature. The next section explains how this is accomplished.

To off set the disadvantage of non-linear resistance change the film ECR offers several advantages. Recall when the gain expression,

$$\Delta T_{out} = \frac{k\ \Delta T_s}{r_v + r_L}\ \Delta T_{in} \qquad (3.5\text{-}7)$$

was derived, three resistor parameters appeared in it. The first was k, of the amount the resistance changed per unit of input temperature. The second and third were the minimum and maximum resistor values, r_L and r_v. The most remarkable characteristic of the film ECR is these three quantities can be tailored almost independently of one another.

There are 3 fluids used in a film ECR. The conducting fluid, the nonconducting fluid, and the vaporization fluid used in the sensor. The parameters k, r_v and r_L depend directly on the properties of these three fluids, on a one to one basis, as shown in figure 3-5.8.

The parameter k depends only on the sensor fluid. The film section changes resistance in response to a pressure input, independent of how the pressure is generated. The amount of resistance change per unit of pressure is determined by the conductivities of the conducting and nonconducting fluid. But the amount of pressure change per degree of input is the slope of the sensor fluid saturated vapor pressure curve. Thus, even with the conducting and nonconducting fluids specified, a desired k value can be achieved by selecting a sensor fluid with the appropriate saturated vapor curve, subject to the constraint of boiling point. A wide range of flurocarbon liquids, with well tabulated properties, can be mixed to get desired property combinations. The result is the ability to tailor the amount of resistance change per degree of temperature input.

The maximum resistor value, r_v, and the minimum, r_L, can be selected almost independently. The film ECR will have the maximum resistance value, r_v, when the whole film chamber is filled with nonconducting fluid, and has no conducting fluid. The resistor will have the value r_L when the film chamber is completely filled with conducting liquid. Thus r_v depends completely on the conductivity of the insulating fluid, and r_L on the conducting fluid. These two properties are com-

pletely independent. The only constraint on the two fluids is they have different densities. It would make no difference if the insulating fluid was heavier and in the bottom of the film section.

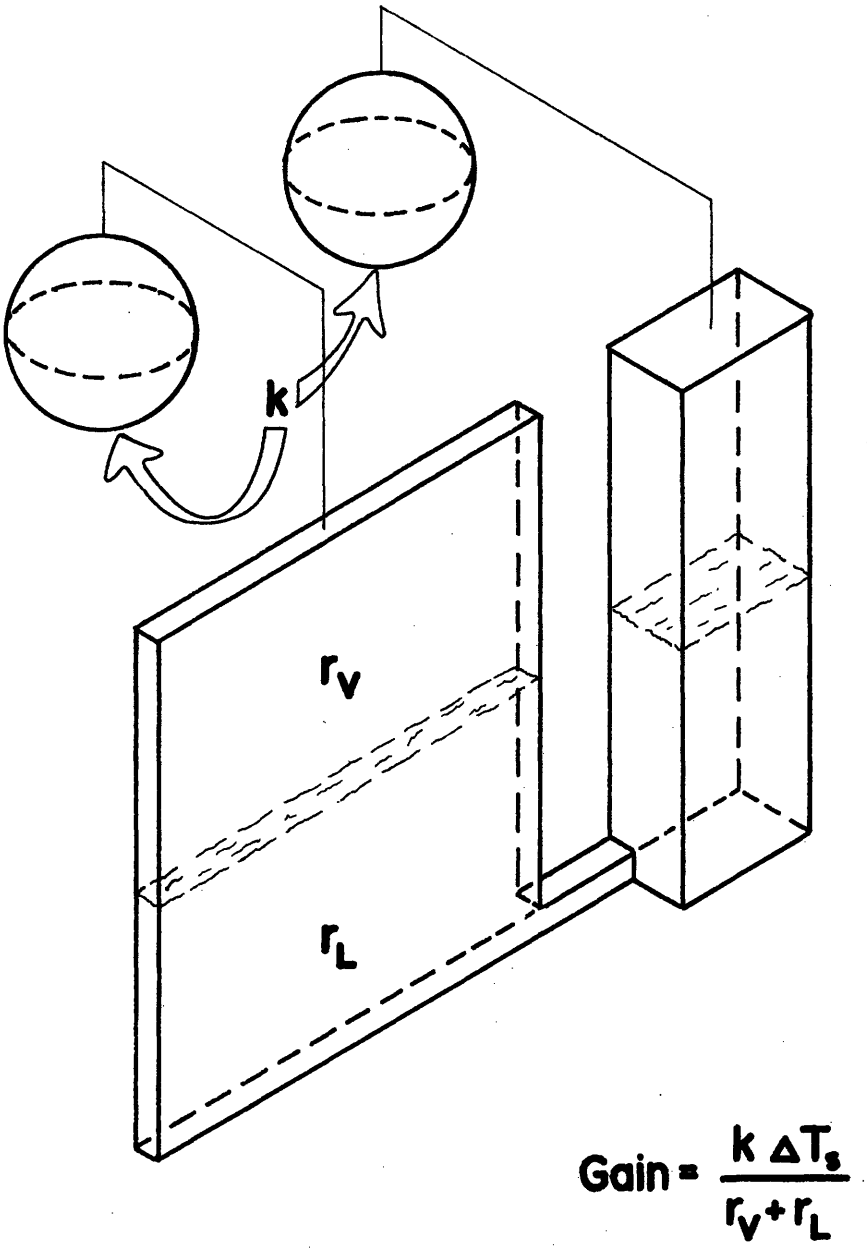

Figure 3-5.8: Correspondence of gain parameters to ECR fluid properties.

In the gain derivation, the dependence of gain and range on the ratio r_v/r_L was demonstrated. Within the limits of available fluid properties this ratio can be selected to produce the optimum amplifier for a given application.

There is one other constraint on the conducting and insulating fluids. Both fluids must have low vapor pressure within the amplifier operating temperature range. One film ECR will be in thermal contact with the temperature source, and one with the temperature sink. If either liquid in the film chamber has a significant vapor pressure there will be unwanted "feed-back" and vapor pumping to the sensor bulbs. The feedback would take the form of pressure signals from the film sections to the sensors, if a film section rose in temperature. If a conducting fluid generated enough pressure, it could cause the sensor fluid to condense completely, and thus decouple the sensor from the resistor.

If the sensor is cooler than the film section, vapor from the film section could condense in the control bulb. This is called "vapor pumping". Both problems are avoided if the fluids used in the film section have low vapor pressures. If the nonconducting fluid is a gas, the portion in the film section will expand as it is heated; however, the effect is usually small. The sensor can compensate for the gas heating by condensation of some vapor.

The film ECR was the logical choice for amplifier construction. It offered independence of all resistor parameters, allowing the gain

and range trade off to be the choice of the designer. The simplicity of the film ECR decreases the likelihood of failure. The sensor can be located far from the modulated film section, if desired, without affecting ECR performance. There is no theoretical limits on the size of a film ECR, the power it can gate, or the operating temperature range. These constraints are imposed by material mechanical properties. The next section will detail how two film ECR's are combined to produce an amplifier.

Section 3-6: Amplifier construction from two film ECR's.

Part 3.6A: Topology of the two film ECR amplifier.

The last section detailed the layout and characteristics of the film ECR. In this section the amplifier built from two such resistors will be detailed. Sections two and three of this chapter deal with the theory of the two resistor amplifier. To create the amplifier of this thesis two film resistors were connected in a "push-pull" configuration around a junction block.

The nonlinearity inherent in the film ECR must be compensated for at this stage to produce a linear amplifier input/output relationship. The two film ECR's and junction plate are shown in figure 3-6.1. For purposes of illustration each resistor is shown with two side walls. In the actual amplifier built and tested the interior wall of each resistor is eliminated, the junction block serving as both interior walls. The junction block is of a highly conductive material. There must not be temperature gradients across the junction block or the output will not be single-valued. The junction block extends above the two ECR's to form an output. Sensors can be attached to this output block to form a feedback loop. The hot source is placed against the outside wall of the ECR R_V. The cold sink is attached to the outside of the ECR R_L. The conductive material in the junction block does not extend to form the interior wall between reservoirs. This would result in needless heat leakage from the junction block to

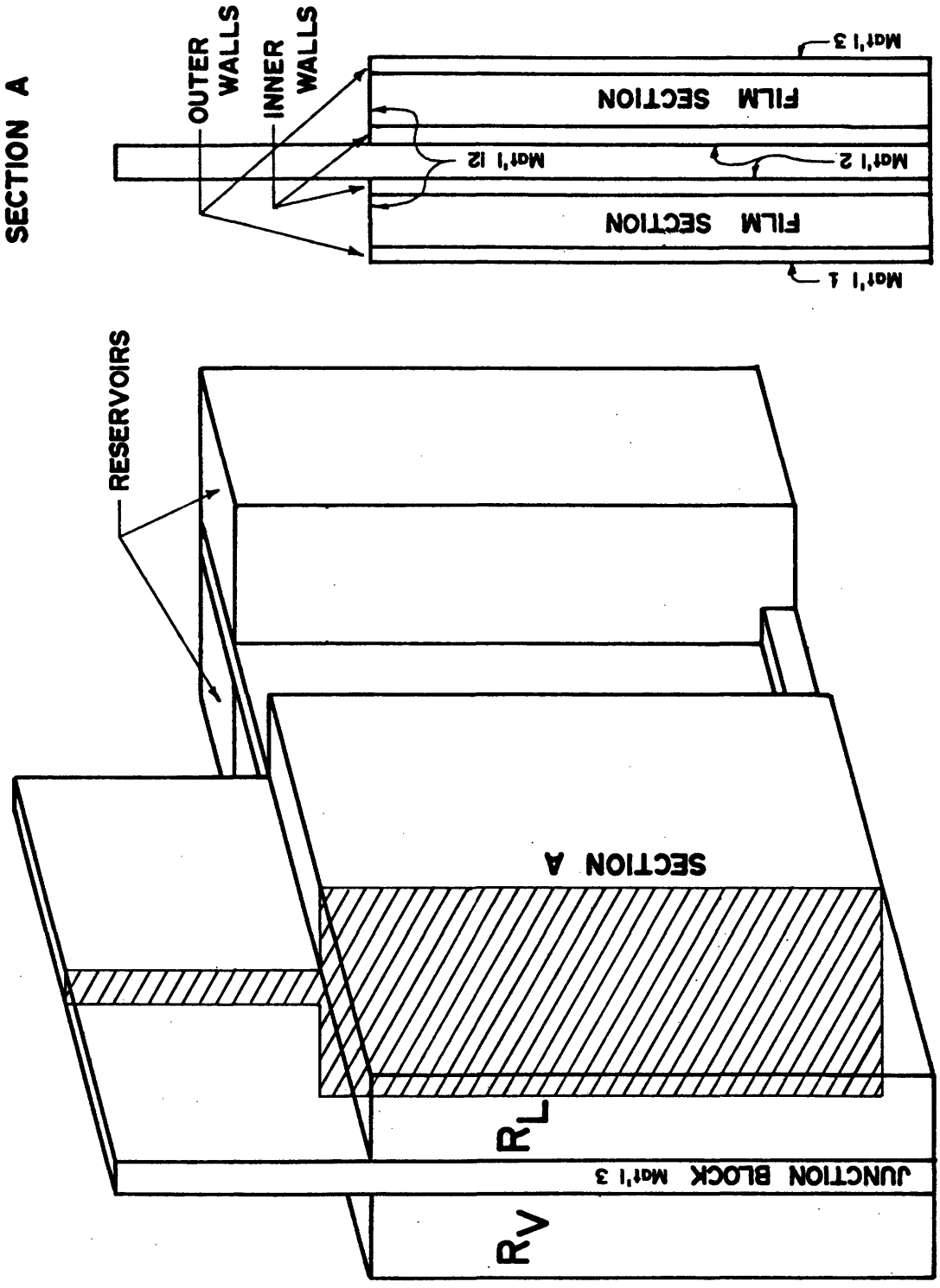

Figure 3-6.1: Amplifier resistor geometry.

the reservoirs. The reservoirs were placed as shown for practical construction considerations, and are separated by an insulating material with the same thickness as the junction block. By making the interior film section wall and the interior reservoir wall colinear, both film section and reservoir could be made from a single piece of continuous, vacuum-molded polycarbonate. This aids considerably in getting an air-tight seal around the film and reservoir chambers. Each film and reservoir chamber has a vent (not shown in figure 3-6.1) for attaching the pressure input from the sensors.

The sensor topology is diagrammed in figure 3-6.2. The conducting plate side is put in thermal communication with the input. The conducting plate should be highly conductive. to prevent temperature gradients; thus the sensor will respond to one input temperature The conductive plate could have a wick attached to keep the sensor liquid in thermal contact at all times. A thin diaphragm separates the sensor fluid from the nonconducting fluid. For this thesis the non-conducting fluid has been assumed a gas with negligible density, which fills the sensors and conveys the sensor pressure to the film and reservoir sections. The total sensor volume is kept limited, to prevent either sensor from blowing all the conducting fluid out of the film section. The recombination of sensor vapor with its liquid, in response to a lower temperature input, is a potential time lag. The aspect ratio of the sensor (the ratio of area to thickness) should be maximized to avoid this problem.

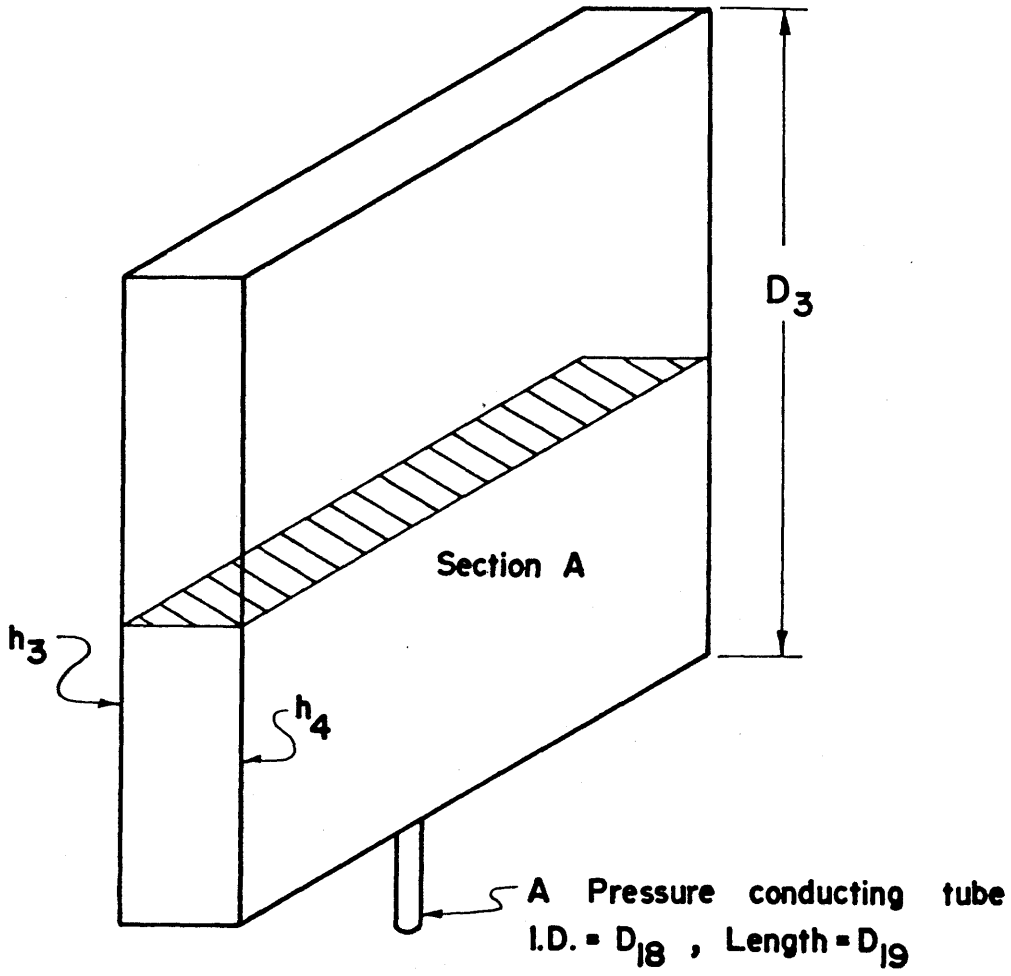

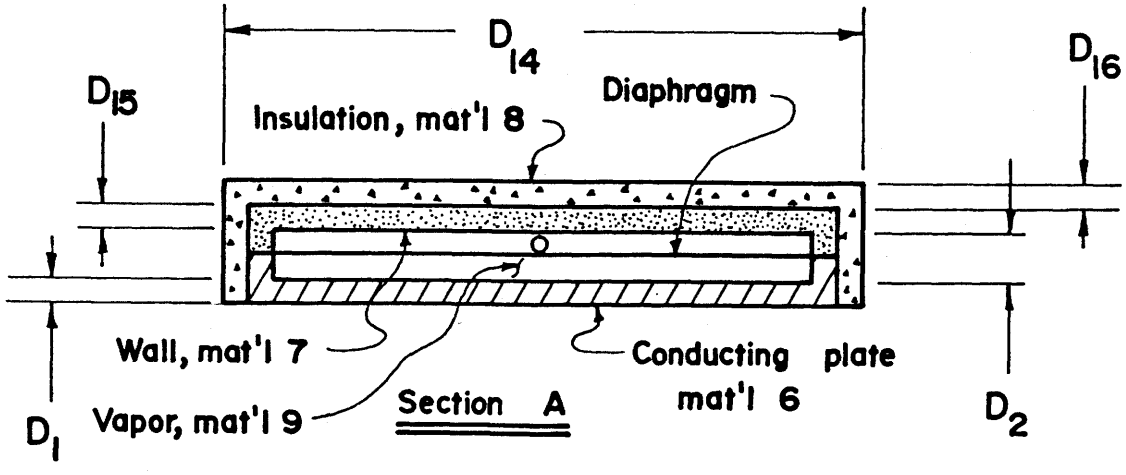

Figure 3-6.2: Sensor topology

Part 3-6B: Compensation for the ECR nonlinearity.

The thermal resistance of the film ECR was shown to be a nonlinear function of the conducting fluid height, h. The expression relating thermal resistance to h was:

$$R = \frac{L/w}{(K_2 - K_2)h + K_1 H} \qquad (3\text{-}6.1)$$

By proper arrangement of the sensors and the conducting fluid levels, the output temperature of an amplifier constructed from two film ECR's, can be made a linear function of the input temperature difference.

The highly nonlinear character of the film ECR is illustrated in figure 3-6.3. For the purpose of illustration the ECR parameters have been assigned the following values:

$$H = 1.0$$

$$w = 1.0$$

$$L = .1$$

$$K_1 = 1.0$$

$$K_2 = 10.0$$

A different set of values would produce a different, but still nonlinear, resistance versus conducting fluid level curve.

The two nonlinear ECR's can be configured to produce an output that is a linear function of the input temperature difference.

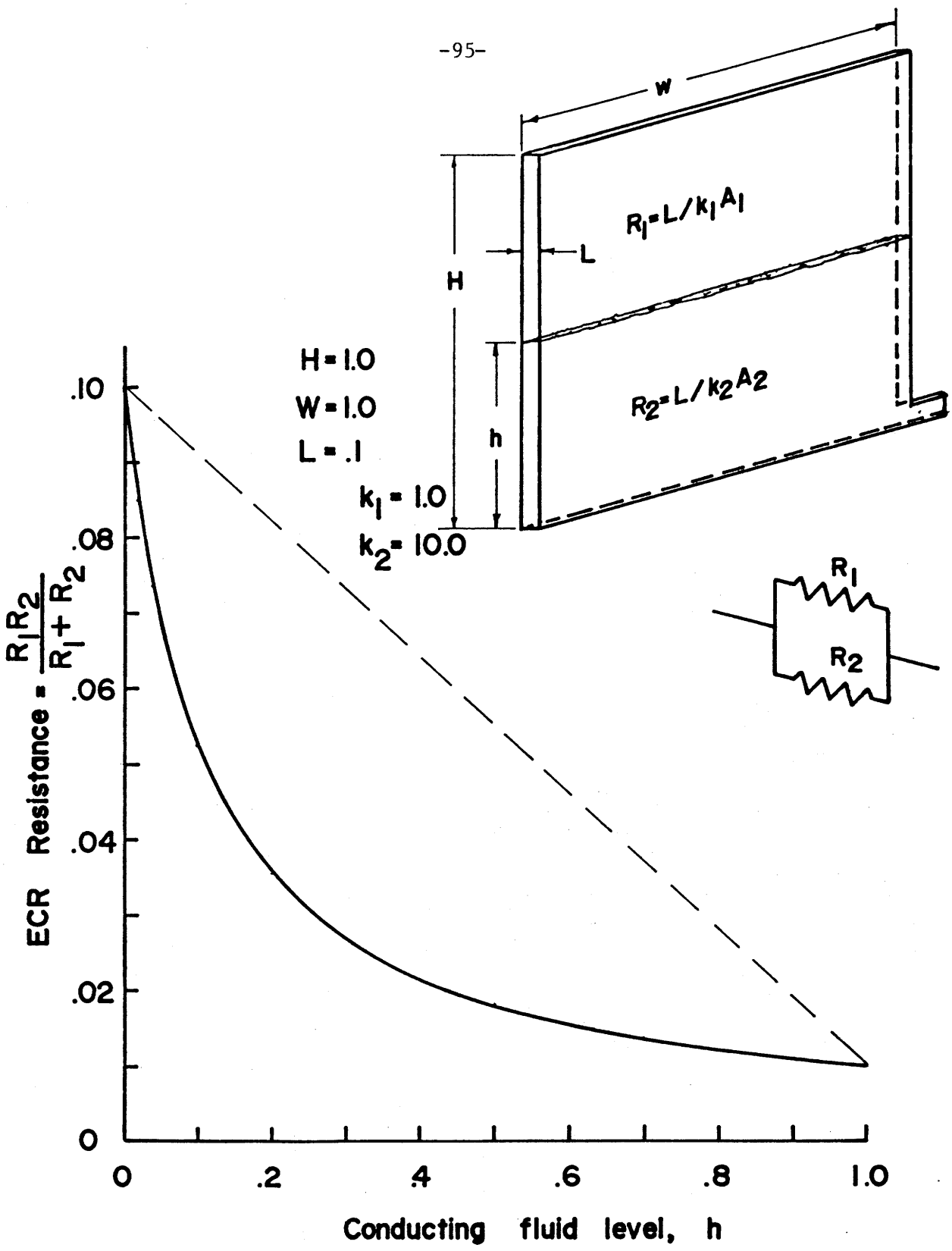

Figure 3-6.3: Nonlinear character of film ECR

The resistor geometry illustrated in figure 3-5.6 will accomplish this goal. The film section and reservoirs must be equal in cross section, and the resistors initially filled to their centerline with the same conducting fluid. Normally two resistors would have four sensors. But combining the four sensors to form two is the final step needed to make the amplifier linear.

The positive sensor of R_V is combined with the negative (fig. 3-6.4) sensor of R_L, and the negative sensor of R_V is merged with the positive sensor of R_L. These combined sensors have double the volume of a single sensor. The combined sensors correspond to the negative and positive amplifier inputs, respectively. The two sensors are connected inversely to the two ECR's; the same pressure difference is seen across both resistors, but the sign is reversed. This means the two film section fluid levels deflect equally, but inversely, relative to the centerline of the film sections. This effect is indicated in figure 3-5.6, with the symmetric deflection, Δh.

Constraining the fluid deflections in R_V and R_L to be symmetric about the center line allows the fluid level in both ECR film sections to be expressed in terms of one variable, h. If the fluid level in R_L's film section is h, then the level in R_V's film section is H-h. The resistance of R_V and R_L can then be expressed:

$$R_L = \frac{L/w}{(K_2 - K_1)h + K_1 H} \qquad (3\text{-}6.2)$$

$$R_v = \frac{L/w}{(K_2 - K_1)(H-h) + K_1 H} = \frac{L/w}{(K_1 - K_2)\, h + K_2 H} \qquad (3\text{-}6.3)$$

Previously, the output temperature of the amplifier was expressed by the relation:

$$\Delta T_{out} = \Delta T_s \left[\frac{R_L}{R_L + R} - \frac{1}{2}\right] \qquad (3\text{-}6.4)$$

which can be rewritten in terms of the expressions for R_v and R_L to form:

$$\Delta T_{out} = \Delta T_s \left[\frac{(K_1 - K_2)h + K_2 H}{(K_2 + K_1)H} - \frac{1}{2}\right].$$

Now the conducting fluid level, h, appears in the numerator, and the output temperature is a linear function of this parameter. The conducting fluid level is a linear function of the pressure difference, which is very close to a linear function of temperature difference between the two input sensors. And thus, the output temperature is a linear function of the input temperature difference.

Once the sensors have been combined, and the geometry of Figure 3-6.1 chosen for the amplifier, there is a very simple way to insure the film section fluid level deflections will the symmetric. The reservoirs could be omitted entirely and the film sections connected at the bottom. Conducting fluid leaving one film section would flow into the other. One sensor would connect to each film section and the amplifier would be complete. The reservoirs offer some experi-

mental and practical advantages that are detailed in appendix three. Thus, even though they cause the amplifier to be mechanically more complex, the reservoirs are retained in the design.

The amplifier configuration in figure 3-6.4 is the topic of this thesis. In addition to being linear, it's performance characteristics can be tailored to specific applications. The next chapter will analyze how specific amplifier parameters and dimensions affect its operation.

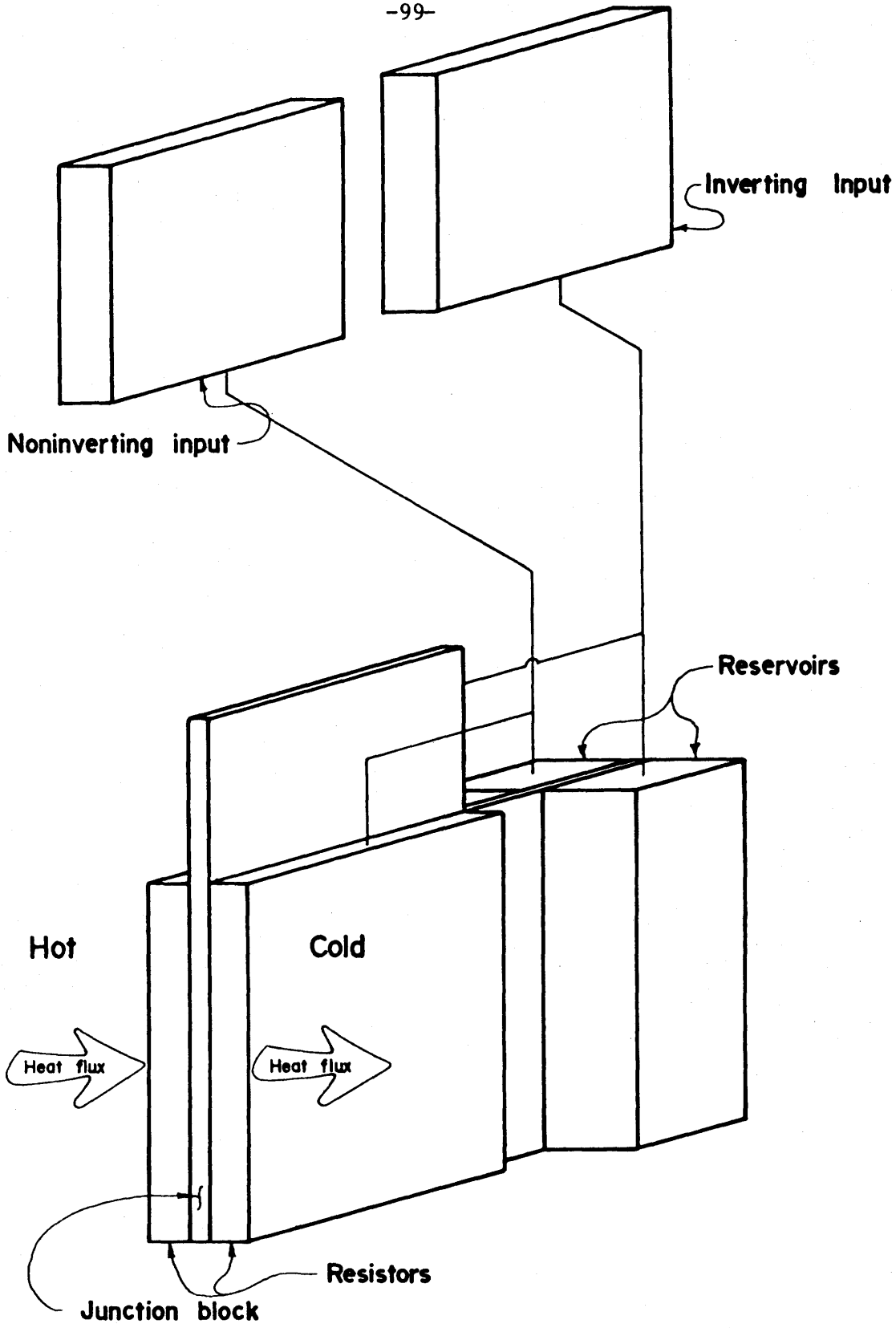

Figure 3-6.4: Final amplifier configuration.

CHAPTER 4: AMPLIFIER MODEL AND DYNAMIC RESPONSE SIMULATION

Section 4-1: Brief chapter summary.

Section two describes the final amplifier dynamic model. A complex twenty-first order model developed in appendix 2 is reduced in appendix 4 to seventh order. This is accomplished by assigning dimensions to the amplifier components with the optimal design technique described in appendix 3. The dimensions allow the model elements to be sized, and the less significant elements eliminated. The result is the final bond graph model with all elements values known.

Section three details the solution to the system dynamic equations, derived in appendix 5. With a bond graph the system state equations can be developed, and the instantaneous dynamic behavior of the amplifier simulated on a digital computer. The results of the simulation are compared with analytic predictions of gain and range in the previous chapter. A simple model of two cascaded lags is presented as a first order approximation to the simulated amplifier behavior.

Section 4-2: Simplified amplifier model.

To predict amplifier dynamic performance analytically a mathematical model of the amplifier must be developed. Expressions for the amplifier steady state gain and range were derived in the previous chapter. These expressions ignored dynamics, and implicitly assumed infinite time for resistances and temperatures to change. In reality some finite time is needed for the conducting fluid levels to change, and for the various thermal elements to come to temperature equilibrium. This section will describe a model that will allow the amplifier output to be predicted as a function of time and the temperature inputs.

An amplifier model will predict the temperature change of the system thermal capacitances as a function of time. All physical parts of the amplifier are characterized as capacitances with a single temperature. The temperature of a thermal capacitance is a single valued function of the heat stored. By accounting for the heat flowing into and out of a thermal capacitance, the amount stored at any instant is known, so the temperature is known. The amplifier thermal capacitances are connected by thermal resistors. Resistance to heat flow is modeled as resistance. A more complex explanation of thermal modeling is presented in appendix 1, along with an explanation of thermal bond graphs.

The final model of the thermal amplifier is shown in figure 4-2.1. This model is a simplification of the more complex and complete

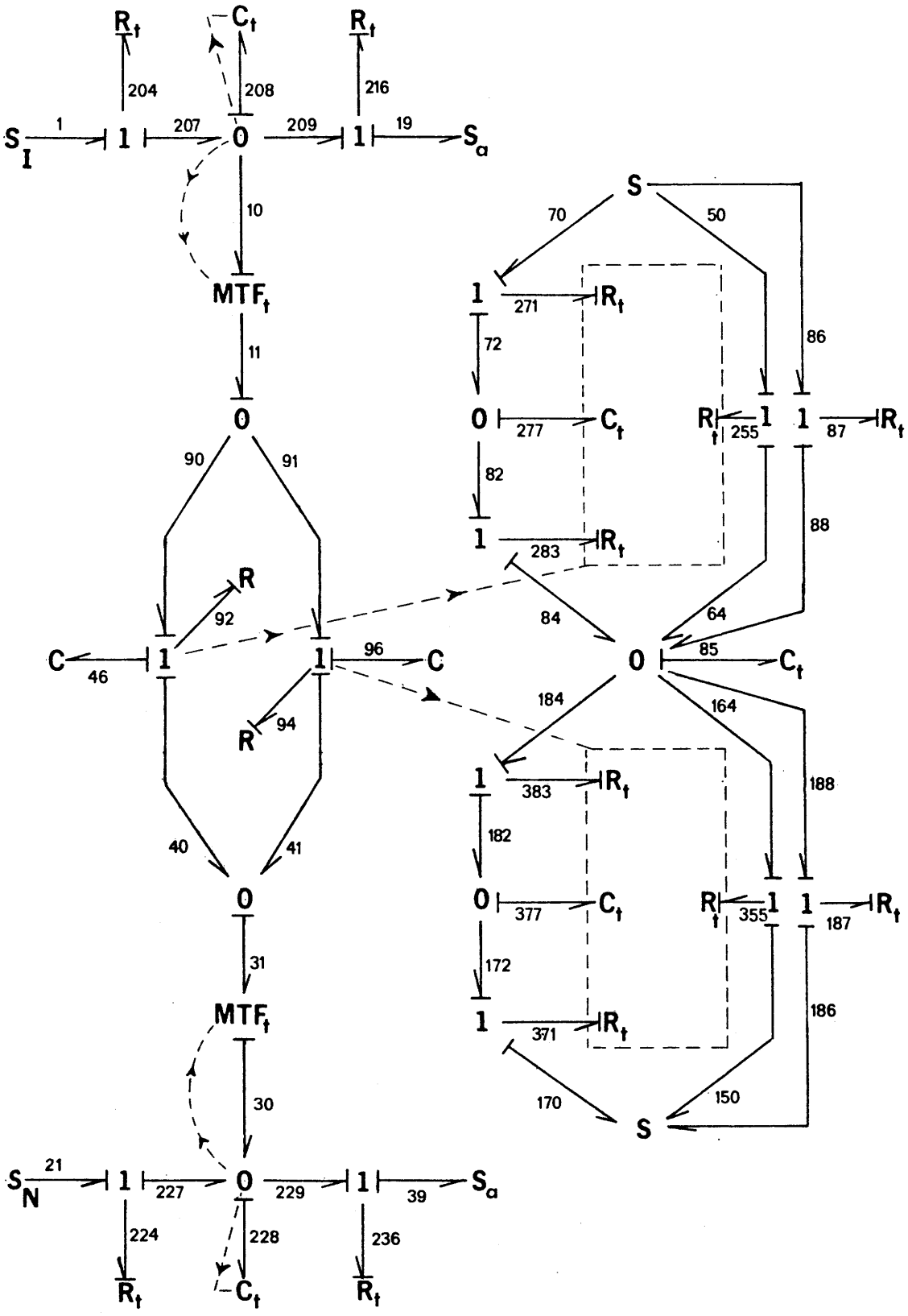

Figure 4-2.1: Final thermal-bond-graph amplifier model.

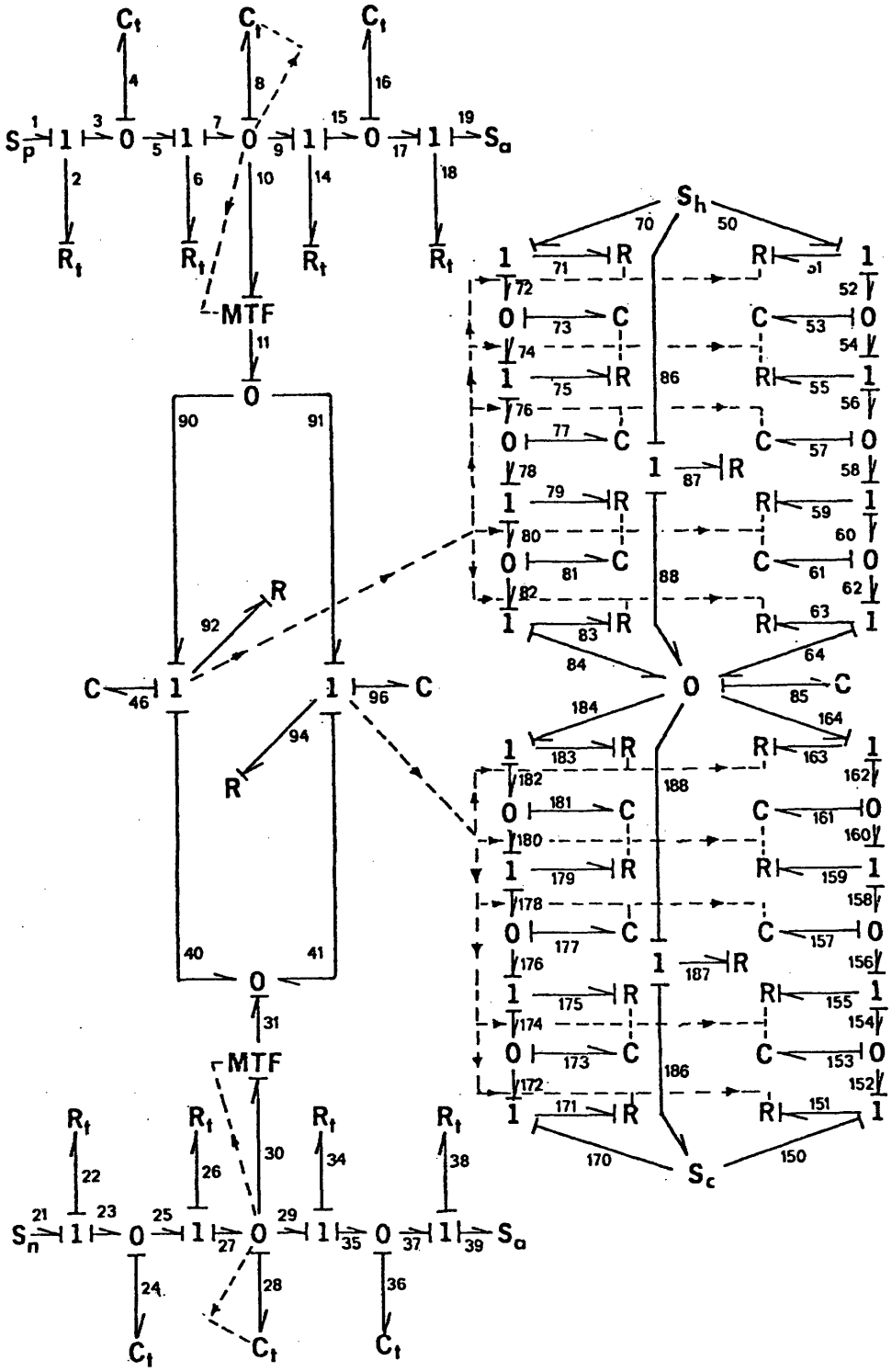

Figure 4-2.2: Twenty-first order amplifier model.

model shown in figure 4-2.2. Model complexity is determined by the detail and accuracy desired in the performance prediction. Ultimately every material particle in the amplifier could be modeled as a separate capacitance. Such detail is seldom necessary and capacitance and resistance are "lumped" into model elements that correspond physically to a distributed part. The complex amplifier model provided more detail than necessary for the amplifier ultimately built and tested. Consequently, it was simplified to the final model.

The final model of the amplifier built and tested for this thesis was developed in three discrete steps. The complex model was developed first. Physical parts of the amplifier were modeled as discrete resistances and capacitances, irrespective of relative magnitude. The values of these model elements were expressed as functions of the amplifier physical dimensions. Second, the amplifier dimensions were selected. Amplifier performance was related to some critical dimensions, which were subject to physical and system constraints. A numerical optimal design technique was employed to select the "optimum" amplifier dimensions for desired performance. Third, the selected dimensions were inserted into the complex model element expressions, and the magnitude of each element determined. The less significant elements were eliminated or combined with larger elements to create the final seventh order model shown in figure 4-2.1. Each step will be described in more detail.

Appendix 2 explains the development of the complex model. The physical correspondence of model elements to physical amplifier parts is described in detail. The complex model represents an attempt to create model elements that correspond roughly to the physical divisions of the amplifier. The elements are expressed in terms of amplifier dimensions. The resulting model is twenty-first order, i.e., there were twenty-one capacitances identified that could have independent effort values (temperature or pressure) as a function of time and inputs.

Optimal design was used to select amplifier dimensions, via the complex method of Box, a procedure described in appendix 3. To select amplifier dimensions rationally these dimensions had to be related to the amplifier performance. The selection of desired performance would then generate a set of dimensions. A mathematical expression, called a performance index, relates the dimensions to be optimized to a product that reflects performance. The generation of this index is not a rigorous procedure, but can be done more or less rationally. While being optimized the physical dimensions can be constrained to lie within certain limits with inequality constraints. The dimensions in the performance index are varied within their constraints to maximize the value of the performance index. The dimensions that maximize the performance index are the "optimum" for that index. A different index usually produces a different set of optimum dimensions.

The performance index used to design the test amplifiers merely penalized physical size. A smaller amplifier of the same shape will respond faster, since less heat flow is needed to change the temperatures of its thermal capacitances, which are smaller. The performance indices and their generation is described in appendix 3, as well as the dimensions produced by the optimization.

Dimensions dictated by the optimization allowed the model elements to be sized. The complex model was derived with all the element values expressed in terms of dimension variables. The relative significance of the different model elements could be compared once their magnitudes were known. The model simplification, described in appendix 4, resulted in the final model of figure 4-2.1. Table 4-2.1 summarizes each element (an element is designated by the bond number attached to it) and what it corresponds to physically in the amplifier. Basically there are two circuits in the amplifier that can be decoupled and discussed individually.

The circuit shown in figure 4-2.3 is formed by the sensors and manometers. There are nominally, four independent energy storage elements. These are the two fluid capacitances associated with the manometers, C_{46} and C_{96}, and the thermal capacitance of each sensor, C_{208} and C_{228}. If the pressure conducting tubes are matched in length, making the two fluid resistances R_{92} and R_{94} equal, the two fluid manometers could be characterized as one element, since the in-

Table 4-2.1 Summary of final model elements.

$R_{t_{204}}$	The thermal resistance into the inverting sensor. Includes the conducting plate surface film coefficient, all the conducting plate conduction resistance, and the sensor fluid conduction resistance.
$C_{t_{208}}$	The inverting sensor thermal capacitance. Includes all heat stored in the sensor mass, plus heat stored in the vaporized sensor fluid.
$R_{t_{216}}$	The thermal resistance of the inverting sensor back wall to ambient heat leakage. Includes the thermal resistance of the sensor walls and insulation.
$R_{t_{224}}$	Same quantity as $R_{t_{204}}$ for the noninverting sensor.
$C_{t_{228}}$	Same quantity as $C_{t_{208}}$ for the noninverting sensor.
$R_{t_{236}}$	Same quantity as $R_{t_{216}}$ for the noninverting sensor.
C_{46}	Fluid capacitance of resistor $R_{v's}$ manometer.
C_{96}	Fluid capacitance of resistor $R_{L's}$ manometer.
R_{92}	Fluid resistance to conducting fluid flow in R_v.
R_{94}	Fluid resistance to conducting fluid flow in R_L.
MTF_t	The temperature to vapor pressure conversion in either sensor.
$R_{t_{271}}$	Includes all the contact thermal resistance with the hot source, all the outside wall resistance for the wall portion in contact with the conducting fluid, and half the conducting fluid resistance for R_v. Thus, the value of this parameter is determined by the conducting fluid level.
$C_{t_{277}}$	Is all the thermal capacitance of $R_{v's}$ outside wall and conducting fluid in $R_{v's}$ film section, which varies with film level.

Table 4-2.1: Summary of final model elements. (Con't.)

$R_{t_{283}}$	Includes the other half of R_v's conducting fluid resistance and half the junction block resistance for the block portion in contact with the conducting fluid.
$R_{t_{383}}$	Is the same quantity as $R_{t_{283}}$ for R_L.
$C_{t_{377}}$	Is the same quantity as $C_{t_{277}}$ for R_L.
$R_{t_{371}}$	Is the same quantity as $R_{t_{271}}$ for R_L.
$C_{t_{285}}$	Is the thermal capacitance of the junction block.
$R_{t_{255}}$	Is the thermal resistance encountered by heat flowing from the hot source to the junction block through the insulating fluid of R_v. It includes all the outside wall, insulating fluid, and half the junction block resistance for that portion of the outside wall and junction block in contact with the insulating fluid, which is a function of the film level.
$R_{t_{355}}$	Is the same quantity as $R_{t_{255}}$ for R_L.
$R_{t_{87}}$	Represents the resistance to heat flowing from the hot source to the junction block through the side walls of R_v.
$R_{t_{187}}$	Is the same quantity as $R_{t_{87}}$ for R_L.

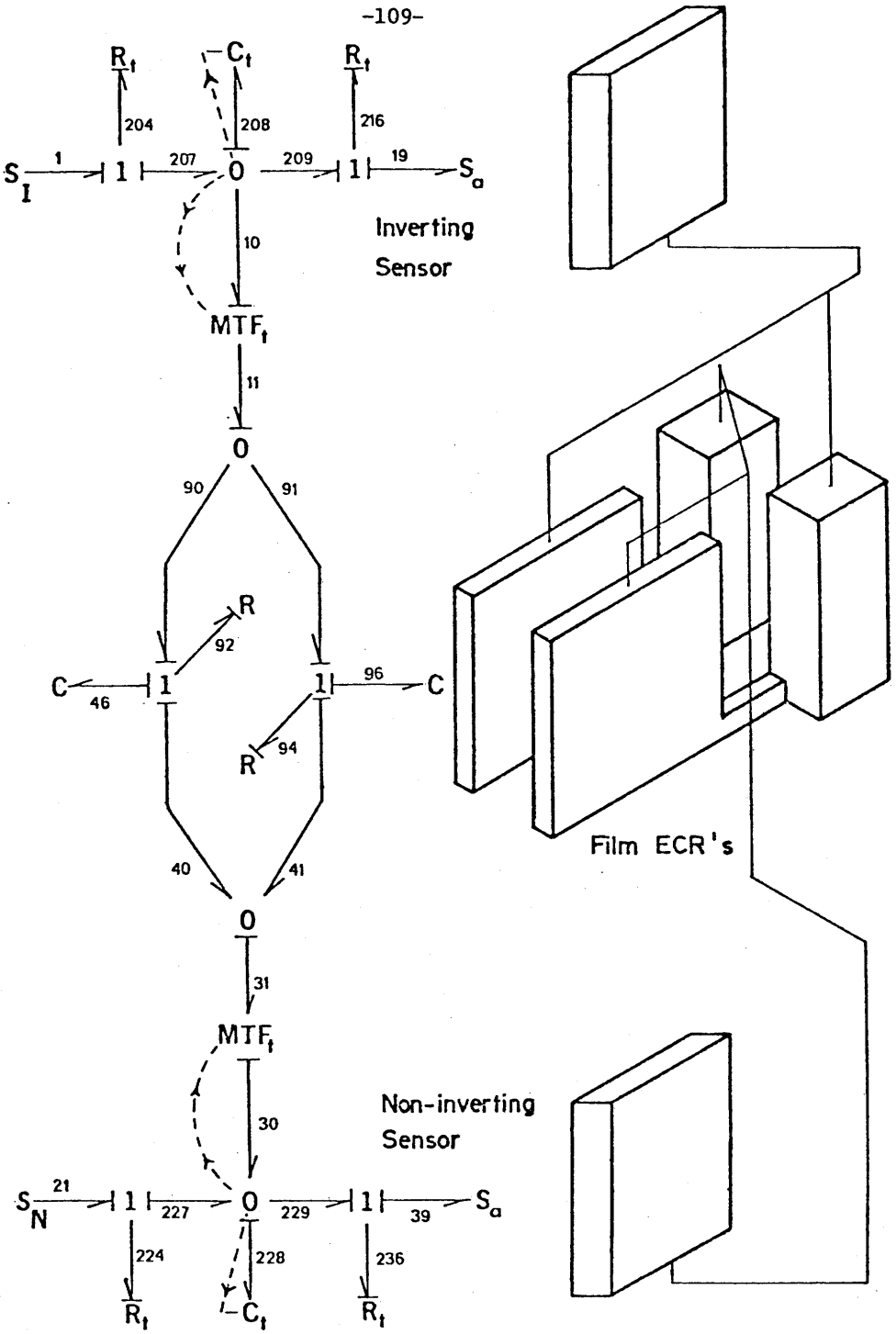

Figure 4-2.3: Diagram of sensor/manometer circuit and parallel bond graph model.

stantaneous pressure across both would be the same. Unless the conducting fluid is very dense or the operating frequency high, the energy storage effects of the manometer capacitance is small. The manometer fluid level determines thermal resistances in the thermal circuit, so the fluid capacitance is included in the model.

The two modulated thermal transformers (MTF_t) represent the effect of using saturated vapor in the sensors. The vapor converts a temperature in an associated pressure, and thus "transforms" the effort variable in the thermal energy domain, temperature, into the effort of the fluid domain, pressure. The moduli of these two transformers are equal, and is the slope of the saturated vapor curve.

The sensor/manometer circuit has no power bonds connecting it to the thermal-resistor circuit, because there is no power exchange between the two. Strictly speaking, any power dissipated in the fluid resistances R_{92} and R_{94} would appear as heat in the conducting fluid. But this effect is normally miniscule. The dashed lines represent signal flow between the two circuits, in this case the manometer levels.

The thermal resistor circuit is illustrated in figure 4-2.4, with the bond graph model and the physical part shown in parallel. Table 4-2.1 summarizes the model elements and what they represent physically in the amplifier. Inspection of the bond graph reveals there are three independent heat flow paths from the source to sink through the junction block.

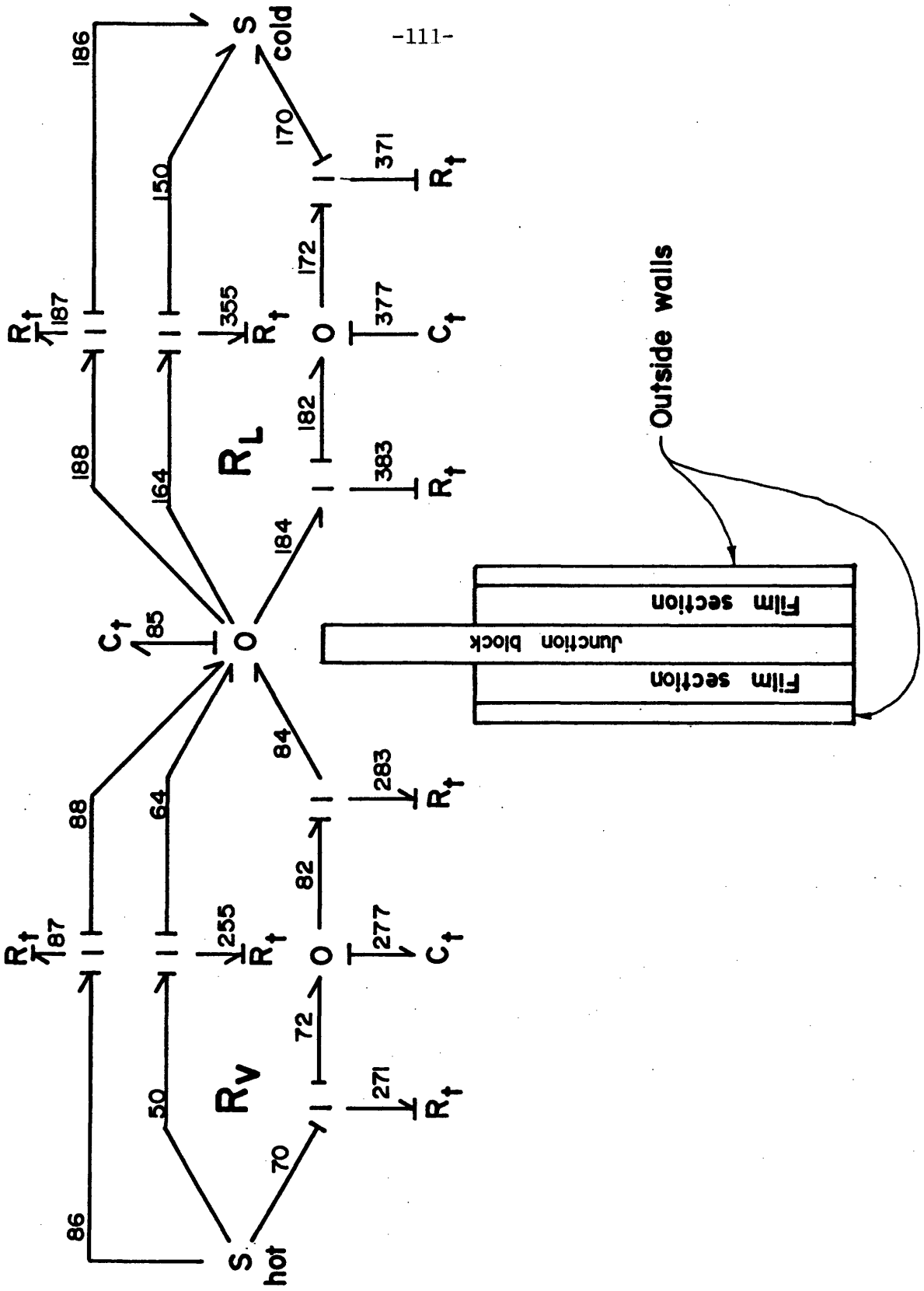

Figure 4-2.4: Diagram of thermal resistor circuit and parallel bond graph model.

The lowest path is the flow through the conducting fluid in R_v and R_L. The resistance and capacitance values are modulated by the conducting fluid level. Note there is no longer an interior wall to both R_v and R_L, the junction block serving as interior wall to both. An inner wall would serve to reduce temperature gradients in the junction block, by providing resistance to heat flow into and out of the block. However, since the junction block is made from copper, whose thermal resistance is approximately $1/5000^{th}$ of the conducting fluid, there will be an infinitesimal temperature gradient.

The middle path is through the insulating fluid in both resistors, air, whose capacitance is so small it can be ignored. The value of the resistance R_{t255} or R_{t355} is modulated by the volume of the film section filled with insulating fluid.

The upper path of figure 4-2.4 is the heat leakage through the edges of both resistors. This is an unwanted effect, but always present to some degree. If the edges are kept thin the resistance is made large. Radiation effects, if any, would be lumped with this resistor. However, the outer and inner walls of both R_v and R_L are polished copper. The emissivity of copper is so low, approximately .07, (Ref. 18) that radiation effects can be ignored; only conduction effects need be included in the model.

The two circuits previously described are connected by the signal flow bonds to form the complete model. The next step is to solve the equations derived from the model to simulate amplifier behavior.

Section 4-3: Computer simulation of amplifier dynamic performance.

This section details the predictions made from the model described in the previous section. Once a bond graph has been developed for a system the derivation of the system state equations is a straightforward process, described at length in appendix 5. These equations were solved numerically on a digital computer.

Two model simulations were performed for this research. An initial simulation was done of an "ideal" amplifier before any experimental work was performed. All assumptions made for model deviation were carried into the simulation. A second simulation was performed of an amplifier later experimentally tested, with simulation parameters, such as source and sink temperature, slightly altered due to experimental findings.

The "ideal" amplifier has the dimensions generated in appendix 3, table A3-5.1, under the heading "ideal" amplifier. The material selected for the various amplifier parts are listed in table A4-4.1, along with their critical thermal properties.

A number of simulations of the ideal were performed, for different temperature step inputs. For each simulation, the source temperature was 212°F, or boiling water. The cold sink was an ice bath at 32°F. This resulted in a "ground" temperature (the temperature midway between the source and sink) of 122°F. This is also the output temperature with no differential temperature input. Temperature output

at the junction block with a differential temperature input is measured relative to the ground temperature. Figure 4-3.1 summarizes the computer simulation data for the ideal amplifier. Step inputs of different sizes and signs generated the curve shown. An input greater than .6°F, plus or minus, saturates the amplifier. This corresponds physically to the sensors producing a pressure difference in excess of 4.4 inches of silicone oil head. At this point one film section is completely filled with conducting fluid, and the other is empty. No further thermal resistance changes can then occur. The amplifier fails to respond to any greater temperature differences, and the output curve becomes horizontal. A gain of 80 was calculated with the program.

Recall that in chapter 3 an analytical expression was determined for gain and range:

$$\text{Gain} = \frac{k\,\Delta T_s}{r_v + r_L} \qquad (4\text{-}3.1)$$

$$\text{Range} = \frac{\frac{r_v}{r_L} - 1}{\frac{r_v}{r_L} + 1} \qquad (4\text{-}3.2)$$

The amplifier dimensions and materials determine all the parameters in these expressions. For this amplifier $k = 2.77 \frac{BTU}{hr\ ft\ °F}$, $\Delta T_s = 180°F$ The maximum resistance, $r_v = 4.621 \frac{hr°F}{BTU}$, and the minimum resistance, $r_L = 1.517 \frac{hr°F}{BTU}$. The result is a resistance ratio of 3.05, very close to the design value of 3.0. In figure 3-4.1 gain and range values were plotted as a function of the resistance ratio r_v/r_L. To use figure 3-4.1,

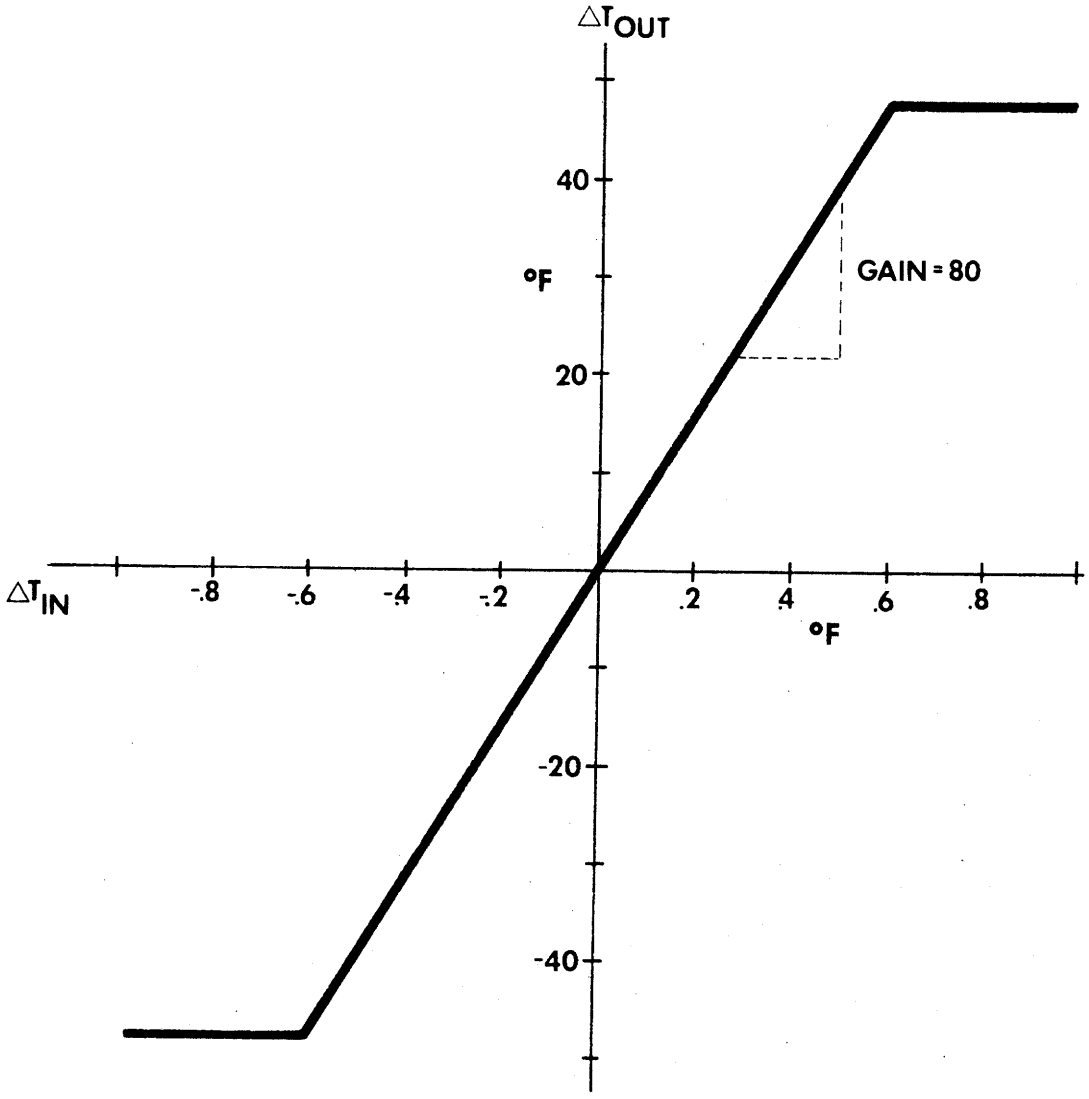

Figure 4-3.1: Summary of computer simulation data for ideal amplifier.

the maximum gain and range must be defined. The maximum range is 180°F, the total temperature difference between source and sink. The maximum gain;

$$\text{gain}_{max} = \frac{k\ \Delta T}{2r_L} = 164 \qquad (4\text{-}3.3)$$

Reading the gain fraction for $r_v/r_L = 3.05$, the value is 49%. The range fraction is 51%. This results in a gain of 81, and a range of 91°F.

The computer simulation predicted a gain of approximately 80, and a range of 90°F. The analytic prediction agreed within 2% of the simulation results. The response shown in figure 4-3.2 indicates an amplifier response time constant of 5.8 minutes, and is essentially first order. The dominant system time constant is related to the time required for the junction block to change temperature.

The sensors, which are independent thermal capacitances, also have a characteristic time constant, which the simulation predicted to be less than 20 seconds. That is, the conducting fluid level comes to equilibrium in both film sections in about five time constants or in less than two minutes. The sensor thermal dynamics are approximately 20 times faster than the junction block dynamics. Generally, when dynamics differ by an order of magnitude, as in this case, the faster dynamics can be ignored. Hence the sensor dynamics can be neglected by comparison to the much slower junction block dynamics.

The amplifier time constant is a constant value, regardless

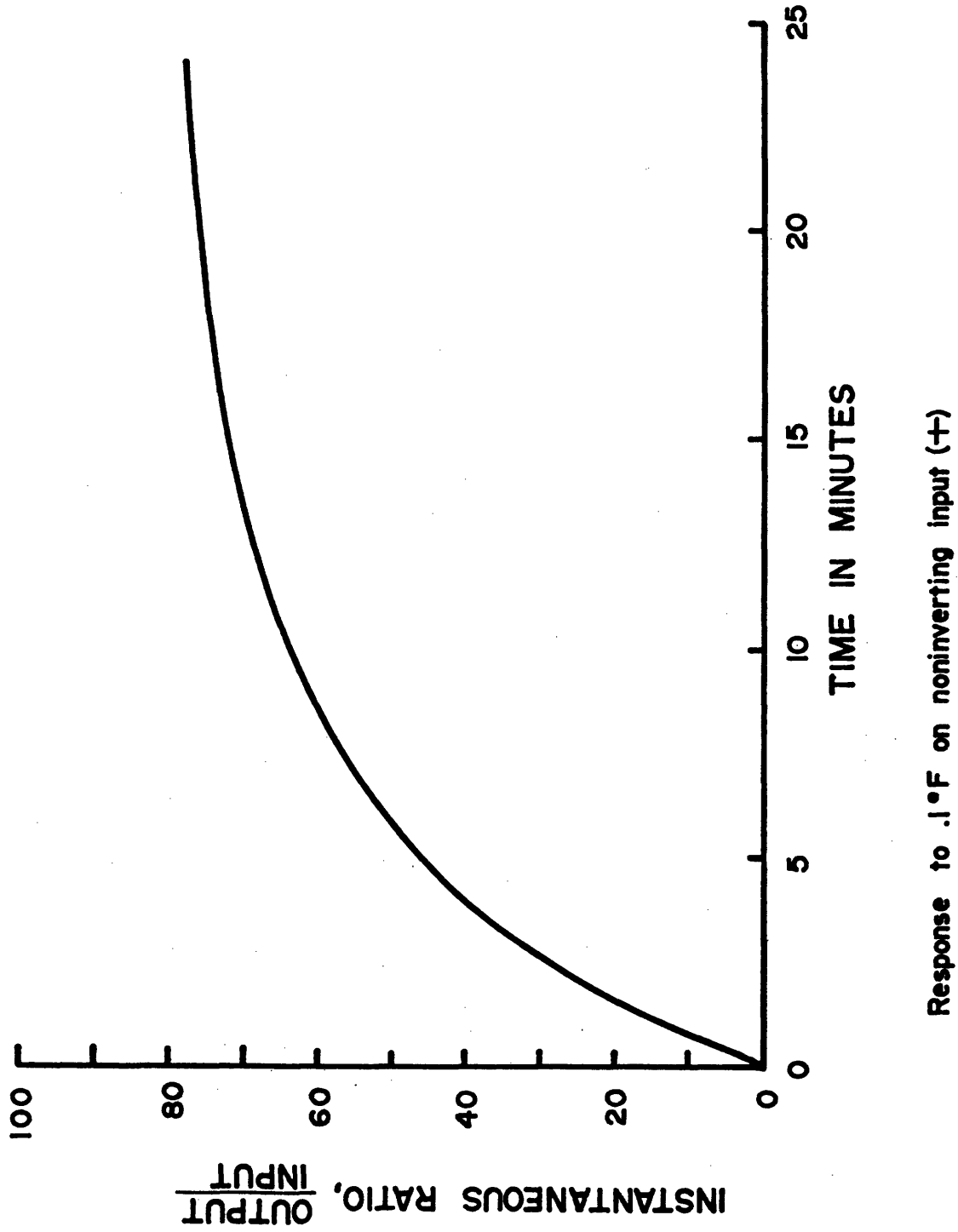

Figure 4-3.2: Simulation of amplifier response to step input.

of input level. It depends on fixed system parameters which are independent of the highly nonlinear character of the resistors R_v and R_L. The first order character of the amplifier response justifies the use of a first order model to determine the parameters which govern the time constant. Assume the resistor-amplifier circuit can be modeled with the simple circuit of figure 4-3.3:

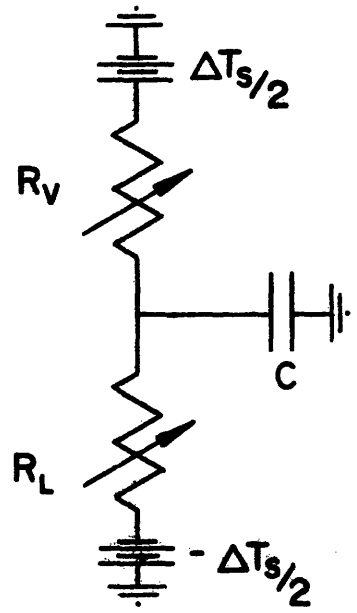

Figure 4-3.3: Circuit to model amplifier response.

The two resistors, R_v and R_L, are the variable resistors, but the capacitor, C, is the total thermal capacitance of both resistors. Referring to figure 4-2.4 C is defined as:

$$C = C_{t277} + C_{t85} + C_{t377} \qquad (4\text{-}3.4)$$

Fortunately this capacitance is constant, even though the value of C_{t277} and C_{t377} is modulated by the conducting fluid levels in the two

resistors. Since the conducting fluid level changes inversely in these capacitances, the net thermal mass of conducting fluid in the thermal circuit remains constant.

The circuit of figure 4-3.3 can be characterized with the bond graph of figure 4-3.4:

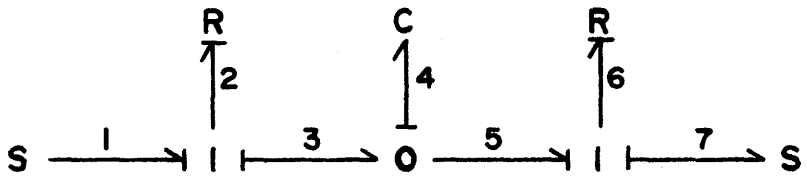

Figure 4-3.4: Thermal bond graph of first order amplifier model.

Since there is only one independent energy storage element, the capacitor, this model is first order. The one governing differential equation is found to be:

$$\dot{e}_4 = \frac{1}{C}\left[\frac{\Delta T_s/2 - e_4}{R_v} - \frac{e_4 - (-\Delta T_s/2)}{R_L}\right] \qquad (4\text{-}3.5)$$

which reduces to:

$$\dot{e}_4 = \frac{e_4}{C\left(\frac{R_v R_L}{R_v + R_L}\right)} \qquad (4\text{-}3.6)$$

This means the system time constant, τ, is defined as

$$\tau = C\left(\frac{R_v R_L}{R_v + R_L}\right) \qquad (4\text{-}3.7)$$

The time constant is invariant despite the nonlinear behavior of R_v and R_L. This can be demonstrated by substituting the defining relations of R_v and R_L (Equations 3-6.2 and 3-6.3 respectively) into equation 4-3.7, yielding:

$$\tau = \frac{L/w}{K_1 H + K_2 H} \qquad (4\text{-}3.8)$$

which equates the time constant to fixed parameters. Unfortunately 4-3.8 cannot be used to calculate time constants, since edge leakage has not been included in the resistor defining expressions, equations 3-6.2 and 3-6.3. But equation 4-3.7 can be easily employed to compute the time constant, since any instantaneous resistor values will yield the same result.

Returning to the simulated amplifier the preceeding calculations can be employed to characterize the amplifier with a very simple model, shown as a block diagram in figure 4-3.5.

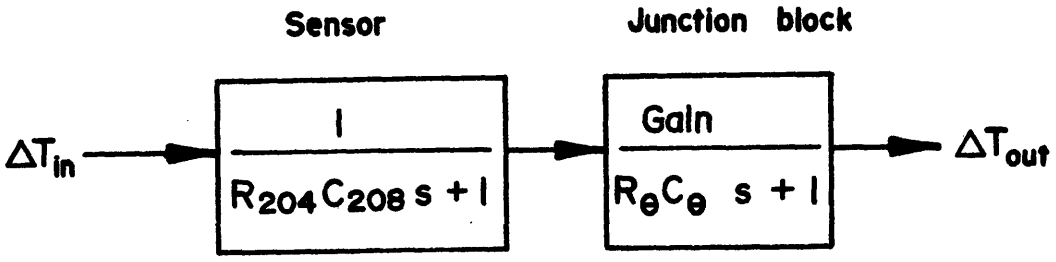

Figure 4-3.5: Block diagram of simplified amplifier model.

Bascially the amplifier is characterized by two cascaded lags, the sensor lag and amplifier lag. The time constant of the sensor is:

$$\tau_{sensor} = R_{204}C_{208} \tag{4-3.9}$$

and the resistor-amplifier time constant:

$$\tau_{resistor} = R_{\theta}C_{\theta} \tag{4-3.10}$$

where:

$$R_{\theta} = \frac{R_v R_L}{R_v + R_L} \tag{4-3.11}$$

$$C_{\theta} = C_{t277} + C_{t85} + C_{t377}$$

Using these relations the simulated amplifier can be examined. For the sensor:

$$R_{204}C_{208} \tilde{=} .14 \frac{hr°F}{BTU} \times .03 \frac{BTU}{°F} \tilde{=} .25 \text{ minutes.}$$

For the resistor section:

$$R_{\theta} = \frac{2.29^2}{2.29+2.29} \frac{hr°F}{BTU}$$

$$C_{\theta} = .0951$$

$$\therefore R_{\theta}C_{\theta} \tilde{=} 6.53 \text{ minutes}$$

This is close to the higher order model prediction of 5.8 minutes. This means, for low frequency inputs, the device is essentially first order, and dominated by the RC time constant of the resistors. Thus a faster response can be obtained by decreasing the resistance and

capacitance of the resistors and junction block.

Experimental results showed that the ideal amplifier presented above required slight modifications to be consistent with the physical amplifier system. Most notably, the sensor fluid must be contained in a metal enclosure, necessitating the addition of a spring rate to the sensor model; however, the bond graph model in unaffected by this change. Also, certain material property values were changed to agree with experimentally determined values.

CHAPTER 5: EXPERIMENTAL PROCEEDURE AND RESULTS

Section 5-1: Brief chapter summary.

Section 2 details the experimental equipment arrangement used to test amplifier performance. The amplifier power supply, temperature, inputs, and instrumentation are described, with references to appropriate appendices for more detail.

Section 3 discusses the open loop amplifier response tests performed on the apparatus of section 2. The tests were done in two sections. The first tests were performed to determine the gain value throughout the input temperature range of amplifier operation. The second part compared the prediction of dynamic open loop response to a step, done with second and seventh order model, to experimental measurements.

Section 4 describes the closed loop response and prediction. The lower order model is not adequate to describe the much faster response of a system configured as an effort follower. The seventh order model agrees with the experimentally measured dynamics, but predicted slightly greater temperature excursions. The seventh order model was then used to generate open and closed loop bode plots for an input temperature range within which the resistors did not saturate.

Section 5-2: Experimental apparatus and procedure

The amplifier experiments were performed with the system diagrammed in figure 5-2.1. The components form three broad categories; the amplifier power supply, amplifier inputs, and the instrumentation to monitor the experiments. Appendix 6 describes experimental equipment construction in greater detail, but each category will be discussed briefly.

The power supply, a hot source and cold sink, were tanks of boiling and ice water respectively. The source and sink tanks had a thick copper wall on one side which formed the contact for attachment to the amplifier. Immersion heaters maintained boiling, while ice was added to the sink, manually, as it melted. Both were highly agitated with magnetic stirrers to maintain a uniform, constant temperature on the copper contact plate. The amplifier was clamped between the source and sink with thermally conductive paste between the mating copper surfaces, as shown in figure 5-2.1.

The temperature inputs to the amplifier were accomplished with agitated temperature baths. Two tanks were constructed, with heaters and temperature controllers, that were stirred magnetically. Sensors were immersed in the bath, supported on stands that allowed the water to flow freely over the conducting plates. A desired temperature could be dialed on the controller, which would turn on the heater as necessary to maintain the set point temperature.

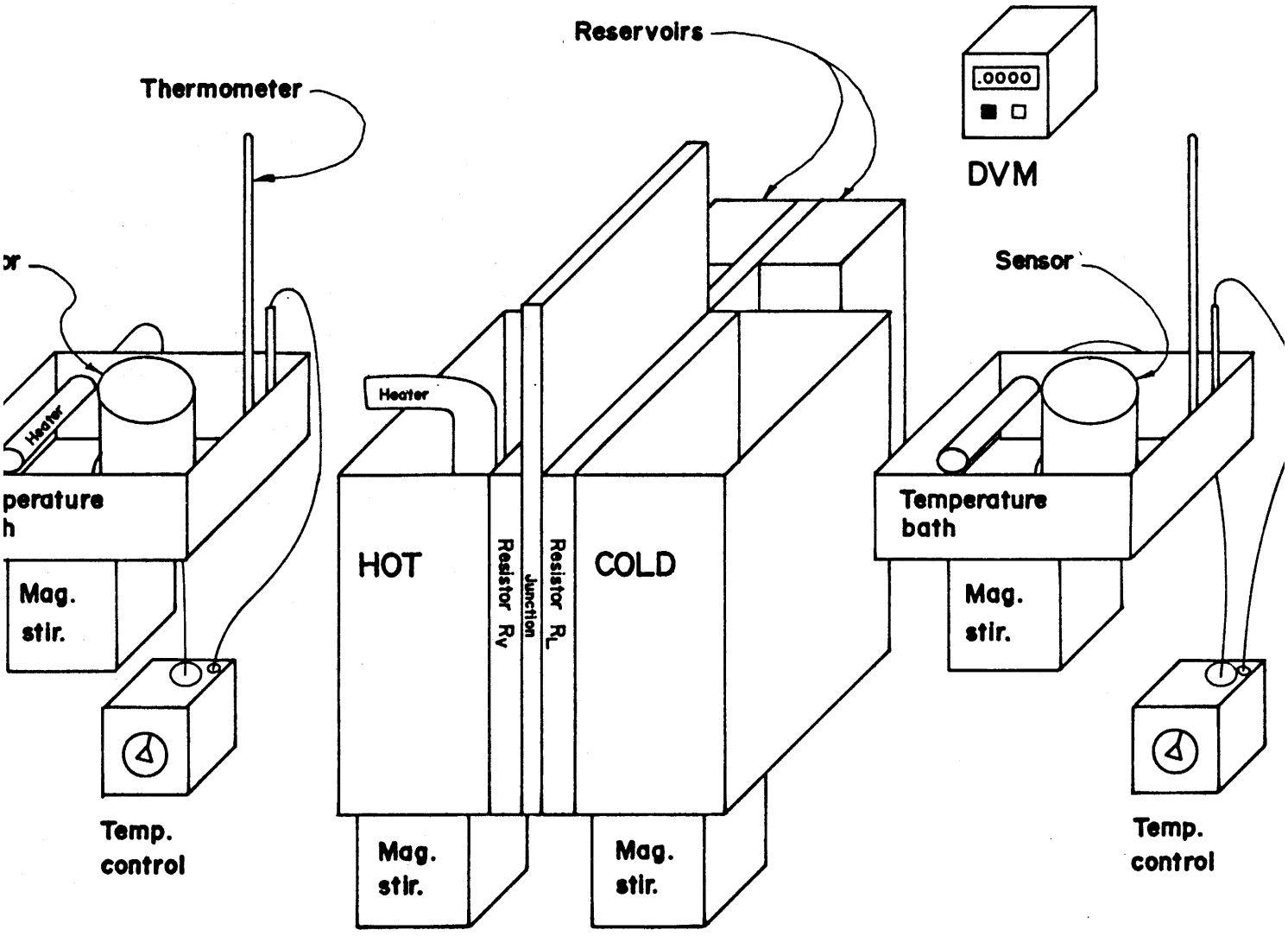
Thermometer
Reservoirs
.0000
DVM
Sensor
Heater
perature
h
Mag.
stir.
Temp.
control
Heater
HOT
Resistor Rv
Junction
Resistor RL
COLD
Mag.
stir.
Mag.
stir.
Temperature
bath
Mag.
stir.
Temp.
control

The instrumentation used in the experiments measured the source, sink, output, and sensor temperatures. The sensor temperature was monitored by a shielded thermocouple embedded in the copper conducting plate. The resulting sensor and amplifier combination had 5 thermocouple outputs: one from each sensor; one each from the outside walls of R_V and R_L; and one from the junction block. The outside wall temperatures of the resistors were considered to be the source and sink temperature. The temperature data was read on a digital voltmeter or recorded on a strip chart recorder.

Section 5-3: Open Loop Response Tests

Open loop response data was gathered from prototypes built according to the ideal and modified amplifier dimensions of Appendix 3. The testing was divided into two parts. One set of tests-the "gain test" - measured the gain, and traced the gain across the spectrum of potential amplifier inputs, from negative to positive output saturation. The other test set-the "open-loop dynamic test" - measured the actual temperature change of the output as a function of time, to compare the actual system time constants and thermal dynamics with the predictions.

The gain tests were performed by changing the bath temperatures to produce a small negative or positive input. The output was then given enough time to stabilize, and a reading was taken. This procedure was repeated in small input temperature increments, through the complete range of the amplifier.

For the gain test a typical data set is shown by the solid line in figure 5-3.1. The direction of temperature change is indicated by the arrowheads on the line. The dotted line represents the computer prediction for comparison.

The measured gain of 20 appears to be slightly less than the predicted gain of 23, although the experimental error alone is enough to account for the difference. The heat lost to ambient from the junction block is not accounted for in the prediction. This leakage would

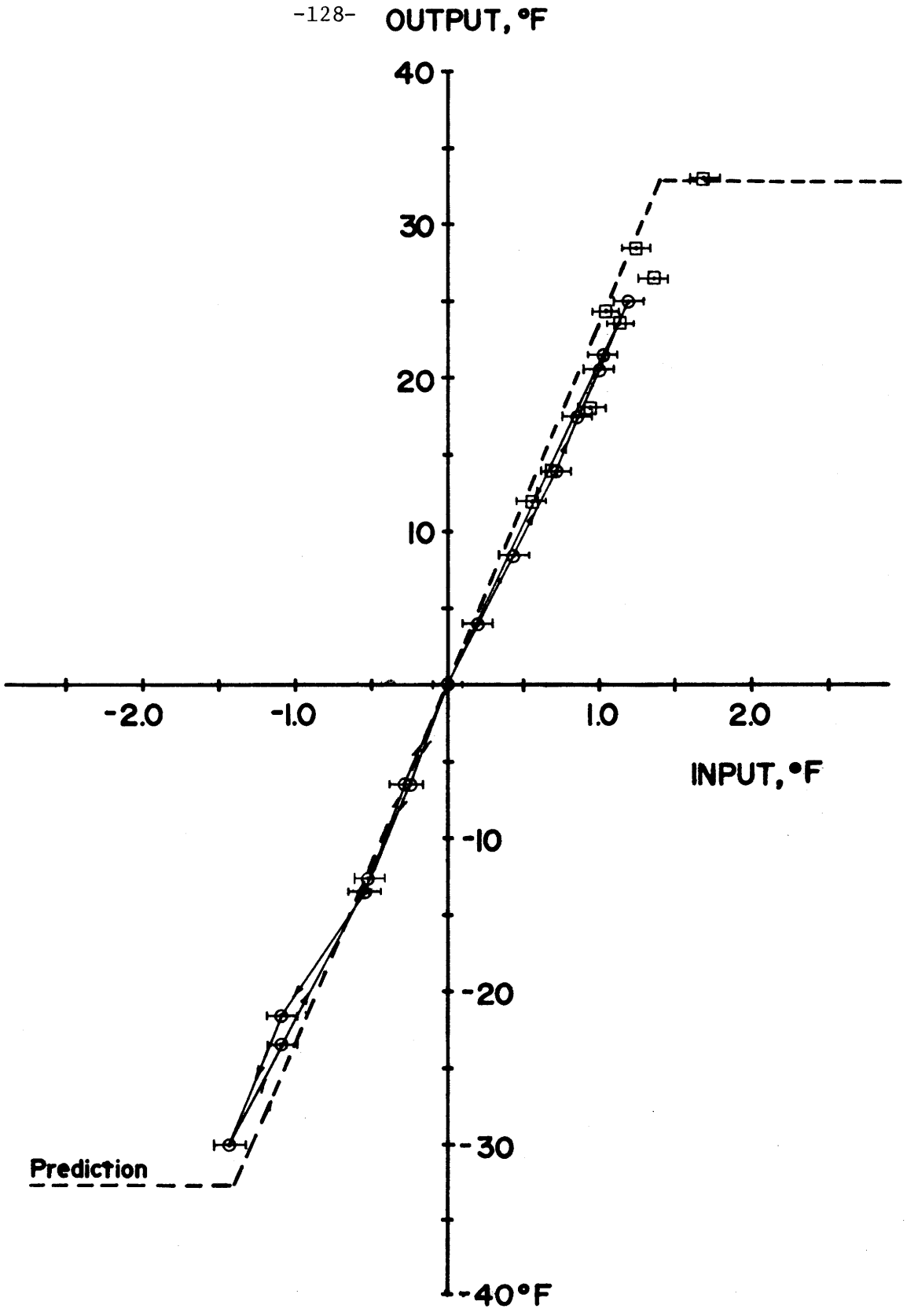

Figure 5-3.1: Summary of open loop gain data.

cause the measured gain to be slightly less than prediction. The junction block was insulated with polyurethane foam ($k = .02 \frac{BTU}{hr\ ft^{\circ}F}$), to minimize this leakage.

The arrows permit evaluation of hysteresis. There doesn't appear to be detectable hysteresis, if time is provided for the output to reach thermal equilibrium. However, finer measurements would be required to detect a small hystersis effect. The results appear to agree acceptably with prediction, and they exhibited a high degree of repeatability.

The dynamics of the open loop response were evaluated on the ideal amplifier with the sensors disconnected. The computer simulations, predicted, and experimental tests confirmed, the sensor time constant was an order of magnitude less than the time constant of the resistor-junction block combination. To test the thermal dynamics of the amplifier section the conducting fluid levels were quickly changed by a predetermined amount, and the temperature of the junction block monitored as a function of time.

A comparison of the data and predictions are shown for several different runs in figure 5-3.2. Note the predictions of both the simple second order model and the seventh order model agree within experimental error. It appears the more complex model is not needed for simple open loop step response.

The agreement between open-loop prediction and response indi-

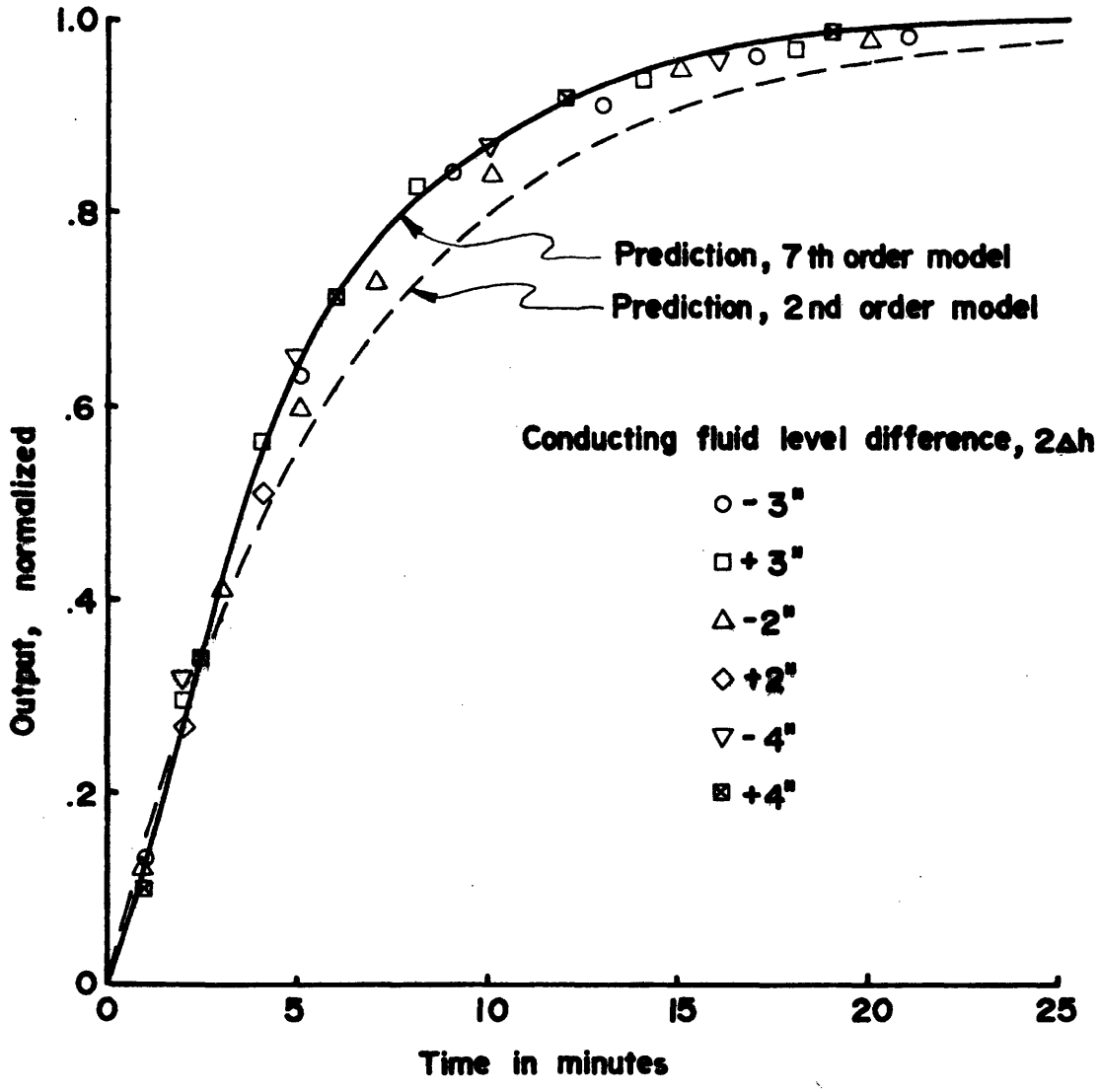

Figure 5-3.2: Dynamic amplifier response to step input.

cated that the close loop response should be investigated. If the open loop experiments had proved unsatisfactory there would have been little purpose in closed loop investigation. To close the loop, the experimental set-up had to be modified. The next section will describe the experimental method, and the apparatus modifications.

Section 5-4: Closed loop experimental method.

The circuit chosen for closed-loop simulation and testing was that of an effort follower. A diagram of this circuit is shown in figure 5-4.1.

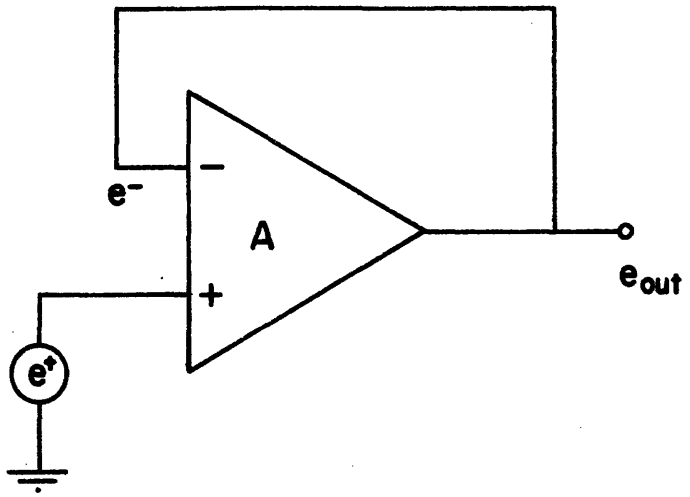

Figure 5-4.1: Effort follower circuit used for closed loop simulation.

The connection from the output to the negative input is the "feedback" loop. This circuit forms a follower of the positive input because:

$$e_{out} = A(e^{+} - e^{-}) \qquad (5\text{-}4.1)$$

but $e^{-} = e_{out}$

$$\therefore \quad e_{out} = A(e^{+} - e_{out}) \qquad (5\text{-}4.2)$$

$$\therefore \quad e_{out} = \frac{A}{A + 1} e^{+} \qquad (5\text{-}4.3)$$

If A>>1 this relation becomes:

$$e_{out} \tilde{=} e^{+}$$

and the output always has approximately the same level as the input. This assumption is less accurate if the gain is small. A plot of the gain versus the ratio e_{out}/e^{+} is shown in figure 5-4.2. Therefore, with the modest gain of 20 the output of the thermal amplifier should always be slightly less than the input.

The negative sensor was mounted on the junction block with the angled copper mounting bracket shown in figure 5-4.3. This complex experimental equipment geometry was difficult to completely insulate. A two-piece polyurethane assembly was used, which was $\frac{1}{4}$" thick on the average. A heat transfer paste was used between the mating copper surfaces to decrease thermal resistance.

To conduct experiments, the junction block and negative sensor were allowed to come to thermal equilibrium with pressure conducting tubes disconnected, while the positive sensor was immersed in a temperature bath, and brought up to the junction plate temperature. Then the pressure conducting tubes were connected. With this method the zero input level had the conducting fluid level in both R_v and R_L at mid-point in the film section.

The temperature input was a change in the positive sensor bath temperature. The temperature of the negative sensor was then monitored as the output. Temperature readings were taken every 30 seconds, on the thermocouples, to a resolution of one micro-volt or .03°F.

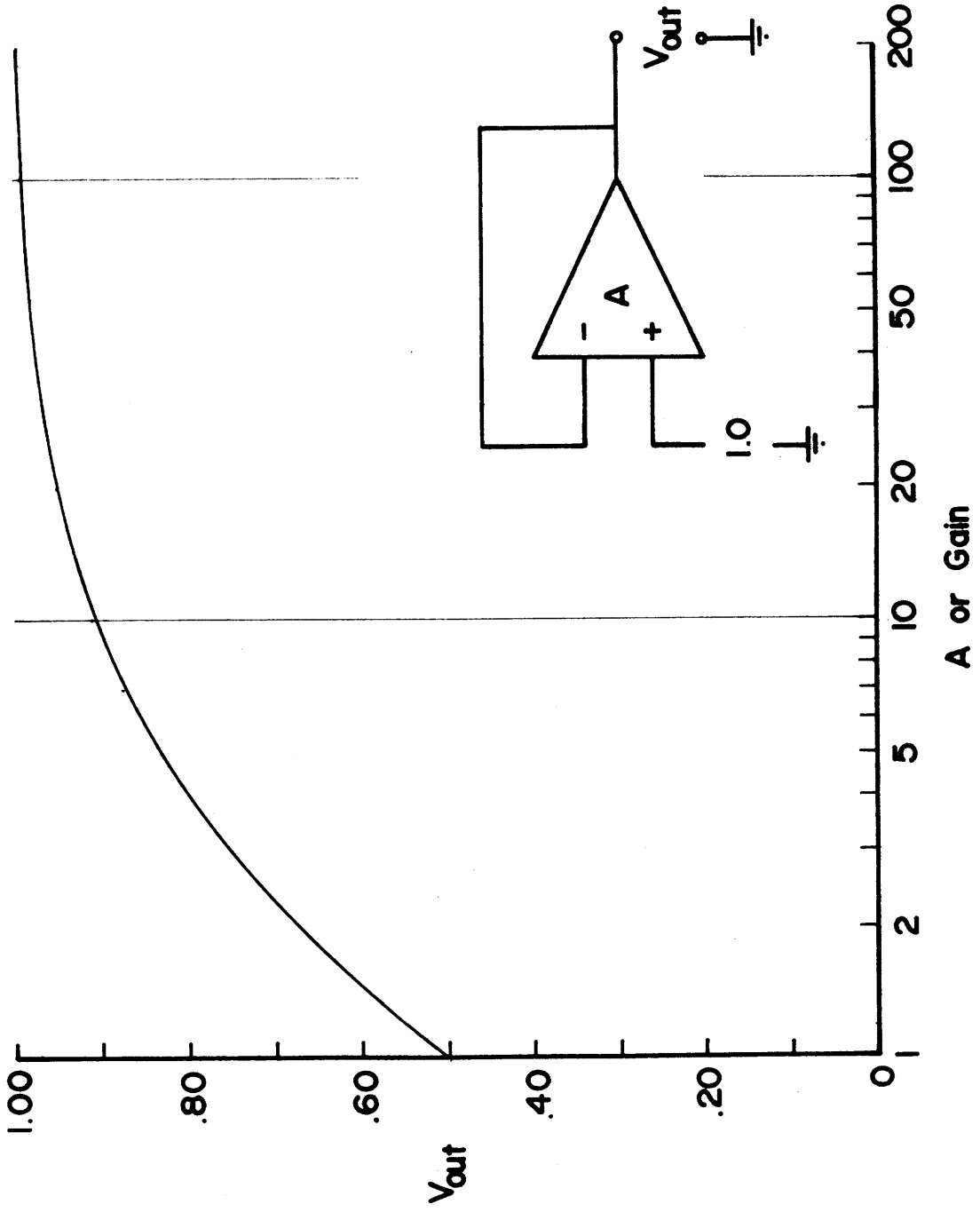

Figure 5-4.2: Plot of gain versus follower error.

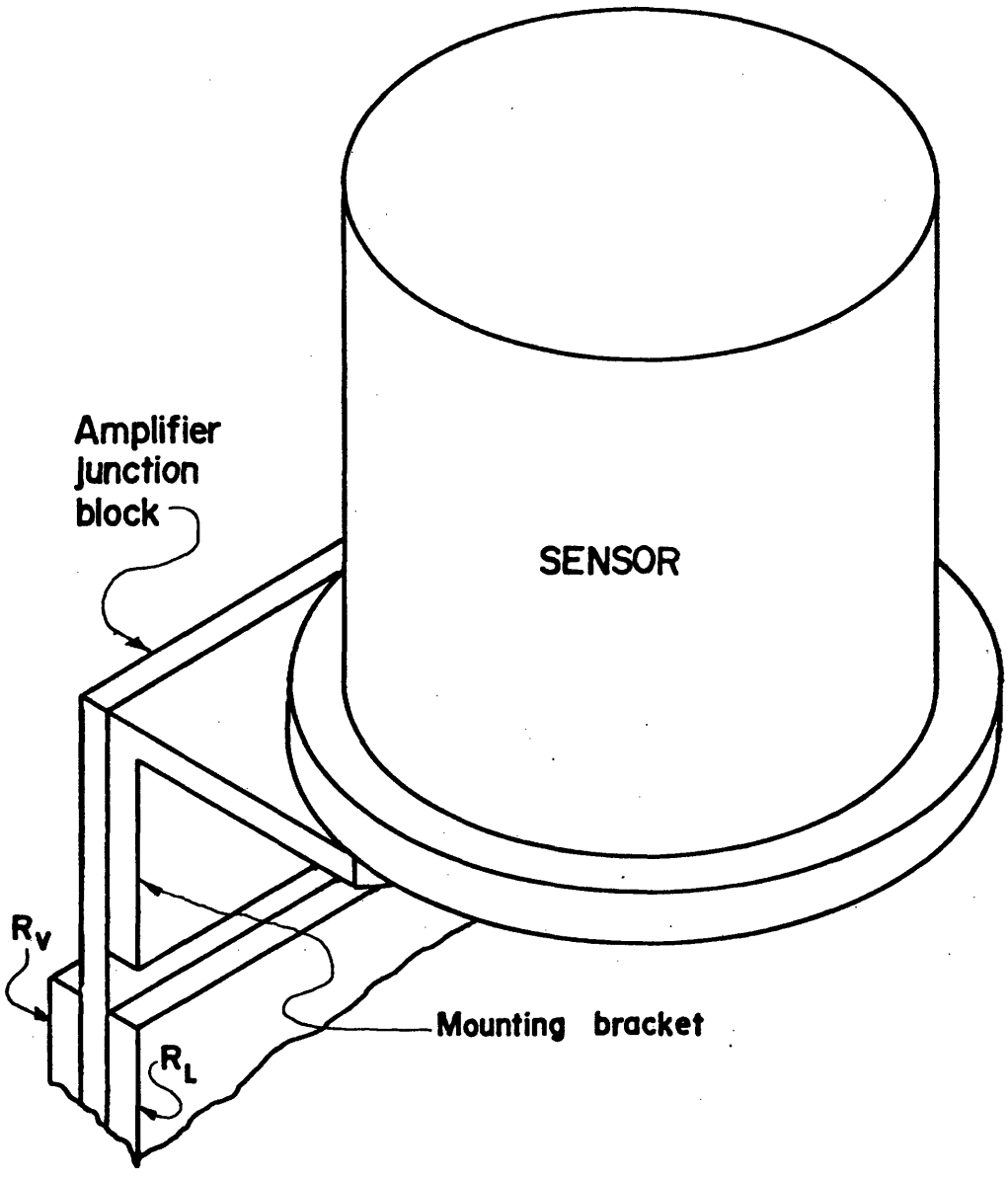

Figure 5-4.3: Closed loop negative sensor attachment.

The model used for the closed loop computer simulation is shown in figure 5-4.4, and is the previously described 7th order model. The inverting temperature input has been replaced with a conducting bond, connected to the junction block capacitance, C_{285}. The capacitance of the junction block has been increased to account for the copper connecting bracket's mass, and a leakage resistance to "ground" or ambient temperature has been added. The experimental prototype had a power consumption of 10 watts.

The second order amplifier model, presented as two cascaded lags in the previous chapter, was very close in predicting open loop step response and low frequency open loop performance, but could not be used for closed loop simulation. The closed loop response was fast enough to require a model with the higher order dynamics, which the seventh order model contained. The low order model ignores the capacitance of the conducting fluid in the resistors, because this effect only becomes significant at higher frequencies. The model employed to analyze amplifier behavior is a function of the circuit configuration and the input frequency the application requires.

The computer prediction of closed loop response is shown by the dotted line in figure 5-4.4, and the experimental data points are indicated and connected by a solid line. The dynamics seem to agree as to the frequency and damping, but the temperature excursions are not as large as predicted. The prediction includes the effect of insulation leakage, which was an experimentally measured quantity. The leakage resulted in a larger follower error than could be accounted for by finite gain. The agreement between theory and experiment are close,

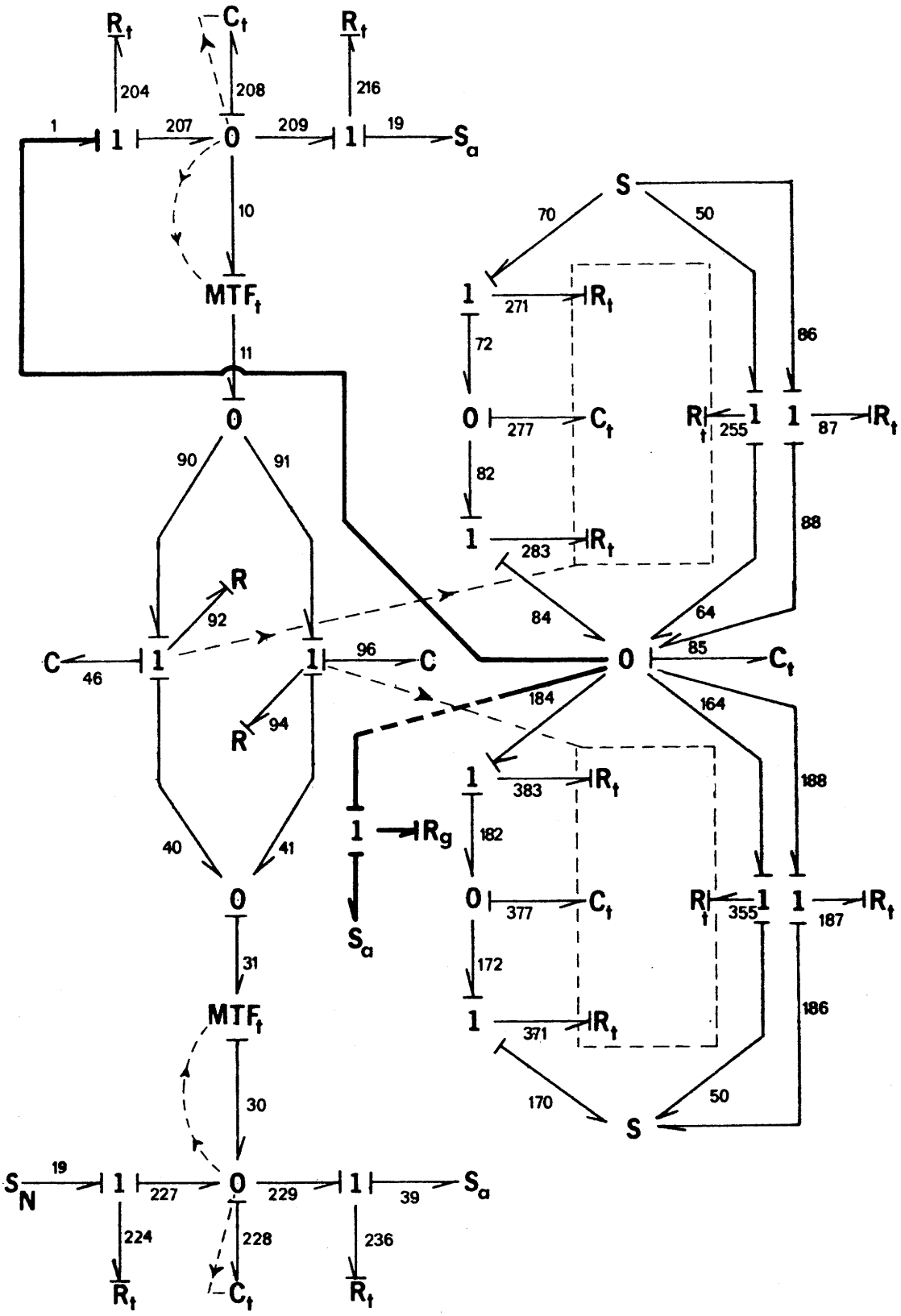

Figure 5-4.4: Bond graph of model used for closed loop simulation.

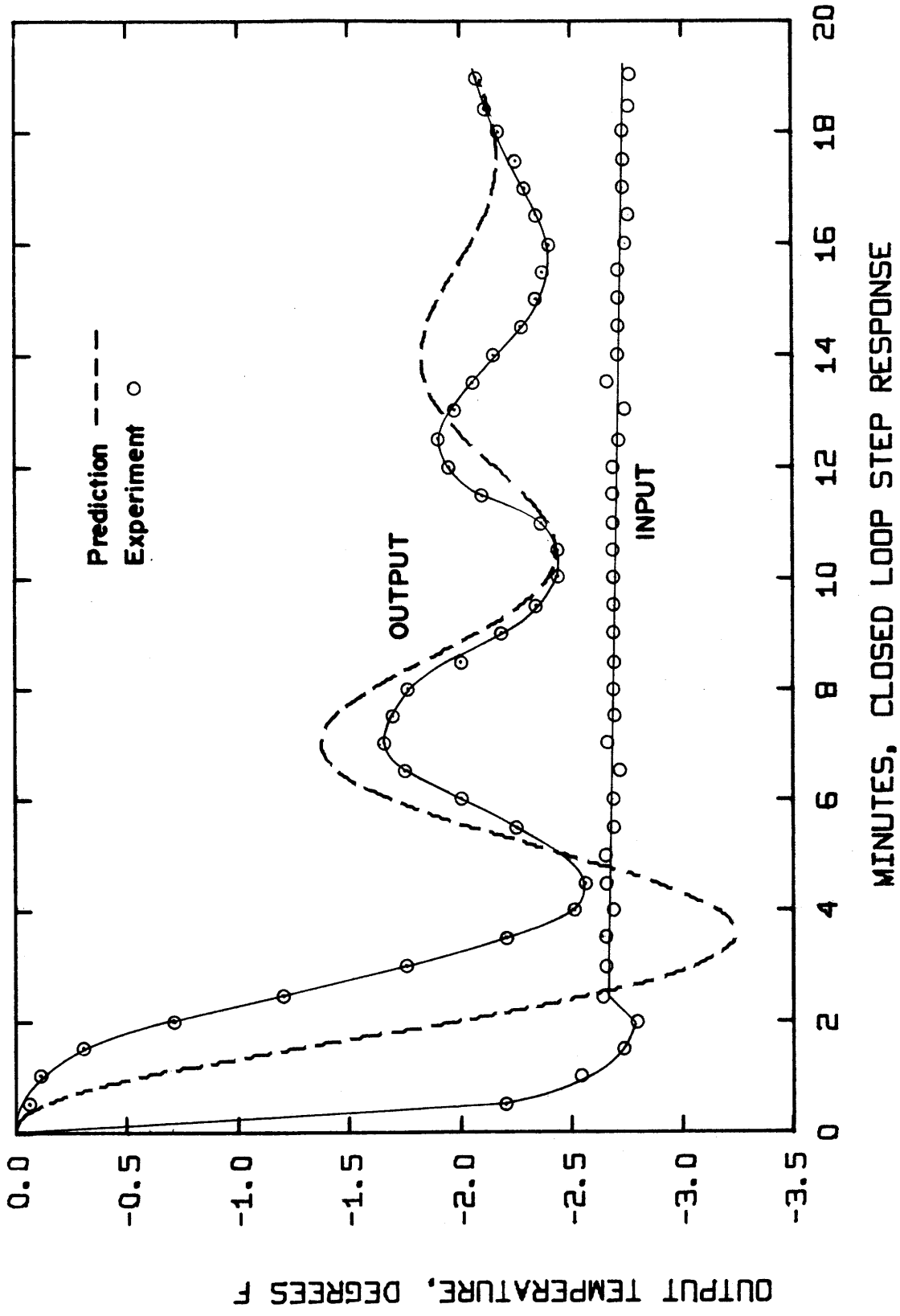

Figure 5-4.5: Comparison of measured and predicted closed loop response.

given the complex thermal behavior of the system.

This marked the extent to which experimental verification of the model could be done on the experimental equipment built. Enough faith had been generated in the amplifier model to continue study by producing open and closed loop bode plot predictions of amplifier behavior. The open loop response was simulated by holding both temperature fixed and varying the other sinusoidally. The output temperature was predicted, and the attenuation and phase lag computed. The results, for the modified amplifier, are shown in figure 5-4.6.

For the closed loop simulation the model described previously was employed. A sinusoidal temperature change was programmed for the positive sensor and the response calculated for various frequencies. The closed loop results are also presented in figure 5-4. .

For a non-linear system the response will be a function of input level. For the bode plots generated the input was kept small enough to avoid the amplifier's resistors saturating. Thus the plots should represent a valid prediction of amplifier response to low level inputs, and is therefore useful in predicting stability limits.

Closing the loop had a substantial impact on the amplifier response. The open loop time constant of the modified amplifier was approximately minutes. Loop closure improved the dynamics substantially, giving a full scale response in 9 minutes, and a 90% rise time

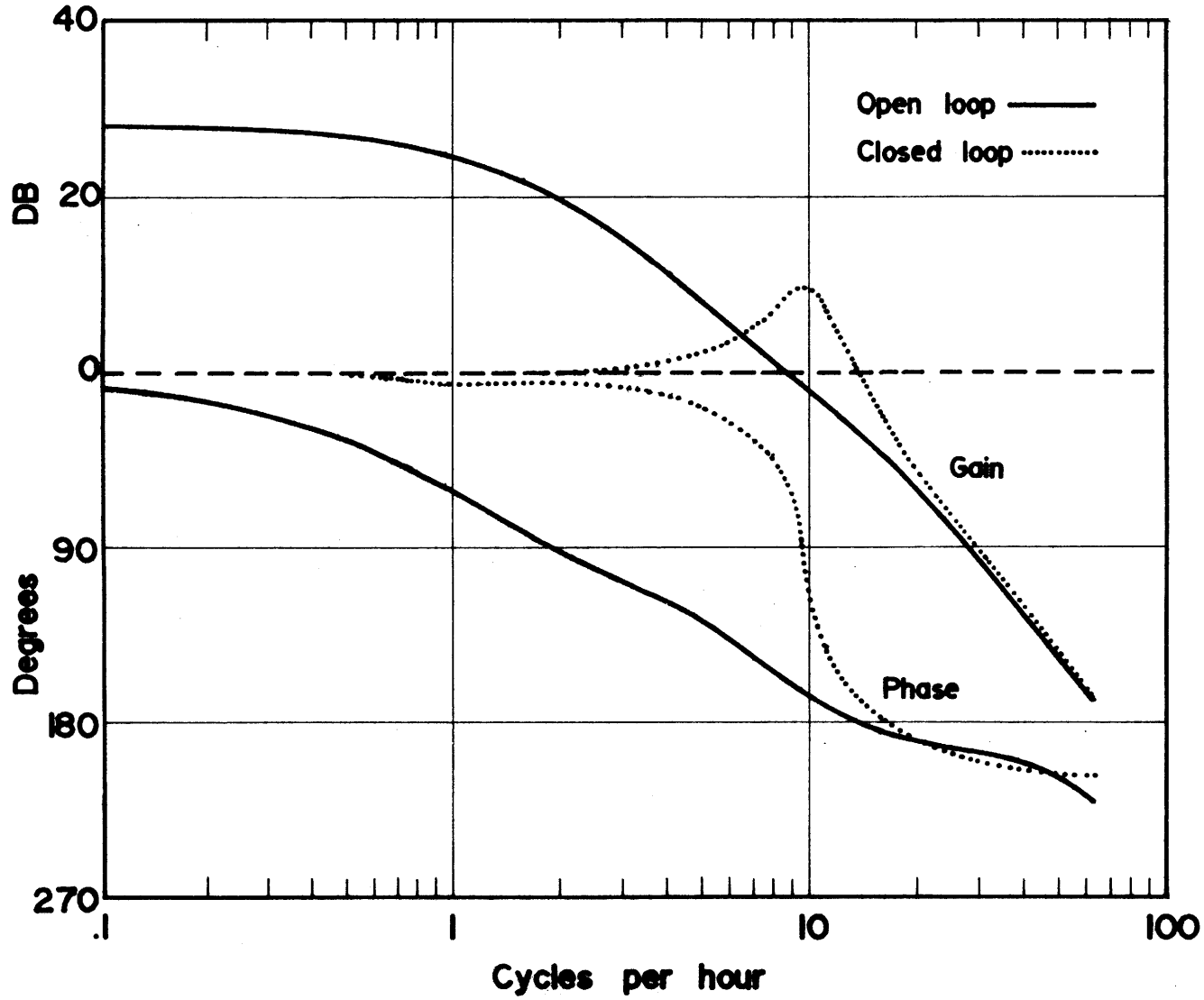

Figure 5-4.6: Bode plot of open and closed loop amplifier performance.

of approximately 2 minutes.

Gain and frequency response represent two of the five parameters useful for analyzing amplifier performance that were discussed in chapter 1. The other three, input impedance, output impedance, and common mode rejection, will be related to the thermal amplifier.

The input impedance is the thermal resistance in the sensor to heat flow from a temperature input. There will be an initial heat flow drawn by the sensor to come into temperature equilibrium with the input. After this transient the steady state heat flow to the sensor will be from heat leakage to ambient, and will be a function only of sensor insulation thickness. Thus, the steady state input impedance can be made arbitrarily large by increasing the sensor insulation.

The output impedance is a function of the load resistance being driven by the amplifier. Ideally there would be no output impedance, but for this design the minimum output impedance will be r_L, or the minimum resistance value of R_v or R_L. Since r_L also appears in the denominator of the gain expression, maximum gain and minimum output impedance occur when r_L is made as small as possible.

Finally, the common mode rejection of the thermal amplifier is theoretically unlimited. The identical temperature input to each sensor, with the same sensor fluid, will create identical pressures, and no change in the resistor-manometer fluid levels. High temperature will create high pressure, but identical construction should produce parts

deflect identically under pressure, until they burst from pressure generated by the sensors. The common-mode operating temperature limit is imposed only by structural considerations, and material limitations.

This completes the discussion of the model and experimental results. The next chapter will discuss these results and suggest conclusions. Finally, recommendations for further research will be presented.

CHAPTER 6: CONCLUSIONS, APPLICATIONS, AND RECOMMENDATIONS FOR FURTHER RESEARCH

Section 6-1: Brief chapter summary.

Section 2 details the six major conclusions that can be drawn from this work. Essentially a working operational amplifier has been developed, and successfully modeled. The model has been directly related to the physical components of the device, and a method suggested to select physical dimensions to produce desired dynamic performance. A small, but significant body of construction expertise has been generated, and the device has shown itself to be worthy of further development and investigation.

Section 3 describes further research that must be done to bring the thermal operational amplifier to a state of practical implementation. The passive thermal circuit elements, such as resistors and capacitors, need to be developed to inter-connect amplifiers and to configure them into operational circuits.

Section 4 illustrates potential applications for the thermal amplifier. The temperature regulator represents the most useful control device that could be readily built. A thermal operational amplifier based control circuit would draw power for the logic from the heat source being controlled, hence would not require outside power, and would consume no power when no heat was available. Such circuits could be redundant safety systems for electronic temperature controls in the event of power failure. They also represent a potentially inexpensive way to implement a high accuracy temperature controller.

Section 6-2: Conclusions.

This section details the six major conclusions that can be drawn from this work. While hardly exhaustive these conclusions represent the major findings of this research, and the goals towards which it was directed.

The first, and most important conclusion, is that a working, differential, thermal, operational amplifier has been built, and shown to be a physically realizable device. The experimental prototype has met the original requirements for such a device, that it: use only heat for energy, amplify the algebraic sum of temperature inputs on differential sensors by some constant factor greater than unity, and produce a temperature output. The gain of 20 proves remarkably constant over the range of operation, and hysteresis appears undetectable.

The second conclusion is the performance of the thermal amplifier can be modeled and predicted. The mathematical model of the amplifier, constructed from lumped parameters, provided good agreement with observed experimental results. A corollary to this conclusion is the necessary degree of model complexity has been delimited. The original twenty-first order model was reduced to a seventh order model based on model element values. This in turn was shown reducable to a simple second order system for open loop step response prediction, while the seventh order model was necessary for the faster

closed loop response. Predictable response with this verified model enables future designers to test a design before construction, and establishes that the important system parameters have been found and defined.

The third conclusion is the amplifier response has been related to the important physical parameters of the amplifier. The dynamic amplifier response has been predicted solely in terms of physical dimensions and material properties. The relative significance of these various properties and dimensions have been assessed and the value of each model element has been quantified in terms of them. The critical trade off of amplifier gain and range has been identified in terms of the dimensionless maximum to minimum resistance ratio of the two resistors. A simple expression for gain has been developed, solely in terms of resistor parameters and source temperature. Finally, experimental results have been in good agreement with the analysis.

The fourth conclusion is that a method of selecting physical amplifier parameters to produce some desired performance has been demonstrated. The optimal design technique, which is not a completely rigorous method to determine the behavior of the amplifier, does prove a simple way to produce specific amplifier dimensions. The resulting design will have the desired resistance ratio, and sufficient sensor capacity to modulate the resistors. The material properties and part dimensions have extremely complex interactions, which would make manual amplifier design a difficult task. This numerical design technique can

maintain amplifier dimensions within innumerable constraints, and produce the "best" design for a given performance measure or index. The technique is illustrated and successfully employed in this work.

Fifth, a small but important body of practical construction experience for thermal amplifiers has been produced. The problems posed by: flexible diaphragms, air diffusion, material specifications, sensor fluid characteristics, and differential thermal expansion have all been encountered and surmounted in this research. This represents a portion of the learning curve the next investigator does not have to produce. Because the final product was a working amplifier, the solutions to the various problems were valid, but not necessarily optimum.

The sixth and final conclusion is the thermal amplifier is worthy of more development. The predictable nature of the amplifier response makes specific application designs possible. The time constant can be tailored with the resistor/junction block RC values over an extremely wide range. The substitution of sodium potassium for silicone oil as the conducting fluid in the test amplifier would reduce the time constant to 22 seconds. The device itself is simple, reliable, and has only one moving part (the diaphragm). Gains as high as 100 could be achieved single stage, giving a two stage amplifier a total gain of 10,000 - more than enough for a practical operational amplifier. With the development of mating passive thermal elements, such as resistors, the amplifier could be configured in standard control circuits to perform many control functions.

Section 6-3: Recommendations for further research.

In this thesis the thermal operational amplifier has been taken from concept to working prototype. Large amounts of experimental work remains to develop thermal resistances and capacitances that can be easily connected with the amplifier in operational circuits. It is also necessary to verify or adjust the amplifier model to accurately predict performance in operational circuits, and over an extended range of frequencies.

This research has been concerned with the active thermal element; the amplifier. Equally important to its practical application are the passive thermal elements; resistors, conductors, and capacitors, that are necessary to create inconnected circuits. Even the best thermal conductors, copper and diamond, have substantial thermal resistance. To minimize unwanted resistance thermal conduction paths are kept as short as possible. This imposes geometry constraints on an amplifier designer for circuit layout. Thermal resistance, and capacitances that can be inserted reliably and repeatedly into circuits, with predictable values, have yet to be developed. These components are the next step for usable thermal logic.

The heat pipe represents a conductor/resistor possibility that should be investigated. Since heat pipes conduct heat long distances with little temperature drop they could function as low resistance conductors between amplifier stages, input and outputs, and circuit components.

The amplifier and model developed has been tested for open and closed loop response. However, for sinusoidal response an experimental apparatus capable of generating a range of thermal input frequencies must be built, and the predicted Bode plots verified. This will be fairly sophisticated equipment, and will represent a significant development project. With foresight the same equipment should be usable to test operational circuit performance as well.

Finally there remains the endless task of making the amplifier more compact and reliable. During the course of this research the amplifier was reduced in size from 9" x 12" to 2-5/8" x 2-5/8", roughly a factor of four. The number of future applications will be a strong function of size and reliability. Better design and materials will hopefully reduce amplifier size by another order of magnitude.

Section 6-4: Potential applications for the thermal operational amplifier.

A logic that "thinks" with heat; using heat for inputs, outputs, and power supply, has obvious application for thermal control. Indeed, efficiency improvements, and the elimination of transduction motivated this development of thermal logic for thermal control. In the broad application category comprised by thermal control, three specific areas have been identified that the thermal amplifier could be particularly well suited. These are: a discreet device temperature regulator, an exothermic reaction safety control system, and totally thermal active control logic. This list is hardly exhaustive, but each example will be discussed briefly to illustrate the nature of potential applications.

A thermal operational amplifier could be the basis for a controller that regulates temperature of a free standing device using only thermal power. For example, a fuel cell must combine its reactants at a fairly constant temperature for maximum efficiency, while giving off heat during the reaction. A thermal logic system could easily regulate the wall conductivity of such a device, metering heat loss to maintain the desired temperature. The logic would use the heat of the cell itself for power. A similar application would be temperature regulation of a board of electronic components, whose constant temperature is important for their operation. The devices give off heat, which would power logic and be metered to the environment.

In both cases a discrete system would be temperature regulated by logic that would not "come alive" or draw power until there was heat present to be controlled.

An exothermic reaction safety, or back-up, control system is primarily configured as a controller. In a great many industrial operations, and certainly in nuclear power generation, the processes involved are exothermic, or heat generating. Generated heat, if not dissipated, would heat the reactants and accelerate the reaction. Most such processes are electronically temperature controlled to avoid a potentially unstable "runaway". A thermal logic controller could be a redundant back up and/or the primary control system for such a process. It would be completely immune to electrical power failure, and highly insensitive to the operating environment. Drawing no power it's presence would not have a noticable affect on the system until needed. The control limits of such a back up system would be set outside an electrical system boundaries, so the thermal logic would become active only if the electrical system failed. In a recent highly publicized incident where a primary and secondary core system cooling failed because of a common power supply failure, a totally thermal back up control would have been ideal.

Finally, the thermal operational amplifier opens the possibility of active totally-thermal control. Active single-element temperature control is available, as described in chapter one. The thermal

amplifier represents the first totally general thermal logic building block. Instead of just modulating thermal resistances the amplifier allows the complex operations of temperature integration and differentiation to be performed totally in the thermal domain. All the control expertise and strategies developed in electronics, including optimal control, can now be applied almost intact to the thermal control. Leads, lags, filters, followers, etc. can be built with time constants tailored to the application. Thermal logic can take its place along side electronics, hydraulics, and fluidics as an independent control discipline with its unique elements.

Interfaces between the thermal and other control disciplines are simple mechanical devices already developed. A temperature can produce an electrical proportional signal through a thermistor or thermocouple. A temperature can turn on or off a control valve through a vapor or wax filled expansion bellows, or produce almost any required mechanical motion. With the sensors removed the amplifier's resistors could respond directly to pressure.

With diverse forms and simple interfaces with other control disciplines thermal logic could assume much of the thermal control performed today in some other medium.

APPENDICES

APPENDIX A1: SYSTEM MODELING WITH THERMAL BOND GRAPHS

In the last generation we have seen the birth of Dynamic System Analysis as a separate discipline; several methods of mathematically modeling a system are in current use. One of the most powerful of these is the bond graph method, invented by H. M. Paynter, circa 1960, at M.I.T., (Ref. 10) This method has been refined to the point that references are easily found on its unambiguous application to fluid, electrical and mechanical systems. (Ref. 17,16,23,28) A similar method of attack is used in each case: one accounts for power (the product of an effort and flow variable) and traces its flow between system elements. However, In purely thermal systems, modeling rules have not been so clearly defined.

The crux of the thermal modeling problem is which effort and flow variables to use. Since there seems to be unanimous agreement that temperature is the most desirable (and perhaps the only possible) effort variable, the choice of flow variable remains the only question. Most bond graph researchers to date have used entropy flow as the flow variable. (Ref. 22,21,27,28). This has the advantage of being consistent with previous system models of other energy domains since the effort and flow variable multiply to give power. However, the traditional heat transfer variable is heat flow; unfortunately the product of heat flow and temperature is not power.

A method eliminating the complexity of entropy flows yet avoiding second law violations, has been developed using effort and flow

variables which do not multiply to give a power product. Equation formulation is not altered from normal bond graph methods except when crossing the boundaries of the thermal domain; a transformer bridges these boundaries. The effort variable is temperature (T) but the flow variable is heat flow (q) - the traditional pair.

A bond graph whose effort and flow variables do not multiply into power have been labeled "pseudo bond graphs". (Ref. 17) In place of this pejorative label the appellation "thermal bond graphs" is offered. Bond graphs, like any modeling system, are a tool used for analyzing and predicting dynamic system behavior. The criteria for deciding how to model any system should be utilitarian and empirical, not doctrinaire or dogmatic. To this end a utilitarian justification for the use of thermal bond graphs is presented: they work.

The 0 and 1 junctions represent common effort and common flow respectively. This remains true if T and q are now the effort and flow variables. It also remains true that for an n-port 0-junction $q_1 + q_2 \ldots q_n = 0$; and for an n-port 1-junction, $T_1 + T_2 \ldots + T_n = 0$. Power flow in each case is identical with q, i.e., the flow variable happens to be the power rather than part of the power product.

The resistance (R) and capacitance (C) elements will represent the same concept in a T-q bond graph model as they do in the traditional heat transfer sense. In basic bond graph theory an R element is that element which has a functional relationship between the effort and flow

variables. The traditional thermal resistance is the constant of proportionality between temperature and heat flow. Hence the traditional thermal resistance is identical to the thermal bond graph resistance. Unlike entropy relationships, thermal conductivities of most materials are easily verified and well-documented. Moreover, such a system modeling method could be more easily employed by those whose background was primarily heat transfer and not system modeling: they are already familiar with heat flow - temperature relationships. In this suggested method, the R element is no longer an energy dissipator, but always appears off a 1-junction and induces a drop in temperature. Heat flow and hence energy flow is the same into and out of a thermal resistance.

A generalized bond graph C element has a functional relationship between the flow varible and the first derivative of the effort variable. The traditional thermal capacitor has a linear relationship between heat flow and the time rate of change of temperature. With temperature and heat flow as our effort and flow variables the traditional capacitor is identical to the bond graph capacitor and all thermal capacitance data can be employed by the thermal modeler.

Besides junctions and 1-ports, transformers and gyrators are needed to bridge the boundaries between thermal domains and non-thermal domains. A transformer is a device 1) with two ports, 2) where the power in equals the power out, and 3) where the input effort and flow variables enjoy complementary functional relationships with the effort and flow variables out. Since the product of the effort and flow variables in

all but the thermal domain equals power, when crossing a domain boundary the product of the e and f variables in the non-thermal domain will equal only the flow variable in the thermal domain.

As in usual bond graphs, non-thermal power is $e_2 \times f_2$; however, thermal power equals simply f_1. An element, - called the Modulated Thermal Transformer (MTF_t) - models energy transfer between other domains and the thermal domain; it is the only new element required. It is shown in figure A1.1.

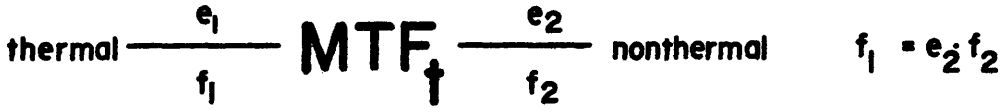

Figure A1.1: Modulated thermal transformer.

If there were some proportional relation between e_1 and e_2, in addition to $f_1 = e_2 \times f_2$, then this device acts exactly like a transformer. A good example of this is a thermocouple, where the temperature, e_1, generates a proportional voltage, e_2. In each case the most important feature of this device is $f_1 = e_2 \times f_2$.

With these small changes in element use bond graphs can be applied with the same clarity and ease of equation derivation to thermal systems as to non-thermal systems. The resulting equations will be familiar heat transfer equations and in terms of the readily

measured variable, temperature.

To illustrate the use of these suggested effort and flow variables, a model of a thermistor, the circuit of which is shown in figure A1.2, will be presented. This will display thermal-domain modeling, as well as the transition between energy domains.

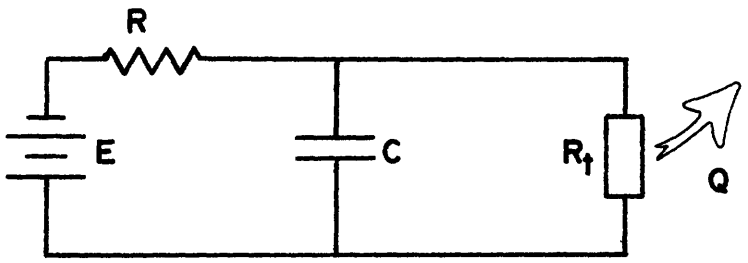

Figure A1.2: Thermistor circuit.

The thermistor is a temperature sensitive resistor. The electrical portion of the circuit is quickly modeled as figure A1.3:

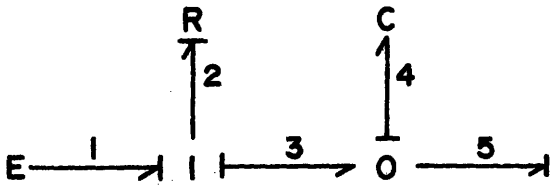

Figure A1.3: Bond graph of electric portion of thermistor circuit.

As a thermal system the thermistor has a surface thermal resistance, a thermal capacitance, and an internal conduction resistance all in series with a transformer that converts electrical energy into thermal

energy. All of the resistances and capacitances can be lumped into single elements in discreet positions to simplify the model. A thermistor (figure A1.4) is a temperature-sensitive transformer converting electric power to heat:

heat flow ▷ Internal conduction resistance of thermistor ▷ Heat stored in mass of thermistor ▷ Surface Heat transfer resistance ▷ Temperature medium

Figure A1.4: Thermistor thermal circuit.

Taking this simple heat flow diagram we can construct the following bond graph model (figure A1.5) of the heat flow:

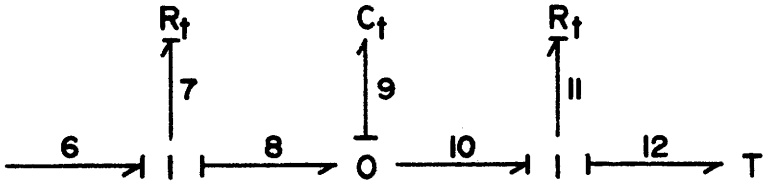

Figure A1.5: Thermal bond graph of thermistor.

These two models can be combined into figure A1.6, the total bond graph of the thermistor,

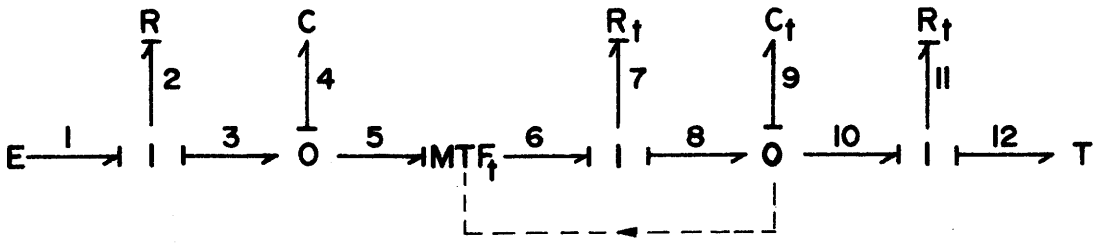

Figure A1.6: Total thermistor bond graph.

where the temperature of the transformer modulates the rate of electrical energy conversion in the thermistor.

Now the equation derivation can go forward in the standard manner for bond graphs, the only exception being the conversion in the transformer, where $e_5 \cdot f_5 = f_6$.

Bond graph equation derivation starts by writing the constitutive relations for the independent energy storage elements. In this case these are capacitors C_4 and C_{t9}:

$$\dot{e}_4 = f_4/C_4 \tag{A1.1}$$

and

$$\dot{e}_9 = f_9/C_{t9} \tag{A1.2}$$

The task is now to express f_4 and f_9 in terms of E, T, e_4, e_9, and physical system element values. From the definitions of '0' and '1' junctions it is known:

$$f_1 = f_2 = f_3 \tag{A1.3}$$

$$f_6 = f_7 = f_8 \tag{A1.4}$$

$$f_{10} = f_{11} = f_{12} \tag{A1.5}$$

$$e_3 = e_4 = e_5 \tag{A1.6}$$

$$e_8 = e_9 = e_{10} \tag{A1.7}$$

From the definition of the R element it follows:

$$e_2 = f_2/R_2 \tag{A1.8}$$

$$e_7 = f_7/R_{t7} \tag{A1.9}$$

$$e_{11} = f_{11}/R_{t11} \tag{A1.10}$$

The thermistor itself acts as a modulated transformer whose electrical resistance depends on its temperature. For the purpose of this example we will assume this resistance can be expressed as a function of the temperature e_9. The voltage across the thermistor and the current through it are related by:

$$e_5 = f_5 R(e_9) \tag{A1.11}$$

The system behavior is completely described by the two equations governing the independent energy storage elements, the two capacitors:

$$\dot{e}_4 = \frac{1}{C_4}\left[\frac{E-e_4}{R_2} - \frac{e_4}{R(e_9)}\right] \tag{A1.12}$$

$$\therefore \quad \dot{e}_9 = \frac{1}{C_{t9}}\left[\frac{e_4^{\,2}}{R(e_9)} - \frac{e_9-T}{B_{t11}}\right] \tag{A1.13}$$

Note that passing through the transformer is the only place where using a non-power pair of effort and flow variables affected the equation derivation process.

The proceeding example also illustrates the ease with which ENPORT-1 could be modified to accept the new element, the thermal transformer. Since the program already accepts the standard transformer,

the addition of this new element would only require a modification and renaming of this existing element. The constitutive relation would change from that of the normal transformer:

$$\begin{bmatrix} e_2 \\ f_2 \end{bmatrix} = \begin{bmatrix} m & 0 \\ 0 & \frac{1}{m} \end{bmatrix} \begin{bmatrix} e_1 \\ f_1 \end{bmatrix} \qquad \text{(A1.14)}$$

to that of the thermal transformer:

$$\begin{bmatrix} e_2 \\ f_2 \end{bmatrix} = \begin{bmatrix} m & 0 \\ 0 & e_1 \end{bmatrix} \begin{bmatrix} e_1 \\ f_1 \end{bmatrix} \qquad \text{(A1.15)}$$

The program could operate on bonds on either side of this element in the normal fashion.

In the preceeding example the second law was not discussed because the only place it would apply is to heat flow, where it would require heat to flow in the direction of the temperature gradient. In the following system heat is converted into work so that a model with a potential second-law violation can be illustrated.

The system in figure A1.7 is the traditional gas-piston where heating the gas causes the piston to exert a force on the connecting rod. This example is used because it will illustrate that the second law can be observed in most systems by demanding that no heat flow against a temperature gradient.

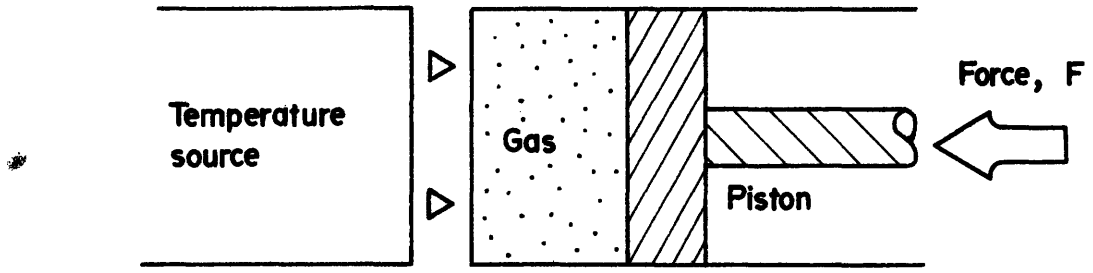

Figure A1.7: Gas-piston system.

The heat flow can be described (figure A1.8) as follows:

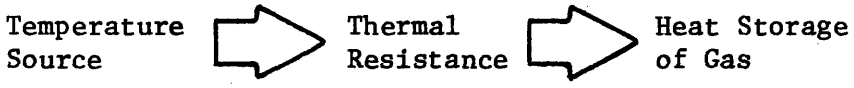

Figure A1.8: Thermal circuit of gas piston system.

There will be one thermal resistor and one thermal capacitor.

Ignoring friction on the piston, the resulting bond graph of the system (figure A1.9) becomes:

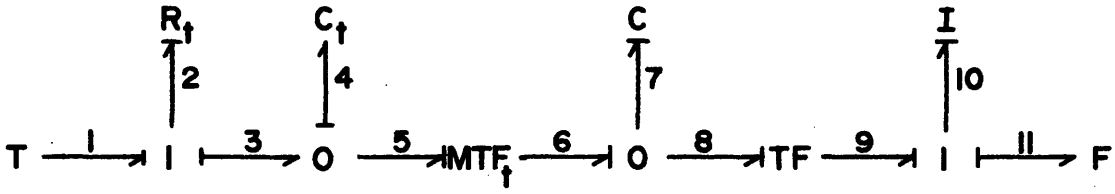

Figure A1.9: Total bond graph of gas-piston system.

Where C_7 is the effect of gas compressibility and I_{10} is the inertia of the mass in the piston.

The two independent energy storage elements are C_{t4} and I_{10}. The constitutive relations for these are:

$$\dot{e}_4 = f_4/C_{t4} \tag{A1.16}$$

and

$$\dot{f}_{10} = e_{10}/I_{10} \tag{A1.17}$$

From the junction definitions the following can be written directly:

$$f_1 = f_2 = f_3 \tag{A1.18}$$

$$f_9 = f_{10} = f_{11} \tag{A1.19}$$

$$e_3 = e_4 = e_5 \tag{A1.20}$$

The resistor behavior is identical to that in the first example. The important aspect of this example is that heat can flow both ways through the thermal transformer. If the system is in equilibrium an increased force on the piston will cause the gas to heat and transfer that heat to the temperature source. The thermal transformer is defined by the equation of state of the perfect gas, PV=nRT, and the relation that $f_5 = e_6 \cdot f_6$. In other words, the PV product of work out the fluid port will equal the heat that is transferred to the gas minus that which is stored by the gas-nothing more than the first law.

The second law is contained in the structure of the system. Any heat to work converter will have some thermal capacitance, however

small. This will require an '0' junction or temperature node next to each transformer. The only way the second law could then be violated is for heat to flow against the temperature gradient into this node. While this is not a rigorous proof that system models properly constructed will not disobey the second law, an exception is not apparent. Since work can be converted with 100% efficiency into heat there is no problem with heat flow in the other direction. Because the first and second laws are built into the system structure, the equations can be derived in the straight forward manner of bond graphs.

Using temperature and heat flow as effort and flow variables one can model what are intuitively thermal resistors and capacitors as such. The resulting system representation preserves the clarity and ease of equation derivation that have traditionally characterized bond graphs. The advantages of using this non-power pair are more than enough to justify the small bit of deviation from standard bond-graph representation. Thus the author perceived this method as the most rational compromise between retaining the intuitive feel of traditional thermal modeling and minimizing the changes to the powerful bond graph technique.

APPENDIX A.2: FILM AMPLIFIER MODEL CONSTRUCTION

Section A2-1: Summary of appendix.

This appendix describes the construction of a mathematical model to predict amplifier behavior.

Section 2 details the translation of the amplifier geometry into specific subscripted dimension variables. The amplifier is modeled as a series of discreet thermal resistances and capacitances, expressed as functions of dimensions and materials. The lumped thermal elements are used to model the corresponding distributed effects in the amplifier. Materials used in different amplifier parts are given subscripted variable designation.

Section 3 describes specific thermal model elements. Using the dimension and material variables of the previous section an expression is derived for the value of each element. The interaction between the different elements is discussed and characterized. A bond graph model of the amplifier is presented.

Section A2-2: Amplifier model topology.

This section details the physical parts that make up the amplifier. In chapter three the relation of amplifier performance to fixed resistor parameters (k, R_v, and R_L) was examined with the linear model. The resistor parameters ultimately derive their value from the physical dimensions of the amplifier. This appendix will relate the physical dimensions of the amplifier to a dynamic model.

Resistor parameters R_v, R_L, and k, are first selected. The selection of physical dimensions, to produce desired resistor parameter values, can be done rationally if the effect of each dimension can be predicted beforehand. Note that some dimensions are constrained by physics to vary in fixed ratios with other dimensions.

A general amplifier layout has been decided from broad practical considerations. Each part will be specifically labeled, and the physical dimensions given a unique label. The sensors and resistors are modeled separately since they are physically separate. The sensors will be examined first.

A detailed diagram of a sensor is shown in figure A2-2.1. The section view labels the various interior parts. The original sensor design called for a diaphragm with a negligible spring rate. This makes the geometry of the edge connections insignificant, because the diaphragm can deflect any amount required to touch both walls. Both sensors are assumed to be identical. The diaphragm material properties

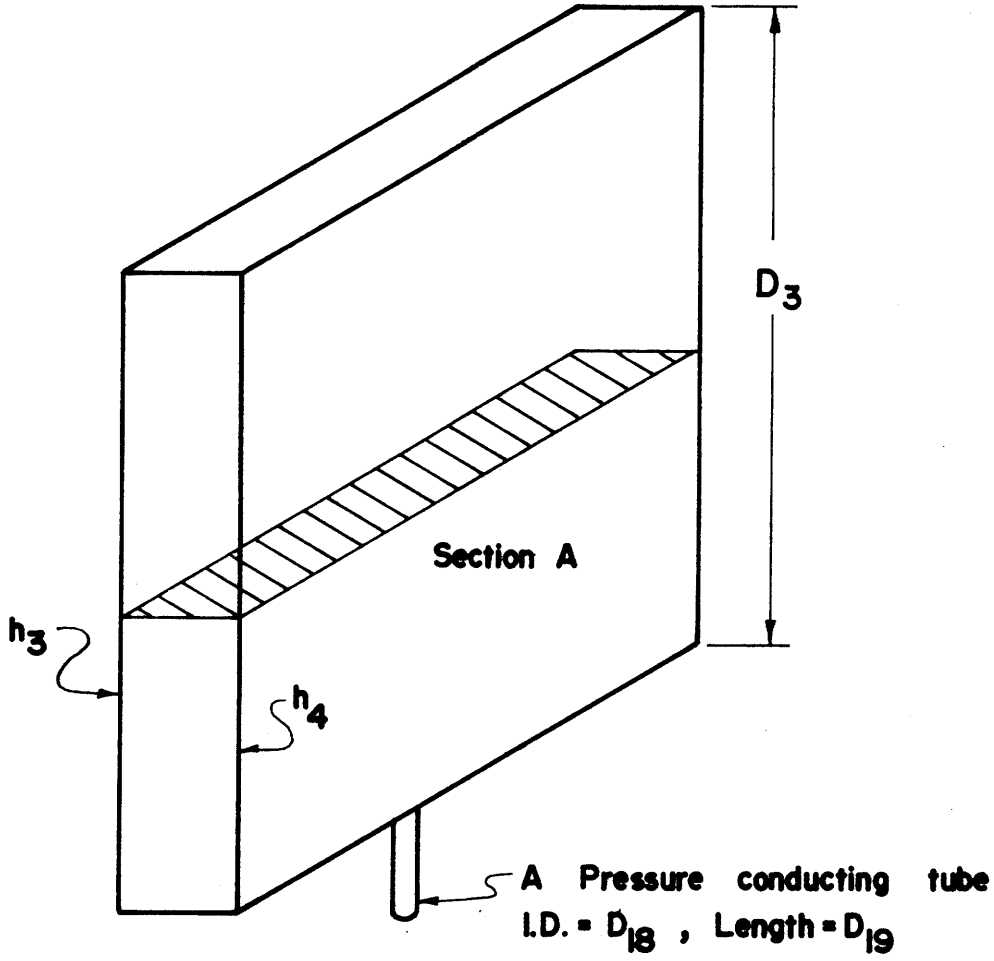

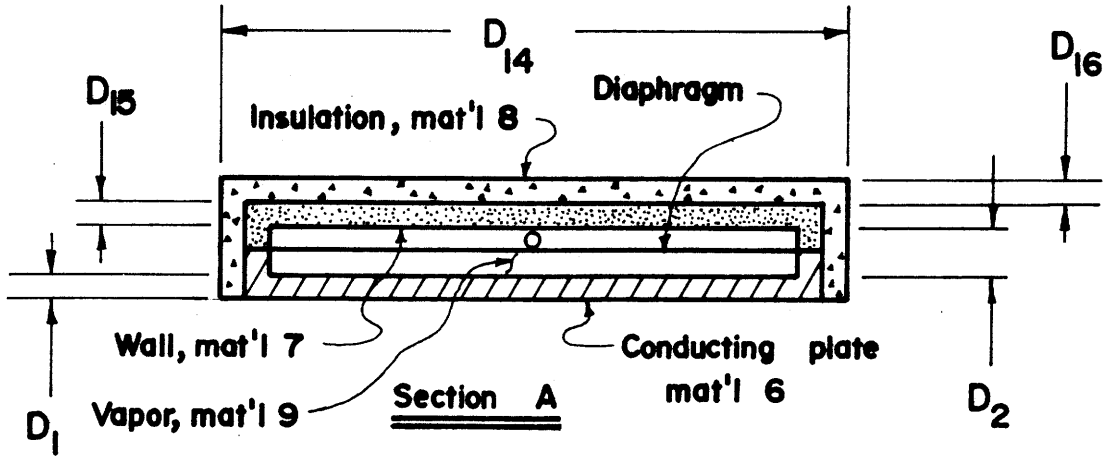

Figure A2-2.1: Sensor dimensions variables.

should not influence the sensor, for the case of a negligible diaphragm spring rate, so are not indicated. The remaining five materials in the sensor are in a heat flow path. They will represent thermal resistance and capacitance, which can be calculated from known material properties. No method of mechanical fastening has been indicated, the surfaces could be assumed bonded to one another. Mechanical fasteners will modify the effective thermal conductivity of the material they pass through and should be accounted for.

All dimensions in figure A2-2.1 are shown as subscripts variables. In numerical order they are as follows:

D_1 ≡ Thickness of the conducting plate

D_2 ≡ Inside thickness of sensor chamber

D_3 ≡ Height of sensor

D_{14} ≡ Width of sensor

D_{15} ≡ Thickness of sensor structural wall, sides, back assumed equal

D_{16} ≡ Thickness of sensor insulation, sides and back assumed equal

D_{17} ≡ Thickness of wick (optional)

D_{18} ≡ Internal diameter of pressure conducting tube

D_{19} ≡ Length of pressure conducting tube

The several materials used in the sensor are numbered, appearing as subscripts on the material property to be identified. The material numbers, in order, indicate:

Material 6 ≡ Conducting plate material

Material 7 ≡ Sensor wall structural material

Material 8 ≡ Sensor wall insulation

Material 9 ≡ The vaporizing fluid

Material 10 ≡ Wick material (optional)

Material 11 ≡ Insulating or nonconducting fluid

Each material will have a thermal conductivity k, a density ρ, and a constant pressure specific heat (or heat capacity) C_p associated with it. Two other parameters, h_3 and h_4, which appear in figure A2-2.1, are the convective heat transfer coefficients to the two sides of the sensor. These coefficients, also called film coefficients, are the surface heat transfer resistance. The film coefficient for the conducting plate is h_3, for the back of the sensor, h_4. The heat loss through the sides is assumed to have the same film coefficient as the sensor back.

Some tacit assumptions have been made in designating significant dimensions. First, the conducting plate and back of the amplifier will have the same outer dimensions. Second, all four sides are assumed to have the same wall and insulation thickness as the back. Finally, the effects of thermal conduction down the pressure conducting tube is ignored.

With these assumptions the description of the sensor parameters is complete. The next task is to examine the two-resistor amplifier section.

The film ECR's and junction plate are shown in figure A2-2.2. The two ECR's are identical, except for the material on the outside walls which can differ, as can the thickness of the outside walls. The subscripted dimensions, in order, are:

D_4 ≡ Width of ECR's and junction block

D_5 ≡ Film section thickness

D_6 ≡ Thickness of ECR interior wall, both ECR's.

D_7 ≡ Thickness of junction block

D_8 ≡ Height of ECR film section

D_9 ≡ Thickness of sides, all equal on film section

D_{10} ≡ Inside width of reservoir

D_{11} ≡ Inside thickness of reservoir

D_{12} ≡ R_V outside wall thickness

D_{13} ≡ R_L outside wall thickness

D_{20} ≡ Height of junction plate

The materials in the two resistors, reservoirs, and junction plate are designated as follows:

Material 1 ≡ R_V outside wall material

Material 2 ≡ Interior wall material of both R_V and R_L

Material 3 ≡ Junction block material

Material 4 ≡ R_L outside wall material

Material 5 ≡ Conducting liquid

Material 12 ≡ Resistor side wall material

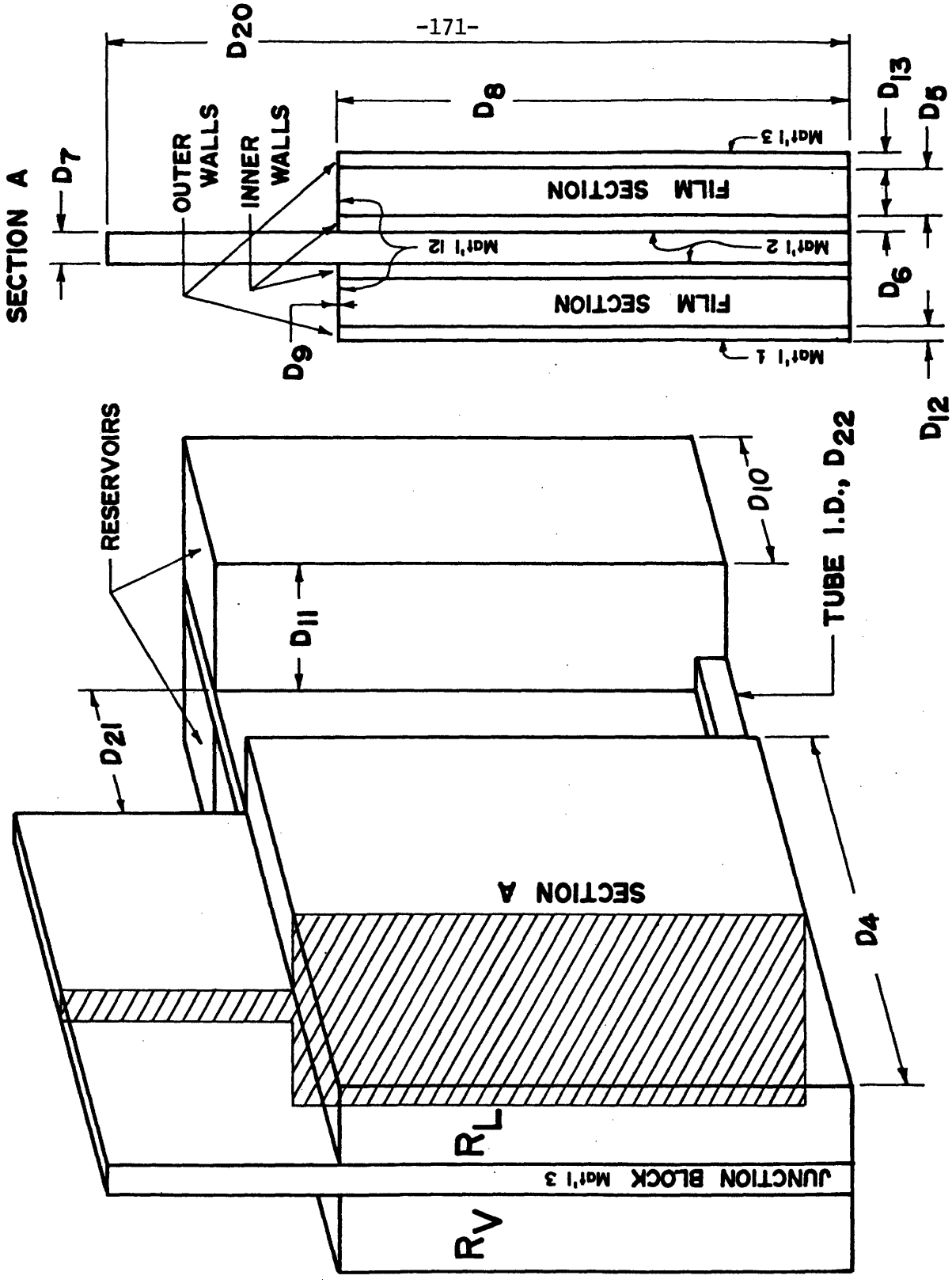

Figure A2-2.2: Amplifier dimension variables.

Finally, there are two film coefficients associated with the amplifier. The convective heat transfer coefficient for R_v's outside wall is h_1. The outside wall film coefficient of R_L is h_2. The amplifier section is more complex than the sensors and has more implicit assumptions.

Assumptions are contained in the parameters designated as significant. First, the film section edges have the same film coefficients as the front and back. Second, the pressure conducting tube attachments to film section and reservoirs have no thermal effect on the system. Third, there are no mechanical fasteners, all surfaces are assumed bonded. The effect of fasteners would be accounted for by altering the thermal conductivity of the side materials. Fourth, the reservoir material is unimportant, and the thermal leakage to the reservoirs is ignored. Fifth, the inside walls of R_v and R_L are made of the same material. This is to minimize the bowing from a "bimetal" effect. Finally, the thermodynamics of the amplifier are considered much slower than the fluid mechanics of the conducting fluid, and the geometry of the flow passage between film section and reservoir is left unspecified.

This completes the labeling of the physical components of the amplifier. With a standardized designation for each part a coherent modeling process can be explained. The next section will translate the physical dimensions into thermal parameters.

Section A2-3: Complete thermal amplifier model.

In this section the thermal model of the amplifier will be described. The previous section labeled the significant dimensions with specific variables. These dimensions explicitly size all the thermal elements in the thermal circuit. There are actually two independent thermal circuits in this amplifier. The two sensors, and the two U-tube manometers formed with the conducting fluid, act independently of the heat flowing from the source to the sink. If the conducting and insulating fluids have no vapor pressure, there is no feedback to the sensors as to the amount of heat is flowing through the conducting fluid, or at what temperature. Thus the thermal model of the amplifier can be broken into two portions. The first will be the two sensors opposing each other through the two legs of the U-tube manometer. The second part will be the purely thermal circuit formed by the source, variable resistors, junction plate, and sink. This second part is dependent on the sensor circuit for the values of R_V and R_L. The independent functioning of these two thermal circuits is critical in developing unilateral thermal control systems. The sensor circuit will be modeled first.

The sensor circuit, and the parallel bond graph model, is shown in figure A2-3.1. Figure A2-3.2 is a more detailed drawing of a sensor and its associated bond graph. The topology of the bond graph parallels the physical layout of the circuit, as much as possible, for clarity. For an explanation of thermal bond graphs see appendix 1. In

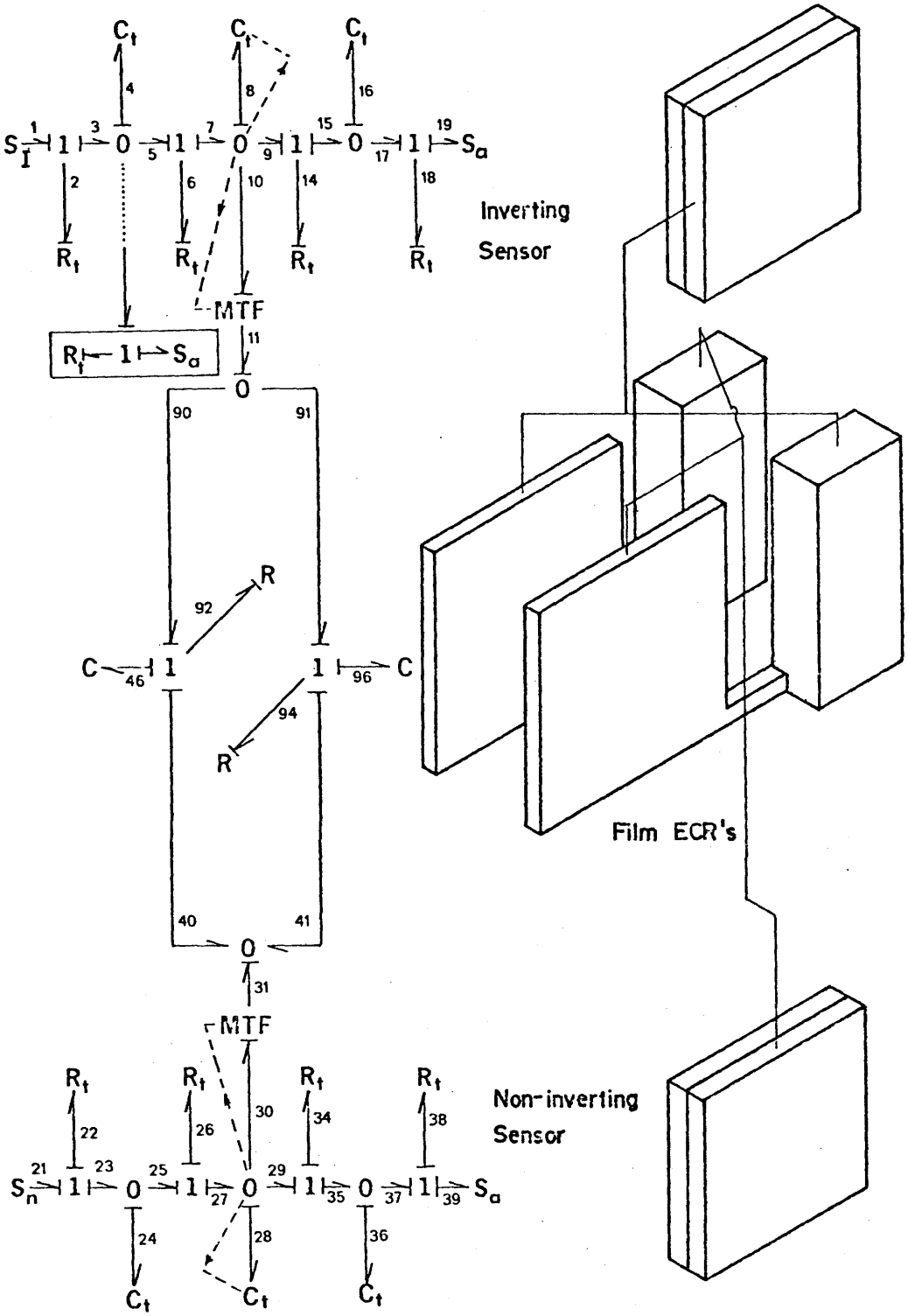

Figure A2-3.1: Sensor circuit and parallel bond graph.

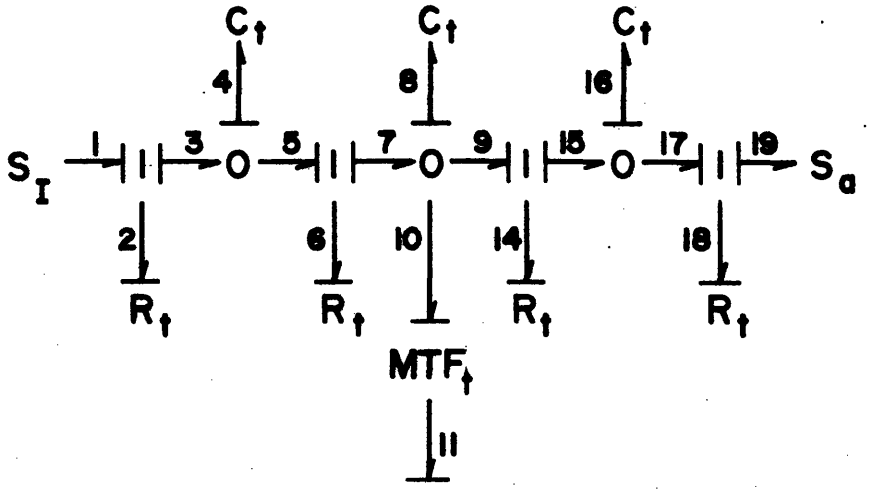

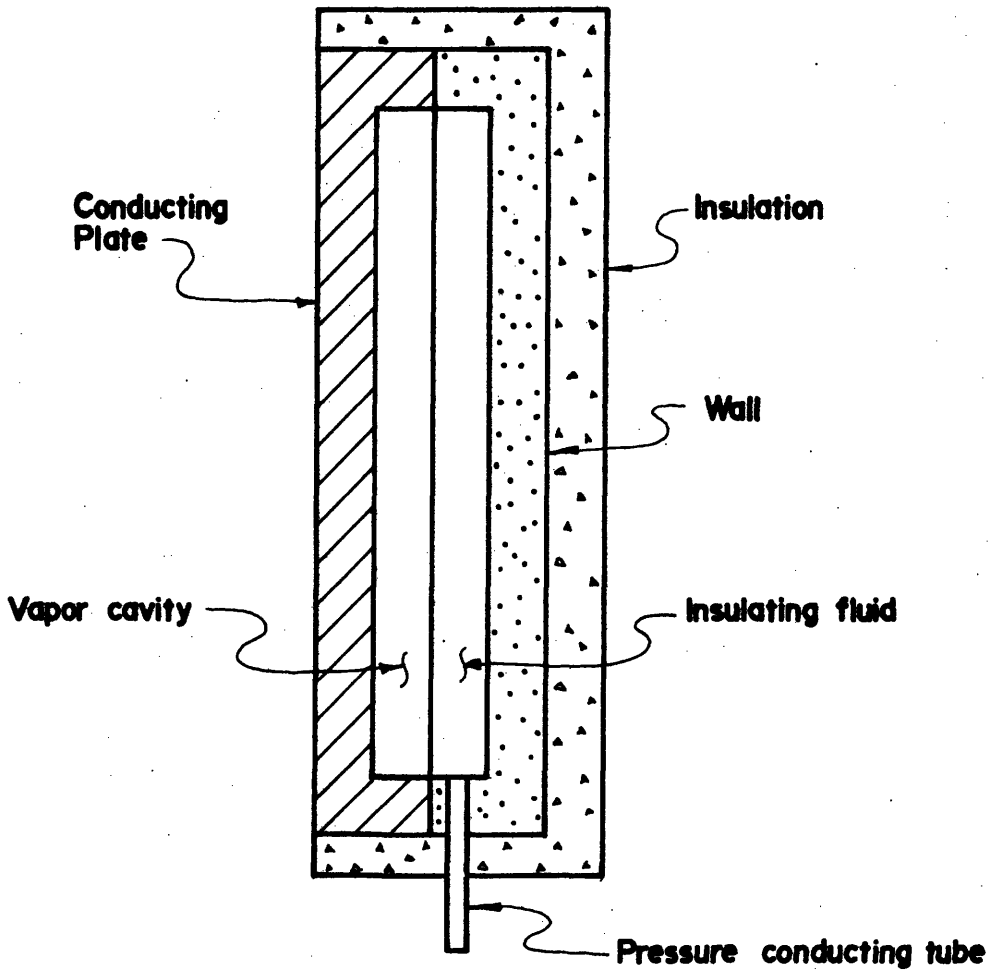

Figure A2-3.2: Detailed sensor diagram and parallel bond graph.

brief;'0' junctions are the temperature nodes, '1' junctions are common flow or series connection, and R's and C's are resistances and capacitances respectively. The bond number is used to designate the element, i.e. C_4 is the capacitor on bond 4. It is appropriate at this point to stop and list what each element corresponds to physically in the circuit.

S_I is the inverting sensor input temperature source. The source is assumed to have no dynamics of its own, but instead can supply, or sink, all the heat necessary to maintain its temperature value. If the heat drawn by the sensor is small, compared to the heat capability of the source, this assumption will be valid. To model a source with dynamics bond 1 can be broken and the source bond graph appended to the sensor graph.

R_2 is the sum of the surface resistance and half the thermal resistance of the conducting wall. All resistances and capacitances in this model will be lumped parameters. This means a distributed quantity is lumped into a single parameter. The resistance of the conducting plate is distributed throughout its entire thickness. For modeling purposes resistance is assumed to lie at the surface, half on each side of the plate. This allows the plate to be modeled at a single temperature, making the capacitance of the plate a function of a single parameter, the plate temperature. The value of R_2 is expressed by the relation;

$$R_2 = \frac{1}{h(3) * D_3 * D_{14}} + \frac{D_1/2}{K_6 * D_3 * D_{14}} \qquad \text{(A2-3.1)}$$

where the dimensions and constants are those of figure A2-2.1.

In this thesis all dimensions are in inches, but unit correction factors have been omitted from the constituitive relations. The computer program listings in Appendix 7 have the complete formulae for all the elements discussed in this section, with units and correction factors.

C_4 is the conducting plate thermal capacitance. Thermal capacitance is the mass of the object multiplied by its heat capacity. A wick was not used in this design, but it's thermal capacitance would lumped with the conducting plate's. The expression for C_4 is:

$$C_4 = D_3 * D_{14}[[C_{P6} * \rho_6] * D_1 + [C_{P10} * \rho_{10}] * D_{17}] \quad (A2\text{-}3.2)$$

The parameter ρ_{10} is the effective or net wick density and not the density of the wick material.

R_6 is the thermal resistance sum of three parts; the other half of the conducting plate, all of any wick, and half of the vapor cavity in the sensor. The diaphragm is assumed to have negligible thermal resistance. The vapor thermal conductivity in the cavity will be some combination of the vaporizing and insulating fluid conductivities. If both fluids are gases they can be characterized by some average value. Where there is a significant conductivity difference the system model will have to be altered. R_6 is expressed by the relation:

$$R_6 = \frac{1}{D_3 * D_{14}} \left[\frac{D_1/2}{K_6} + \frac{D_{17}}{K_{10}} + \frac{D_2/2}{K_9}\right] \quad (A2\text{-}3.3)$$

In this model, the vaporizing fluid conductivity is used for half of the vapor cavity resistance, the insulating fluid value will be used in computing the other half.

C_8 is the thermal capacitance of the vaporized liquid. The vaporizing fluid will have a heat of fusion. As a gas the fluid will store some heat, but significant heat is used to vaporize the liquid. Thus, the heat stored is <u>not</u> a function of temperature, but instead depends, in addition, on the volume of vapor. This means the value of C_8 is a nonlinear function of temperature. It can be characterized by the instantaneous value $C_8 = \frac{q_{stored}}{\Delta T}$, but this number would have little physical meaning. The actual heat stored in C_8 or C_{28} must be computed indirectly. The instantaneous temperatures of the two inputs are examined to determine the pressure difference across the manometers, ΔP. This pressure difference drives the fluid manometers to equal heights. The instantaneous height and the pressure determines the total vapor volume in each sensor. The vapor mass is then determined from the vapor specific volume. The heat stored is found by multiplying this mass by the heat of fusion. This subject will be treated in more detail in section 4. Because of the complexity of C_8, an exact expression will be explained in the dynamic simulation.

R_{14} is the resistance of half the vapor cavity plus half the sensor outside wall. Like the conducting plate, half the thermal resistance of the wall is assumed to lie on each surface. The expression for R_{14} is:

$$R_{14} = \frac{1}{D_3 * D_{14}} \left[\frac{D_2}{2 * K_9} + \frac{D_{15}}{2 * K_7}\right] \qquad \text{(A2-3.4)}$$

The sensor is assumed to have a high aspect ratio (area/thickness), so all heat transfer through the sensor occurs by conduction and none by convection, which eliminates a convective heat transfer coefficient associated with the inside surface of the vapor cavity.

C_{16} is the lumped thermal capacitance of the walls and insulation. The temperature at the '0' junction where C_{16} is attached can be designated the wall temperature. Strictly speaking this will not be the insulation temperature. However, the heat capacity of insulating materials is usually an order of magnitude less than those of solids, so this simplification causes little error. Thus the capacitance are combined. The expression for C_{16} is:

$$C_{16} = \frac{D_2*D_{15}*2*[D_3 + D_{14}]*C_{P7}}{\rho_7} + \frac{D_2*D_{16}*2*(D_3+D_{14})*C_{P8}}{\rho_8} \qquad \text{(A2-3.5)}$$

$$+ \frac{D_3*D_{14}*D_{15}*C_{P7}}{\rho_7} + \frac{D_3*D_{14}*D_{16}*C_{P8}}{\rho_8} \qquad \text{(A2-3.6)}$$

The first term is the capacitances of the sensor wall edges, the second the sensor edge insulation. The third and fourth terms refer to the sensor back wall and insulation respectively.

R_{18} is the resistance of half the sensor wall, all the insulation, and of the surface. The edges were included in the capacitance calculation because they contain mass and store heat. They are not included in the resistance calculation, because the edge heat loss is con-

sidered small. The sensor is assumed to have a large aspect ratio, and thus edge effects are ignored. The expression for R_{18} is

$$R_{18} = \frac{1}{D_3 * D_{14}} \left[\frac{D_{15}}{2 * K_7} + \frac{D_{16}}{K_8} + \frac{1}{h_4}\right] \qquad \text{(A2-3.7)}$$

If the edge effects are to be included a '1' junction with the effective edge resistance should be attached to the first '0' junction, as indicated in the box of figure A2-3.1. The flow through this resistance should go to S_a as shown.

S_a is the temperature of the environment or ambient, assuming this temperature is different from S_I. Once again this temperature is modeled as a source. If the sensor is immersed in a temperature bath $S_2 = S_I$ and the only way the sensor could lose heat is via bond 10. If a sensor was mounted on the output junction to facilitate a feedback configuration, the conducting plate would be against the junction. The back of the sensor would be exposed to ambient. In this situation $S_p \neq S_2$ and heat lost from the flow through the sensor would have to be accounted for. By analogy to electronics this is "leakage current". This completes discussion of the sensor bulb passive elements.

Bond 10 represents energy flow out of the sensor. This energy exits via work done on the fluid manometers. The MTF_t, for modulated transformer, is the vaporizing fluid. It senses a temperature and produces a proportional pressure. Thus the saturated vapor transforms

temperature into pressure. This transformation is modulated by the vapor temperature. The dashed line from the '0' junction to the MTF indicate the temperature modulation. The temperature to pressure conversion need not be linear. The transformer modulation can be a continuous but complex function of input temperature. The output of the transformer is a pressure, the effort variable in the fluid domain.

The modulated transformer also represents the demarcation between the fluid and thermal domains. In the introduction, and appendix 1, the effort and flow variables associated with each energy domain are discussed. A transfer from the thermal domain to any other has special properties. Effort and flow variables in most energy domains multiply to have units of power. For reasons discussed in appendix 1, the variables used in the thermal domains are temperature and heat flow. Heat flow has the units of power.

The rules of this transformation are also covered in the appendix. Bond 11 is in the fluid domain, pressure is the effort variable and volume flow is the flow variable. An equal pressure is put on one leg of both manometers, modeled as bonds 90 and 91. Flow through the manometers will be subject to several effects.

The manometers will have two effects on power flow through them. First, they will store some of the energy in the fluid capacitance associated with the legs of the manometers being at different levels. Second, because the conducting fluid in the manometers must flow to be

at different levels, there will be some small amount of power lost in flow resistance. The fluid flow is assumed to occur so slowly that fluid inertance can be ignored.

C_{46} and C_{96} are the capacitances associated with the manometers. The capacitance value for a standing vertical tank is the tank's area divided by the fluid density. This value can be used in this model only if the film section and reservoir have the same cross-section area. In chapter 3 it was shown the requirement that the amplifier be linear constrained the reservoir to have the same cross-section as the film section.

In figure A2-3.1 the bonds 90 and 91 are attached to the film section of R_v, and the reservoir of R_L. At the same time bonds 40 and 41 have the reverse connections. The result is each sensor pushes on the film section of one resistor and the reservoir of the other. The geometry of both resistors is identical, the manometers will move symmetrically with their respective conducting fluid heights about the resistor midpoint. This will assure amplifier linearity, as was proved in chapter 3.

The expression for C_{46} and C_{96} is:

$$C_{46} = C_{96} = \frac{D_4 * D_5}{\rho_5} = \frac{D_{10} * D_{11}}{\rho_5} \qquad \text{(A2-3.8)}$$

The model has provisions for a reservoir of differing cross-section, the dimensions D_{10} and D_{11} are variables that are not constrained

implicitly. However, for the case where $D_4 * D_5 \neq D_{10} * D_{11}$, a different expression for C_{46} and C_{96} must be used.

R_{92} and R_{94} are fluid resistances the conducting and insulating fluids encounter when shifting levels in the two manometers. Resistance will be a significant effect, even when inertance is not, if the conducting fluid has a high viscosity. The insulating fluid has been assumed a gas, so it will contribute little fluid resistance, but this contribution is calculated. For modeling and construction purposes the tubing connecting the reservoir to the film section will have an internal diameter equal to D_{22}. The length of this conducting tube will be assumed equal to the distance between film section and reservoir, or D_{21}. All flow is assumed laminar, the thermal time constants driving the flow being much larger than those of the fluid system. The expression for R_{92} and R_{94} is

$$R_{92} = R_{94} = \frac{128 * \mu_5 * D_{21}}{\pi * D_{22}^4} + \frac{128 * \mu_{11} * D_{19}}{\pi * D_{18}^4} \qquad \text{(A2-3.9)}$$

The first term is the contribution of the conducting fluid flowing through the convection tube between reservoir and film section. The second term is from non-conducting fluid flowing through the pressure conducting tubing from the sensors. The cross-section of the film section and reservoir is assumed much larger than $\frac{\pi * D_{22}^2}{4}$ and thus all the manometer flow resistance is concentrated in the flow conducting tube. In the event this assumption is not true, an additional resistance term

must be added.

The bond graph model of the sensor and manometer circuit is symmetric about C_{46} and C_{96}. The sensors and manometers are assumed identical. A negative sensor bond, n, corresponds exactly to a bond in the positive sensor N+20. Thus all of the elements and their constituitive relations have been defined, since $R_n = R_{n+20}$, and $C_n = C_{n+20}$. The only exceptions are the bonds 40 and 41 which correspond to bonds 90 and 91.

This completes explanation of the sensor-manometer circuit. This circuit is completely independent of the amplifier-resistor circuit. This means there will be no unwanted feedback from the output to the sensors. The model of the amplifier-resistor circuit will be examined next.

The amplifier-resistor circuit, and the parallel bond graph model, is shown in figure A2-3.3. Only the end view of the resistor film sections is shown, since the reservoirs do not enter into the thermal circuit. Like the sensor-manometer circuit there is complete symmetry about the mid-point capacitor, C_{85}. However, the elements do not have symmetric values since the two resistors change value inversely in their "push-pull" configuration.

Each resistor has three parallel heat flow paths. The upper path is the heat flow through the insulating fluid. The lowest path is through the conducting fluid. The additional third parallel path, not

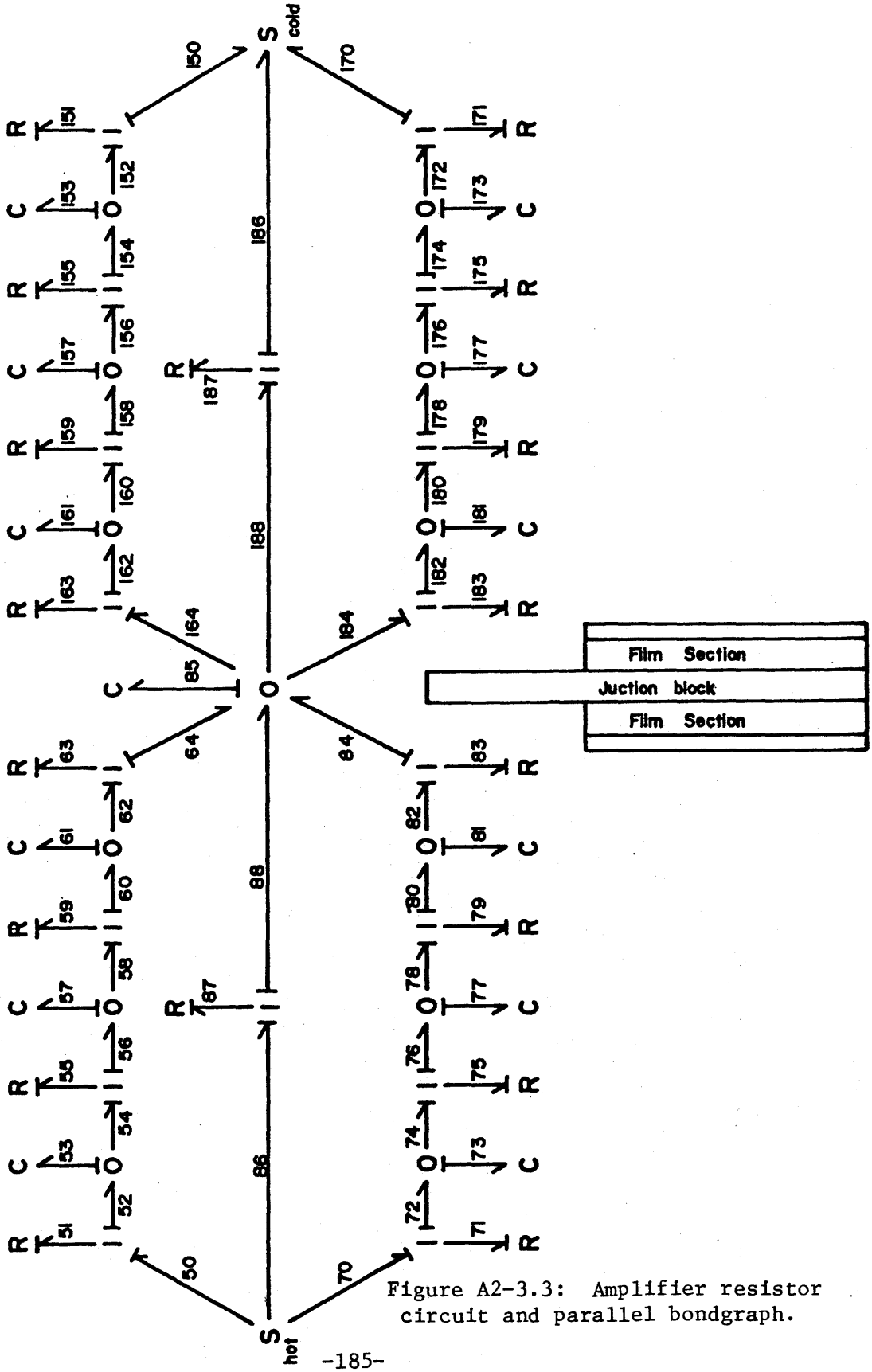

Figure A2-3.3: Amplifier resistor circuit and parallel bondgraph.

discussed earlier, is the heat leakage through the resistor edges and heat transferred by radiation. Identical components in each resistor will be described simultaneously, since and element in R_v, with number n, is the same element in R_L with number N+100.

S_h is the hot source, and is thus a temperature source. As an ideal source it is invariant under load, and the temperature is constant. S_c is the cold sink, with all the same properties.

R_{71} and R_{51} are the same resistance, but differ by an area term. R_{71} is the surface resistance, plus half the outside wall resistance, for the area of R_v in contact with the conducting fluid. R_{51} is the same quantity for the area is contact with the insulating fluid. To calculate these respective areas a convention established in chapter 3 will be used. To prove the output temperature was a linear function of input temperature, the conducting fluid height in one of the resistors was the only variable. Amplifier linearity guaranteed the two conducting fluid heights moved in symmetry about the film section midpoint. For model calculations fluid height is measured from the film section midpoint, as shown in figure 3-5.6. The fluid height in R_v will be called Δh, and will be positive when above the centerline, negative when below. By symmetry the fluid height in R_L, measured from the film section midpoint, will be $-\Delta h$. Given the variable Δh, the areas of both resistors in contact with the insulating and conducting fluids can be calculated. If U designates the area of R_v in contact with the insulating fluid, and B the area in contact with conducting fluid, then:

$$U = D_4 * [D_8/2 - \Delta h] \qquad \text{(A2-3.10)}$$

$$B = D_4 * D_8 - U \qquad \text{(A2-3.11)}$$

The maximum absolute value the variable Δh can assume is $D_8/2$. Symmetry of the system indicates the quantities U and B have complementary values for R_L. In R_L, U will be the area in contact with the conducting fluid, and B will be the area touched by insulating fluid. With these two variables, U and B, expressions for R_{51} and R_{71}, and the symmetric elements in R_L, R_{151}, and R_{171}, can be written:

$$R_{51} = \frac{1}{h_1 * U} + \frac{D_{12}}{2 * K_1 * U} \qquad \text{(A2-3.12)}$$

$$R_{71} = \frac{1}{h_1 * B} + \frac{D_{12}}{2 * K_1 * B} \qquad \text{(A2-3.13)}$$

$$R_{151} = \frac{D_{13}}{2 * B * K_4} + \frac{1}{h_2 * B} \qquad \text{(A2-3.14)}$$

$$R_{161} = \frac{D_{13}}{2 * U * K_4} + \frac{1}{h_2 * U} \qquad \text{(A2-3.15)}$$

The terms are symmetric except for D_{12} and D_{13}, which are different because the outside walls of R_L and R_v were allowed to be different thicknesses, subject to the constraint that their thicknesses and conductivities combine to produce the same thermal resistance in each wall. The surface between the hot source and R_v is designated by film coefficient h_1, while between the sink and R_L the coefficient is h_2.

C_{53}, C_{73}, C_{153} and C_{173} are the outside wall capacitances of R_v and R_L. C_{53} and C_{73} refer to the outside wall of R_v, and represent that part of the wall in contact with the conducting and insulating fluid respectively. C_{153} and C_{173} are the complementary values of

the same quantities, in R_L. Using the area variables U and B, defined earlier, the following expressions can be written:

$$C_{53} = D_{12} * D_4 * [\frac{D_8}{2} - \Delta h] * \rho_1 * C_{P1} = D_{12} * U * \rho_1 * C_{P1} \quad \text{(A2-3.16)}$$

$$C_{153} = D_{13} * D_4 * [\frac{D_8}{2} + \Delta h] * \rho_4 * C_{P4} = D_{13} * B * \rho_4 * C_{P4} \quad \text{(A2-3.17)}$$

$$C_{73} = D_{12} * B * \rho_1 * C_{P1} \quad \text{(A2-3.18)}$$

$$C_{173} = D_{13} * U * \rho_4 * C_{P4} \quad \text{(A2-3.19)}$$

The assumption made about the conducting plate of the sensor is also made for the outside walls of R_v and R_L, all the capacitance in the wall is lumped and assumed at one temperature, and all the wall resistance lies on the surface, half on each side.

R_{55}, R_{75}, R_{155}, and R_{175} are resistances composed of half the outside walls of R_v and R_L, and half the thermal resistance of the fluid in contact with these walls. The fluid has a heat capacity and will store some energy. No accounting is made of the energy put into the fluid and later carried to or from the reservoir. The assumption for the model was; entering fluid has the instantaneous temperature of the film already in the section. Once again R_{55} and R_{75} differ only by a U and B term, and the fluid they are in contact with. R_{155} and R_{175} are the geometrically similar resistances of R_L. The expressions for each are:

$$R_{55} = \frac{D_{12}}{2 * U * K_1} + \frac{D_5}{2 * U * K_{11}} \qquad \text{(A2-3.20)}$$

$$R_{75} = \frac{D_{12}}{2 * B * K_1} + \frac{D_5}{2 * B * K_5} \qquad \text{(A2-3.21)}$$

$$R_{155} = \frac{D_5}{2 * B * K_{11}} + \frac{D_{13}}{2 * B * K_4} \qquad \text{(A2-3.22)}$$

$$R_{175} = \frac{D_5}{2 * U * K_5} + \frac{D_{13}}{2 * U * K_4} \qquad \text{(A2-3.23)}$$

The thermal resistance of the fluid is assumed concentrated at the film section walls.

C_{57}, C_{77}, C_{157}, and C_{177} are the thermal capacitances associated with the fluids in R_V and R_L. C_{57} and C_{157} are the insulating fluid thermal capacitances of R_V and R_L respectively. C_{77} and C_{177} are conducting fluid thermal storage in the same two resistors. The expressions for these four capacitances are:

$$C_{57} = D_5 * U * \rho_{11} * C_{P11} \qquad \text{(A2-3.24)}$$

$$C_{77} = D_5 * B * \rho_5 * C_{P5} \qquad \text{(A2-3.25)}$$

$$C_{157} = D_5 * B * \rho_{11} * C_{P11} \qquad \text{(A2-3.26)}$$

$$C_{177} = D_5 * U * \rho_5 * C_{P5} \qquad \text{(A2-3.27)}$$

R_{59}, R_{79}, R_{159}, and R_{179} are resistances composed of half the fluid thermal resistance (conducting or insulating) and half the interior

wall resistances of both R_v and R_L. R_{59} contains the wall and fluid resistance for area in contact with the insulating fluid in R_v, R_{79} represents wall area in contact with the conducting fluid. R_{159} and R_{179} are the analogous quantities in R_L. The expressions are:

$$R_{59} = \frac{D_5}{2 * U * K_{11}} + \frac{D_6}{2 * U * K_2} \quad \text{(A2-3.28)}$$

$$R_{79} = \frac{D_5}{2 * B * K_5} + \frac{D_6}{2 * B * K_2} \quad \text{(A2-3.29)}$$

$$R_{159} = \frac{D_6}{2 * B * K_2} + \frac{D_5}{2 * B * K_{11}} \quad \text{(A2-3.30)}$$

$$R_{179} = \frac{D_6}{2 * U * K_2} + \frac{D_5}{2 * U * K_5} \quad \text{(A2-3.31)}$$

C_{61}, C_{81}, C_{161}, and C_{181} are the inner wall thermal storages for both R_v and R_L. They differ only by the area term. C_{61} is the capacitance of R_v's inner wall in contact with the insulating fluid, C_{81} is in contact with the conducting fluid. C_{161} and C_{181} are the same quantities in R_L. They are represented by the expressions:

$$C_{61} = D_6 * U * \rho_2 * C_{P2} \quad \text{(A2-3.32)}$$

$$C_{81} = D_6 * B * \rho_2 * C_{P2} \quad \text{(A2-3.33)}$$

$$C_{161} = C_{81} \quad \text{(A2-3.34)}$$

$$C_{181} = C_{61} \quad \text{(A2-3.35)}$$

The symmetry in the above expressions increased because the initial assumptions required the two interior walls to be identical material and thickness.

R_{63}, R_{83}, R_{163}, and R_{183} are composed of half the interior wall thermal resistance and half the junction block resistance, and differ only by area terms. R_{63} and R_{83} are defined by the area in contact with insulating and conducting fluid respectively in R_v. R_{163} and R_{183} are the analogous quantities in R_L. Using the area variable U and B:

$$R_{63} = \frac{D_6}{2 * U * K_2} + \frac{D_7}{2 * U * K_3} \qquad \text{(A2-3.36)}$$

$$R_{83} = \frac{D_6}{2 * B * K_2} + \frac{D_7}{2 * B * K_3} \qquad \text{(A2-3.37)}$$

$$R_{183} = R_{63} \qquad \text{(A2-3.38)}$$

$$R_{163} = R_{83} \qquad \text{(A2-3.39)}$$

The adhesive bonding, if any, between the interior walls and junction block will have some thermal resistance. This resistance can be accounted for by altering the value of the wall conductivity, or adding another term to these resistance expressions.

C_{85} is the most important element in the circuit since it represents the thermal capacitance of the junction block between R_v and R_L. Again, the internal resistance of the block has been modeled as lying half on each surface, so the block can be modeled with no resistance,

and thus is at a uniform temperature. This uniform temperature is the output. Since all amplifier heat output must flow out this block, it should be an inherently conductive material. The expression for C_{85} is:

$$C_{85} = D_{20} * D_4 * D_7 * \rho_3 * C_{P3} \qquad \text{(A2-3.40)}$$

Note that, aside from the sources, C_{85} is the only element in the circuit whose value is constant, and not modulated by the fluid level in the resistors.

R_{87} and R_{187} are the remaining two elements, and they are composed of the undesired thermal short circuits between source, output, and sink. Each term is the sum of two resistances. The first is the thermal resistance of the edges. The second is the radiation resistance between the surfaces.

The exact modeling of the radiation term of R_{87} and R_{187} is a function of the radiation conducting properties of the fluid and walls. The governing parameter of radiative heat flow between reradiating surfaces is called the gray body shape factor, and is generally designated by the letter $\mathcal{F}$. (Ref. 24) Among other things it is a function of the emissivity and absorptivity of the two surfaces, the shape factor, and the absorption of intervening transparent substance. It is beyond the scope of this thesis to deal comprehensively with radiation modeling. Radiation was considered in the initial modeling of the amplifier. The copper walls of the amplifier, which were highly polished, had an emissivity of approximately .1 (Ref. 18) which was too low to have significant

radiation effects. Because infrared behavior is so material dependent there are no feasible, general modeling rules. Radiant heat transfer was not included in this amplifier model.

Without radiation effects the expressions for R_{87} and R_{187} are:

$$R_{87} = \frac{[D_{12} + D_5 + D_6 + D_{7/2}]}{[2 * D_4 + 2 * D_8] * D_9 * K_{12}} \qquad \text{(A2-3.41)}$$

$$R_{87} = R_{187} \qquad \text{(A2-3.42)}$$

Since R_v and R_L are identical in construction the edge leakage is identical.

This completes the discussion of the amplifier-resistor circuit model. Each circuit in the amplifier, the sensor-manometer circuit and the amplifier resistor circuit, have been discussed independently. In figure A2-3.4 the complete bond graph of the amplifier with sensors is shown. The coupling between the manometer conducting fluid levels and the elemental values in the thermal circuit is shown by the signal flow bonds (----) between the fluid '1' junctions and the elements in the thermal circuit. No power is transmitted by a signal flow bond, only information. The information on this bond is the conducting fluid height Δh. This will, in turn, establish the value of U and B. With U and B specified each element in the thermal circuit has a known value.

The complete bond graph of figure A2-3.4 represents a dynamic

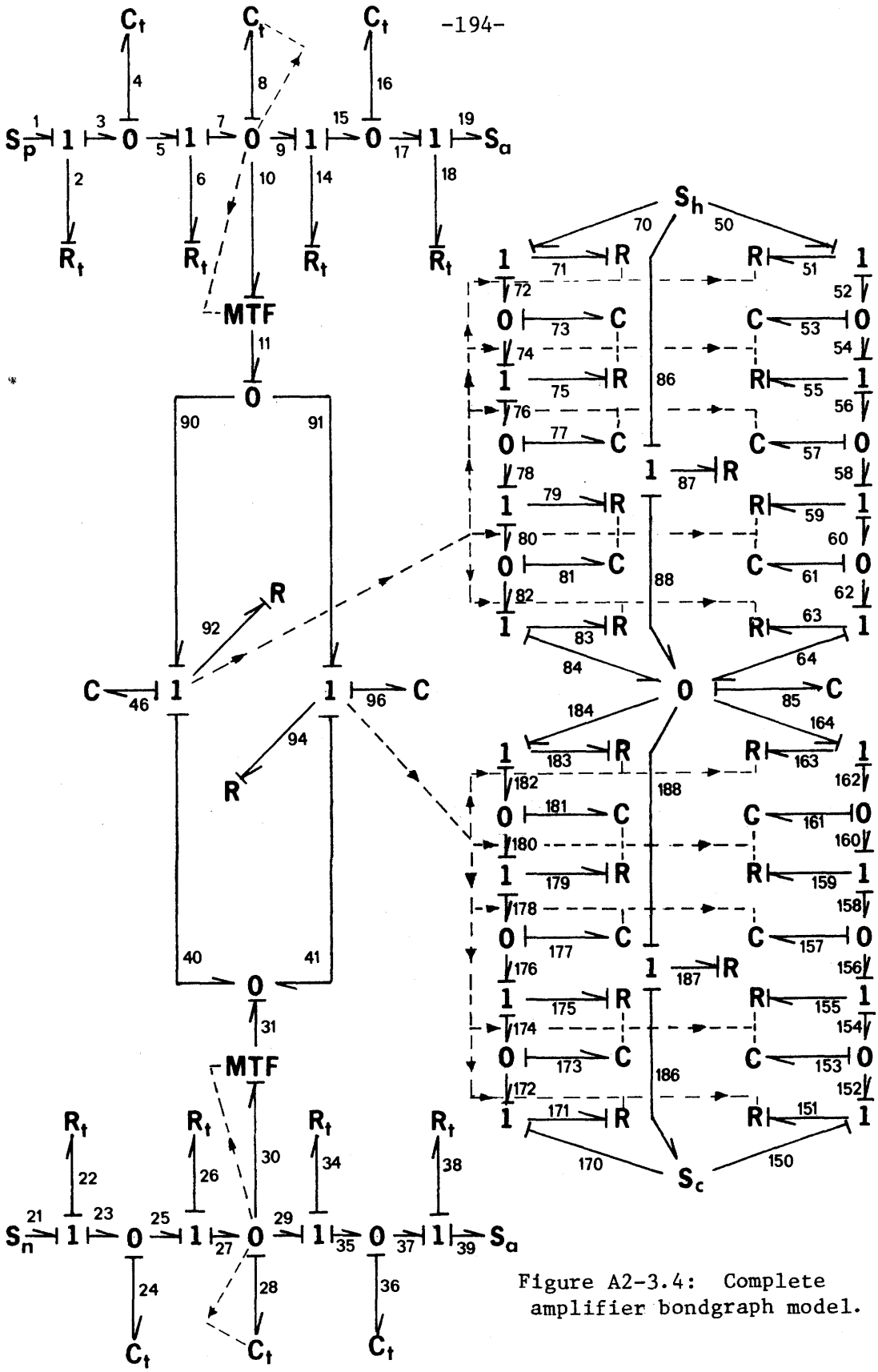

Figure A2-3.4: Complete amplifier bondgraph model.

model of the system. The differential equations can be mechanically derived in a straightforward manner, but the resulting system equations may be linear or nonlinear.

The known nonlinear elements, the modulated transformers, where explicitly designated by signal flow bonds. While linear system equations are far easier to solve, nonlinear equations, which result from this system model, can be solved to any aribtrary accuracy numerically.

The next task is to assign dimensions to all amplifier components. One set of dimensions must be selected, modeled, simulated, built, and tested.

APPENDIX 3: AMPLIFIER DIMENSION SELECTION WITH OPTIMAL DESIGN

Section A3-1: Summary of appendix.

Section 2 introduces the optimization technique. A static rather than dynamic optimization was used, and the difference is explained. A mathematical expression containing the design parameters to be optimized, called the performance index, is brought to a maximum value by changing the values of the design parameters within their individual constraints.

Section 3 explains the six design parameters optimized, and the inequality constraints on each. The parameters being optimized are constrained to lie within bounds specified by the designer.

Section 4 describes the two performance indices used in this thesis, and the meaning of each term. The performance index, a function relating the parameters being optimized, is defined. The initial amplifier design, called "ideal" had to be modified in light of experimental results. The second index produced the "modified" amplifier.

Section 5 tabulates the results of the optimization, and the selected amplifier dimensions.

Section A3-2: Introduction to the optimal design techniques.

This appendix will explain a procedure for amplifier dimension selection. In the previous appendix the dimensions of amplifier parts were related to dynamic model component values. Each model element value has been expressed in terms of the subscripted amplifier physical dimensions and material properties. The dynamic model relates model element values to the dynamic performance of the amplifier. All information necessary to relate physical dimensions to dynamic performance is present.

The dimensions for the test amplifier were found using the Complex Method of Box (Ref. 15). This is an iterative method for solution of nonlinear optimization problems. The presence of nonlinear elements in the model guarantees the resulting system equations will be nonlinear. In addition, the interaction of the different amplifier parameters makes the optimization problem a nonlinear one.

First, a brief description of the optimization technique.

One process of selecting parameters on the basis of their effect on performance is called optimization. The dimensions are selected to be optimum in light of a given performance criteria, a performance index. The parameters are mathematically related in the index, while being subject to internal and external constraints. Their values are iterated until the index is minimized or maximized. Op-

timization falls into two broad categories, static and dynamic. In a static optimization a performance index is based on model parameters that are independent of time, and the parameters are adjusted so they minimize or maximize the index. A dynamic optimization has a performance index composed of static and time or path dependent quantities. The particular time history or path history of the system will affect the index, and a dynamic optimization results in a system that is optimum for a certain dynamic history or path. A different path may require different element values to be the "optimum" system. It is extremely difficult to predict a priori what path will fairly represent the dynamic path that will be seen by the "average" thermal amplifier. The selection of the performance index is a similar problem.

The problem of the performance index, static or dynamic, is how to translate desired system performance such as, "fastest response possible with less than 5% overshoot" into a algebraic combination of system parameters. This function, when minimized, should generate parameter values that will make the system perform as desired. There is currently no systematic method for index generation. The normal procedure is to generate a performance index, optimize, and solve the resulting differential equations on a digital computer. This simulated system performance is analyzed. If necessary, the performance index is adjusted and the process repeated. The direct translation of a performance criteria for the system into a performance index for the optimization is still somewhat an art.

The dimensions for the amplifier simulated in this thesis were selected by a static optimization. There are two important parts to a static optimization problem. The first is detailing the constraints between the variables in the performance index. The second, generation of the performance index itself. Once both parts of the problem have been solved a computer program can maximize the performance index subject to the constraints.

Section A3-3: Inequality constraints on amplifier parameters.

The complex method of Box maximizes a performance index composed of parameters which are constrained by inequalities. Each parameter can be constrained between an upper and lower bound, both of which can be functions of other parameters. Constraint selection is similar to performance index generation, in that there is no systematic method to generate constraints.

The static optimization optimizes six amplifier parameters. In the program (see Appendix 7 for listing) the constrained variables appear as subscripted x's where:

$x(1) \equiv$ conducting plate area of the sensor bulb, $D_{14} \times D_3$

$x(2) \equiv$ sensor bulb vapor chamber thickness, D_2

$x(3) \equiv$ film section thickness, D_5

$x(4) \equiv$ thickness of the walls bonded to junction, D_6

$x(5) \equiv$ thickness of junction block, D_7

$x(6) \equiv$ length of one side of the film section, D_4 or D_8

Both sensors and the film section were assumed square, so $D_{14} = D_3$ and $D_4 = D_8$.

A slightly more complex optimization, including the width of both sensor and film section as independent variables, could be constructed. There would have to be a specific importance to these dimensions to make it worthwhile.

The optimization required a total of 10 constraints on ten variables, six of which are in the performance index and consequently "optimized". A constraint is an inequality expression of the form:

$$x_L \leq x_n \leq x_u \qquad \text{(A3-3.1)}$$

where x_L is the lower bound on the variable being constrained, x_n, and x_u is the upper bound. The constrained variable, x_n, does not have to be optimized. Only variables that appear in the performance index are iterated to their optimum value. The following paragraphs will describe each variable and the constraints upon it.

The first variable, x_1, is the conducting plate area of the sensor bulb, $D_{14} \times D_3$. This value was bracketed between two functions. The lower limit constrained the sensor to have 210% more volume than a film section. A full scale deflection of conducting fluid in both R_V and R_L requires a sensor to pump an insulating fluid volume equal to half a film section and half a reservoir. The film section and reservoir have equal cross-section and height, and half of each totals one full film section. This volume must be pumped by a diaphragm starting in the middle of the vapor cavity, so one film section volume is on each side of the diaphragm. The insulating fluid may have some compressibility so 10% additional volume was added to the sensor. The constraint is expressed by the inequality:

$$2.1*D_4 * D_8 * D_5 \leq x_1 * D_2 \qquad \text{(A3-3.2)}$$

But $D_4 = D_8 = x_6$, $D_5 = x_3$, and $D_2 = x_2$, so this expression can be rewritten:

$$2.1 * x_6^2 * x_3 \leq x_1 * x_2 \qquad \text{(A3-3.3)}$$

This expression is now rewritten to form a lower bound on the value of x_1, by simply dividing both sides by x_2.

$$x_1 \geq \frac{2.1 * x_6^2 * x_3}{x_2} \qquad \text{(A3-3.4)}$$

The upper bound on conducting plate area is a practical consideration. When the amplifier is in a feedback configuration the sensor will be attached to the output junction plate. This plate has width D_4. If the conducting plate area becomes larger than the film section area, assuming they are both square, part of the sensor conducting plate would protrude beyond the edges of the junction block. This has the potential of introducing temperature gradients across the conducting plate. To avoid a sensor larger than the output plate the sensor area is constrained to be less than the film section area. The expression for this constraint is:

$$x_1 < x_6^2 \qquad \text{(A3-3.5)}$$

Upper and lower bounds can be combined into one constraint expression for x_1:

$$\frac{2.1 * x_6^2 * x_3}{x_2} \leq x_1 \leq x_6^2 \qquad \text{(A3-3.6)}$$

The performance index will be maximized while x_1 is held within these boundaries.

The second variable, x_2, is the control bulb or sensor vapor cavity thickness, D_2. This variable has no direct constraints but must be large enough to produce a volume 10% larger than the film section, within some practical limits. As a minimum, .125" was set. A rubber diaphragm thinner than .010" is difficult to fabricate. If the sensor cavity thickness fell to .100", then 10% of the cavity volume would be diaphragm. This would magnify the effects any manufacturing defects the diaphragm, a small error in thickness could cause the sensor to have insufficient volume.

As an upper limit the cavity is constrained to be less than 1.0". Convection must not be a significant heat transfer mode inside the sensor or the thermal model would have to be revised, and beyond one inch convection would be significant. The two limits combine to make the following constraint expression for x_2

$$.125 \leq x_2 \leq 1.0 \qquad \text{(A3-3.7)}$$

The third variable, x_3, is the film section thickness, D_5. The minimum for silicone oil was established at .062 in, by considering surface tension effects of the oil. Other fluids would have other constraints. Capillary effects could cause fluid to "hang-up" in the section due to surface tension, and would invalidate the pressure balance assumptions. The manometer levels would then reflect a balance of sur-

face tension and pressure effects. For the first optimization of the amplifier, the lower bound on x_3 held at .125". Later experimental tests established a .062" gap was permissible. A second optimization was performed with .062" as a lower bound. The two optimizations and the two performance indices will be discussed in greater detail in section 4.

An upper limit on the film section was placed at 1.0". This was a somewhat arbitrary value; but there are two important drawbacks to a thick film section. A thick film section requires a large mass of vaporized sensor fluid to pump the required volume of conducting fluid. This lowers the input impedance of the amplifier, and would excessively load a sensitive temperature source. Second, for fluid of moderate viscosity, convection could become the dominant heat transfer mode in the film section. The model has been developed assuming pure conduction; the optimization must guarantee this assumption. The resulting constraint expression is:

$$.062 \leq x_3 \leq 1.0 \qquad \text{(A3-3.8)}$$

The fourth variable, x_4, is the thickness of the wall bonded to the junction, D_6. This thickness has thermal importance that will be discussed with variable nine. There are no structural considerations since this wall can be supported by the junction block, so a lower limit on the value of x_4 is zero. Thermal considerations place an

upper limit on x_4 of .125. Above this thickness the thermal gradient in the wall could become so great as to cause significant warping. The resulting constraint expression for x_4 is:

$$.010 \leq x_4 \leq .125 \qquad \text{(A3-3.9)}$$

The fifth variable, x_5, is the junction block thickness, D_7. This dimension has thermal significance also explained with variable nine.

The thickness is constrained to be greater than .010" and has less than .125". If too thin, fabrication is difficult, if too thick thermal gradients may cause warping. The constraint expression is:

$$.010 \leq x_5 \leq .125 \qquad \text{(A3-3.10)}$$

The sixth variable, x_6, is the length of one side of the film section, D_4 or D_8. The film section has been assumed square. Selecting a minimum and maximum value is somewhat arbitrary, but practical considerations again dictate limits. If x_6 shrinks below 1" the part size will make construction difficult. If the amplifier is more than 10" on a side, it will be unwieldy and too large for a signal processing device. These two dimensions were the upper and lower bound on x_6.

$$1.0 \leq x_6 \leq 10.0 \qquad \text{(A3-3.11)}$$

The seventh variable, x_7, is the control bulb volume, $D_3 * D_2 * D_{14}$, or in terms of optimization variables, $x_1 * x_2$. x_1, the conducting plate area, was constrained to guarantee 10% more volume in the control bulb than in 2 film sections. Nothing constrained this volume from being far greater than 10%, so it will be limited to less than 50% larger. The expression for the volume of the film section is $D_5 * D_4 * D_8$, or in terms of optimization variables, $x_6^2 * x_3$. The following expression constrains x_7:

$$2.1 * x_6^2 * x_3 \leq x_7 \leq 2.5 * x_6^2 * x_3 \qquad \text{(A3-3.12)}$$

The eighth variable, x_8, is the thermal resistance of a film section when completely filled with insulating fluid, r_v. This variable is constrained to be some multiple of r_L, thus constraining the r_v/r_L ratio.

The most important parameter to amplifier performance is the maximum to minimum resistance ratio, r_v/r_L, of R_V and R_L. In figure 3-4.1 the percentage of theoretical gain and range realizable were expressed as a function of this ratio. Without edge leakage this ratio would be equal to the conductivity ratio of the conducting and insulating fluids. Because of leakage, the resistance ratio of the two fluids must be higher than the desired resistance ratio. The optimization program will adjust the size of the film section until the edge leakage reduces the overall resistance ratio to the one specified.

In addition to edge leakage, the resistance of the walls is a fixed value and limits the minimum value of r_L. The film section must be thick enough so its resistance when filled with insulating fluid is the necessary r_v. The edge leakage and residual wall resistance combine to constrain the geometry of the film resistors, since the former constrains the D_4 and D_8 dimensions and the latter the D_5 dimension.

The geometric variables of the resistors will be forced by the optimization to produce the required resistance ratio. If a large minimum resistance is desired, to limit power drain, a larger value is used for the lower bound.

The maximum value, r_v, is the sum of the film section and interior wall resistance, when the film section is filled with insulating fluid. The film section resistance is the parallel sum of the edge and film resistance.

The edge thermal resistance can be expressed as,

$$R_{edge} = \frac{x_3}{4 * x_6 * D_9 * K_{12}} \qquad \text{(A3-3.13)}$$

and the film section resistance, in the insulating mode, is,

$$R_{film} = \frac{x_3}{x_6^2 * K_{11}} \qquad \text{(A3-3.14)}$$

The two resistances in parallel sum to be,

$$R_{net} = \frac{R_{edge} * R_{film}}{R_{edge} + R_{film}} \qquad \text{(A3-3.15)}$$

The interior wall resistance is:

$$R_{wall} = \frac{x_4}{x_6^2 * K_2} \qquad \text{(A3-3.16)}$$

and this resistance is in series with R_{net}, so:

$$r_v = R_{net} + R_{wall} = x_8 \qquad \text{(A3-3.17)}$$

This value is constrained to be larger than r_L, by a multiple called the resistance ratio. The value of r_L is computed the same way as r_v. The only difference is K_{11} is replaced with K_5, the conductvity fluid. Let,

$$R'_{film} = \frac{x_3}{x_6^2 * k_5} \qquad \text{(A3-3.18)}$$

and,

$$R'_{net} = \frac{R'_{film} * R_{edge}}{R'_{film} + R_{edge}} \qquad \text{(A3-3.19)}$$

then,

$$r_L = R'_{net} + R_{wall} \qquad \text{(A3-3.20)}$$

The lower constraint on x_8 then becomes:

$$\text{resistance ratio} * r_L \leq x_8 \qquad \text{(A3-3.21)}$$

The upper constraint placed on x_8 is unimportant.

One ideal amplifier characteristic was zero output impedance. Since the resistance of R_v and R_L is the output impedance, r_L should be as small as possible. The maximum resistance r_v, will depend on desired gain or range.

The ninth variable, x_9, is the junction block thermal resistance from the middle to top of the film section, which is x_6 high. In the model the junction block is assumed at a uniform temperature. This requires the internal resistance of the block to be small compared with the rest of the amplifier. A highly conductive material may be used for the junction. However, thermal resistance is a function of both material conductivity and conductor cross-sectional area. If the junction block is made too thin, its internal resistance will grow too high. Variable five, the junction block thickness, determined the cross-section area, since the block is assumed to be x_6 wide. Variable nine is constrained to have less resistance than the film section filled with conducting fluid and interior wall in series. This constraint is illustrated in figure A3-3.1. As shown, the resistance through the junction block to the output is made less than the resistance into the junction block. There is no minimum placed on the resistance through the junction block, so the lower constraint is zero. The expression for this constraint is:

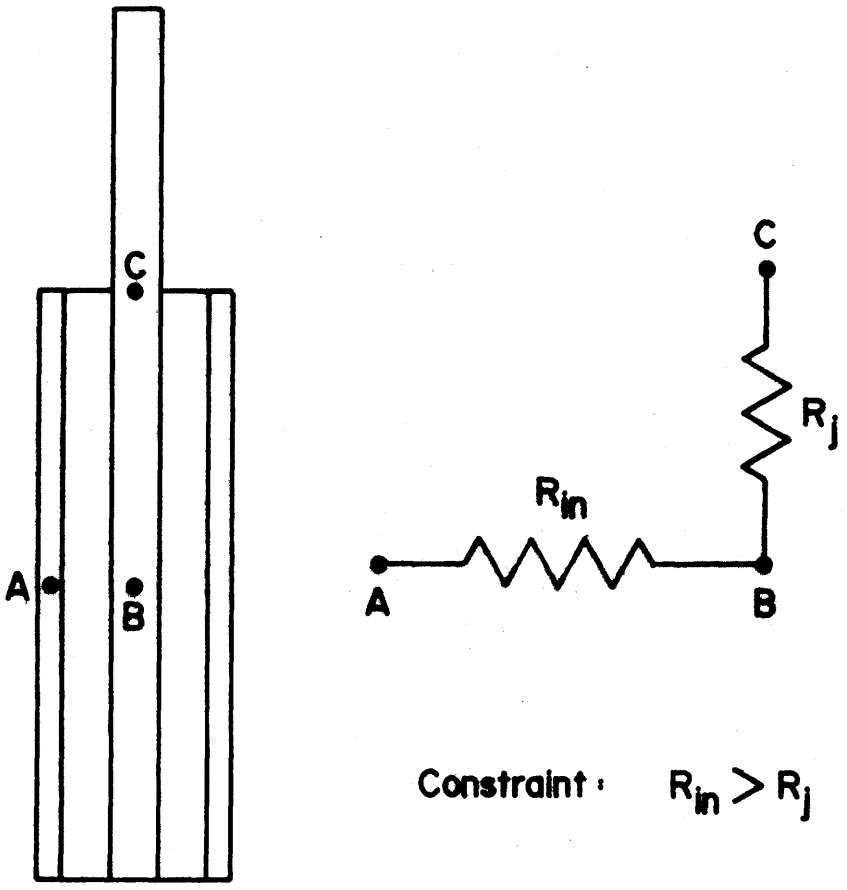

Figure A3-3.1: Junction block resistance constraint

$$0 \leq \frac{x_6}{2 * x_5 * K_3 * x_6} \leq \frac{x_4}{x_6^2 * K_2} + \frac{x_3}{K_5 * x_6^2} \qquad \text{(A3-3.22)}$$

where $x_9 = \frac{x_6}{2 * x_5 * K_3 * x_6}$

Any resistance in the amplifier walls should be concentrated in the walls next to the junction block, if fixed resistance is intentionally added to reduce power drawn. Variable four is the thickness of the inner walls, and determines their resistance. Interior wall resistance will help prevent temperature within the junction block. The "optimum" amplifier will have no resistance in the outer wall, since this resistance would increase r_L.

The tenth and last variable, x_{10}, is the lower constraint on x_1, which is itself bounded. The expression for x_{10} is:

$$x_{10} = \frac{2.1 * D_4 * D_8 * D_5}{D_2} = 2.0 * x_6^2 * x_3/x_2 \qquad \text{(A3-3.23)}$$

It is constrained to be less volume than the film section one inch thick. The constraint expression is:

$$0 \leq x_{10} \leq x_6^2 * 1.0 \qquad \text{(A3-3.24)}$$

and it prevents the lower boundary on x_1 from crossing the upper boundary and fouling the constraints.

Descriptions of the ten constrained variables are now complete. Only the first six variables were carried into the performance index, and thus were iterated to an optimum value. The next section of this chapter will explain how the index was constructed and justify the selection of the six variables chosen.

Section A3-4: The performance index.

The performance index is an algebraic expression containing only the variables to be optimized. The values of the variables are adjusted, within their respective constraints, until the performance index reaches its maximum numeric value. The program stops, and returns the various parameter values that made the performance index a maximum, and these values are optimum.

The performance index is the mechanism through which a designer attaches importance to particular design parameters. Unfortunately, there is no systematic way to relate dynamic system performance to the weighting given these variables in the performance index. There are, however, general directions that the physics of the amplifier dictate. The two performance indices used to design the two test amplifiers evolved through several iterations. The static optimization described in this section is concerned with one goal, to minimize response time.

The original performance index was:

$$P.I. = -[x_2 + x_3 + 9x_4 + x_5 + x_6^2] \qquad \text{(A3-4.1)}$$

The variable x(I,1), or x_1, did not appear in the expression, because it is constrained to be just slightly less than x(I,6). The double subscripts are used to make the notation of this explanation consistent with the computer program listing in Appendix 7. Experimental results, ex-

plained in detail in chapter 5, dictated some changes. The resistor sides were reduced from .062" to .020"; because the .062" was too thick to vacum mold. Because air diffusion through flexible diaphragms could not be prevented, sensors were constructed with metal bellows instead of diaphragms. Proper bonding of polycarbonate could not be executed between the junction block and the inner wall of R_V and R_L, because thermally conductive adhesives chemically attacked polycarbonate. The result was the evolution of a second performance index of the form:

$$P.I. = .1 * x_1^{.5} - 10\,[x_2 + x_3 + 5 * x_4 + x_5] - x_6 \qquad (A3\text{-}4.2)$$

The critical difference between these two indices is the value of the coefficients. The coefficient values are the mechanism that assigns relative weighting to the variables. For example, the interior wall bonding difficulty translated itself into a higher penalty for any interior wall thickness. The result was to increase, from 9 to 50, the coefficient of the interior wall thickness, x_4. This section will describe the second performance index in detail, since this index dictated the design of the successful test amplifier.

The optimization program optimizes six dimensions. All materials, and the resistance ratio, have been assumed selected. Materials were selected for practical and construction considerations. Materials will be discussed in numerical order. Table A3-4.1 summarizes the material properties.

Table A3-4.1: Material Table.

No.	Material	Part Material is Used For	ρ, Density lbm, ft^3	C_p, Specific Heat, Btu/lbm°F	K, Conductivity Btu/ft hr°F
1	Polycarbonate (Copper)	Outside wall, R_V	74.88 (555.36)	.30 (.092)	.111 (230.12)
2	Polycarbonate	Interior wall, both R_V & R_L	74.88	.30	.111
3	Copper	Junction Block	555.36	.092	230.12
4	Polycarbonate (Copper)	Outside wall, R_L	74.88 (555.36)	.30 (.092)	.111 (230.12)
5	Silicone Oil	Conducting fluid	60.59	.380	.049*
6	Copper	Conducting plate of sensors	555.36	.092	230.12
7	Polycarbonate	Sensor bulb walls	74.88	.30	.111
8	Urethane Foam	Sensor insulation	2.50	.250	.022
9	Air	Pressure conducting fluid	.071	.241	.016
10	Fibre-Glass	Sensor wick (optional)	158.50	.197	.500
11	Air	Insulating fluid	.071	.241	.016
12	Polycarbonate	Amplifier side walls	74.88	.30	.111

*Experimentally Determined

No.	Material	Part Material is Used for	ρ, Density lbm, ft^3	C_p, Specific Heat, Btu/lbm°F	K, Conductivity Btu/ft hr°F
13	a. FC-88		115	.25	.032
	b. F-11	Sensor Fluid	93.6	.212	.0503
	c. F-113		97.61	.229	.0432

Vapor Pressure, Temperature, and Volume Relationships for Sensor Fluids P in psi, T in °F, v in ft^3/lbm

a. FC-88 (Floriert^R) $P = 51.71[10^{(7.9768 - \frac{860}{459.69+T})}]$ $v = 3.555 - .0370T + 10^{-4}T^2$

b. FC-11 (Freon^R) $P = 8.106 - .1295T + .00284T^2$ $v = 9.076 - .1107T + .00037T^2$

c. F-113 (Freon^R) $P = 8.144 - .1619T + .001853T^2$ $v = 13.139 - .14896T + .00047T^2$

Table A3-4.1: Material Table (con't.).

Material 1, used for R_v's outside wall, and Material 4, R_L's outside wall, did not enter into the optimization. Their resistance should be kept as small as possible. Any desired resistance should be concentrated in Material 2, to prevent temperature gradients in the junction block. The original design used polycarbonate outside walls, with 2 copper plates bonded to their outside for stiffness. Polycarbonate would allow the entire film section and reservoir to be vacuum molded in one piece. Bond problems between the polycarbonate and copper resulted in the outside walls of the experimental model being solid copper.

The interior wall of both R_v and R_L, material 2, is also polycarbonate. This polymer is high in strength and thermal resistance. Polycarbonate also retains its mechanical properties to a moderate temperature. The high thermal resistance means a resistance value can be achieved with a small amount of material, and with less unwanted thermal capacitance.

Material 3 is used in the junction block and is copper. This metal has the highest thermal conductivity of readily available materials, and reasonably low capacitance. For the same reasons material 6, for conducting plate of the sensor, was copper. While not as thermally conductive, aluminum is stronger mechanically and could be substituted for either of these materials if the stress level due to high sensor pressure required it.

Material 5, the conducting fluid, is the most critical material selection in the amplifier. The ideal fluid will have high conductivity and no density. The best actual material is sodium potassium (NaK). A conductivity close to that of steel and a density less than water makes the material ideal. However, it is explosive in the pressure of water, making it dangerous. Sodium-potassium is also incompatible with many common metals. The requirement of low vapor presence eliminates many fluids, like water. Mercury is highly conductive, but very dense. The large pressure difference required to drive the manometers full of mercury reduces the gain. The material selected was a chemically inert, moderate viscosity, silicone oil. The thermal conductivity is not high, but adequate for the selected resistance ratio.

Figure 3-4.1 illustrated the trade-off of gain and range as a function of the resistance r_v/r_L. The parameter r_v was the maximum resistance value of the film resistor, and r_L the minimum. A logical selection for symmetry reasons was $r_v/r_L = 3$. This would give half the theoretically possible gain and range.

For practical reasons air is an overwhelming choice for an insulating fluid, material 11. It has high thermal resistance, and a pressure that is relatively insensitive to temperature. In addition to being chemically stable it is of negligible density. Air is compatible with most materials.

Silicone oil has a thermal conductivity roughly 3-1/2 times that of air. The resistance ratio has to start slightly higher than desired because edge leakage will reduce the ratio of r_v/r_L to a value below that of the fluids.

Materials do not offer a continuous spectrum of properties. A specific material parameter value is not always obtainable. Thus, the size of the amplifier is adjusted by the optimization until the resistance ratio is reduced to the desired value, 3.0, by edge leakage.

The sensor bulb walls, material 7, and the amplifier sides, material 12, are both polycarbonate. Polycarbonate has excellent mechanical strength and toughness. It can also be vacuum formed into very complex shapes. This considerably aids in the actual fabrication of the amplifier.

Material 10, the wick, and material 8, the sensor insulation, did not enter the optimization and do not have to be selected at this time. In the experiments a close cell polyurethane foam was used for insulation. This completes material selection.

A priori it is known the amplifier with the smallest internal resistance and capacitance will respond fastest. A small capacitance requires less heat to change its temperature, and a small resistance provides less of a barrier to this heat flow. Small resistances and capacitances produce a low output impedance, and small size and weight. The performance index was constructed to produce the smallest amplifier

compatible with the desired resistance ratio, having the smallest internal resistance and capacitance. The performance index used to produce minimum resistance and capacitance was:

$$P.I. = .1 \times x_1^{.5} - 10*[x_2 + x_3\ 5 * x_4 + x_5]-x_6 \qquad (A3\text{-}4.3)$$

All dimensions are positive. The method of Box trys to maximize the value of the performance index. All parameters with a negative sign will be minimized, all parameters with a positive sign will be maximized. The program will iterate the variables within the constraints to achieve the smallest negative value or the largest positive value for the performance index.

In the above performance index all variables are given a negative weight except x_1, the area of the sensor conducting plate. By rewarding the control bulb area slightly, and penalizing its thickness, x_2, the control bulb produced will have the highest aspect ratio permissible within the constraint, and consequently the fastest response time. A thin control bulb will also require less diaphragm or bellows deflection for pumping a given volume, and lessen any unwanted feedback from a diaphragm or bellows spring rate. The square-root of x_1 is taken to bring the value of x_1 down to the magnitude of x_6, otherwise the area term would dominate the performance index. When experiments revealed a flexible polymer diaphragm impractical, a metal bellows was substituted. By rewarding the sensor area the maximum sensor dia-

meter is produced by the optimization. Thus x_1 has a positive coefficient in the second performance index.

The remaining variables in the performance index; x_2, x_3, x_4, x_5 and x_6, all have a negative coefficient. This serves to penalize them. The variables x_2, x_3, x_4 and x_5 are multiplied by 10 because they are constrained to be an order of magnitude less than x_6. To make the P.I. equally sensitive to each parameter all variables must affect its absolute value equally, thus the coefficient is an attempt to match the variable magnitudes. Equal variable magnitudes resulted in much faster optimization solutions, and less computer time. Variable x_4 has an additional penalty of 5. This variable is the thickness of the interior wall of R_V and R_L. It desirable to keep this value small, so the residual resistance of the amplifier is minimized. Thus, x_4 is penalized heavily in the first performance index. Experimental results revealed difficulties in getting a good thermal bond between junction block and wall, and the second performance index placed an extremely heavy penalty on x_4. If the wall is not needed to prevent temperature gradients in the junction block, the optimization will eliminate it completely, by reducing its thickness to 0. A thicker film section can also prevent thermal gradients in the junction block. By weighting x_4 more heavily than x_3, the program will build more film gap in preference to the fixed wall resistance.

The film section length or height, x_6, is not modified with

any coefficient and is penalized. It was used as the base magnitude to size the coefficients of the other variables.

The design criteria of minimum response time has been translated into a performance index that minimizes all physical dimensions in the amplifier. This will cause the thermal element values to be small. The rewarded dimension x_1, is constrained to lie between penalized parameters and thus is held to a minimum. Other design goals would require different performance indices, and would produce amplifiers with different physical dimensions.

The next section will discuss the results of this optimization program. The resulting dimensions, combined with some practical considerations, size all the parameters in the amplifier model.

Section A3-5: Optimization results.

This part of Appendix 3 presents the output of the optimization program. Basically there were two optimizations performed on the amplifier. The first, using the first performance index presen- was done before any experimental results. Experimental necessities dictated some design changes that required a modification of the performance index. Details of the experimental results are presented in chapter 5. The modifications were described in the previous section. For simplification the amplifier generated by the first performance index:

$$P.I. = -(x_2 + x_3 + 9x_4 + x_5 + x_6^2) \qquad (A3\text{-}5.1)$$

will be termed an ideal amplifier. The amplifier designed by the second performance index:

$$P.I. = .1 * x_1^{.5} - 10[x_2 + x_3 + 5x_4 + x_5] - x_6 \qquad (A3\text{-}5.2)$$

will be called a modified amplifier. Below is a table summarizing the result of both optimizations; and the values of all dimensions on both types of amplifiers.

The dimensions of the ideal amplifier actually built and tested differ from those of the preceeding table. Practical construction considerations dictated some alterations. The specific changes will be explained in appendix 6. The dimensions listed in the table were these used to simplify the analytical model. The next section will describe the simplification possible with dimensions assigned to each model element.

Table A3-5.1: Dimensions.

Variable	Corresponding Amplifier Dimension (see figures 4-2.1 and 4-2.2)	Parameter Values Ideal	Modified
x_1	D_4 x D_3	18.5in^2	6.74in^2
x_2	D_2	.306in	.135in
x_3	D_5	.125in	.062in
x_4	D_6	.064in	.0001in
x_5	D_7	.057in	.020in
x_6	D_4, D_8	4.39in	2.60in
	D_1	.031in	.125in
	D_9	.063in	.030in
	D_{10}	1.476in	.883in
	D_{11}	.375in	.186in
	D_{12}	.063in	.187in
	D_{13}	.063in	.187in
	D_{15}	.063in	.375in
	D_{16}	.250in	0.0in
	D_{17}	.031in	0.0in
	D_{18}	.125in	.062in
	D_{19}	18.00in	18.0in
	D_{20}	6.6in	4.75in
	D_{21}	1.0in	.750in
	D_{22}	.125in	.125in
	D_{23}	.010in	.010in

The original model included all thermal lumped parameters that were judged significant in the amplifier geometry. No attention was given to the relative size or importance of different reistances or capacitances. With dimensions the value of each parameter can be examined, and the less significant parameters further lumped or eliminated to simplify the model. The simplification is described in Appendix 4.

APPENDIX A4: SIMPLIFICATION OF AMPLIFIER MODEL THROUGH COMPARISON OF PARAMETER MAGNITUDES

This appendix details the simplification of the original amplifier thermal model. The dimensions of appendix three are inserted into the element definition expressions of appendix four, and the element values are then known. The different magnitudes of element values allow some to be combined or eliminated, reducing the system from a 21st to a 7th order model.

Considerable simplification of the original amplifier model results from sizing the elements. The dimensions produced by the optimization determines each resistance and capacitance value. The model described in appendix two and shown in figure A2-3.4 has twenty-one independent energy storage elements. A twenty-first order model is extremely high order. In figure A4.1 the values of each parameter are shown for the ideal amplifier, which was dimensioned in the previous section. Because of the wide variation of parameter values the model of figure A4.1 can be condensed into the model of figure A4.2.

Several simplifications have occurred. The capacitance of the control bulb is dominated by the sensor fluid and vaporization effects. Therefore, all the sensor capacitance is lumped into one capacitative element whose value depends on the amount of fluid vaporized. But there is a fixed component to the sensor capacitance that is not less than 0.1 Btu/°F. In figure A4.2 this lumped capacitance is C_{208} and C_{228}. By similar reasoning all the resistance in the control bulb is lumped

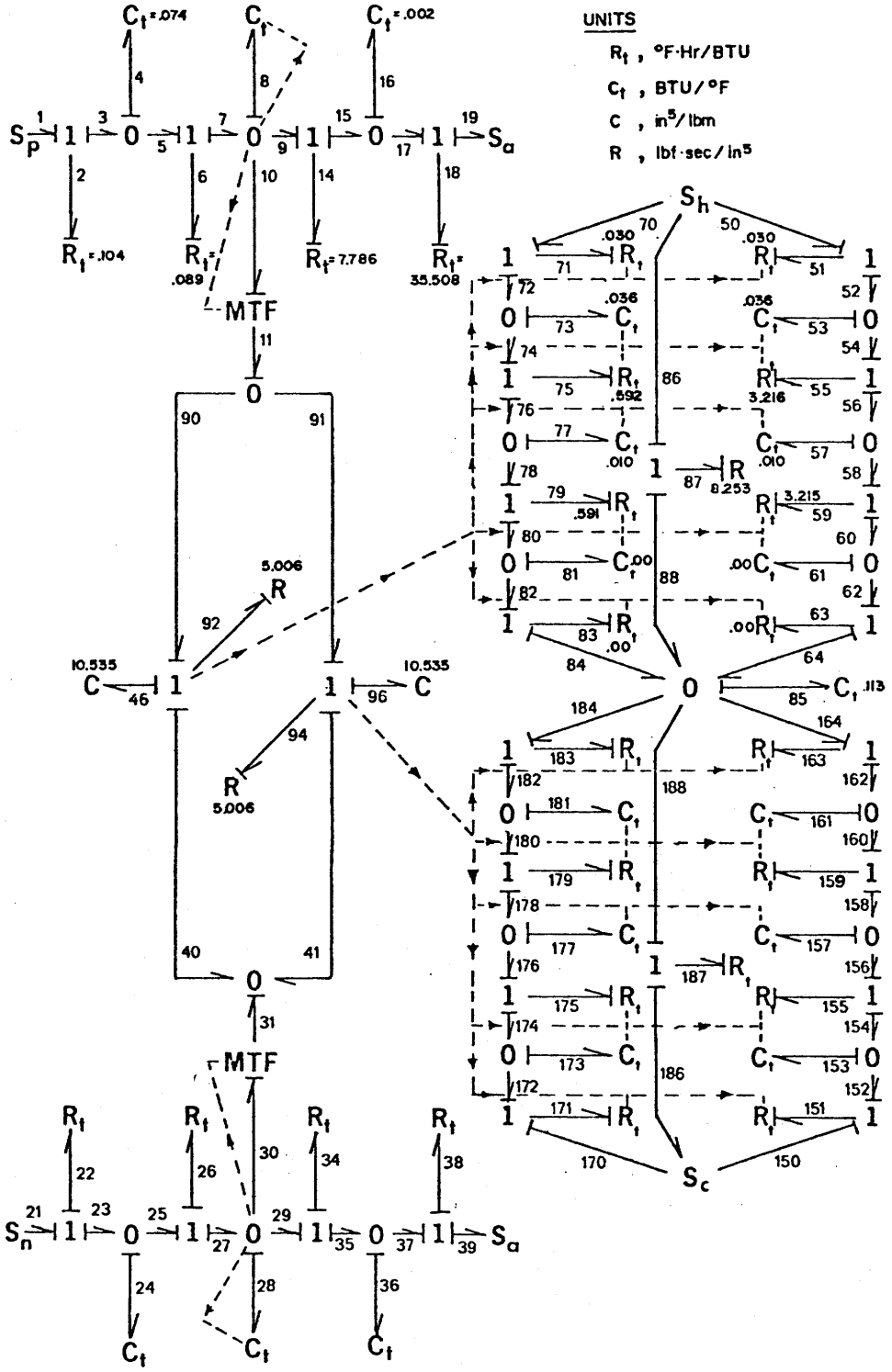

Figure A4.1: Amplifier bond graph with element values "ideal" amplifier.

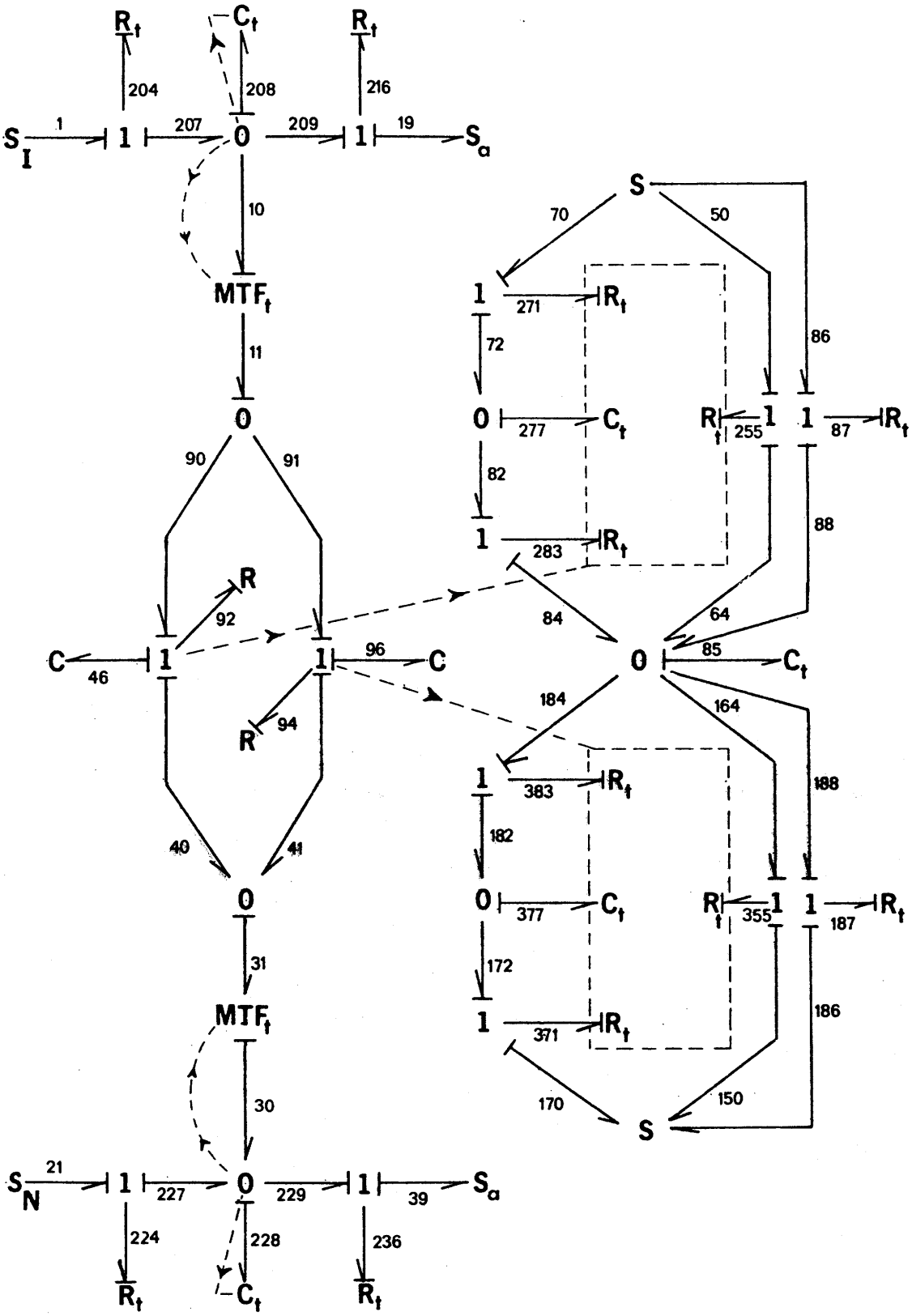

Figure A4.2: Final, simplified amplifier bond graph.

into two elements. The first is the thermal resistance to heat flow into the sensor fluid, the second is resistance to flow through the sensor fluid and out of the sensor. The flow through the second resistor would be called "leakage to ground" in electronics and effectively lowers the input impedance of the amplifier. These are shown as R_{204} or R_{224}, and R_{216} or R_{236}. The values of these lumped parameters are defined as follows:

$$C_{208} = C_4 + C_{16} + \text{variable component due to vaporization} \quad \text{(A4.1)}$$

$$C_{228} = C_{24} + C_{36} + \text{variable component due to vaporization} \quad \text{(A4.2)}$$

$$R_{204} = R_2 + R_6 \quad \text{(A4.3)}$$

$$R_{224} = R_{22} + R_{26} \quad \text{(A4.4)}$$

$$R_{216} = R_{14} + R_{18} \quad \text{(A4.5)}$$

$$R_{236} = R_{34} + R_{38} \quad \text{(A4.6)}$$

R_{204} and R_{224} are identical, and represent the thermal resistance of each sensor conducting plate.

C_{208} and C_{228} are identical, and represent all the thermal capacitance of each sensor. This includes heat stored in the sensor walls as well as the sensor vaporizing fluid.

R_{216} and R_{236} are identical, are representative of all the thermal resistance in the sensor outside walls and insulation.

C_{46}, R_{92}, R_{94}, and C_{96} remain unchanged.

R_{271} and R_{371} are identical, and represent the thermal resistance of the outside wall of both R_v and R_L, in contact with the conducting fluid, as well as $\frac{1}{2}$ the resistance of the conducting fluid.

C_{277} and C_{377} are identical, and represent all the thermal capacitance of the R_v and R_L. This includes the capacitance of conducting and insulating fluids, as well as the resistor walls.

R_{283} and R_{383} are identical, and represent the other half of the conducting fluid thermal resistance, and half of the junction block resistance, for that portion of the junction block in contact with the conducting fluid.

C_{85} remains unchanged, and is the thermal capacitance of the junction block.

R_{255} and R_{355} are identical, and represent the thermal resistance of the outside wall of each resistor in contact with the insulating fluid, as well as the resistance of the insulating fluid. In addition, each contains $\frac{1}{2}$ the junction block resistance for that portion of the junction block in contact with the insulating fluids.

The new model elements have values defined as:

$$R_{271} = R_{371} = R_{71} + R_{75} \qquad \text{(A4.7)}$$

$$C_{277} = C_{377} = C_{73} + C_{53} + C_{77} + C_{57} + C_{81} + C_{61} \qquad \text{(A4.8)}$$

$$R_{283} = R_{383} = R_{79} + R_{83} \tag{A4.9}$$

$$R_{255} = R_{355} = R_{51} + R_{55} + R_{59} + R_{63} \tag{A4.10}$$

All thermal capacitance has been removed from the insulating fluid heat path.

The simplified model is seventh order. By combining elements the resulting system has only seven independent energy storage elements. These elements are not of equal importance for the amplifiers tested. However, if a different conducting fluid were selected, such as mercury, it's density and heat capacity would give capacitances C_{46}, C_{96}, C_{277}, and C_{377} much more importance than they have with silicone oil. In Table 4-2.1 a brief summary is made of each model element and what it corresponds to, physically, in the amplifier.

This completes the description of the simplified model of the thermal operational amplifier. In appendix A5 the relevant differential equations describing this model will be derived, and the model equations solved numerically. The results will be predictions of performance for a thermal amplifier.

APPENDIX 5: DERIVATION OF THE STATE EQUATIONS FOR THE SIMPLIFIED AMPLIFIER MODEL

Section A5-1: Summary of appendix.

Section two describes the mathematical characterization of the complex sensor thermal capacitances, C_{208} and C_{228}. An expression for these capacitances must be in terms of system inputs and state variables. The total heat stored in a sensor is divided by its instantaneous temperature to find the capacitance value at a particular moment.

Section three details the remainder of the state equation derivation for the seventh order system.

Section A5-2: Characterizing the thermal capacitances C_{208} and C_{228}.

The final model of the thermal amplifier has seven independent energy storage elements, as shown in figure A4.2. A rate equation can be written for each element, describing its instantaneous energy storage. The seven equations that result, when solved simultaneously, completely describe the model behavior. This description will be the amplifier output temperature variation as a function of time, and the temperature inputs. In this section the equations describing the energy storage in the two sensors will be derived.

For derivation of the state equations some variables have to be defined. In table A5-2.1 the bond graph effort, and equivalent computer simulation variables, are summarized, with explanations. Variables Y(1) through Y(7) are called state variables, because the values of these variables totally determine the instantaneous state of the system. There are seven independent energy storage elements in the system, and the state variable values determine the amount of energy stored in each. Sensor pressure is a function of sensor temperature from the saturated vapor assumption. A different variable is used for sensor and amplifier section pressures, because instantaneously the two quantities may not be equal, since there is some small fluid resistance in the pressure conducting tubes. However, they seldom differ significantly since the thermal time constants are very much longer than the propagation time of pressure pulses down the conducting tubes. With the above variables, and

Table A5-2.1

	Bond Graph Effort		Equivalent Computer Program Variable		Description
1.	e_{208}	=	Y(1)	≡	Temperature of inverting sensor in degrees F
2.	e_{228}	=	Y(2)	≡	Temperature of noninverting sensor in degrees F
3.	e_{1}	=	XTI	≡	Temperature input to inverting sensor, °F
4.	e_{21}	=	XTN	≡	Temperature input to noninverting sensor, °F
5.	e_{46}	=	Y(3)	≡	Pressure across film section and reservoir of $R_{v,psi}$
6.	e_{96}	=	Y(4)	≡	Pressure across film section and reservoir of $R_{L,psi}$
7.	$e_{86}=e_{70}=e_{50}$	=	XTSCE	≡	Hot source temperature, °F
8.	$e_{186}=e_{170}=e_{150}=$		XTSNK	≡	Cold sink temperature, °F
9.	e_{227}	=	Y(5)	≡	Temperature of R_v's conducting fluid, °F
10.	e_{285}	=	Y(6)	≡	Junction block temperature, the output, °F
11.	e_{377}	=	Y(7)	≡	Temperature of R_v's conducting fluid, °F
12.			Y(8)	≡	Amount of heat stored in negative sensor, in Btu's
13.			Y(9)	≡	Amount of heat stored in positive sensor, in Btu's
14.	e_{11}	=	E11	≡	Pressure in negative sensor, in psi
15.	e_{31}	=	E31	≡	Pressure in positive sensor, in psi
16.			HITE	≡	Conducting fluid level in R , relative to the film section center line, in inches

those previously cited, an expression for the sensor heat storage can be derived. The negative sensor will be referred to as the noninverting sensor, the positive sensor is noninverting.

The sensors are the most difficult energy storage elements to characterize mathematically. The vapor heat storage has to be expressed as a temperature dependent thermal capacitance to combine the heat storage effects of all sensor parts. The sensor fluid heat storage can be characterized by an instantaneous thermal capacitance,

$$C_{sensor} = \frac{q}{T} = \frac{\text{Total heat stored}}{\text{Temperature}} \qquad \text{(A5-2.0)}$$

To compute the capacitance the total heat stored must be expressed in terms of the amplifier geometry, materials, and the sensor temperatures.

The computation of heat stored in the sensors will proceed as follows. The heat stored in each sensor is directly proportional to the mass of vaporized sensor fluid. The mass of sensor vapor is the vapor volume divided by its specific volume. The specific volume is a function of temperature and pressure. The sensor temperature is known, because it is an input, and so is the pressure, because the vapor is saturated. The vapor volume is equal to the total gas volume of the system minus the volume of the insulating gas. The total system gas volume is equal to the total volume of both sensors, film sections, and reservoirs, minus the volume of conducting fluid. All these quan-

tities are known. The insulating gas volume is found by the perfect gas law. The result is the heat storage in both sensors is known as a function of sensor temperatures. This development will now be repeated mathematically.

Heat stored in the positive and negative sensors is expressed by the relations:

$$Y(8) = [\text{Mass of vapor in inverting sensor}] \times h_{fg} \qquad \text{(A5-2.1)}$$

$$Y(9) = [\text{Mass of vapor in noninverting sensor}] \times h_{fg} \qquad \text{(A5-2.2)}$$

where h_{fg} is the sensor fluid heat of vaporization. The mass of saturated vapor can be determined from its volume and temperature:

$$\text{Mass of vapor} = \frac{\text{volume of vapor}}{v(T)} \qquad \text{(A5-2.3)}$$

where v(T) is the specific volume of the saturated vapor expressed as a function of the particular sensor's temperature. The saturated vapor volume is the difference between the insulating fluid volume and the total system volume, v_{total}. Since the sensors can be at different temperatures the insulating fluid in contact with each sensor will be at different pressures. Therefore the volume of insulating fluid must be calculated separately for each sensor.

$$\text{Volume of air, inverting sensor} = \frac{\text{Mass} \times R \times Y(1)}{e_{11}} \qquad \text{(A5-2.4)}$$

$$\text{Volume of air, noninverting} = \frac{\text{Mass} \times R \times Y(2)}{e_{31}} \qquad \text{(A5-2.5)}$$

The air temperature and pressure are assumed the same as the saturated

vapor. The modified amplifier used sensors with metal bellows. The bellows' spring rate will cause the saturated vapor pressure to be different from the insulating fluid. The error will be small if the spring rate is moderate. The air will not be at a uniform temperature, but will be assumed at sensor temperature. Since temperature is absolute, the percentage error caused by this assumption of uniform temperature is small. The air mass is known from initial charging. An expression for the vapor can be written:

vapor volume, inverting sensor = [total system volume (HITE), inverting sensor] - [volume of air, inverting sensor]

vapor volume, non-inverting sensor = [total system volume (HITE), non-inverting sensor] - [volume of air, non-inverting sensor]

The total system volume is a constant. But the portion of this total volume occupied by a particular sensor and its insulating fluid is <u>not</u> a constant, but a function of the conducting fluid level, expressed with the variable HITE. The conducting fluid height changes with the pressure difference between sensors. The vaporization of fluid in the sensor causes the diaphragm to expand, pumping air out of the sensor and into a film section and reservoir. At the same time the diaphragm in the other sensor will be contracting in response to the pressure increase. The total heat stored in each sensor can now be written as a function of sensor temperature and conducting fluid level; HITE:

$$Y(8) = \frac{h_{fg}}{v(Y(1))} \left[V_{total,\,inverting} - \frac{\text{Air Mass} \times R \times Y(1)}{e_{11}(Y(1))}\right] \quad \text{(A5-2.6)}$$

$$Y(9) = \frac{h_{fg}}{v(Y(2))} \left[V_{total,\,non\text{-}inverting} - \frac{\text{Air Mass} \times R \times Y(2)}{e_{31}(Y(2))}\right] \quad \text{(A5-2.7)}$$

The two sensors will have inverse vapor volume changes, one volume increasing, the other decreasing. The change can be computed directly from the sensor temperatures.

The variable HITE is the variable Δh, discussed in Chapter 3, and representing the film section conducting fluid height above the film section mid-point, in $\underline{R_v}$:

$$HITE = \frac{e_{11}[Y(1)] - e_{31}[Y(2)]}{2\rho_5}$$ where ρ_5 is the density of the conducting fluid (A5-2.8)

The conducting fluid will have a height-Δh in the film section of R_L. The value of HITE is multiplied by the cross-section area of either the reservoir or film section (because they are equal) and the product is a volume change. Twice this volume change is the total change from the initial condition, HITE = 0, for each sensor:

$$V_{total,non\text{-}inverting} = \text{total initial volume} - D_9 * D_{10} * \frac{(e_{11}[Y(1)] - e_{31}[Y(2)]}{\rho_5}$$

(A5-2.9)

$$V_{total,inverting} = \text{total initial volume} - D_9 * D_{10} * \frac{(e_{31}[Y(2)] - e_{11}[Y(1)])}{\rho_5}$$

(A5-2.10)

Now the heat storage of each sensor can be written completely as a function of temperature:

$$Y(8) = \frac{h_{fg}}{v(Y(1))} \left[\text{total initial volume} - D_9 * D_{10} * \frac{(e_{31}(Y(2)) - e_{11}(Y(1)))}{\rho_5} - \frac{\text{Air Mass x R x } Y(1)}{\rho_{11}(Y(1))}\right.$$

(A5-2.11)

$$Y(9) = \frac{h_{fg}}{v(Y(2))} \left[\text{Total Initial Volume} - D_9 * D_{10} * \frac{(e_{11}(Y(1)) - e_{31}(Y(2)))}{\rho_5} - \frac{\text{Air Mass x R x } Y(1)}{e_{11}(Y(1))}\right] \quad \text{(A5-2.12)}$$

Note the equations are coupled. The heat storage is now totally in terms of Y(1) and Y(2), but each temperature appears in both equations. This heat storage represents only the heat stored in the sensor fluid vapor.

A value for the thermal capacitance of the sensor walls was calculated in chapter four. All the capacitance in both sensors can be characterized by the following expressions:

$$C_{208} = \frac{Y(8)}{Y(1)} + C_4 + C_{16} \quad \text{(A5-2.13)}$$

$$C_{228} = \frac{Y(9)}{Y(2)} + C_{24} + C_{26} \quad \text{(A5-2.14)}$$

have been defined previously. This analysis is valid for a sensor with metal bellows instead of a flexible diaphragm, when an additional term is added to account for the thermal capacitance any volume of sensor liquid in the bellows. Previously this term was ignored, however, a bellows has substantially more volume than the ideal flat sensors, and the sensor liquid capacitance effects cannot be ignored. It is a simple matter to lump this effect with C_4 and C_{24}.

Section A5-3: Equation derivation.

With the capacitances C_{208} and C_{228} characterized, the bond graph of figure 4-5.2 provides all the information necessary to derive the governing differential equations. The equations will be written in terms of the bond graph variables. Each bond will have an effort and flow associated with it. The effort, temperature or pressure, will be represented by e; the flow, heat flow or volume flow by f. The subscript will reference the particular bond the variable is associated with. The physical meaning of the system model elements has been described previously. The governing equations are rate equations, that express effort variable change as a function of time.

The sensor capacitance rate of temperature change is expressed by the relations:

$$\dot{e}_{208} = \frac{1}{C_{208}}\left[\frac{1}{R_{204}}[e_1-e_{208}] - e_{11}[\frac{1}{R_{92}}[e_{11}-e_{31}-e_{46}] + \frac{1}{R_{94}}[e_{11}-e_{31}-e_{96}]] - \frac{1}{R_{216}}[e_{208}-e_{19}]\right] \qquad \text{(A5-3.1)}$$

$$\dot{e}_{228} = \frac{1}{C_{228}}\left[\frac{1}{R_{224}}[e_{21}-e_{228}] + e_{31}[\frac{1}{R_{92}}[e_{11}-e_{31}-e_{46}] + \frac{1}{R_{94}}[e_{11}-e_{31}-e_{96}]] - \frac{1}{R_{236}}[e_{228}-e_{39}]\right] \qquad \text{(A5-3.2)}$$

The two efforts e_{11} and e_{31} are the saturated pressures of the vapor in each sensor and are a function only of the sensor fluid's temperature. Specific functions for specific fluids are indicated in table A4-4.1.

The remaining state variables are much simpler to characterize. The state equations are:

$$\dot{e}_{46} = \frac{(e_{11} - e_{31} - e_{46})\, R_{92}}{C_{46}} \qquad \text{(A5-3.3)}$$

$$\dot{e}_{96} = \frac{(e_{11} - e_{31} - e_{96})\, R_{44}}{C_{96}} \qquad \text{(A5-3.4)}$$

$$\dot{e}_{227} = \left[\left(\frac{e_{70} - e_{227}}{R_{271}} \right) - \left(\frac{e_{227} - e_{85}}{R_{283}} \right) \right] \frac{1}{C_{227}} \qquad \text{(A5-3.5)}$$

$$\dot{e}_{85} = \frac{1}{C_{85}} \left[\left(\frac{e_{227} - e_{85}}{R_{283}} \right) + \left(\frac{e_{50} - e_{85}}{R_{255}} \right) + \left(\frac{e_{86} - e_{85}}{R_{87}} \right) - \left(\frac{e_{85} - e_{186}}{R_{186}} \right) - \left(\frac{e_{85} - e_{377}}{R_{383}} \right) - \left(\frac{e_{85} - e_{150}}{R_{355}} \right) \right]$$

$$+ \text{radiation effects (if any)} \qquad \text{(A5-3.6)}$$

$$\dot{e}_{377} = \frac{1}{C_{377}} \left[\left(\frac{e_{85} - e_{377}}{R_{383}} \right) - \left(\frac{e_{377} - e_{170}}{R_{371}} \right) \right] \qquad \text{(A5-3.7)}$$

When the preceeding equations are integrated with respect to time, performance of the amplifier is predicted.

APPENDIX 6: CONSTRUCTION AND RECONSTRUCTION OF TEST AMPLIFIER

Section A6-1: Summary of appendix:

This appendix presents the experimental effort spent building the test amplifiers. It includes more detail in order that the construction mistakes made by the author be not repeated by future investigators of this topic. The ideal amplifier represents the amplifier constructed with the belief that all modeling assumptions were true. The modified amplifier was the final amplifier constructed with the benefit of the experience gained from the ideal amplifier.

Section two describes the problems encountered in building the ideal amplifier that was computer simulated in chapter four. The resistor side wall thickness proved to great to vacuum mold the resistor as a single piece, and was reduced. The resistors, originally completely polycarbonate, could not be effectively bonded to copper contact plates with thermal epoxy.

Section three details the ideal amplifier design changes to solve the problems of section 2. The polycarbonate in the amplifier is substantially reduced, and the outer walls are made solid copper. The assembly method is described. The method of Boys was used to evaluate the capillarity of the conducting fluid, and the film section gap was reduced. An amplifier with this improved ideal design was constructed.

Section four narrates the unsuccessful attempts to make the flexible diaphragm sensors work. Air diffusion through the diaphragm proved an unsolvable problem. A sensor design using a metal bellows is selected as an alternative. The bellows spring rate substantially reduces amplifier gain. To compensate for this effect the performance index is changed to penalize amplifier volume, which lessens bellows deflections, and the modified amplifier is designed with this optimization program change.

Section five describes experiments performed with the modified "ideal" amplifier. Even though there are no sensors to drive the amplifier, simulated pressure inputs are used to evaluate its response. The experimental procedure is outlined. The time response was found to agree with prediction, but the measured range was 30% below expectation. The published conductivity of the conducting fluid, silicone oil, was found to be 50% high.

Section six details the construction of the modified amplifier and its metal bellows sensors. Dimensions and construction details are given. The model remains valid for the bellows sensors if the assumed density of the conducting fluid is increased to compensate for the bellows' spring rate. A method to determine the increase is described.

Section A6-2: Unsuccessful attempt to construct an ideal amplifier.

The initial design of the ideal amplifier is shown in figure A6-2.1. In appendix two, figures A2-2.1 and A2-2.2, the significant dimensions of the amplifier parts were designated by subscripted variables. Table A3-5.1 assigned values to these dimensions for both types of amplifiers optimized. Actual construction required some deviation from the design used to construct the mathematical models. Most of the changes involved problems with mechanical assembly of the device.

Vacuum molding was the method selected to construct the film section and reservoir assembly. Originally the inner and outer walls of both R_v and R_L were specified to be .062 polycarbonate. Polycarbonate can be vacuum molded; a process where a sheet of thermoplastic material is heated, and then placed against a male die of the desired shape. A vacuum is drawn between the die and heated sheet. Atmospheric pressure forces the sheet to stretch and conform to the die shape. When the sheet cools it will permanently retain the die shape. An illustration of a single piece, resistor-reservoir combination with a back plate is shown in figure A6-2.2. It eliminates sealing problems at joints by reducing the total number of joints required. A large flange was left around the vacuum molded part to facilitate bonding to the back plate. The resulting assembly of R_v and R_L had only 2 pieces.

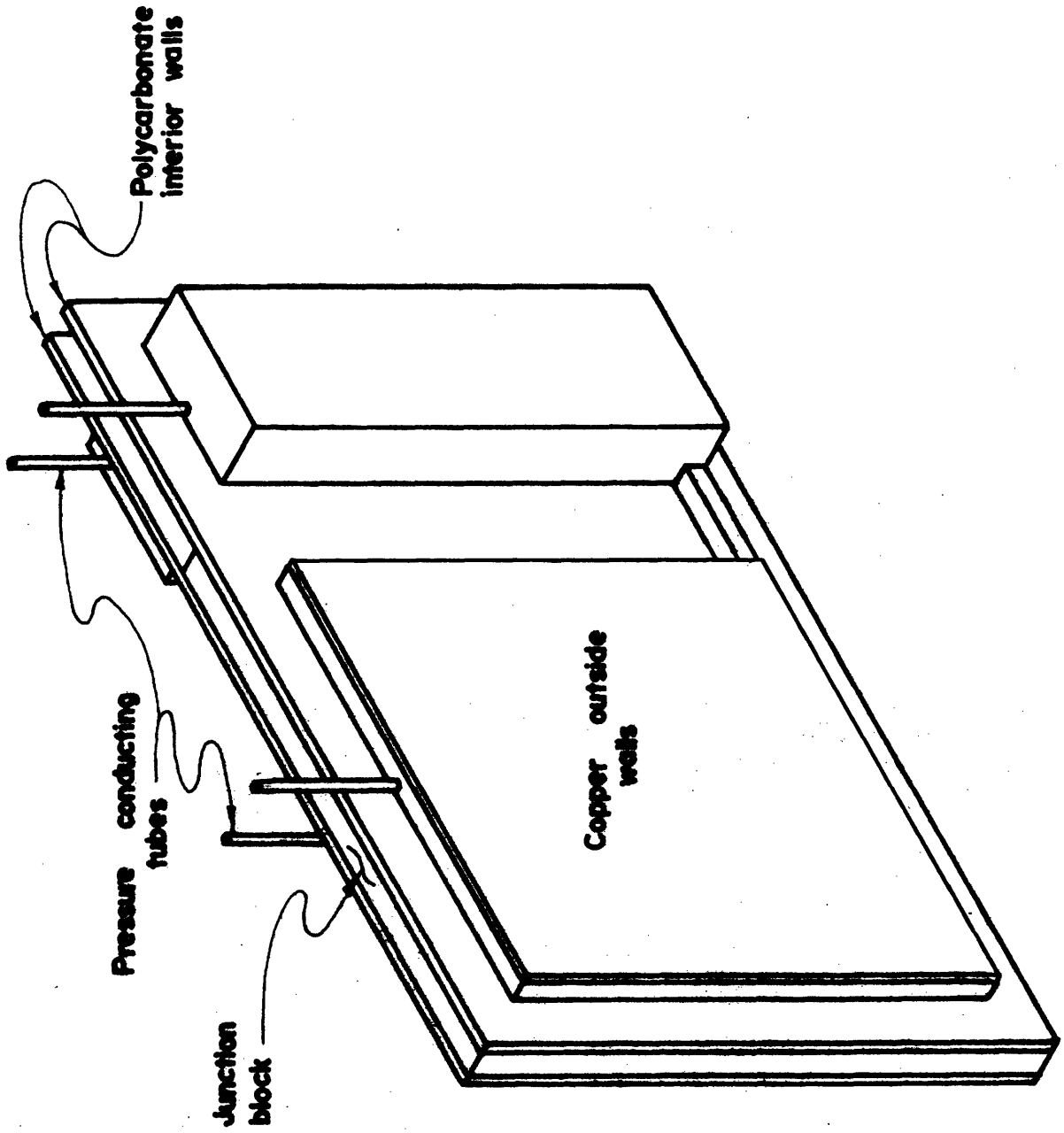

Figure A6-2.1: Initial ideal amplifier design.

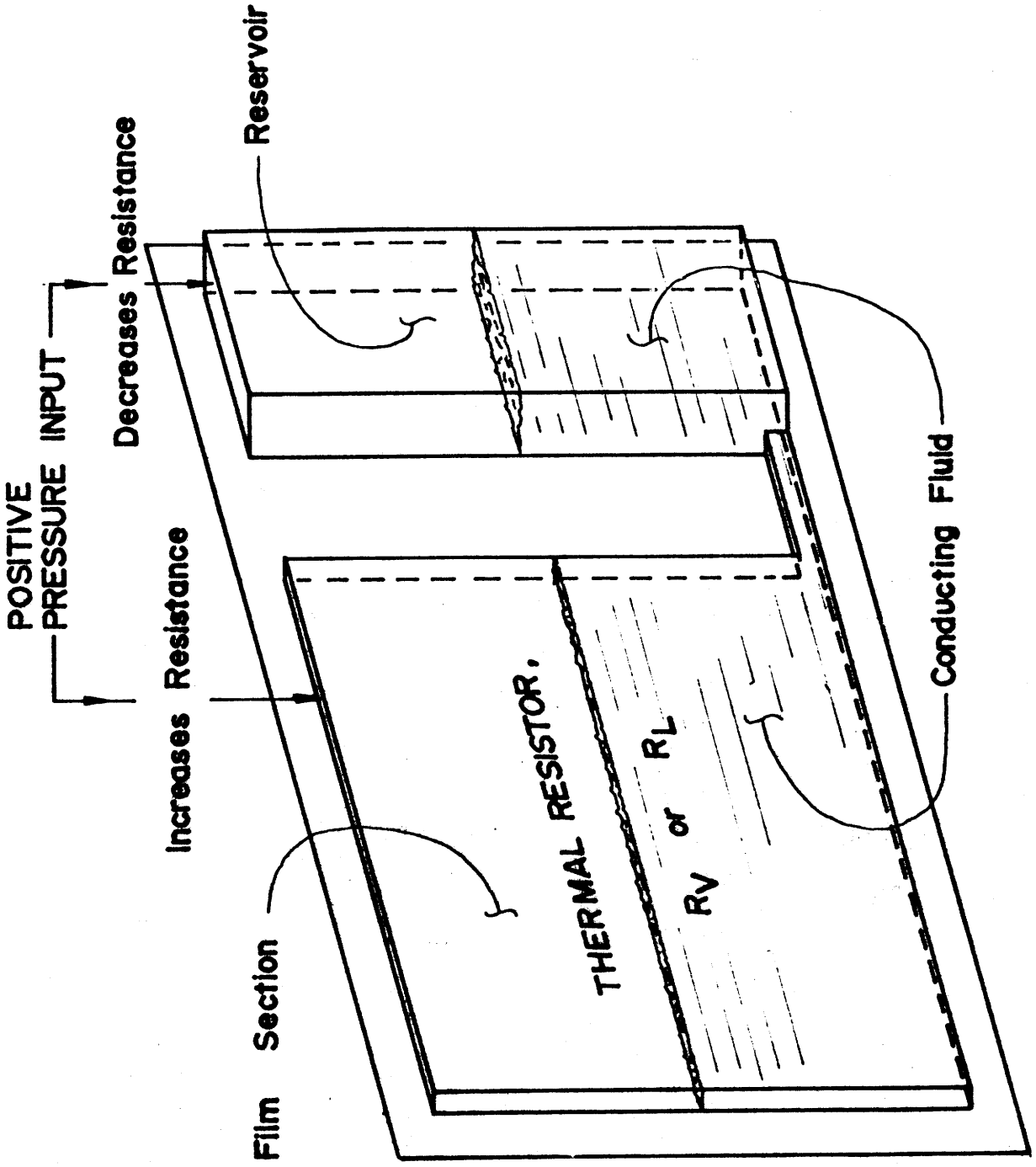

Figure A6-2.2: Vacuum-molded resistor-reservoir combination

Several unsuccessful attempts were made to vacuum mold .062" polycarbonate: it was much too thick to conform properly to the mold shape. Thick material leaves a large fillet in mold corners. Since it was important the film section and reservoir have equal volumes, this proved intolerable. Thus the outer sheet of polycarbonate was reduced to .030" in thickness.

To provide good thermal contact with the source and sink a .032" thick copper plate was to be bonded to the outside wall of R_v and R_L. The new .030" polycarbonate outer wall of R_v and R_L proved too flexible, and the addition of the copper would have given the outside wall necessary rigidity. Rigidity is important to good thermal contact between the resistor outside walls and the temperature source and sink. Thermal contact is achieved by spreading a thermally conducting paste between closely mated surfaces. If the surfaces are not flat and rigid, they will bend and leave air pockets or excessive paste thickness, vastly reducing the quality of the thermal contact.

The amplifier had four pressure taps, one on each film section and reservoir, which were originally brass tubes glued in place with an epoxy. The vacuum molded film section and reservoir was bonded to the backplate with a solvent cement. The junction plate was bonded to each resistor with a layer of thermally conductive epoxy. The copper plates attached to each resistor outside wall were adhered in the same manner.

The design shown in figure 6-2.1 required substantial modification. Attempts to bond the polycarbonate resistor walls to the copper plates failed. Two thermal epoxys were tried; TRA-BOND 2151, and EPO-TEK 90. In each case the polycarbonate in contact with the epoxy crazed and fractured, having been chemically attacked by the epoxy. Attempts to substitute standard epoxy for the thermal variety resulted in extensive "peel" problems, especially at elevated temperatures. The two materials differ in thermal expansion by 40% (9×10^{-6}/°F for copper, 5.6×10^{-6}/°F for polycarbonate), which created bonding difficulties due to thermal stresses for joints operating over a 180°F temperature range.

The differential thermal expansion of the epoxy and polycarbonate also created problems in bonding the pressure tap tubes. To operate correctly the amplifier had to be air tight as well as structurally sound. Any local peel of the epoxy created an air leakage path.

The bonding and vacuum drawing construction-problems dictated some design modifications. The next section will describe the design changes and the ideal amplifier actually built and tested.

Section A6-3: Revised design and construction of ideal amplifier.

The wall bonding problems described in the previous section were solved by the design changes shown in figure A6-3.1, a drawing of the revised ideal amplifier design. Vacuum molded polycarbonate still forms the reservoir and the film section edges, but there is no polycarbonate inner wall attached to the junction block. Instead, the molded part is bolted directly to the copper junction block. Long screws pass through the junction block, and the small piece of polycarbonate which separates the reservoirs, (the reservoir block) and clamp both vacuum molded sheets simultaneously. The junction block and reservoir block were threaded, so the molded sides could be attached separately. A silicone sealant was applied to the molded flange just prior to assembly. To insure the conducting tube between film section and reservoir was sealed, a thin polycarbonate backing sheet was applied to the vacuum molded piece in the area of the conducting tube and was bonded with a solvent.

The break between the reservoir block and the junction block could be a potential source of leaks. The small backing piece bridges the gap behind the conducting tube and provides a flat surface to seal. In the vacuum mold a thin recess for this backing plate was provided, so the back plane of the vacuum molded piece remained flat.

The outside of R_v and R_L is formed by joining two pieces of copper plate. The base plate is .062" copper that is drilled and tapped

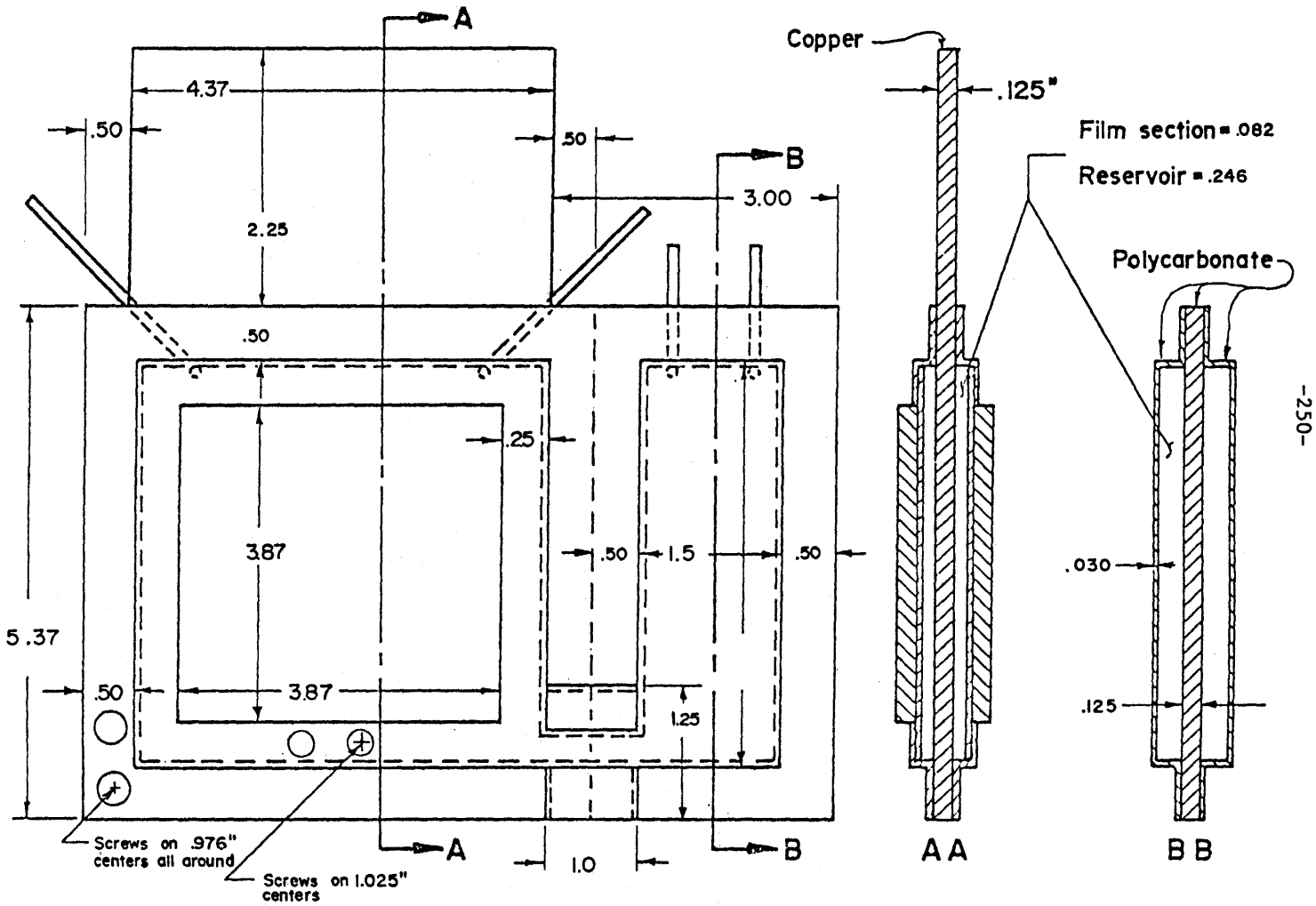

Figure A6-3.1: Revised ideal amplifier design

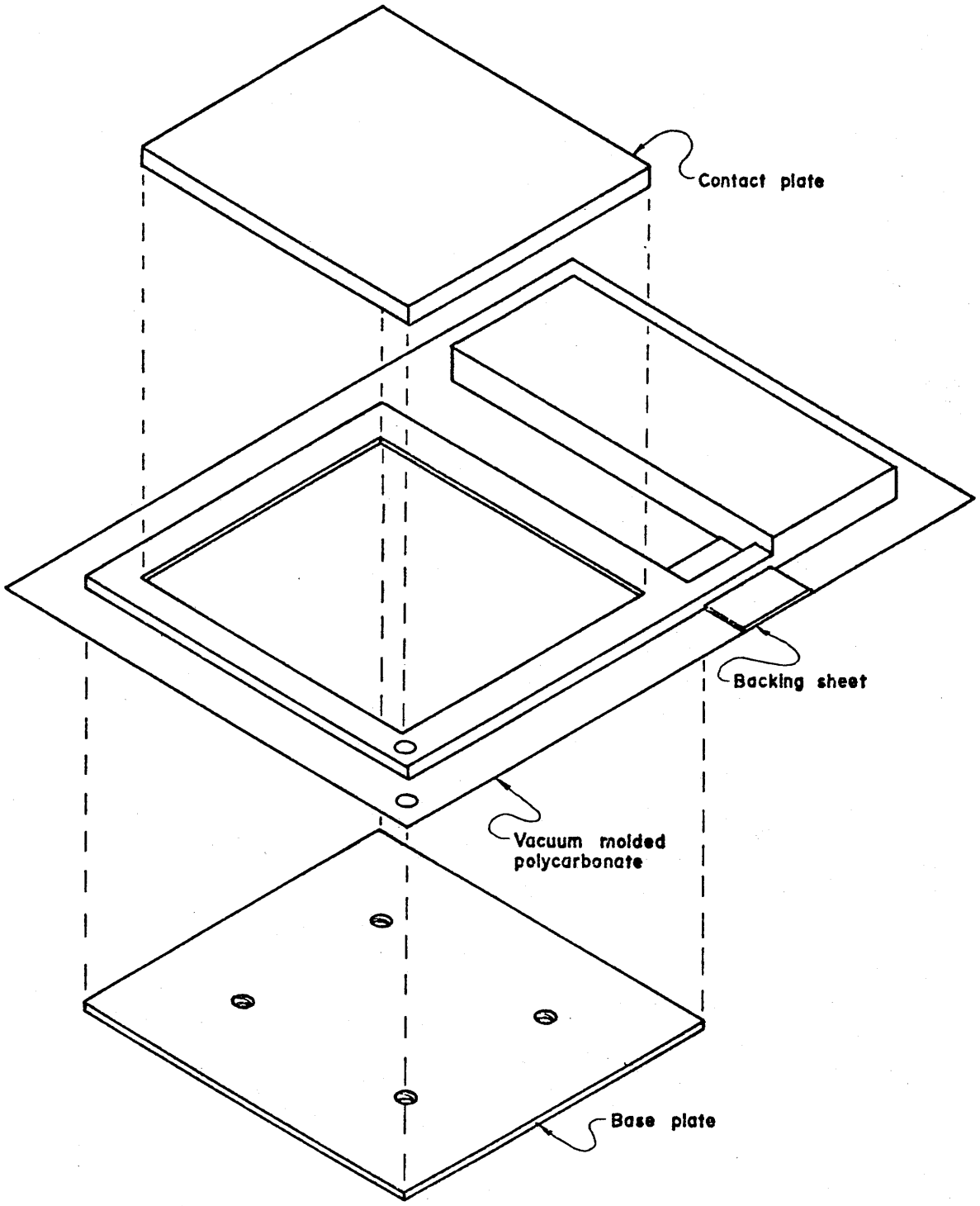

Figure A6-3.2: Resistor outside wall assembly.

on its perimeter. These holes accept the short screws which bolt a polycarbonate flange to the plate. This flange is left when a square hole is cut in the vacuum molded part, as shown in figure A6-3.2. This base plate also has holes that nylon spacers are screwed into. These spacers hold the base plate and junction block precisely separated, while at the same time keeping the fixed heat path between the outside wall and junction block as small as possible. The spacer holes are drilled and tapped, and then the contact plate is soldered to the base plate. The two plates are pressed together while cooling to keep the solder thickness very small. The contact plate makes the threaded holes in the base plate "blind" holes, which are air tight. The nylon spacers are threaded into these blind holes, and cut roughly to length. Once in place each spacer is then precisely ground to exact length, to insure the accuracy of the film section thickness. The ideal amplifier had 9 spacers; in the modified, only four spacers were used. When the outside wall assembly is bolted to the polycarbonate flange a silicone sealant is used, again to insure air tightness. The contact plate is thick enough, .125 inch, to stand above the heads of the button head socket screws used to attach the polycarbonate to the copper.

During the amplifier wall redesign the thickness of the film section was reduced from .125 inch to .082 inch. In the optimization the film section thickness was constrained to be greater than .125 inch. This was to insure no significant capillary action would occur in the film section. However, testing had not been done to find the minimum

thickness possible with insignificant capillary action. The silicone oil was tested for capillarity by the method of Boys. (Ref. 6).

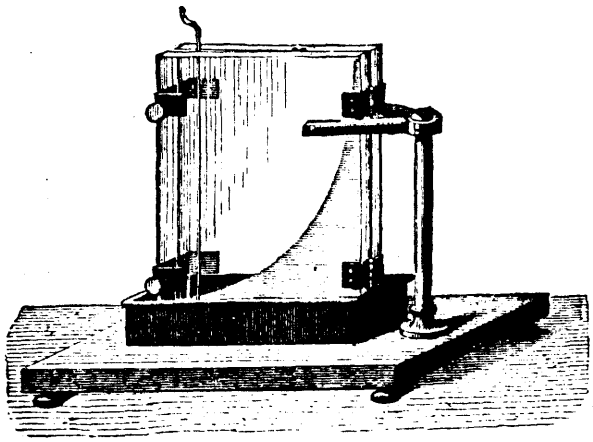

Figure A6-3.3: Method of Boys for capillarity testing.

Figure A6-3.3 illustrates the method. Two transparent plates are allowed to touch at one edge and are separated by a known gap on the other. The plates are then set in a shallow dish containing the fluid whose capillarity is to be evaluated. The fluid will rise between the plates forming a hyperbolic curve, the fluid height at any point being a direct function of the gap between plates. The gap required to keep capillary effects below some acceptable value is then observed. For silicone oil, with a viscosity of .134 reyns, a gap of .053 inch was the minimum feasible. This gap represented only .125 inch of capillarity, reducing the minimum used in the optimization of .062 inch.

The optimization program was run again for an ideal amplifier with the new lower limit of .062 inch on film section thickness. The

program returned a value of .082 inch for the film section thickness. It also reduced the sensor volume by a commensurate percentage. All other dimensions on the amplifier remained unaffected.

The temperature source and sink are attached to the contact plates, which are coated with a thermally conductive paste. The outside wall thickness, a total of .187 inches, make it extremely rigid. The revised design eliminates polycarbonate from the heat conduction path through the film sections. Originally the interior polycarbonate wall was to prevent temperature gradients across the junction block. However, the thermal resistance of silicone oil is 2000 times greater than copper. Therefore, the conductive fluid alone has enough resistance to guarantee the junction block will be at a uniform temperature.

The revised design of figure A6-3.1 eliminates the adhesive "peel" problem caused by differential thermal expansion. There is no parallel wall bonding. The silicone sealant used for the joints is flexible. The rigid walls, all copper, are the main structural members of the amplifier. The thin polycarbonate side walls serve only to seal the edges.

In use, the amplifier is clamped between the source and sink, and the compressive force is transferred from the contact plates to the junction block by the spacers. The copper plates have little internal thermal resistance and so have an almost uniform temperature. Thus, even though the three main structure members, the two outside walls and junction block, are at different temperatures, each is uniform in

temperature. There are no thermal stresses introduced by this arrangement, and no warping or peel problems.

The adhesive peel problems around the pressure taps were avoided by moving the taps into a body of uniform temperature, the junction block. As shown in figure A6-3.1, the pressure input to the film sections is brought through holes in the junction block. Stainless steel 16 gauge tubes are soldered in the block to connect the pressure tubes. The pressure taps to the reservoirs are holes drilled in the polycarbonate reservoir block, with stainless steel tubing sealed into them.

Ports were attached to the side of each reservoir for conducting fluid filling. These ports were small polycarbonate blocks, solvent-bonded to the reservoir walls, tapped with a #4-40 tap. The hole allows a hypodermic needle to fill the reservoir and film section. The hole was sealed by a flat head screw with an '0' ring under the head.

This amplifier proved very leak resistant. It was tested by immersion in water while internally pressurized at 3 psi. The reservoir shape distorted at this pressure, but sealing integrity remained.

This section has discussed the resistor-reservoir construction with no mention of the sensors. The next section will describe the original sensor design, and the associated problems,

Section A6-4: Unsuccessful ideal sensor design and testing.

The sensors originally designed to drive the ideal amplifier are shown in figure 3-6.2. The volume inside the sensor was specified by the BOX routine used to optimize the amplifier dimensions. The conducting plate is aluminum, with a cavity milled out. The cover is polycarbonate, which has #4-40 clearance holes for the the screws which clamp the two halves together. The conducting plate is drilled and tapped for the screws. A seal between the two halves is achieved by making the flexible diaphragm the same outside dimensions as the sensor, and punching holes in the diaphragm to allow the clamping screws to pass through. Vacuum grease was applied to each side of the diaphragm, before installation, to insure a good seal. The diaphragm divides the sensor cavity. To inject the sensor fluid a #2-56 access hole is provided in the conducting plate. The air pumped by the diaphragm enters or exits via a #4-40 threaded hole in the cover. A 16 gauge stainless steel tube with a #4-40 thread is inserted. Both threaded openings are sealed with '0' rings.

Unfortunately, this sensor could not be made to work. The problem was air consistently permeated the diaphragm. The air quickly destroyed the temperature/pressure functional relationship the saturated fluid is assumed to possess. Air in the sensor fluid gave the flexible diaphragm a highly nonlinear effective spring-rate, contrary to the assumption of flexibility. If given enough time the diaphragm

would "inflate" until the diaphragm was pressed tightly against the cover.

Several different diaphragm materials were tested. The original sensor fluid was 3-M's Florinert, FC-88, which did not chemically attack most polymers. Diaphragms were made from: dental dam, neoprene, buna-N, polyester, and vinyl. While all the materials would retain the sensor fluid, all failed to prevent air seepage. Attempts were made to coat the polymer diaphragm with a metal film. While slowing the air infiltration rate by a factor of 10, the pin-holes and cracks in the metal film (the latter resulting from the metal film's inability to stretch with the polymer backing) still admitted too much air. Thicker, nonstretching polymer diaphragms were considered, but such diaphragms would have a highly nonlinear spring rate, and tend to be viscoelastic.

Corrugated metal diaphragms were considered. Empirical and closed form data exist for the spring rate and geometry of thin, metal, circular diaphragms (Ref. 29,30). Corrugated diaphragms have two disadvantages. First, the spring rate of such diaghragms is very high. The corrugations make the diaphragm elastic over a wide range of displacement, but actually cause the small displacement spring rate to be higher than for a flat plate of the same thickness. Only when the metal becomes extremely thin does the spring rate become low enough to be practical. Second, for this application, the elastic spring rate of a corrugated diaphragm is not constant, but rather a function

of deflection. This would render the amplifier performance nonlinear as well, unless a compensation technique was found.

The decision was made to construct the sensors with metal bellows. A bellows has a very linear spring rate, which can also be very low if the corrugations and material thickness can be properly combined. However, for this particular amplifier sizing, no combination of material and geometry made the spring rate negligible.

A spring rate reduces amplifier gain. A pressure difference generated by a temperature difference between sensors must now perform two tasks. The pressure has to deflect the bellows and cause a conducting fluid level change. With a completely flexible diaphragm in the sensor all the pressure difference would be compensated for by conducting fluid level change. But a bellows spring rate will compensate for some pressure difference and cause the conducting fluid level deflection to be less. The output temperature change will be less for a given temperature input. Hence gain is reduced.

The effect of a bellows spring rate can be reduced if a given bellows deflection produces a greater conducting fluid level change in the resistors. A spring rate puts a premium on the air volume pumped by the sensor. The highest gain amplifier will be configured to require the lowest pumping volume to effect the resistance change in R_V and R_L.

The ideal amplifier was designed with little consideration for volume pumped. The optimization program returned the smallest size consistant with the other constraints. But total volume pumped was not penalized and no effort was consciously made to minimize it.

The amplifier design was modified to account for gain lost through additional volume pumped, by changing the performance index used in the optimization. The result was generation of the modified amplifier, which was built and tested.

Even though a new amplifier was built to employ bellows sensors, much valuable design data was gained from the ideal amplifier constructed. The next section will outline tests on the ideal amplifier.

Section A6-5: Tests on the ideal amplifier.

The sensors designed for the type 1 amplifier could not be made to function correctly. However, the amplifier body functioned as designed, and was tested for time response and gain. Small differential pressure inputs were substituted for sensor inputs.

Two important pieces of data were gathered. First, the thermal time constant proved very close to that originally predicted. Second, the predicted output range was about 30% less than predicted.

The amplifier tests were performed in the experimental apparatus diagrammed in figure 5-2.1, and photographed in figure A6-5.1. The hot source and cold sink were constructed identically. A stainless steel beaker was sawed to create a flat side approximately 5 inches across. A 1/8 inch copper plate was soldered onto the beaker to provide a rigid, flat, conductive surface to place against the contact plate of the amplifier. The stainless steel permitted the use of magnetic stirrers to agitate both source and sink. Two 300 watt immersion heaters were used to keep the source boiling. The heaters were AC powered through a variac to control the violence of boiling. An automatic syphon was used to keep the water level in the source constant; as the water boiled away it was syphoned from a large flat pan, which was on a level with the top of the source.

The sink was an agitated ice bath. As the ice melted the water was syphoned off and the ice manually replaced. The source,

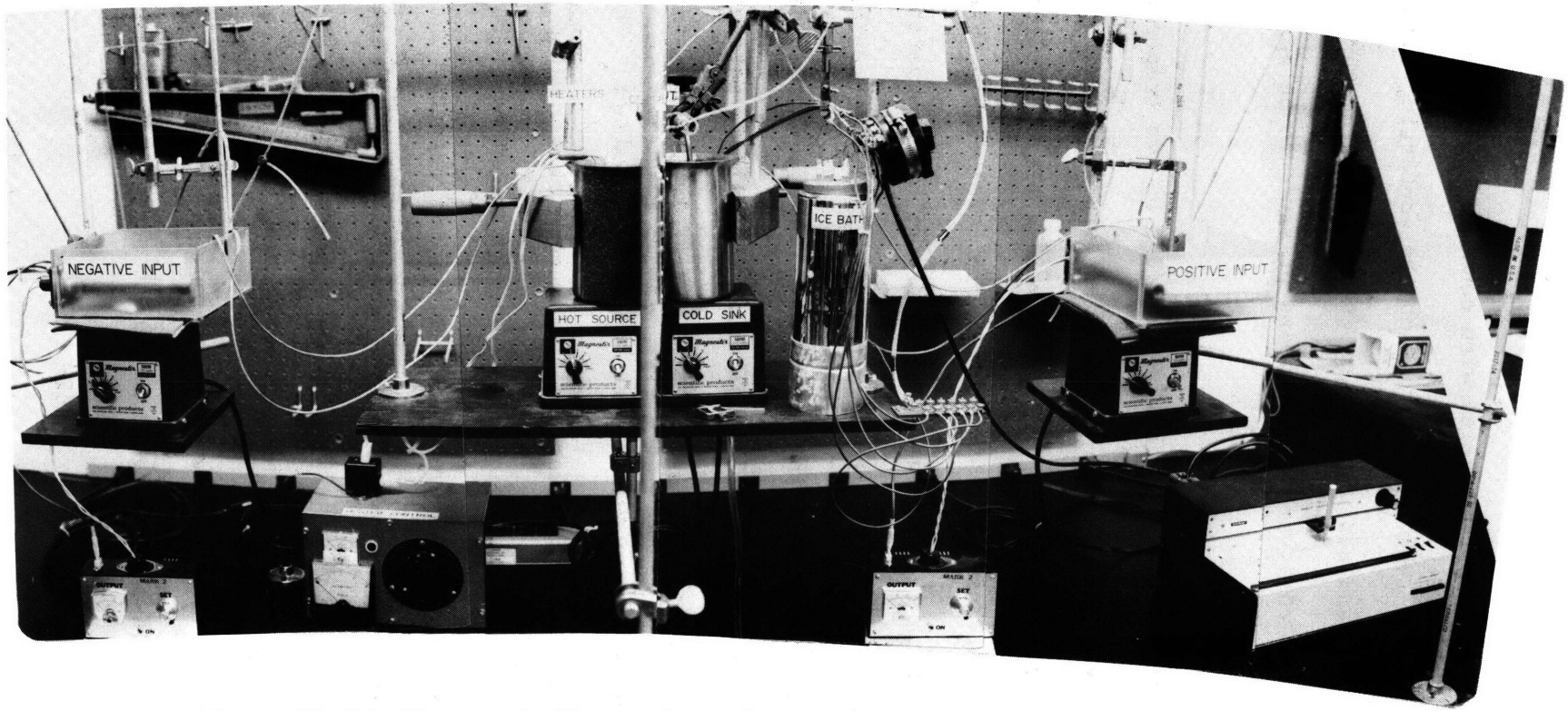

Figure A6-5.1: Photograph of experimental apparatus

amplifier, and sink were connected with conductive Thermacoat ($K = .43 \frac{Btu}{hr\ ft^2 {}^\circ F}$), which was spread on the contacting surfaces. A large Jorgensen hand screw clamp was used to hold the three parts together. It enabled a variable clamping pressure to be applied to the assembly.

The temperature inputs were provided by two temperature baths, one for each sensor, in which the sensors were immersed. The baths were rectangular tanks, $6\frac{1}{2}$" x 7" x 3" constructed from 1/4" polycarbonate, solvent bonded into tank form. Polycarbonate was chosen for its high thermal resistance and good high temperature mechanical properties. A Watlow Firerod, 2Ω, 550 watt modulated heater, #N 7Jx2A, was built into each tank. This heater, under the control of an RFL Model 70-115 temperature controller, motivated and maintained the bath temperature at some preset level above ambient, being a proportional controller with thermistor feedback. The logic was bought separately and assembled into a controller. This allowed the installation of a more sensitive 10-turn potentiometer for the temperature setpoint, and a voltmeter to monitor output. The maximum current capacity of the controller was 15 amperes, which resulted in a maximum power input to the bath of 450 watts. A magnetic stirrer was used to agitate each bath. The sensors were supported in the bath by polycarbonate rings that were perforated. This was to allow free water flow over the whole conducting plate of the sensor.

A precision thermometer was suspended in each bath as a visual indicator of temperature. The baths were thermally insulated from the magnetic stirrers, which tended to have a high steady state operating temperature.

Type E (chromel-constantan) thermocouples were embedded in the conducting plates of both sensors, to monitor their temperature. Type E thermocouples were also embedded in the outside wall of R_V and R_L, and the junction block. A thermal epoxy was employed for this task. An ice reference point was used, rather than an electronic ice point. The latter being found too variable to produce consistent results.

The thermocouple outputs were read and recorded on three different instruments. For the open loop gain experiments the sensor thermocouples were wired differentially. This differential signal was sent through an Omega OMNI-AMPI thermocouple amplifier, with a gain setting of 100. The signal was then read by a calibrated HP 970A digital multimeter. The combination yielded a resolution of one micro volt on the input. In practice noise reduced resolution to $\pm$ 3 micro volts ($\simeq \pm$ .1°F).

The absolute temperatures of the source, sink, junction block, and sensors were recorded on a Heath 201A Strip Chart recroder, with a sensitivity of ten milli-volts full scale. Resolution was only to $\pm$ 30 microvolts, which is approximately $\pm$ 1°F.

For the closed loop experiments the thermocouple voltages were read on a model 8350A Fluke digital multimeter, with a resolution to 1 micro volt ($\simeq$ .03°F) chart recorder and later converted to temperatures from thermocouple tables. Accuracy of measurement was approximately one tenth degree farenheit.

The amplifier response is a temperature change in the junction block. The junction block temperature changes in response to a conducting fluid level change in R_V and R_L. For tests on the type one amplification the inputs were small pressure differences across the reservoirs and film sections. The pressure were scaled to produce 2", 3", and 4" differences in the film section fluid levels. Computer simulations were run for the same inputs.

A comparison of the measured and predicted time response is illustrated in figure 5-3.2. The response is normalized to the steady state, and is plotted against time. The data points are from experimental runs, the dashed lines are computer prediction. The segment seems very good, especially considering this is heat transfer data, which is generally difficult to make consistent.

The absolute temperature change of the junction block for a given input did not agree with prediction. Figure A6-5.2 plots the predicted and measured junction temperature change for a given conducting fluid level difference between R_V and R_L. The problem was determined to be the reservoir temperatures assumed for simulation, and the con-

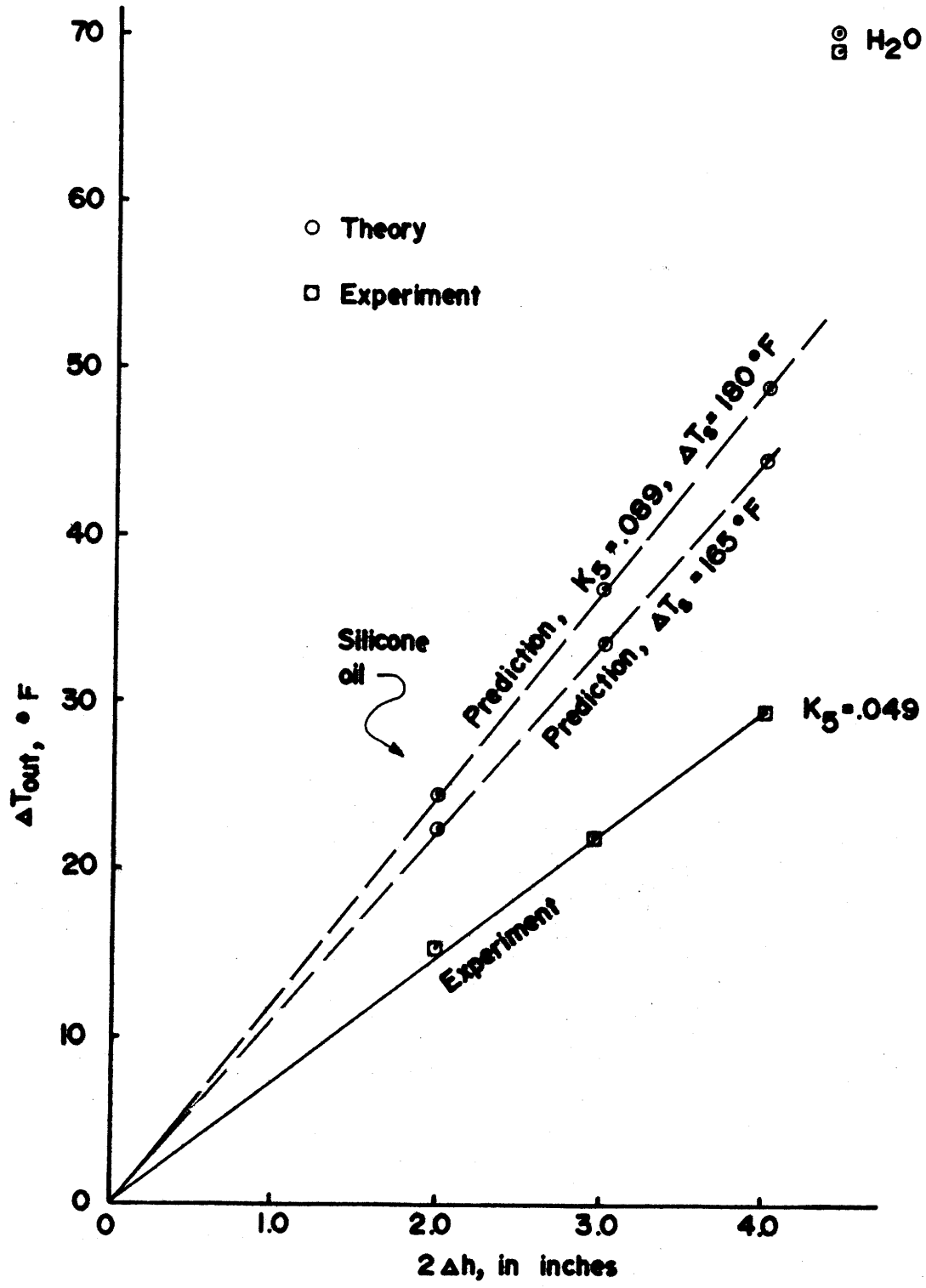

Figure A6-5.2: Predicted versus measured junction temperature change.

ductivity value of the oil.

The prediction assured a source temperature of 212°F and a sink temperature of 32°F. In actual experiments the outside walls of R_v and R_L could not be made to hold these levels. The actual source temperature ran about 202°F and the sink temperature about 37°F. This results in some adjustment in the prediction, as shown by the dotted curve in figure A6-5. .

To determine a conductivity value for the silicone oil a fluid of known thermal conductivity was substituted for the oil inside the amplifier. Water was selected. A computer prediction of junction temperature change for water was made, that agreed closely with the experimental results. This verified the suspicion the oil conductivity was in error, and allowed the oil conductivity to be calculated by a ratio of the oil to water experimental results. The result was a value of the silicone oil conductivity of .049 $\frac{\text{Btu}}{\text{hr ft°F}}$. This value is 44% lower than Dupont's listed specification.

This completed the experimental work that could be done with the ideal amplifier. The data gathered was used to design the modified amplifier, which will be described in the next section.

A6-6: Design of construction of the modified amplifier.

The critical dimensions of the modified amplifier were listed in table A3-5.1. The need to penalize the insulating fluid volume pumped by the sensors required a change in the performance index, as discussed briefly in section A3-4. The new performance index resulted in an amplifier considerably smaller than the ideal amplifier. The most significant difference between ideal and modified amplifiers is the sensor.

In figure A6-6.1 a sensor for the modified amplifier is diagramed. The bellows, manufactured by Cliflex Bellows Corp. of Boston, Mass., were brass, .0055 inches thick. The dimensions shown in the diagram resulted in a spring rate for the bellows of 4.2 lbf/in. Since the effective area of the bellows was 3.6 in^2, the pressure spring rate was 1.17 $lbf/in^2/in$. The cap for the top end of the bellows, which came open at both ends, was cold formed from .008 inch brass shim stock. They were soldered in place with 60/40 solder. The bellows base was soldered to a copper plate, which had been predrilled with a fill hole. A 1" high, 6 inch long, spiral heating fin was soldered to the copper plate inside the bellows, to aid fast condensation of the Freon.
A top for the bellows-plate assembly was fabricated from acrylic, the parts of which were solvent-assembled. The copper plate and flange were drilled for 4 attachment screws. The top was tapped and threaded for $\frac{1}{8}$" NPT to accommodate the specially fabricated pressure tap, which

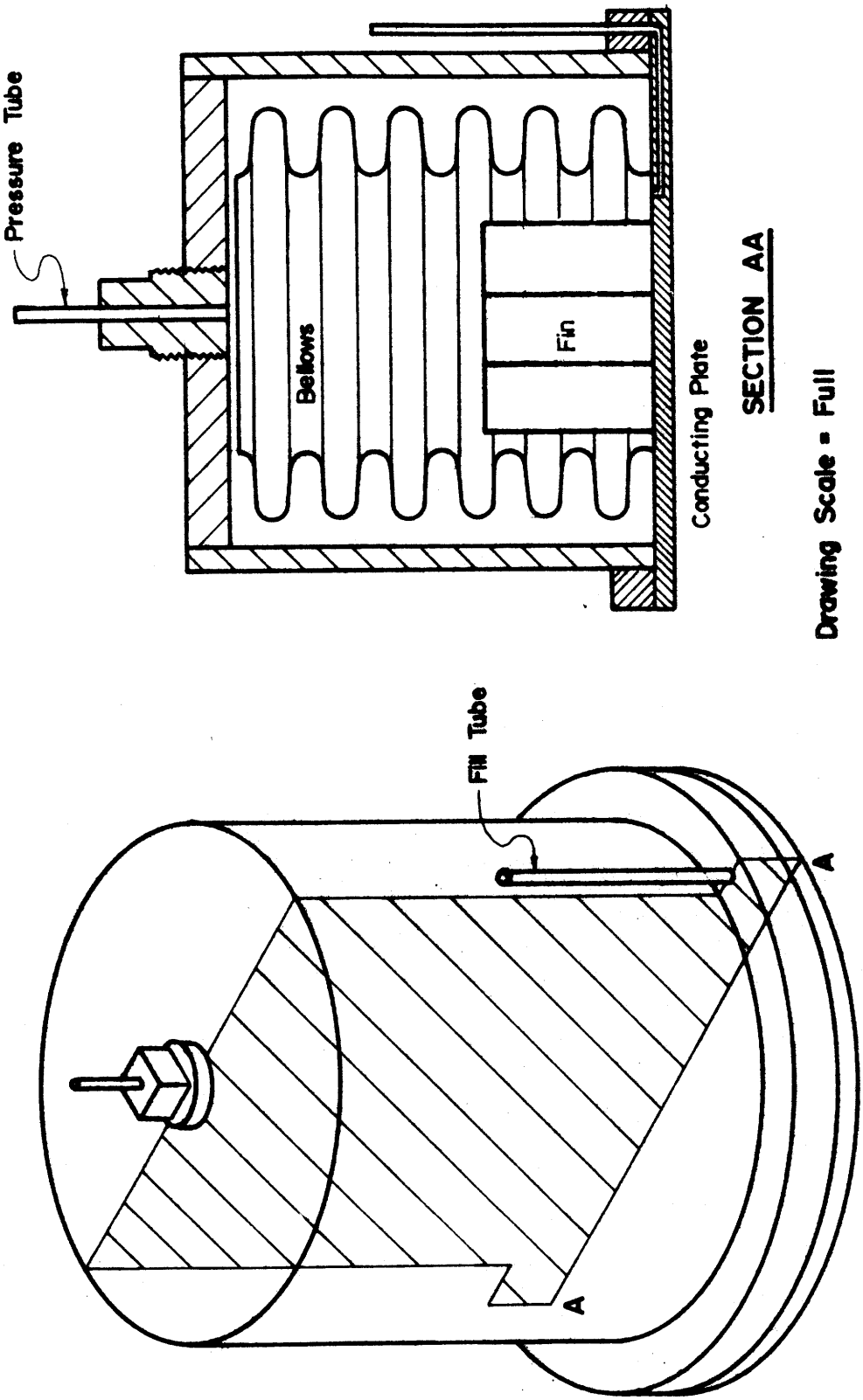

Figure A6-6.1: Diagram of modified amplifier sensor.

is also diagramed in figure A6-6.1. The top was sealed air tight to the copper plate with silicone sealant to insure a bellows displacement resulted in equivalent air displacement. The filling of the sensor is described in section seven.

The modified amplifier is shown in figure A6-6.2. The construction is identical to the type one amplifier, the only differences being size and bolt spacing. Also, the junction plate was made a simple rectangle, rather than the slightly more complex shape of the ideal amplifier. The number of air gap spacers was reduced from 9 to 4.

The substantially smaller volume of the modified amplifier required only .427 in^3 of air displacement to drive the amplifier to complete saturation. This translated into .123 inch of bellows displacement, ignoring compressibility effects of the air.

The bellows in the negative and positive sensors are in pressure communication through the conducting and insulating fluids. An expansion of either bellows requires an identical contraction of the other. This causes the pressure loss to bellow spring rate to be twice the value for a single bellows. ($.117 \frac{lb_f/in^2}{in.}$) In addition, a volume change generates a fluid level difference in the manometers formed by the film sections and reservoirs. The manometer effect acts as a fluid spring, requiring a pressure difference to be deflected. The fluid level change and the bellows' spring rate add as springs in parallel. A temperature difference between sensors creates a pressure

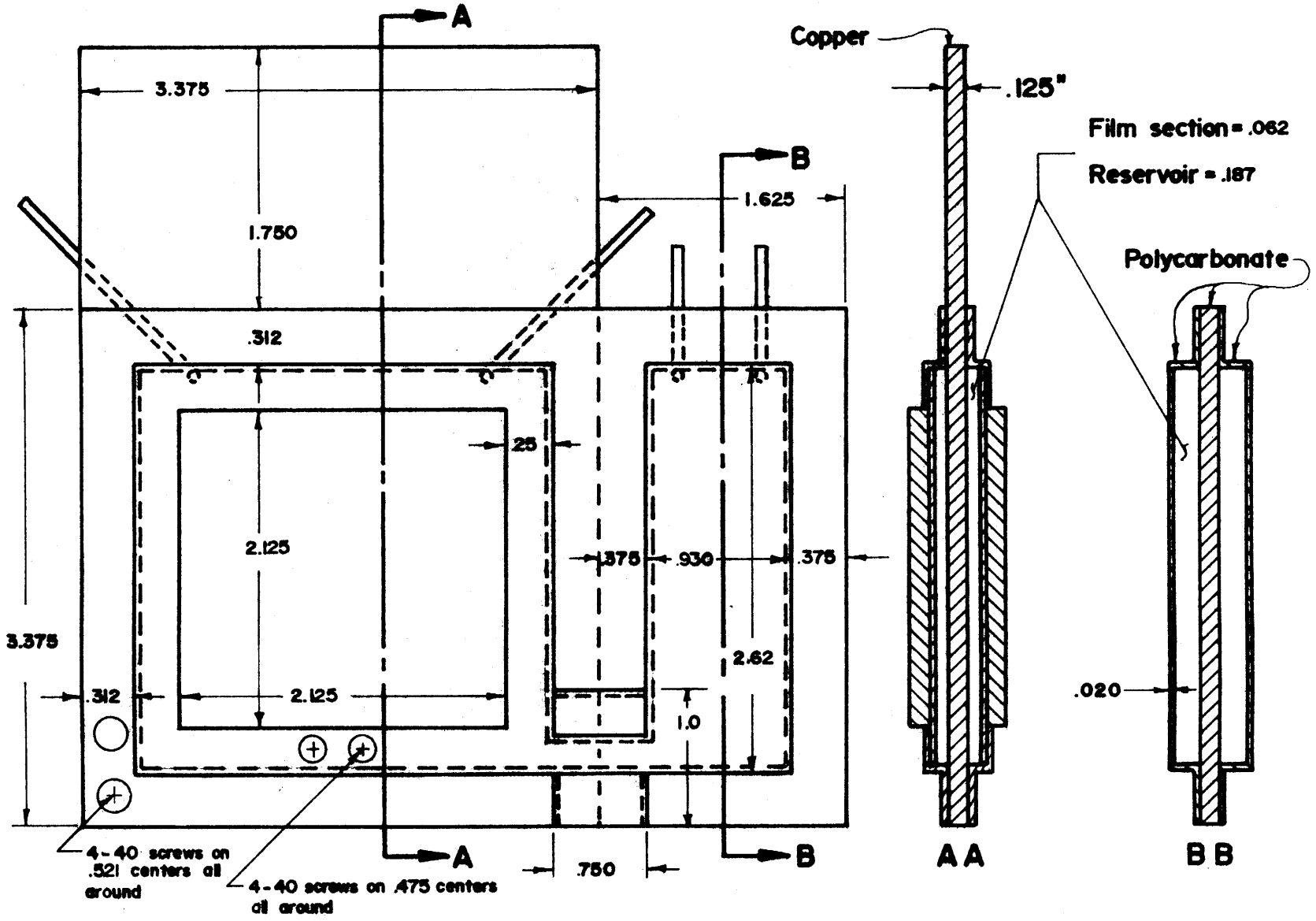

Figure A6-6.2: Drawing of modified amplifier.

difference, causing a change in the film section-reservoir manometers until the product of displacement and the combined spring rate equals the pressure difference. The model derived previously, for sensors with no spring rates does not require modification for sensors with spring rates. The effect of a diaphragm spring rate can be included simply by modifying the conducting fluid density to account for the spring rate.

The effective conducting fluid density is derived by calculating the pressure required to cause a unit of conducting fluid displacement with and without a sensor spring rate. The density of the conducting fluid is then multiplied by this ratio to calculate the effective density.

First, the pressure/unit volume with no diaphragm spring rate is calculated. For a given fluid level change:

$$\text{total air volume-displaced} = \text{cross sectional area} \times \Delta h \times 2 \qquad \text{(A6-6.1)}$$

where the cross sectional area is that of the film section or reservoir. The pressure difference required to pump this volume:

$$\text{pressure difference} = 2 \times \Delta h \times \rho_{\text{conducting fluid}} \qquad \text{(A6-6.2)}$$

Therefore,

$$\frac{\text{Pressure difference}}{\text{Unit Volume}} = \frac{\rho_{\text{conducting fluid}}}{\text{Cross section area}} \qquad \text{(A6-6.3)}$$

Therefore,

$$\frac{\text{Pressure difference}}{\text{Unit volume}} = \frac{.0361 \ \frac{\text{psi}}{\text{in}}}{.1628 \ \text{in}^2} = .222 \ \frac{\text{psi}}{\text{in}^3} \qquad \text{(A6-6.6)}$$

Now the same quantity is calculated for the bellows. The bellows pressure spring rate was calculated previously to be 1.17 psi/in. With an effective area of 3.6 in^2, this results in a volume spring rate of .325 $\frac{\text{psi}}{\text{in}^3}$. One bellows most compress as the other expands, so the effective spring rate doubles to .650 psi/in^3. The total bellows/fluid system spring rate is:

$$K_{\text{total}} = .650 + .222 = .872 \ \frac{\text{psi}}{\text{in}^3} \qquad \text{(A6-6.7)}$$

with approximately 3/4 of the spring rate due to the bellows. This is modeled in the program as an effective density increase of the conductive fluid.

$$\text{New Conducting Fluid Density} = \frac{.872}{.222} \times \rho_f = 3.93 \ \rho_f. \qquad \text{(A6-6.8)}$$

Thus, increasing the density by a factor of 4 accounts for the bellows spring rate. This method was employed in Chapter 5 to predict the the behavior of the modified amplifier. The bellows sensors and the modified amplifier formed the working experimental model.

Section A.7: Sensor fluid selection for the experimental amplifier.

The material tables in appendix four, A4-4.1, listed the properties of several sensor fluids. (that fluid which generates a saturated vapor pressure in proportion to a temperature), specifically FC-88, Freon-11, and Freon-113. The latter was finally chosen, but not before considerable experimentation had been done.

The original choice for sensor fluid was FC-88, one of the Florinert products manufactured by 3M corporation. FC-88 is a flurocarbon liquid which does not attack polymers, and was selected because it would not attack polymer diaphragms. Even though the sensors now had metal bellows, due to the air diffusion problem, the sensor fluid was not changed. FC-88 had a high vapor pressure change for a given temperature change, and a boiling point slightly above ambient. Unfortunately FC-88 is not a solution, but a mixture of different isomers with different vapor pressures. The original data provided by 3M failed to indicate the properties of the fluid varied depending on the exact mix.

Later data provided by the manufacturer indicated different boiling points, which varied as much as six degrees, Fahrenheit. This information was discovered only after extensive testing of the sensors.

The procedure used to fill the sensors aggravated the tendency of the lighter isomers to boil off first in the FC-88. To insure

there was no air in the bellows a hard vacuum was drawn inside through the fill tube. The bellows could not support a 15 psi pressure differential, which would result with a vacuum inside and atmospheric pressure outside. To avoid this problem a vacuum was drawn outside the bellows through the pressure tap. The degassed sensor fluid was connected (this procedure is described later in this section) to the vacuum lines through a valve. The vacuum was monitored with a Mercury manometer. When there was no dectable air pressure in the sensor, the vacuum line was pinched off and a small amount of sensor fluid was introduced inside and outside the bellows. This was to prevent a large pressure gradient across the bellows while being filled. The flow to the outside of the bellows was then pinched off, and the inside filled with the desired amount of fluid. When filling was complete the stainless steel fill tube was pinched off with specially ground clamping pliers. The tube was then sealed with solder.

Because the sensor fluid fills an evacuated cavity the initial fill contains a higher proportion of the lighter isomers. The amount of fill thus affects the properties of the resulting sensor fluid. This made FC-88 useless as a sensor fluid.

Freon-113 (trichloro-trifluoroethane) was substituted for FC-88; Freon-11 was considered, but its boiling point was too close to room temperature. To hold temperatures close to room temperature would require chillers in addition to the heaters on the temperature

input baths. The Freon-113 has a nominal boiling point of 117°F. At room temperature the pressure of saturated F-113 is approximately 6 psi. This would put a 9 psi pressure differential across a filled bellows, at room temperature, which it could accommodate.

The saturated vapor pressure-temperature curve for Freon-113 was presented in figure 3-5.4. The pressure change for Freon-113, over the range of 100°F to 124°F, is about .435 psi/°F. This constant, and high, parameter made Freon-113 an acceptable sensor fluid. The Freon was degassed, prior to filling, by freezing it, in a bath of alcohol and dry ice, and allowing it to thaw under a hard vacuum. The dissolved gas, forming bubbles in the Freon ice, are drawn off by the vacuum instead of re-entering solution.

APPENDIX 7: COMPUTER PROGRAM LISTING

Section A7-1: Listing of optimal design program.

AMPLIFIER DIMENSION SELECTION
OPTIMIZATION PROGRAM

```
C
C
C
C           PROGRAM DESCRIPTION
C
C     THIS IS A PROGRAM TO SELECT THE AMPLIFIER DIMENSIONS WITH THE
C     THE COMPLEX METHOD OF BOX.  THE USER MUST ENTER THE  MATERIAL
C     PROPERTIES AND THE DESIRED RESISTANCE RATIO ( VARIABLE RR) AND
C     THE PROGRAM WILL RETURN THE SIX OPTIMIZED DIMENSIONS.
C
C
      SUBROUTINE CONST(N,M,K,X,G,H,I)
      DIMENSION X(16,15),G(15),H(15)
      CONDJ=240.0
      CONDW=.1113
      AR=1.0/144.0
      DC=.08333
      WTH=.030
      CONDK=.090
      RESTK=.016
      CONDS=.1113
C
C     YETA IS THE RESISTANCE RATIO TIMES THE MINIMUM RESISTANCE OF
C     THE FILM SECTION.
C
      RFILM= (X(I,3) * .08333) / (X(I,6)*X(I,6)*.00694*CONDK)
      RSIDE= (X(I,3) * .08333) / (4.*X(I,6)*WTH*.00694*CONDS)
      RAIR= RFILM * CONDK/RESTK
      YETA= RR *(RFILM*RSIDE/(RFILM + RSIDE))
C
C  ZETA IS A CONSTRAINT ON BULB VOLUME THAT MAKES IT 10% LARGE THAN FILM
C
      ZETA= X(I,6)*X(I,6)*X(I,3)*2.1
C
C   XETA IS THE RESISTANCE OF THE INTERIOR WALL AND CONDUCTING FLUID
```

```
C
      XETA=((X(I,4) * DC) / (X(I,6)**2.0*CONDW) + (X(I,3)*DC)/(X(I,6)**2
     1 * CONDK))*144.0
C
C   WETA IS THE 10% GREATER VOLUME CONSTRAINT ON THE CONTROL BULB
C
      WETA=X(I,6)*X(I,6)*X(I,3)*2.1/X(I,2)
      IF(I.GT.1) GO TO 901
      A=X(I,1)
      B=X(I,2)
      C=X(I,3)
      D=X(I,4)
      E=X(I,5)
      F=X(I,6)
  901 CONTINUE
C
C
      G(1)=WETA
      H(1)=X(I,6)*X(I,6)
      G(2)=.125
      H(2)=1.0
      G(3)= .062
      H(3)=1.0
      G(4)=.000
      H(4)=.125
      G(5)=.010
      H(5)=.125
      G(6)=2.0
      H(6)=9.0
C
C    X(1) IS THE CONDUCTING PLATE AREA IN INCHES
C    X(2) IS THE CONTROL BULB THICKNESS IN INCHES
C    X(3) IS THE FILM SECTION THICKNESS IN INCHES
C    X(4) IS THE THICKNESS OF THE WALL BONDED TO JUCTION IN INCHES
```

```
C    X(5) IS THE JUNCTION THICKNESS (OF COPPER) IN INCHES
C    X(6) IS THE LENGTH OF A SIDE OF THE FILM SECTION IN INCHES
C
      G(7)=ZETA
      H(7)=X(I,6)**2.0*X(I,3)*2.5
      G(8)=YETA
      H(8)=10000.
      G(9)=0.0
      H(9)=XETA
      G(10)=0.0
      H(10)=X(I,6)*X(I,6)*.98
C
C    X(7) IS THE CONTROL BULB VOLUME
C
      X(I,7)= X(I,1) * X(I,2)
C
C   X(8) IS THE RESISTANCE OF THE FILM SECTION IN THE RESISTING MODE
C
      X(I,8)= (RSIDE*RAIR) / (RSIDE + RAIR)
C
C   X(9) IS THE RESISTANCE OF JUNCTION BLOCK TO MIDPOINT OF FILM SECTION
C
      X(I,9)= (.5/(X(I,5)*DC*CONDJ))
      X(I,10)=WETA
      RETURN
      END
      SUBROUTINE FUNC(N,M,K,X,F,I)
      DIMENSION X(16,15),F(16)
C
C   THIS IS THE OJECTIVE FUNCTION BOX IS TRYING TO MAXIMIZE.
C
      F(I)=X(I,1)**.5*.9 -(X(I,2)+X(I,3)+5.*X(I,4)+X(I,5))*10.0 -X(I,6)
C
      RETURN
      END
```

Section A7-2: Listing of seventh order model simulation program.

AMPLIFIER DYNAMIC SIMULATION PROGRAM

```
      SUBROUTINE EQSIM
      COMMON T,TSTEP,Y(20),F(20),STIME,FTIME,NEWDT,IFWRT,N,IPR,
     *  ICD,ICN,TNEXT,PNEXT,TRACK
      DIMENSION D(25),        R(200), C(200),RHO(20), CP(20)
      REAL K(20),H(20),HITE, MASVN, MASVI
      IF (NEWDT.GE.0) GO TO 909
      READ (8,101) D
  101 FORMAT (7F10.0)
      READ (8,201) (RHO(I),I=1,15,1)
      READ (8,201) (CP(I),I=1,15,1)
      READ (8,201) (K(I),I=1,15,1)
  201 FORMAT (7F10.0)
      READ (8,301) (H(I),I=1,4,1)
  301 FORMAT (4F10.3)
C
C*****************************************************************************
C
C        THIS SECTION IS USED TO DEFINE BASIC INPUT PARAMETERS AND
C        VARIABLES THAT AN INTIAL VALUE MUST BE PROVIDED FOR
C
C*****************************************************************************
C
      XTN=118.3
      XTI=121.0
      XTA=121.0.
      S=.08333
      PI=3.14159
      HITE=0.0
      G=32.2
      XMU5=4.2E-3
      XMU11=4.0E-7
      XNFG=75.0
      AC= 1.0/ 144.0
      GASF= .7094
      SC= .1714E-8
```

```
      XNUMS=4.0
      XTSNK=35.5
      XTOB=121.0
      XTSCE=206.5
      XTB=115.9999
      SRAD=.0625
      TSNK= XTSNK + 459.69
      TSCE= XTSCE + 459.69
C
C*****************************************************************************
C
C        THIS SECTION IS USED TO CHANGE PARAMETERS FROM THE BASIC LEXAN
C        SIDED OP AMP TO ANY CONFIGURATION IT IS DESIRED TO TEST
C
C*****************************************************************************
C
      K(5)=.049
      D(23)=.06
C
C        THIS SECTION HAS ALL INPUT DATA PRINTED
C
      DO 105 I=1,25
      WRITE (5,106) I,D(I)
  106 FORMAT (1X,'D(',I2,')= ',F10.3)
  105 CONTINUE
      DO 208 J=1,15
      WRITE (5,209) J,RHO(J),CP(J),K(J)
  209 FORMAT(1X,'FOR MATERIAL ',I2,' RHO=',F10.3,' CP=',F10.3,' K=',F10
     1.3)
  208 CONTINUE
C
C*****************************************************************************
C
C     DIMENSIONS OF THE DATA IN VARIOUS MATRICES:
C
```

```
C         ALL FLUID RESISTANCES ARE IN LBF*SEC/INCHES**5
C         RHO IS IN LBM/FT**3
C         D IS IN INCHES
C         R IS IN F*HR/BTU
C         C IS IN BTU/F
C         ALL PRESSURES ARE IN LBF/IN**2
C         C FLUID IS IN  INCHES**5/LBF
C         CP IS IN BTU/(LBM*F)
C         H IS IN BTU/(HR*FT**2*F)
C         K IS IN BTU/(HR*FT*F)
C         ALL VISCOSITIES ARE ABSOLUTE, IN LBF*SEC/FT**2
C
C*************************************************************************
C
C      MATERIAL(1) IS THAT OF THE HOT SIDE AMPLIFIER WALL
C      MATERIAL(2) IS THAT OF THE WALLS NEXT TO THE JUNCTION BLOCK
C      MATERIAL(3) IS THAT OF THE JUNCTION BLOCK
C      MATERIAL(4) IS THAT OF THE COLD AMPLIFIER WALL
C      MATERIAL(5) IS THAT OF THE CONDUCTING FLUID
C      MATERIAL(6) IS THAT OF THE CONDUCTING PLATE OF THE CONTROL BULB
C      MATERIAL(7) IS THAT OF THE CONTROL BULB WALLS
C      MATERIAL(8) IS THAT OF THE CONTROL BULB INSULATION
C      MATERIAL(9) IS THAT OF THE PRESSURE VAPOR
C      MATERIAL(10) IS THAT OF THE WICK
C      MATERIAL(11) IS THAT OF THE INSULATING FLUID
C      MATERIAL(12) IS THAT OF THE AMPLIFIER SIDES
C      MATERIAL (13) IS THAT OF THE CONTROL BULB VAPORIZING FLUID
C
C*************************************************************************
C
C      D(1)= CONDUCTION WALL THICKNESS ON CONTROL BULB
C      D(2)= THICKNESS OF AIR CHAMBER IN CONTROL BULB
C      D(3)= HEIGHT OF THE CONTROL BULB
C      D(4)= WIDTH OF AMPLIFIER SECTION
C      D(5)= WIDTH OF FLUID GAP IN AMPLIFIER SECTION
```

```
C      D(6)= THICKNESS OF POLYMER WALL NEXT TO JUCTION BLOCK
C      D(7)= THICKNESS OF JUNCTION BLOCK
C      D(8)= HEIGHT OF AMPLIFIER FLUID RESERVOIR
C      D(9)= THICKNESS OF AMPLIFIER SIDE WALLS
C      D(10)= WIDTH OF FLUID RESERVOIR
C      D(11)= THICKNESS OF FLUID RESERVOIR
C      D(12)= THICKNESS OF AMPLIFIER HOT SIDE WALL
C      D(13)= THICKNESS OF AMPLIFIER COLD SIDE WALL
C      D(14)= WIDTH OF CONTROL BULB
C      D(15)= THICKNESS OF CONTROL BULB SIDE WALLS
C      D(16)= THICKNESS OF INSULATION ON BACK OF CONTROL BULB
C      D(17)= THICKNESS OF WICK IN CONTROL BULB
C      D(18)= I.D. OF AIR CONDUCTION TUBE
C      D(19)= LENGTH OF AIR CONDUCTION TUBE
C      D(20)= HEIGHT OF JUNCTION BLOCK
C      D(21)= DISTANCE BETWEEN FILM SECTION AND RESERVOIR
C      D(22)= HYDRAULIC DIAMETER OF TUBE CONNECTING RESERVOIR
C      D(23)= THICKNESS OF VAPORIZING FLUID IN CONTROL BULB
C
C*****************************************************************************
C
C      SURFACE(1) IS THAT OF THE HOT SIDE OF THE AMPLIFIER
C      SURFACE(2) IS THAT OF THE COLD SIDE OF THE AMPLIFIER
C      SURFACE(3) IS THAT OF THE CONDUCTING PLATE SURFACE OF THE BULB
C      SURFACE(4) IS THAT OF THE OUTSIDE OF THE CONTROL BULB
C
C*****************************************************************************
C
       AREA= D(3)* D(14) / 144.0
       A= AREA
C
C*****************************************************************************
C
C      THE CONTROL BULB CALCULATIONS WILL BE DONE FIRST.  THE RESIST-
C      ANCES HAVE THE FOLLOWING PHYSICAL MEANINGS.
```

```
C      R(2)= ALL SURFACE RESISTANCE + 1/2 WALL CONDUCTION RESISTANCE
C      R(6)= 1/2 WALL + WICK + 1/2 VAPOR CAVITY RESISTANCES
C      R(14)= 1/2 VAPOR CAVITY + 1/2 WALL RESISTANCE
C      R(18)= 1/2 WALL + INSULATION + SURFACE RESISTANCE
C
C      CAPACITANCES IN THE CONTROL BULB:
C      C(4)= THE HEAT STORAGE OF THE WALL AND WICK
C      C(8)= THE HEAT STORAGE OF THE VAPORIZED FLUID
C      C(16)= THE HEAT STORAGE OF THE WALLS AND INSULATION
C
C      SOME ASSUMPTIONS HAVE BEEN MADE. FIRST, THE CONDUCTION THROUGH
C     THE SIDES OF THE CONTROL BULB ARE SMALL ENOUGH TO IGNORE.
C      SECOND, THE CONDUCTIVITY OF THE VAPOR CAVITY IS AN AVERAGE
C      OF THE AIR AND VAPORIZED FLUID.
C
*****************************************************************************

      R(2)= 1./(H(3) * A) + ( D(1) /  24.) / (A * K(6))
     1 + (D(23) / (24.0 * A * K(13)))
      R(6)= (D(1)/24.) / (A*K(6)) + (D(17)/12.) / (A*K(10))
     1 + (D(23) / (24.0 * A * K(13)))
      R(14)= (D(2)/24.) / (A*K( 9)) +(D(15)/24.) / (A*K(7))
      R(18)= (D(15)/24.) / (A*K(7)) + (D(16)/12.) / (A*K(8)) +
     1  1./(H(4)*A)
      R(22)=R(2)
      R(26)=R(6)
      R(34)=R(14)
      R(38)=R(18)
      RS=(D(5)*S)/(XNUMS*PI*SRAD**2.0*AC*K(12)*1.25)
      RSIDE= (D(5)*S)/(2.*(D(4)+ D(8))*D(9)*AC*K(12))
      RLEAK=(.125*S)/(4.4*AC*K(11))
      RADD= (RSIDE*RLEAK) / (RSIDE + RLEAK)
      R(87)= (RS * RADD) / (RS + RADD)
      R(187)=R(87)
      R87= R(87)
```

```
      R187=R(187)
      C(46)= D(4)*D(5)*1728.0 / RHO(5)
      C(96)=C(46)
      R(92)= 128.*XMU5*D(21)/((PI*D(22)**4.0) * 144.0) + (128.0*XMU11*
     1 D(19))/(PI*D(18)**4.0*144.0)
      R(94)=R(92)
      R(42)=R(92)
      R(44)=R(92)
      C(4)= A*(( CP(6)*RHO(6))*D(1)/12. +(CP(10)*RHO(10))* D(17)/12.)
     1 + A*(CP(13)*RHO(13)*D(23)*S)
      C(16)= (D(2)*D(15)*2.*(D(3) + D(14))*CP(7)) / (1728.*RHO(7))
     1 + (D(2)*D(16)*2.*(D(3) + D(14))*CP(8)) / (1728.*RHO(8))
     2 +(D(3)*D(14)*D(15)*CP(7)) / (1728.*RHO(7))
     3 + (D(3)*D(14)*D(16)*CP(8)) / (1728.*RHO(8))
      C(24)=C(4)
      C(36)=C(16)
      C208=.1
      C228=.1
      SENVOL= PI*2.75*2.75*.25*3.0*AC*S
      BELVOL= 3.6*2.0*AC*S
      SENAIR=SENVOL-BELVOL
      AIRM=((SENAIR           + ((PI*D(18)*D(18))/4.0)*D(19))
     1/(         1728.0) + D(4)*D(5)*D(8)/(2.0*1728.0)) * RHO(11)
      R204=R(2) + R(6)
      R302 = ((D(2) - D(8)) + D(14)/2.0)*S/(K(3)*D(4)*D(7)*AC)
      C304=((D(2)-D(8)) +D(14)/2.0)*D(4)*D(7)*RHO(3)*CP(3)*S*AC
      R216=R(14) + R(16)
      R224=R(22) + R(26)
      R236= R(34) + R(38)
      R94= R(94) + R(44)
      R92=R(92) + R(42)
  909 CONTINUE
      RITE=Y(15)
C
C*******************************************************************************
```

```
C
C     AMPLIFIER PARAMETERS:
C     C(85)= JUNCTION BLOCK HEAT STORAGE
C     C(53),C(73) ,C(61), C(81) ARE ALL WALL HEAT STORAGES, THEIR
C     SIZE BEING DETERMINED BY THE FLUID LEVEL IN THE FILM SECTIONS
C     C(57), C(77) ARE THE HEAT STORAGES OF THE RESISTING AND CONDUCT-
C     ING FLUIDS
C     R(51),R(71),R(63),R(83) ARE ALL 1/2 THEIR RESPECTIVE WALL
C     RESISTANCES PLUS SURFACE RESISTANCE
C
C     R(55), R(75), R(59), R(79) ARE ALL 1/2 THE WALL AND 1/2 THE
C     FLUID RESISTANCE OF THE FLUIDS THEY ARE IN CONTACT WITH
C     R(87) IS THE FIXED RESISTANCE OF THE AMPLIFIER SECTION WALLS.
C
C     THE VARIABLE HITE WILL BE THE FLUID LEVEL IN THE HOT SIDE FILM
C     CHAMBER.  IT WILL BE MEASURED FROM A POINT HALF WAY UP THE
C     CHAMBER WALLS..  THUS IT WILL BE POSITIVE FOR A HIGH INPUT
C     TO THE POSITIVE SENSOR
C
C*************************************************************************
C
      C(53)= D(12)*D(4)*RHO(1)*CP(1)*(D(8)/2. - HITE)    *5.787E-4
      C(73)= D(12)*D(4)*RHO(1)*CP(1)*(D(8)/2. + HITE)    *5.787E-4
      C(57)=D(5)*D(4)*RHO(11)*CP(11)*(D(8)/2. - HITE)    *5.787E-4
      C(77)=D(5)*D(4)*RHO( 5)*CP( 5)*(D(8)/2. + HITE)    *5.787E-4
      C(61)=D(6)*D(4)*RHO( 2)*CP( 2)*(D(8)/2. - HITE)    *5.787E-4
      C(81)=D(6)*D(4)*RHO( 2)*CP( 2)*(D(8)/2. + HITE)    *5.787E-4
      C(85)=D(20)*D(4)*D(7)*RHO(3)*CP(3)/1728.
      C(161)= C(81)
      C(181)= C(61)
      C(157)= D(5)*D(4)*RHO(11)*CP(11)*(D(8)/2. + HITE) *5.787E-4
      C(177)= D(5)*D(4)*RHO( 5)*CP( 5)*(D(8)/2. - HITE) *5.787E-4
      C(153)=D(13)*D(4)*RHO( 4)*CP( 4)*(D(8)/2. + HITE) *5.787E-4
      C(173)=D(13)*D(4)*RHO( 4)*CP( 4)*(D(8)/2. - HITE) *5.787E-4
      U= D(4)*(D(8)/2. - HITE) / 144.
```

```
B= D(4)*D(8)/144. - U
R(51) = 1./(H(1)*U)+ (.5*D(12)*S) / (U*K(1))
R(71) = 1./(H(1)*B)+ (.5*D(12)*S) / (B*K(1))
R(55) = (.5*D(12)*S) / (U*K(1)) + (.5*D(5)*S) / (U*K(11))
R(75) = (.5*D(12)*S) / (B*K(1)) + (.5*D(5)*S) / (B*K(5))
R(59) = (.5*D(5) *S) / (U*K(11))+ (.5*D(6)*S) / (U*K(2))
R(79) = (.5*D(5) *S) / (B*K(5)) + (.5*D(6)*S) / (B*K(2))
R(63) = (.5*D(6) *S) / (U*K(2)) + (.5*D(7)*S) / (U*K(3))
R(83) = (.5*D(6) *S) / (B*K(2)) + (.5*D(7)*S) / (B*K(3))
R(163)= (.5*D(7) *S) / (B*K(3)) + (.5*D(6)*S) / (B*K(2))
R(183)= (.5*D(7) *S) / (U*K(3)) + (.5*D(6)*S) / (U*K(2))
R(159)= (.5*D(6) *S) / (B*K(2)) + (.5*D(5)*S) / (B*K(11))
R(179)= (.5*D(6) *S) / (U*K(2)) + (.5*D(5)*S) / (U*K(5))
R(155)= (.5*D(5) *S) / (B*K(11))+ (.5*D(13)*S)/ (B*K(4))
R(175)= (.5*D(5) *S) / (U*K(5)) + (.5*D(13)*S)/ (U*K(4))
R(151)= (.5*D(13)*S) / (B*K(4)) + 1. / (H(2)*B)
R(171)= (.5*D(13)*S) / (U*K(4)) + 1. / (H(2)*U)
C2177= C(173) + C(153) + C(181) + C(161) + C(177)
C277= C(73) + C(53) + C(77) + C(81) + C(61)
C285= C(81) + C(61) + C(85) + C(181) + C(161) + C304
R2155= R(151) + R(155) + R(159) + R(163)
R255= R(51) + R(55) + R(59) + R(63)
R2183= R(183) + R(179)
R271= R(71) + R(75)
R283= R(79) + R(83)
R2171= R(175) + R(171)
E11 = 8.144 - .1619*Y(1) + .001853*Y(1)*Y(1)
E31 = 8.144 - .1619*Y(2) + .001853*Y(2)*Y(2)
DELP=E11-E31
VAIRI=(AIRM*53.3*(Y(1) + 456.)*12.0)/E11
VAIRN=(AIRM*53.3*(Y(2) + 456.)*12.0)/E31
VTOTN=SENVOL          + ((PI*D(18)*D(18)*D(19))/4.0) + ((D(8)/2.0
1 +Y(15))*2.0)*D(5)*D(4)
VTOTI=SENVOL          + ((PI*D(18)*D(18)*D(19))/4.0) + ((D(8)/2.0
1 -Y(15))*2.0)*D(5)*D(4)
```

```
      IF (VAIRN.GE.VTOTN) VAIRN=VTOTN
      IF (VAIRI.GE.VTOTI) VAIRI=VTOTI
      VVAPI= VTOTI - VAIRI
      VVAPN= VTOTN - VAIRN
      MASVN = VVAPN/((13.138 - .14896*Y(2) + 4.732E-4 *Y(2)*Y(2))*1728.)
      MASVI = VVAPI/((13.138 - .14896*Y(1) + 4.732E-4 *Y(1)*Y(1))*1728.)
      Y(8)=MASVI*XHFG
      Y(9)=MASVN*XHFG
      IF (NEWDT.GE.0) GO TO 2
      PUT R302,C304
      PUT RS,RSIDE,RLEAK,RADD
      PUT R204,C208,R216,R224,C228,R236
      PUT C2177,C277,C285,R2155,R255,R2183,R271,R283,R2171,R87,R187
      PUT VAIRI,VAIRN,VTOTN,VTOTI,VVAPN,VVAPI,MASVI,MASVN,AIRM
      PUT XMU11,XHFG,AC,GBSF,BC,XNUMS ,SRAD
      PUT XTA,XTI,XTN,XTSCE,XTSNK,TSNK,TSCE,XTP, XTOB,S,PI,HITE,G,XMU5
      PUT OMEGA
    2 CONTINUE
      C208=Y(8)/Y(1) + C(4) + C(16)
      C228=Y(9)/Y(2) + C(24) + C(36)
C
CC*****************************************************************************
C
C
C        XTSCE IS THE SOURCE TEMPERATURE, XTSNK IS THE SINK TEMPERATURE
C        XTI IS THE TEMPERATURE INPUT TO THE INVERTING BULB.  XTN IS
C        THE NONINVERTING INPUT, AND XTA IS ATMOSPHERE TEMPERATURE
C        LET Y(1)=E208, Y(2)=E228, Y(3)=E46, Y(4)=E96, Y(5)=E277
C        HITE VARIABLE WILL BE Y(15)
C
C
C        Y(1)= TEMPERATURE OF INVERTING BULB IN DEGREES F
C        Y(2)= TEMPERATURE OF NON-INVERTING BUIB IN DEGREES F
C        Y(3)= PRESSURE ON FILM CHAMBER OF HOT SIDE IN PSI
C        Y(4)= PRESSURE ON RESERVOIR OF COLD SIDE IN PSI
C        Y(5)= TEMPERATURE OF HOT SIDE FILM IN DEGREES F
```

```
C         Y(6)= TEMPERATURE OF JUNCTION BLOCK IN DEGREES F
C         Y(7)= TEMPERATURE OF COLD SIDE FILM IN DEGREES F
C         Y(15)= HEIGHT OF CONDUCTING FLUID ABOVE CENTER OF AMPLIFIER
C                IN FILM CHAMBER ON HOT SIDE IN INCHES
C
C*************************************************************************
C
      XTI=Y(6)
      F(1)= ((XTI-Y(1))/R204 - (E11*.3856)*((DELP-Y(3))/R92+(DELP -
     1 Y(4))/R94)    - (Y(1) - XTA)/R216)/C208
      F(2)= ((XTN-Y(2))/R224 + (E31*.3856)*((DELP-Y(3))/R92  + (DELP-
     1 Y(4))/R94)    - (Y(2) - XTA)/R236)/C228
      F(3)=(DELP - Y(3))/(C(46)*R92 * 2.7778E-4 )
      F(4)=(DELP - Y(4))/(C(96)*R94 * 2.7778E-4 )
      F(5)= ((XTSCE -Y(5))/R271 -(Y(5) - Y(6))/R283)/C277
      F(6)= ((Y(5) - Y(6))/R283 + (XTSCE- Y(6))/R255 + (XTSCE - Y(6))/
     1 R(87) - (Y(6) -XTSNK)/R(187)-(Y(6) - Y(7))/R2183 - (Y(6) - XTSNK)
     2/R2155)/C285
      F(7)= ((Y(6) -Y(7))/R2183 - (Y(7) - XTSNK)/R2171)/C2177
      Y(10)=Y(2) - 121.0
      Y(11)=Y(1)-121.0
      Y(12)=XTN - 121.0
      Y(13)= MASVI*XHFG
      Y(14)= MASVN*XHFG
      Y(15)= 1728.0*( -Y(3)    )/(RHO(5)  *2.0)
      Y(17)= Y(6) - 121.0
      Y(19)= T * 60.0
      IF (Y(15).GE.1.310) Y(15)=1.310
      IF (Y(15).LE.-1.310) Y(15)=-1.310
      IF (T.LE..9983) GO TO 99
      PUT C2177,C277,C285,R2155,R255,R2183,R271,R283,R2171,R87,R187
      PUT R204,C208,R216,R224,C228,R236,E11,E31,DELP
   99 CONTINUE
      RETURN
      END
```

APPENDIX A8: AUTHOR'S BIOGRAPHICAL SKETCH

The earliest known record of the author is Nov. 28, 1948 in the town of Battle Creek, Michigan. Born into a middle class family he is reputed to have enjoyed a more or less normal childhood. Spending his earlier years on a farm, where he learned all the virtues of hard work with his hands, he arrived at Harper Creek High School in 1962 with a law career in mind. Finding little in his high school curriculum that challenged his formidable analytical talents he excelled in even his most academic subjects-shop and drafting.

Failing, by some administrative oversight, to get into Harvard the author entered the University of Michigan in 1966, and commenced the study of Philosophy to prepare for the bar. Near the end of his studies, and upon hearing the author was now contemplating a career in philosophy, his philosophy advisor counseled him to apply his formidable analytical talents to some other field of human knowledge. Engineering was suggested. Concluding he had solved all the current problems in the field of philosophy the author commenced the mastery of the sciences; specifically, the study of mechanical engineering. Near the end of his studies, upon hearing the author was now contemplating a career in engineering, his engineering faculty adivsor counseled him to apply his formidable analytical talents to some other field of human knowledge. Philosophy was suggested. Upon learning the author had previously mastered the field he was then advised to continue his engineering studies - at some other institution - to broaden his exposure.

Heeding what he deemed sound advice the author entered the Massachusetts Institute of Technology in 1972, having graduated from Michigan that same year with an A.B. in philosophy, and a B.S.E. in Mechanical Engineering.

He completed a Master's under Professor David Gordon Wilson in 1973, thesis titled, "Design of a vortex section for density sorting of particles". Having finished his thesis the author's advisor counseled him to consider a career in public service. The U.S. Army was suggested. Heeding the advice the author entered the Ordinance Corps in June of 1973.

In a scant 90 days the Army realized the author's formidable analytical talents would be wasted in the armed forces, and discharged him to return his skills to the civilian sector. The author then worked for Procter and Gamble, who suggested he should have academic credentials that accurately reflected his metal prowess and advised him to complete his studies. The author returned to M.I.T. in February 1974.

He commenced work on this thesis under his current advisor B. Shawn Buckley. The author received his Mechanical Engineer's Degree in 1975. In 1977 he co-authored "Planar Thermic Elements for Thermal Control Systems" (ASME Trans., Vol. 99, Series G, No. 1, March 1977).

Having analyzed his career options in light of the credo that has governed his life-the needs of his fellow man-the author has accepted a position with Foster Miller Associates of Waltham, Massachusetts.

REFERENCES

1. A.S.T.M., Manual on the Use of Thermocouples in Temperature Measurement. Philadelphia: A.S.T.M. Special Technical Publication #470A, 1974.

2. Barna, Arpad. Operational Amplifiers. New York: John Wiley & Sons, Inc., 1971.

3. Belsterling, Charles A. Fluidic Systems Design. New York: John Wiley & Sons, Inc., 1971.

4. Bienert, Walter B. "Feedback Control of Variable Conductance Heat Pipes." NASA Tech Brief, No. 72-10169, 1972.

5. Bienert, W. and P.J. Brennan. "Transient Performance of Electrical Feedback Controlled Variable Conductance Heat Pipes." SAE/ASME/AIAA Life Support and Environmental Control Conference, 1971, San Francisco, California.

6. Boys, C.V., Soap Bubbles. New York: Dover Publications, Inc., 1959.

7. Buckley, S. "Thermic Diode Solar Panels: A Brief Summary." Proceedings of International Solar Energy Conference, Winnipeg, Canada, August 1976, Vol. 2, pp. 1-23.

8. Burr-Brown Research Corp. Operational Amplifiers, Design and Applications. New York: McGraw-Hill Book Co., 1971.

9. Christopher, William F. and Daniel W. Fox. Polycarbonates. New York: Reinhold Publishing Corp., 1962.

10. Evans, F.J. and J.J. Dixhoorn. Physical Structure in Systems Theory. London: Academic Press, 1974.

11. Fleischman, G.L. and D.J. Wanous. "Active Control Heat Pipe Performance for Long Life Battery Cooling." ASME Paper No. 72-WA/HT43, 1972.

12. Groll, M. and M. Hage. "Development of an Electrical Feedback Controlled Variable Conductance Heat Pipe for Space Applications." AIAA Paper No. 74-752, 1974.

13. Haringx, J.A. 1957. "Design of Corrugated Diaphragms." Trans. of ASME 79: 55-64.

14. Harrison, H.L., and J.G. Bollinger. Introduction to Automatic Controls, 2ed. Scranton, Pa: International Textbook Co., 1969.

15. Jacoby, S.L.S., J.S. Kowalik, and J.T. Pizzo. Iterative Methods for Nonlinear Optimization Problems. Englewood Cliffs, N.J.: Prentice-Hall, Inc., 1972.

16. Karnopp, D. and R.C. Rosenberg. Analysis and Simulation of Multiport Systems. Cambridge, Mass.: The M.I.T. Press, 1968.

17. Karnopp, D. and Ronald C. Rosenberg. System Dynamics: A Unified Approach. New York: John Wiley & Sons, Inc., 1975.

18. Krieth, Frank. Principles of Heat Transfer, Scranton: International Textbook Co., 1965.

19. Mayr, O. The Origins of Feedback Control. Cambridge, Mass.: The M.I.T. Press, 1970.

20. Mock, P.R., B.D. Marcus, and E.A. Edelman. "Communications Technology Satellite: A Variable Conductance Heat Pipe Application." AIAA Paper No. 74-749, 1974.

21. Oster, G.F. and D.M. Auslander. "Topological Representations of Thermodynamic Systems." Journal of the Franklin Institute, Vol. 292, No. 1, July 1971, pp. 1-17.

22. Oster, G.F. and D.M. Auslander. "Topological Representations of Thermodynamic Systems." Journal of the Franklin Institute, Vol. 292, No. 2, August 1971, pp. 77-92.

23. Paynter, Henry M. Analysis and Design of Engineering Systems. Cambridge, Mass.: The M.I.T. Press, 1961.

24. Rohsenow, Warren M. and Harry Y. Choi. Heat, Mass, and Momentum Transfer. Englewood Cliffs, N.J.: Prentice Hall, Inc., 1961.

25. Shearer, L., A. Murphy, and H. Richardson. Introduction to System Dynamics. Reading, Ma.: Addison-Wesley, 1967.

26. Sun, T.H. and R.C. Prager. "Development of a Switchable Cryogenic Heat Pipe for Infrared Detector Cooling." AIAA Paper No. 74-751, 1974.

27. Thoma, J.U. "Bond Graphs for Thermal Energy Transport and Entropy Flow." Journal of the Franklin Institute, Vol. 292, No. 2, August 1971, pp. 109-120.

28. Thoma, Jean U. Introduction to Bond Graphs and Their Applications. Oxford: Pergamon Press Ltd., 1975.

29. Van Der Ply, L. M. ed. 1960. "Bibliography on Diaphragms and Aneroids." ASME Paper 60-WA-122.

30. Wildhack, W.A., R.F. Dressler, and E.G. Lloyd. 1957. "Investigation of the Properties of Corrugated Diaphragms." Trans. of ASME 79: 65-82.